



EVALUATION OF A METAL SHEAR WEB SELECTIVELY REINFORCED WITH FILAMENTARY COMPOSITES FOR SPACE SHUTTLE APPLICATION

NASA-CR-132320) EVALUATION OF A METAL SHEAR WEB SELECTIVELY REINFORCED WITH FILAMENTARY COMPOSITES FOR SPACE SHUTTLE APPLICATION. PHASE (Boeing Co., Seattle, Wash.) 213 p HC \$12.75

N73-31774

Unclass

G3/31 14752

188

PHASE I REPORT

by

J. H. Laakso & D. K. Zimmerman

Prepared under Contract NAS1-10860

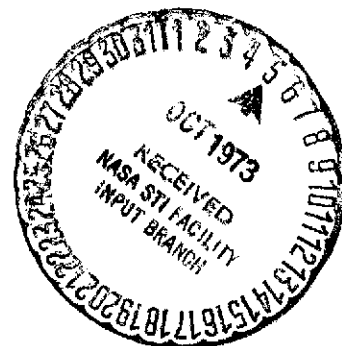
THE BOEING COMPANY

Prepared for

NATIONAL AERONAUTICS AND SPACE ADMINISTRATION

Langley Research Center

Hampton, Virginia



D180-15104

EVALUATION OF A METAL SHEAR WEB
SELECTIVELY REINFORCED WITH FILAMENTARY
COMPOSITES FOR SPACE SHUTTLE APPLICATION

PHASE I SUMMARY REPORT - SHEAR WEB DESIGN DEVELOPMENT

By

J. H. Laakso and D. K. Zimmerman

Prepared by the
Research and Engineering Division
Aerospace Group
The Boeing Company
Seattle, Washington

for

Langley Research Center
National Aeronautics and Space Administration

THIS PAGE INTENTIONALLY LEFT BLANK

ABSTRACT

An advanced composite shear web design concept has been developed for the Space Shuttle orbiter main engine thrust beam structure. Various web concepts were synthesized by a computer-aided adaptive random search procedure. A practical concept is identified having a titanium-clad $\pm 45^\circ$ boron/epoxy web plate with vertical boron/epoxy reinforced aluminum stiffeners. The boron-epoxy laminate contributes to the strength and stiffness efficiency of the basic web section. The titanium-cladding functions to protect the polymeric laminate parts from damaging environments and is chem-milled to provide reinforcement in selected areas. Detailed design drawings are presented for both boron/epoxy reinforced and all-metal shear webs. The weight saving offered is 24% relative to all-metal construction at an attractive cost per pound of weight saved, based on the detailed designs. Small scale element tests substantiate the boron/epoxy reinforced design details in critical areas. The results show that the titanium-cladding reliably reinforces the web laminate in critical edge load transfer and stiffener fastener hole areas.

A program is defined for testing three large scale shear webs. Detail design drawings are presented for the required test beam fixture and boron/epoxy reinforced test webs. Finite element static and buckling analyses of a detailed finite element model (using the NASTRAN computer code) are employed to establish the initial test instrumentation requirements.

THIS PAGE INTENTIONALLY LEFT BLANK

FOREWORD

This report was prepared by the Research and Engineering Division, Aerospace Group, The Boeing Company, under NASA Contract NAS 1-10860, Evaluation of a Metal Shear Web Selectively Reinforced with Filamentary Composites For Space Shuttle Application. The program is being sponsored by the Design Technology Branch of the Langley Research Center under the direction of the contracting officer's representative, Mr. James P. Peterson, Assistant Branch Head.

The technical performance reported summarizes Phase 1 contract activities during the period of May 1971 to June 1972.

Performance of the contract is under the management of Mr. Donald K. Zimmerman, Supervisor, Structures Development Group; Mr. John H. Laakso is the Technical Leader.

The authors wish to acknowledge the contributions of the following program participants:

| | |
|------------------|-------------------------------|
| D. D. Smith | - Design |
| M. M. House | - Element Testing |
| R. L. Egger | - Test Instrumentation |
| M. W. Ice | - NASTRAN Output Modification |
| D. R. Giesecking | - Manufacturing |
| R. Nelson | - Manufacturing |
| J. T. Hoggatt | - Materials and Processing |

Special acknowledgment is made to the Langley Research Center for program guidance and to the Grumman Aerospace Corporation for furnishing structural design and loads information on their Space Shuttle orbiter configurations.

TABLE OF CONTENTS

| | <u>Page</u> |
|--|-------------|
| ABSTRACT | iii |
| FOREWORD | v |
| TABLE OF CONTENTS | vii |
| LIST OF FIGURES | ix |
| LIST OF TABLES | xii |
| 1.0 INTRODUCTION | 1 |
| 2.0 SUMMARY | 3 |
| 3.0 DESIGN STUDIES | 7 |
| 3.1 Component Selection | 7 |
| 3.2 Structural Requirements | 11 |
| 3.3 Material Selection | 13 |
| 3.4 Computer-Aided Design Concept Screening Study | 15 |
| 3.5 Computer-Aided Detailed Design Definition | 26 |
| 3.6 Detailed Design of B/E Reinforced and All-Metal Shear Webs | 38 |
| 3.7 Detailed Design Comparisons | 45 |
| 4.0 ELEMENT TEST PROGRAM | 49 |
| 4.1 Tension Element Testing | 50 |
| 4.2 Shear Web Element Testing | 70 |
| 4.3 Bending Stiffness Element Testing | 103 |
| 4.4 Stiffener Element Testing | 105 |
| 4.5 Corner Element Testing | 108 |
| 4.6 Bearing Element Testing | 112 |
| 4.7 Flaw Growth Element Testing | 116 |
| 5.0 SHEAR WEB TEST COMPONENT DESIGN AND ANALYSIS | 121 |
| 5.1 Shear Web Test Component Design | 122 |
| 5.2 Shear Web Test Component Analysis | 127 |
| 5.3 Component Test Planning | 146 |
| 6.0 CONCLUSIONS | 149 |
| 7.0 REFERENCES | 150 |
| APPENDIX A - Analyses Used in OPTRAN Code for Vertically Stiffener, Shear Resistant Shear Web | A1 |
| APPENDIX B - Detailed Design Drawings | B1 |
| APPENDIX C - Test Plan for the Shear Web Test Components | C1 |

THIS PAGE INTENTIONALLY LEFT BLANK

LIST OF ILLUSTRATIONS

| <u>Figure Number</u> | | <u>Page</u> |
|--------------------------|--|-------------|
| 1: | Grumman H-33 Orbiter Thrust Structure | 8 |
| 2: | Shear Structure Comparisons - Grumman Orbiters | 9 |
| 3: | Shear Web Structural Requirements | 12 |
| 4: | Material Selection | 14 |
| 5: | Computer Aided Design/Analysis Activities | 16 |
| 6: | OPTRAN Code Flow Chart | 17 |
| 7: | OPTRAN Optimization Strategy (Two Variable Example Problem) | 19 |
| 8: | Design Concept Screening Summary | 21 |
| 9a: | OPTRAN Shear Web Model | 27 |
| 9b: | OPTRAN Shear Web Model | 28 |
| 10: | Shear Web Weight Trades | 29 |
| 11a: | Structural Analysis Data for Baseline | 35 |
| 11b: | Structural Analysis Data for Baseline | 36 |
| 12: | Baseline Nominal Laminate Stiffness Properties | 37 |
| 13a: | B/E Reinforced Shear Web Design Details | 39 |
| 13b: | B/E Reinforced Shear Web Design Details | 40 |
| 13c: | B/E Reinforced Shear Web Design Details | 41 |
| 13d: | B/E Reinforced Shear Web Design Details | 42 |
| 14: | Shear Web Design Cost Comparisons | 47 |
| 15: | Tension Test Elements | 51 |
| 16: | Tension Test Element | 51 |
| 17: | Tension Test Element Lay-Up Arrangements | 52 |
| 18: | Data Used in Optran to Establish Ti-Cladding Reinforcement Requirement | 58 |
| 19: | Shear Webs Tension Element Test Data Comparison | 59 |
| 20: | Strain Gaged Tension Specimen SG-2 | 61 |
| 21: | Strain Gaged Tension Specimen SG-3 | 61 |
| 22: | Strain Gaged Tension Specimen SG-4 | 61 |
| 23: | Hole Strain Gage Locations | 62 |
| 24: | Tension Test Strain/Acoustic Emission Results | 63 |
| 25: | Titanium Clad Boron Composite Test Specimens No. SG-6 (Gage 1 Free Field) | 65 |
| 26: | Titanium Clad Boron Composite Test Specimens No. SG-6 (Gage 3 Hole on Titanium) | 66 |
| 27: | Titanium Clad Boron Composite Test Specimens No. SG-6 (Gage 4 in Hole on B/E) | 67 |
| 28: | Strain Concentration Data Comparisons | 68 |
| 29: | Failed Shear Web Element 1 in Test Frame | 71 |
| 30: | Web Element No. 1 | 72 |
| 31: | Test Web Element No. 1 (Ti-Cladding Chem-milled off) | 73 |
| 32: | Corner A | 74 |
| 33: | Corner B | 75 |
| 34: | Corner C | 76 |
| 35: | Corner D | 77 |

LIST OF ILLUSTRATIONS (Cont.)

| <u>Figure Number</u> | | <u>Page</u> |
|--------------------------|---|-------------|
| 36: | Web Element No. 2 | 79 |
| 37: | X-Ray of Shear Web Element No. 2 After Test | 80 |
| 38: | X-Ray of Shear Web Element at Reaction Corner After Test | 80 |
| 39: | Shear Web Element Test Beam | 81 |
| 40: | Strain Gage Locations | 82 |
| 41: | Principal Strain Data for Web Element 1, Rosette 1 | 83 |
| 42: | Principal Strain Data for Web Element 1, Rosette 2 | 84 |
| 43: | Principal Strain Data for Web Element 1, Rosette 5 | 85 |
| 44: | Principal Strain Data for Web Element 1, Rosette 7 | 86 |
| 45: | Principal Strain Data for Web Element 1, Rosette 8 | 87 |
| 46: | Principal Strain Data for Web Element 1, Rosette 12 | 88 |
| 47: | Strain Gage Locations | 90 |
| 48: | Reinforced Cladding Strain Data Used in Tension Element Data Correlation | 91 |
| 49: | Principal Strain Data for Web Element 2, Rosette 8 | 93 |
| 50: | Principal Strain Data for Web Element 2, Rosette 9 | 94 |
| 51: | Principal Strain Data for Web Element 2, Rosette 12 | 95 |
| 52: | Principal Strain Data for Web Element 2, Rosette 13 | 96 |
| 53: | NASTRAN P Quad Element Model (Half Span Modeled) | 97 |
| 54: | Principal Tension Strain Distribution (Microstrain) | 98 |
| 55: | Principal Compression Strain Distribution (Microstrain) | 99 |
| 56: | Principal Shear Strain Distribution (Microstrain) | 100 |
| 57: | Principal Strain Axis Angle Distribution (Microstrain) | 101 |
| 58: | Bending Element Test Data | 104 |
| 59: | Stiffener Test Element | 106 |
| 60: | Stiffener Element Test Data | 107 |
| 61: | Corner Test Element With and Without Loading plates Attached | 109 |
| 62: | Spliced Step-Lap Detail Element Test Data | 110 |
| 63: | X-Ray of Corner Test Element No. 2 Before Test | 111 |
| 64: | X-Ray of Corner Test Element No. 2 After Testing | 111 |
| 65: | Bearing Test Specimen | 113 |
| 66: | Bearing Element Test Data | 114 |
| 67: | Bearing Test Load-Deflection Data | 115 |
| 68: | Flaw Growth Element Test Data | 117 |
| 69: | Fractograph - Titanium | 118 |
| 70: | Fractograph - B/E Reinforced Titanium | 118 |
| 71: | Test Beam Aluminum Frame Work | 124 |
| 72: | B/E Reinforced Joggled Stiffener | 125 |
| 73: | Test Web Beam Assembly (Without B/E Reinforced Stiffeners) | 126 |
| 74: | NASTRAN Finite Element Model Nodes | 128 |
| 75: | Web Plate Elements (NASTRAN P Quad Elements) | 129 |
| 76: | Beam Elements (C Bar NASTRAN Elements) | 130 |
| 77: | NASTRAN Static Solution Data | 131 |

LIST OF ILLUSTRATIONS (Cont.)

| <u>Figure Number</u> | | <u>Page</u> |
|--------------------------|---|-------------|
| 78: | Principal Tension Strains in Test Web Quadrant 1 | 132 |
| 79: | Principal Tension Strains in Test Web Quadrant 2 | 132 |
| 80: | Principal Tension Strains in Test Web Quadrant 3 | 133 |
| 81: | Principal Tension Strains in Test Web Quadrant 4 | 133 |
| 82: | Principal Compression Strains in Test Web Quadrant 1 | 134 |
| 83: | Principal Compression Strains in Test Web Quadrant 2 | 134 |
| 84: | Principal Compression Strains in Test Web Quadrant 3 | 135 |
| 85: | Principal Compression Strains in Test Web Quadrant 4 | 135 |
| 86: | Principal Shear Strains in Test Web Quadrant 1 | 136 |
| 87: | Principa; Shear Strains in Test Web Quadrant 2 | 136 |
| 88: | Principal Shear Strains in Test Web Quadrant 3 | 137 |
| 89: | Principal Shear Strains in Test Web Quadrant 4 | 137 |
| 90: | Principal Strain Axis Angles in Test Web Quadrant 1 | 138 |
| 91: | Principal Strain Axis Angles in Test Web Quadrant 2 | 138 |
| 92: | Principal Strain Axis Angles in Test Web Quadrant 3 | 139 |
| 93: | Principal Strain Axis Angles in Test Web Quadrant 4 | 139 |
| 94: | NASTRAN Buckling Analysis Correlation | 142 |
| 95: | NASTRAN Buckling Solution for Test Web Component | 143 |
| 96: | NASTRAN Buckling Solution for Test Web Component | 143 |
| 97: | NASTRAN Buckling Solution for Test Web Component | 144 |
| 98: | NASTRAN Buckling Solution for Test Web Component with Debonded Stiffener Reinforcement | 145 |
| 99: | Data Acquisition Requirements for the First Web Component Test | 147 |

LIST OF TABLES

| <u>Table Number</u> | | <u>Page</u> |
|-------------------------|--|-------------|
| 1a: | Optimum Shear Web Design Data Bank | 31 |
| 1b: | Optimum Shear Web Design Data Bank | 32 |
| 2: | Laminate Analysis Data Bank (Baseline - Type Laminate with 0.020 in. Ti-Cladding) | 34 |
| 3: | Tension Element Test Data Coupon Specimens | 53 |

1.0 INTRODUCTION

This report presents the results of Phase I of a program for the development of a practical advanced composite shear web concept which is a candidate for near-term application to primary flight vehicle structure. The program consists of three phases:

- Phase I Shear Web Design Development
- Phase II Shear Web Component Fabrication
- Phase III Shear Web Component structural Testing

The culmination of this work will be the testing of three large scale composite reinforced shear webs which include design details that meet the requirements of a main engine thrust structure application on the Space Shuttle Orbiter.

In the Phase I activities, an integrated design development approach was taken which involved computer-aided design and analysis, detailed design evaluation, testing of unique and critical details, and structural test planning. Particular emphasis was placed on computer-aided design to screen candidate concepts and to establish a rational basis for detailed design. Considerable use was made of the NASTRAN computer code to define structural test requirements. It should also be noted that some aspects of the program drew from previous Boeing and Langley Research Center programs; namely, in the computer-aided design, material selection and step-lap joint design areas.

A unique feature of the program is the development of a metal-clad laminate for the shear web plate: chem-milled titanium-clad $\pm 45^\circ$ boron-epoxy (B/E). While the usual form of selective reinforcement is unidirectional strips, it was necessary to apply $\pm 45^\circ$ B/E reinforcement in laminate form to the developed

shear web concept in order to produce significant weight savings. However, the basic intent contained in the selective reinforcement philosophy has been retained; i.e., use a metal-composite material mix in a structural concept that effectively satisfies the design requirements. The web laminate concept that was selected for development has $\pm 45^\circ$ composite reinforcement clad with thin-gage metal skins. The composite reinforcement serves to reduce weight; the metal cladding provides isotropic bending stiffnesses, local reinforcement at joints and stiffener fastener holes and protection from damaging environments.

2.0 SUMMARY

An advanced composite shear web design concept is being developed for the Space Shuttle orbiter main engine thrust beam structure. The selected application area has high shear loading and beam bending strains with the structure at essentially room temperature, which makes the use of B/E reinforcement advantageous. In addition, the thrust structure has large total weight and is located in an area where weight savings assist in vehicle balancing. The multiple limit loading requirements (engine operation for 100 flight service life) dictates the use of a shear-resistant web design concept. The assumed basic dimensions of the selected center-loaded thrust beam are 40 in. deep by 200 in. span.

Various web design concepts, having both B/E reinforced and all-metal construction, were synthesized by a comprehensive computer-aided adaptive random search procedure. Up to eight dimensional variables (continuous and integer) and three material combinations were treated in optimizing the various web concepts for varying shear and bending load conditions.

As a result of the design concept evaluation study, a practical shear web concept was identified having a titanium-clad $\pm 45^\circ$ B/E web plate with vertical B/E reinforced aluminum stiffeners; the net web weight saving offered is 24% relative to all-metal construction at a cost of \$247 per pound of weight saving. The stiffeners are attached to the web laminate with mechanical fasteners for increased reliability and are joggled in the all-metal end regions for attachment to beam chord members. An important product of the computer-aided synthesis activity is a data bank of optimum designs (which can be expanded for input to large scale vehicle optimization programs).

Design details are presented for the selected B/E reinforced design concept and an all-metal web. Critical details, cost comparisons and reliability considerations for the B/E reinforced design are described. A unique aspect of the design is how the web plate laminate is locally reinforced at stiffener fastener holes and edge step-lap joint details. The titanium is chem-milled leaving thickened lands where reinforcement is required.

Structural element test results substantiate the design details in critical areas. The tension element test data provides a basis for preliminary design allowables for designing reinforced stiffener fastener holes. The tension element data demonstrates that the step-lap joint details are not strength critical. This is also shown by tension tests of corner element specimens which simulate the web laminate corner details.

Two shear web element (18 x 25 in. laminates) tests verify the performance of the basic web laminate details with respect to material strength under cyclic loading. Strains were measured at levels which exceed the baseline design requirements and which show good correlation with finite element strain analysis.

Laminate bending stiffness and stiffener crippling test data show good correlation with computer-code predictions. Fastener bearing tests on laminates with reinforced titanium resulted in bearing strength equivalent to the base titanium metal. Tension testing of laminate specimens with flawed cladding demonstrated that flaw growth does not penetrate into the composite material; noninspectable cladding flaws will not grow critical based on the test results.

A test program is defined to substantiate the performance of large scale (36 by 47 in.) assembled B/E reinforced shear webs in an equivalent design load environment. Three component tests are planned. Detailed designs are presented for the test beam fixture and the initial B/E reinforced web component. Finite element strain and buckling analyses, using the NASTRAN computer code, are employed to define the test web instrumentation requirements. The NASTRAN buckling analysis is correlated with a classical solution for a pure shear simplified orthotropic web model to give confidence to the buckling solutions obtained for the detailed (192 plate elements) finite element test web model. As an assessment of fail-safety, a NASTRAN buckling analysis was conducted that indicates that the test web component is fail-safe at limit load with one stiffener having debonded B/E reinforcement.

THIS PAGE INTENTIONALLY LEFT BLANK

3.0 DESIGN STUDIES

3.1 Component Selection

A review of shear web structure on the candidate Space Shuttle orbiters was performed to identify a component that can significantly benefit from the use of advanced composites. Through the Grumman/Boeing Space Shuttle Study arrangement, the Grumman Aerospace Corporation furnished structural information on their orbiters and loads data from finite element analysis of their H-32 Orbiter configuration.

This data was used to establish the upper main engine thrust structure shear webs, shown in Figure 1, as the component area for development. The selected component area has:

- relatively simple structural interfaces;
- relatively large weight in a location where weight savings assist vehicle balancing;
- the webs are relatively accessible in the assembled vehicle.

The thrust structure consists of double web box beams which span the vehicle connecting to side body longerons and which fasten to beam flanges that are integral with fore and aft bulkheads. An upper beam supports the upper main engine and a lower beam of similar construction supports the two lower engines. Conventionally stiffened, built-up titanium construction was specified for the thrust structure webs⁽¹⁾ and so is adopted in this program as the baseline all-metal web construction for weight comparison purposes.

The Grumman loads data is summarized in Figure 2. The thrust structure webs have the highest loading compared to the other candidate areas. The other

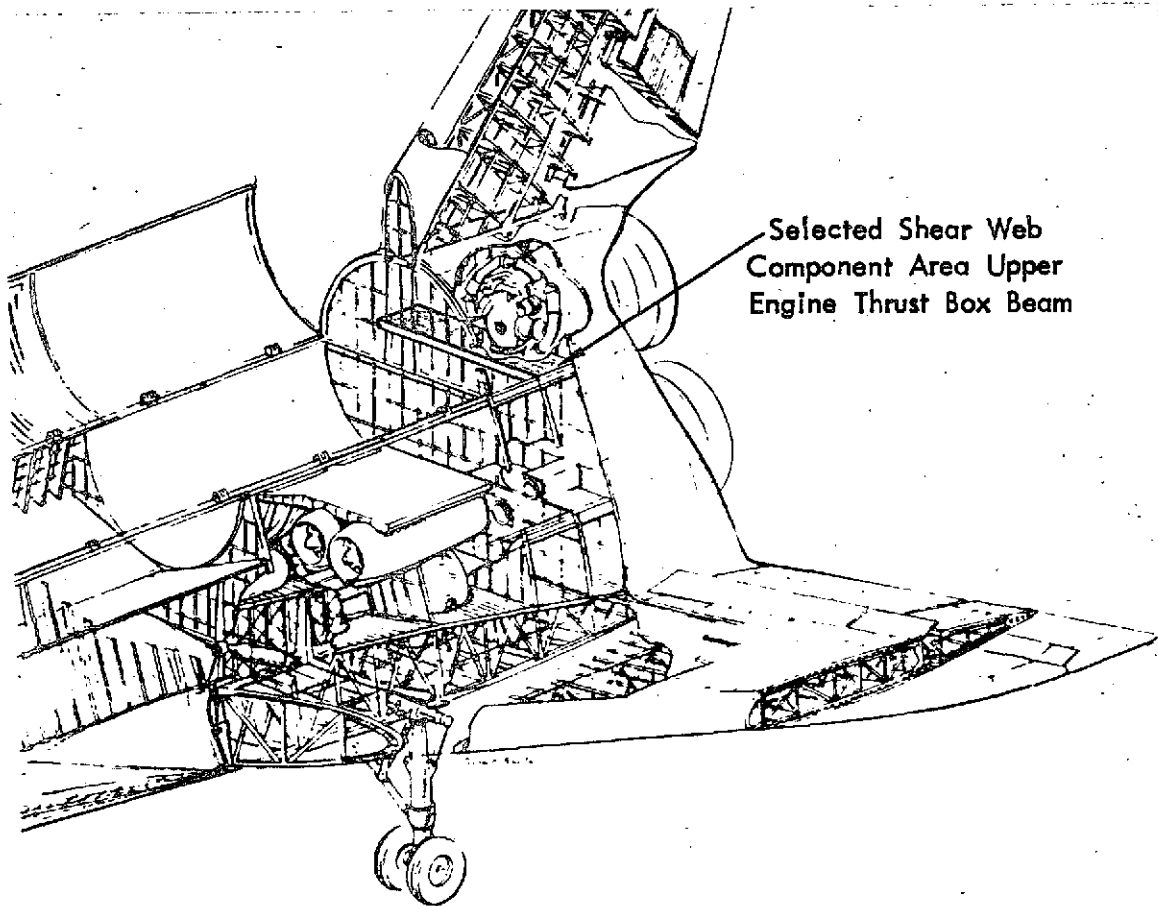
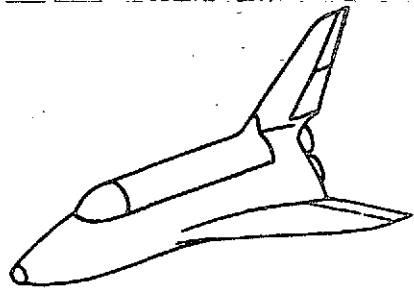
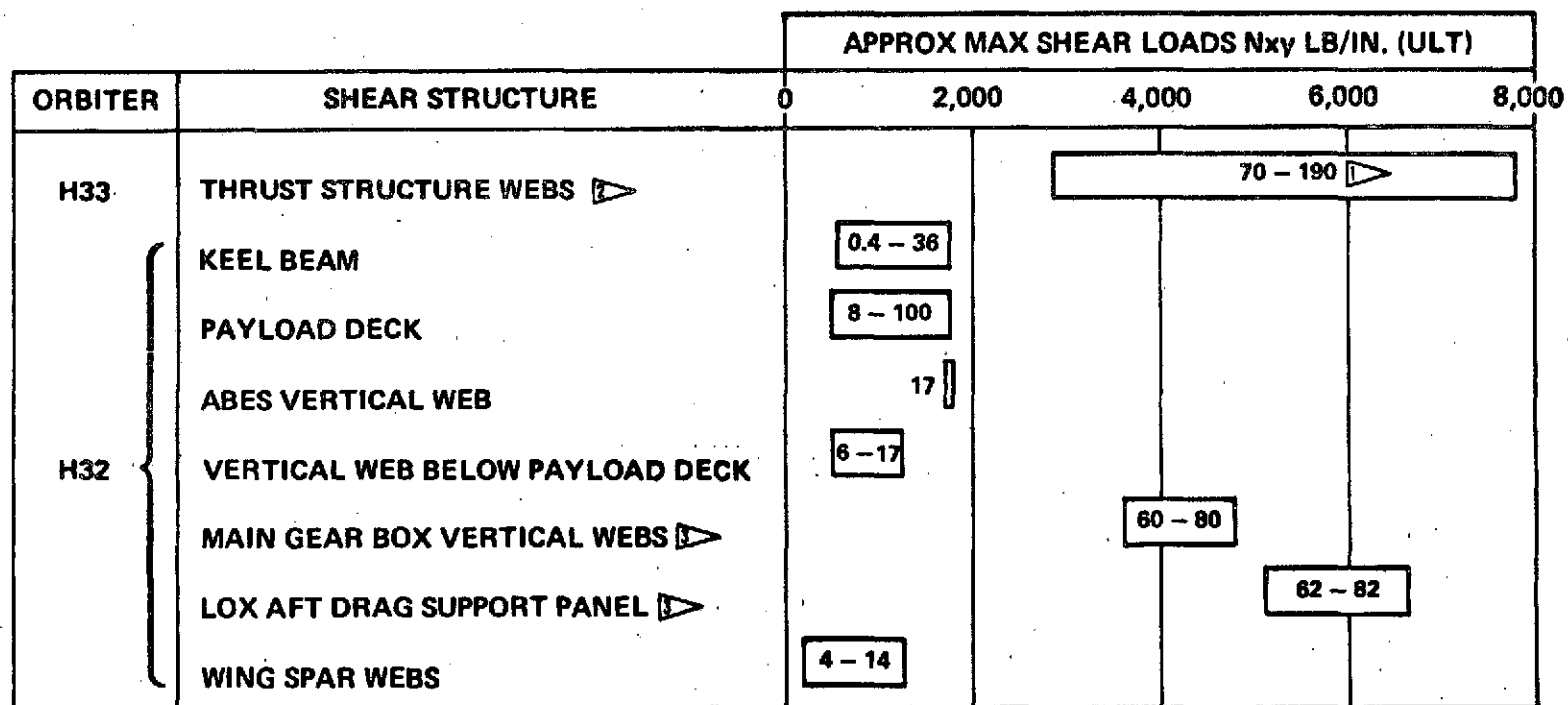


Figure 1: GRUMMAN H-33 ORBITER THRUST STRUCTURE






-  SHEAR STRUCTURAL INDEX N_{xy}/H
-  DOUBLE WEB BOX-TYPE BEAMS
-  COMPLEX LOADED STRUCTURE

Figure 2: SHEAR STRUCTURE COMPARISONS- GRUMMAN ORBITERS

areas shown in Figure 2 are not attractive for advanced composite application because of very light loads or complex configuration. In the lightly loaded areas, minimum gage metal webs or truss-type structure would be more advantageous than advanced composite web structure which is the subject of this program.

3.2 Structural Requirements

Structural requirements were established for the selected thrust beam web from data given in References 1 and 2. Figure 3 presents the general web interfaces and ultimate design load. Since the engine thrust occurs on each flight and is the limit load, the web must be shear buckling resistant to preclude panel fatigue problems in buckled areas. The ultimate design load is based on the following:

550,000 lbs. sea level thrust engine (emergency power level maximum thrust 699,000 lbs.);

Dynamic magnification factor 1.25;

Ultimate factor of safety 1.4.

The environmental conditions that the web design must comply with are:

- Design load occurs with structure at ambient launch pad temperature
- 400 flight life
- -100 to +250°F cyclic temperature excursion on each flight
- 9 hours total acoustic environment (150 db maximum)
- 30 hours total low frequency thrust oscillation environment

In addition to the diaphragm and thrust post structure interfaces shown in Figure 3, the web design concept must be capable of accepting miscellaneous small cutouts in a practical manner without large weight penalty. The web concept must also be resistant to damage from ground handling environments.

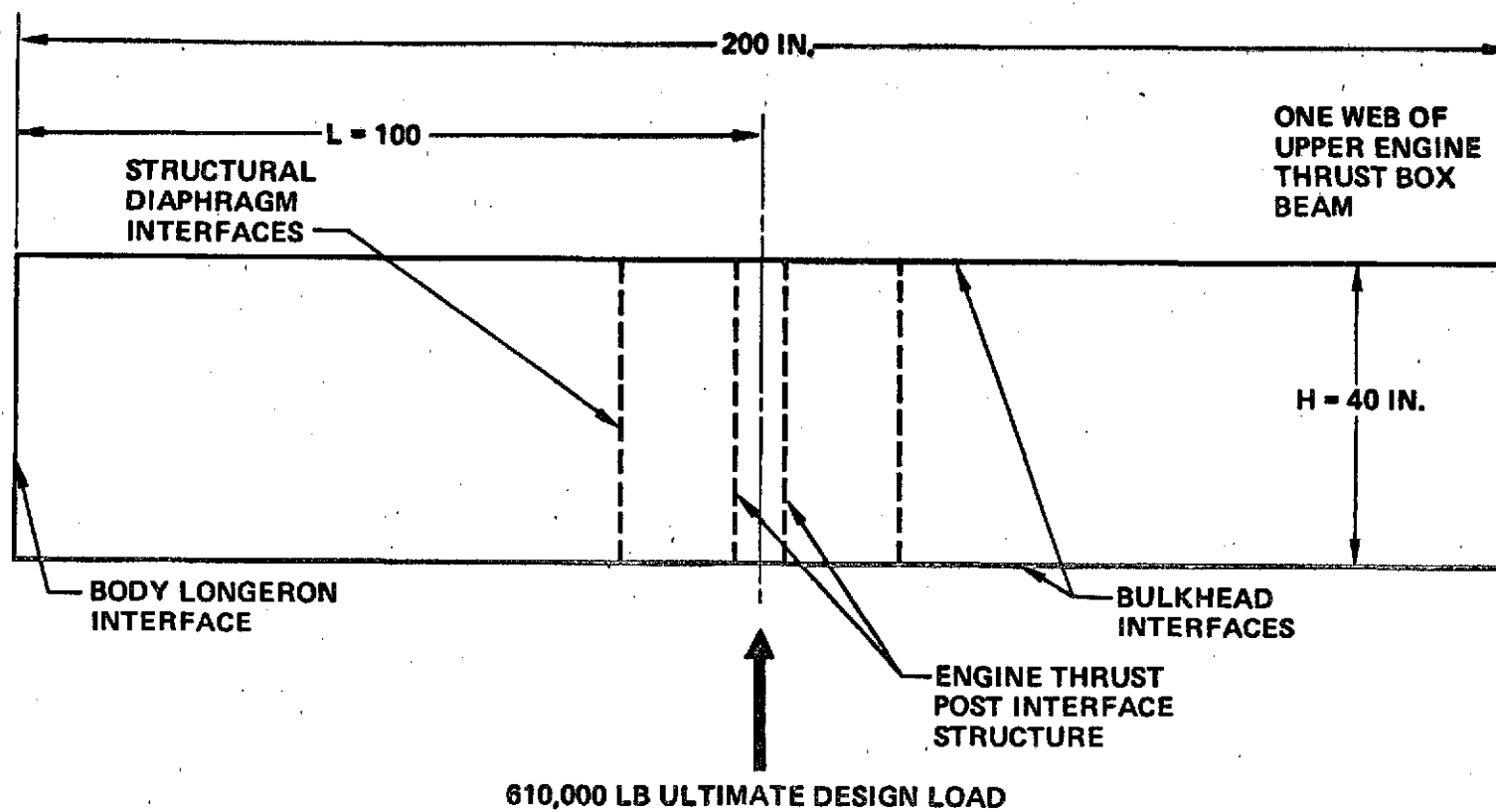


Figure 3: SHEAR WEB STRUCTURAL REQUIREMENTS

3.3 Material Selection

The materials selected for this program satisfy the requirements that (1) sufficient material property and process data exists for design, (2) the materials are commercially available in quantity, and (3) production bonding shop facilities can be used for test article fabrication. The selected materials are shown in Figure 4 and are described in References 3 to 6.

From a structural efficiency point of view, B/E was selected because of its superior strength/density ratios at room temperature compared to graphite-based and other advanced composites, which is important in highly loaded shear web applications. Titanium was chosen over aluminum for laminate material also because of strength/density advantages at room temperature which are amplified by the presence of high residual thermal stresses after curing of aluminum-B/E laminates. Aluminum was adopted for metal stiffener parts based on crippling efficiency factor ($E^{1/3}/\rho$) considerations.

| | |
|--------------------------------------|---|
| ADVANCED COMPOSITE | RIGIDITE 5505/4 BORON/EPOXY PREPREG. TAPE |
| PRIMARY ADHESIVE | METLBOND 329 |
| WEB LAMINATE METAL PARTS | 6 AL-4V M.A. TITANIUM |
| TITANIUM BOND SURFACE PREPARATION | FACE SHEETS - PHOSPHATE FLOURIDE COATING PROCESS STEP-LAP DETAILS & TEST SPECIMENS - VACU-BLAST & SILANE RINSE ALL - 3M EC 2333 PRIMER |
| METAL STIFFENER PARTS | 7075-T6 ALUMINUM (EXTRUSIONS FORMED IN THE O CONDITION) |
| SECONDARY ADHESIVE | MODERATE TEMPERATURE CURING EPOXY BMS 5-51 FOR LOW STRESSED STIFFENER ASSEMBLY |

Figure 4: MATERIAL SELECTIONS

3.4 Computer-Aided Design Concept Screening Study

A computer-aided synthesis approach allowed screening of optimum designs of several B/E reinforced and comparative all-metal shear web concepts. The screening study is integrated in the general study approach as shown in Figure 5. The concepts were divided into two categories; statically determinate and indeterminate models under combined beam bending and shear loading. A multi-variable optimization code technique could be applied to the statically determinate models while a manual iteration technique, using NASTRAN stress analysis data, was necessary for the one indeterminate model that was treated.

The multivariable design optimization activity was accomplished using the OPTRAN computer code (OPTimization by RANdom search algorithm) which employs an adaptive random search algorithm. Figure 6 presents the operational features of the OPTRAN code. A specialized OPTRAN code was constructed for each specific shear web concept that was studied by addition of appropriate code modules for weight, constitutive stiffness, and failure mode analyses. OPTRAN establishes candidate designs by random selection of dimensional variable values from input search ranges, which can specify minimum gages, and then checks for weight savings relative to the best preceding design. If the candidate design offers weight savings, then the failure mode constraints are checked in succession. A design that makes it through all of the failure mode checks then becomes the best current design. However, if a violation of a failure mode constraint occurs, a new random design is established without wasting time on further failure mode checks. Ordering of the analyses, so that active constraints are treated first, decreases run time. After a certain number of good designs have been found, the parameter search ranges are squeezed down in a manner that is adaptive to the history

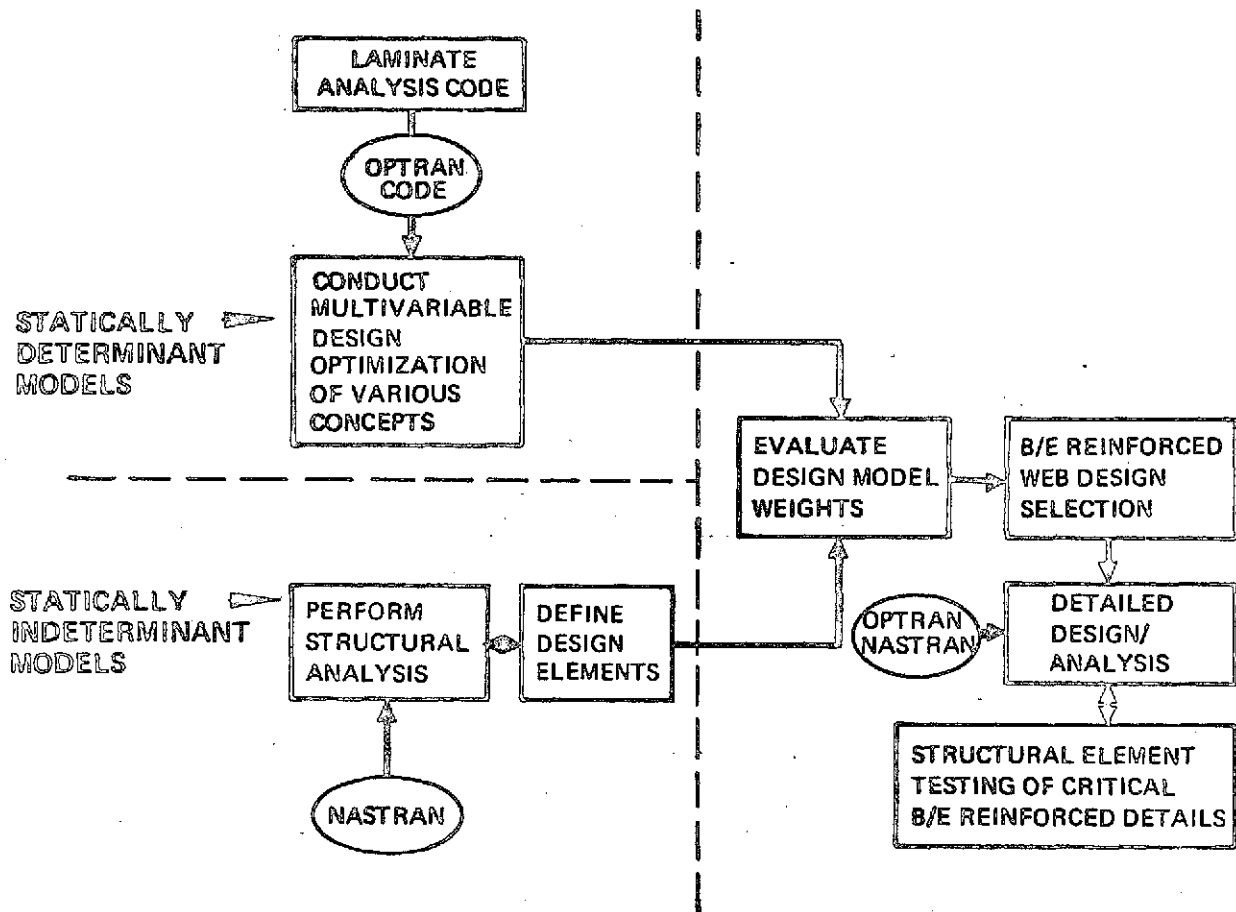


Figure 5: COMPUTER-AIDED DESIGN/ANALYSIS ACTIVITIES

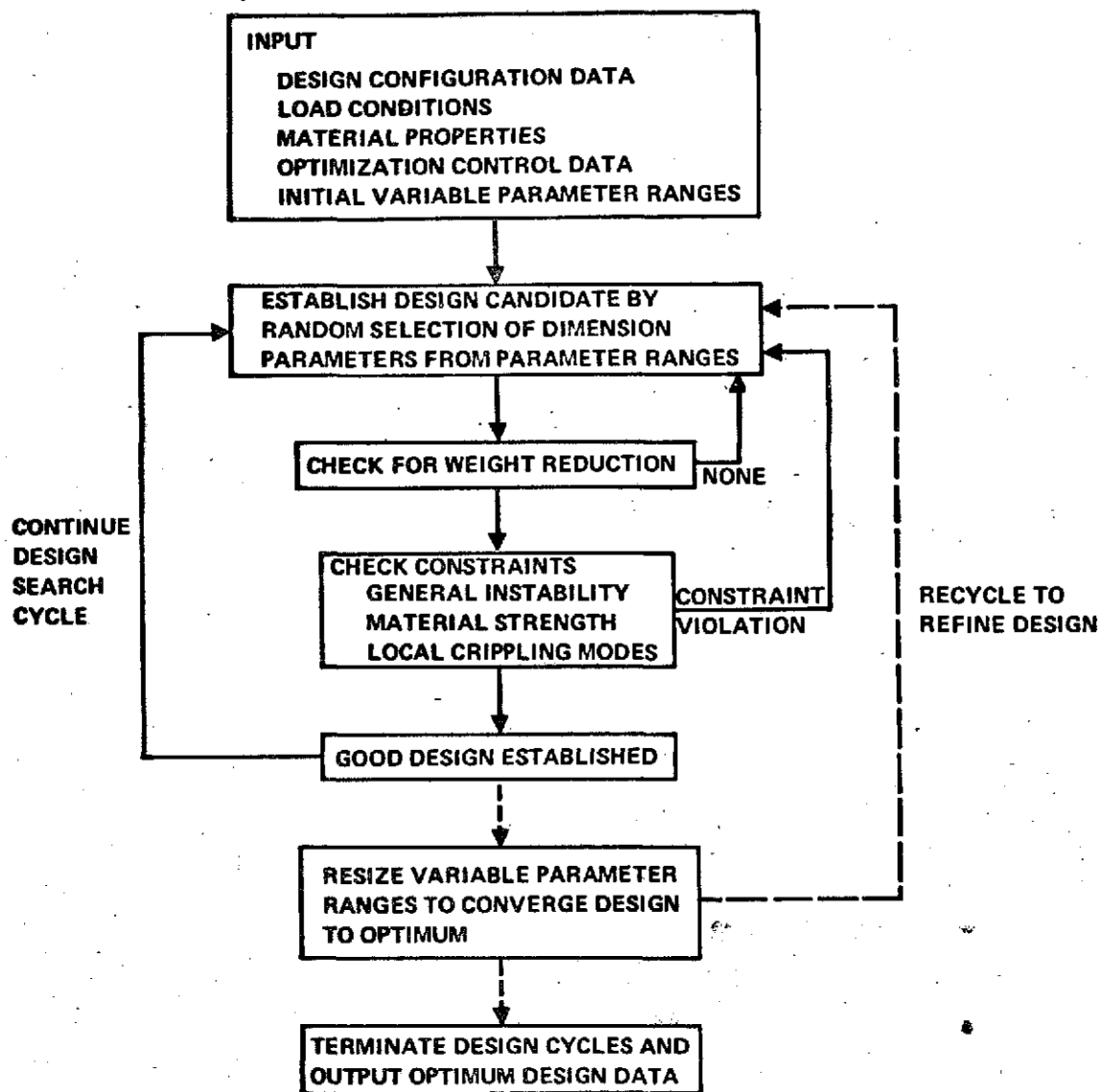


Figure 6: OPTRAN CODE FLOW CHART

of the best previous designs and then another search cycle is conducted. If one variable shows greater variation from cycle to cycle, its range is made broader to increase the probability of directing the design to a true minimum. Experience has shown that trapping of the process at a nonglobal minimum is avoided by seeking a large number of good designs (say 5) in the first search cycle. The search cycles are terminated after the search ranges converge to a desired minimum size. The use of discrete variables (standard structural sections, number of composite laminate plies, etc.) presents no difficulties in this search method.

The optimization strategy coded in OPTRAN is illustrated in Figure 7 by a simplified two variable design optimization problem having linear weight characteristics. The feasible design space at the beginning of the first cycle consists of the unshaded area which contains all possible configurations that do not violate any constraints. The point 1 represents the values of the design parameters x_1 and x_2 constituting the best design found during the first cycle. The feasible design space for the second cycle is established by applying an arbitrary factor to the input search ranges. For following cycles, the boundaries are established as a function (subject to an arbitrary minimum band width) of the variations of x_1 and x_2 for successive best designs found during the preceding two cycles. The current best weight forms an upper boundary to the new feasible design space because each new best design must show a decrease in weight. The optimum minimum weight design, point n, is the best design from the final cycle and is bounded by the two constraint functions, $g_1 = 0$ and $g_2 = 0$. The third constraint function does not govern the final design, although it might have been encountered during previous cycles.

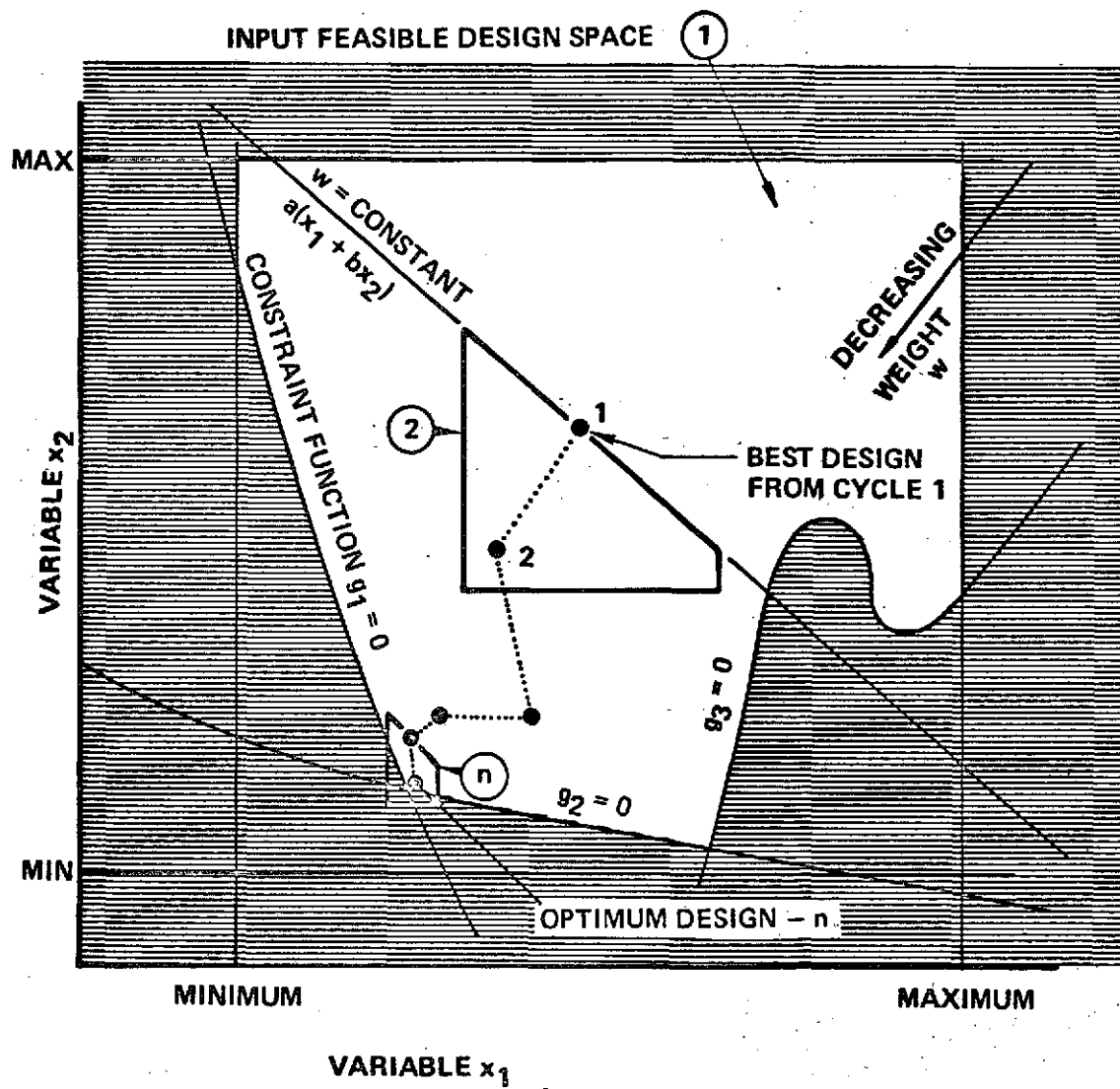


Figure 7: OPTRAN OPTIMIZATION STRATEGY
(TWO VARIABLE EXAMPLE PROBLEM)

A summary of the basic design concept candidates that were evaluated in the screening study is given in Figure 8. The first concept is an extension of conventional, vertically stiffened construction. The diagonally stiffened web explored the benefits of inclined stiffening in a one-way loaded shear web situation. With the largest part of the total weight being in the web plate, both of the above concepts required B/E reinforcement of the web plate to produce significant overall weight savings. The corrugated web is inherently an efficient metal concept and requires a relatively small amount of B/E reinforcement to improve its efficiency; however, it is a concept that requires manufacturing development for application to highly loaded shear web structure and would be costly to fabricate. The sandwich concept was derived from the brazed titanium sandwich developments in the Boeing Supersonic Transport Program. The B/E reinforced brazed sandwich is nominally efficient and overcomes the drawbacks of adhesively bonded sandwich construction in primary structure applications; however, it is also a concept that is expensive to fabricate.

The B/E reinforced web concept that was selected for development is the first concept in Figure 8: the vertically stiffened B/E reinforced titanium web configuration. This configuration was selected because of the following factors:

- Low web weight
- Low potential weight penalties in the final detailed design
- The design concept is statically determinate which simplifies design and analysis
- The design can accept loading reversal (important to other shear web applications)


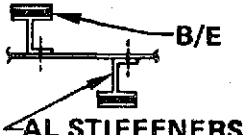


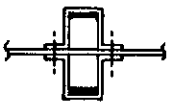




| CONFIGURATION | B/E STIFFENING REINFORCEMENT | WEB PLATE SECTIONS | NOMINAL WEB WEIGHT (LB/LIN FT) | RELATIVE DEVELOPMENT, FABRICATION COST |
|--|---|--|--------------------------------|--|
| VERTICALLY STIFFENED WEB  | ALTERNATING J  | TI-CLAD $\pm 45^\circ$ B/E  CLADDING REINF AT STIFFENERS | 10.6 | LOW |
| DIAGONALLY STIFFENED WEB  | BALANCED HAT  | TI-CLAD $\pm 45^\circ$ B/E | 11.0 | LOW |
| CORRUGATED WEB  |  | TITANIUM | 10.4 | HIGH |
| SANDWICH WEB  | NONE | TI-CLAD $\pm 45^\circ$ B/E FACES  ALUMINUM BRAZED TI HONEYCOMB SANDWICH | 9.3 | HIGH |

Figure 8: DESIGN CONCEPT SCREENING SUMMARY

- The titanium cladding can be reinforced at the web's edges to produce, together with titanium step-lap joint details, metal edge joints that can be mechanically fastened and that are not strength critical in the B/E transition areas
- Cutouts can be accomplished with simple titanium reinforcement inserts (with step-lap B/E transition details), reinforced cladding thickness and fastened reinforcement collars
- The development/fabrication cost is low relative to the more complex advanced composite concepts.

The remaining discussion in this subsection briefly describes the approaches and assumptions made in the computer-aided synthesis of the candidate web concepts.

The primary constraints that were applied to the concepts are the B/E lay-up configuration selection, placement of metal in the web laminates and minimum material thicknesses. Because of the dominance of the high shear loading in all areas of the web structure, a constant thickness $\pm 45^\circ$ B/E lay-up was selected as an efficient lay-up which is practical to fabricate in conjunction with step-lap edge joint details (except for the corrugated web which was constrained to have unidirectional reinforcement because of fabrication problems associated with other lay-ups). An analysis was conducted of the option where the metal is located at the middle surface of the first concept in Figure 8. The analysis indicated that the critical local orthotropic panel buckling load is reduced by 40%. Therefore, the placement of the metal parts of the laminate on the exterior promotes an optimum design condition in shear web structure while affording protection to the laminate. A titanium thickness of 0.020 in. was established as a practical minimum in normal fabrication conditions; this

constraint governed all of the clad-laminate cases. In areas of stiffener fastener holes, the titanium thickness was set to 0.050 in a 1.0 in. wide land to provide local reinforcement. Other minimum constraints considered include 0.090 in. J-stiffener gage, 0.040 in. hat stiffener gage and 4.9 lb/ft^3 titanium honeycomb core.

Optimum designs were synthesized using OPTRAN for the 40 in. web depth and load requirements shown in Figure 3; a uniform strain of $\pm 4000 \text{ } \mu\text{in/in}$ was assumed at the beam chords to account for beam bending effects on the web weight. All structural dimensions and gages were treated as continuous variables in the optimizations with the exception of stiffener metal gages and honeycomb core which were fixed. For example, the vertically stiffened web and the corrugated web both have 5 variables. The laminate properties required for structural analyses were obtained from input tables of stiffnesses relative to properties for equal thickness titanium and were determined from separate classical analysis (7) of laminates having discrete titanium cladding and adhesive plies.

The design weights shown in Figure 8 are OPTRAN results except for the statically indeterminate diagonally stiffened web which was manually iterated using NASTRAN stress analysis data. The stiffened webs have weight allowances included for titanium lands at stiffener holes. None of the weights have allowances for edge details or fasteners. Honeycomb braze material and laminate adhesive ply weight allowances were made. Because the computer-aided synthesis approach involves considerable idealization, detail design weight increases are expected with all of the concepts; the highest increases are anticipated with the corrugated and the sandwich webs.

Analysis of stresses and strains in the Ti-clad B/E web plate parts was accomplished using classical laminate analysis. A maximum filament strain criteria was applied to the composite parts and the von Mises yield criterion was used to evaluate the stress margin of safety in the titanium. The material design allowables that governed are given in Appendix A. The important instability failure modes that were analyzed are summarized below:

- Diagonally-stiffened web
 - stiffener column-type buckling⁽⁹⁾
 - stiffener side crippling⁽⁹⁾
 - local panel buckling under combined loads⁽⁹⁾
- Corrugated web
 - general instability⁽¹⁰⁾
 - local isotropic and orthotropic panel buckling⁽¹⁰⁾
- Sandwich web
 - general instability under combined shear and bending loads⁽³⁾
 - intracell face buckling⁽¹¹⁾
 - intercell face buckling⁽¹²⁾
- Vertically stiffened web
 - metal yielding⁽⁸⁾
 - composite strain
 - local panel instability^(18,23)
 - general instability^(10,18)

Because of the nearly isotropic bending stiffness properties possessed by the metal-clad laminates, isotropic plate buckling theory was used for conservative local panel buckling analysis. Simple edge supports were assumed, with no

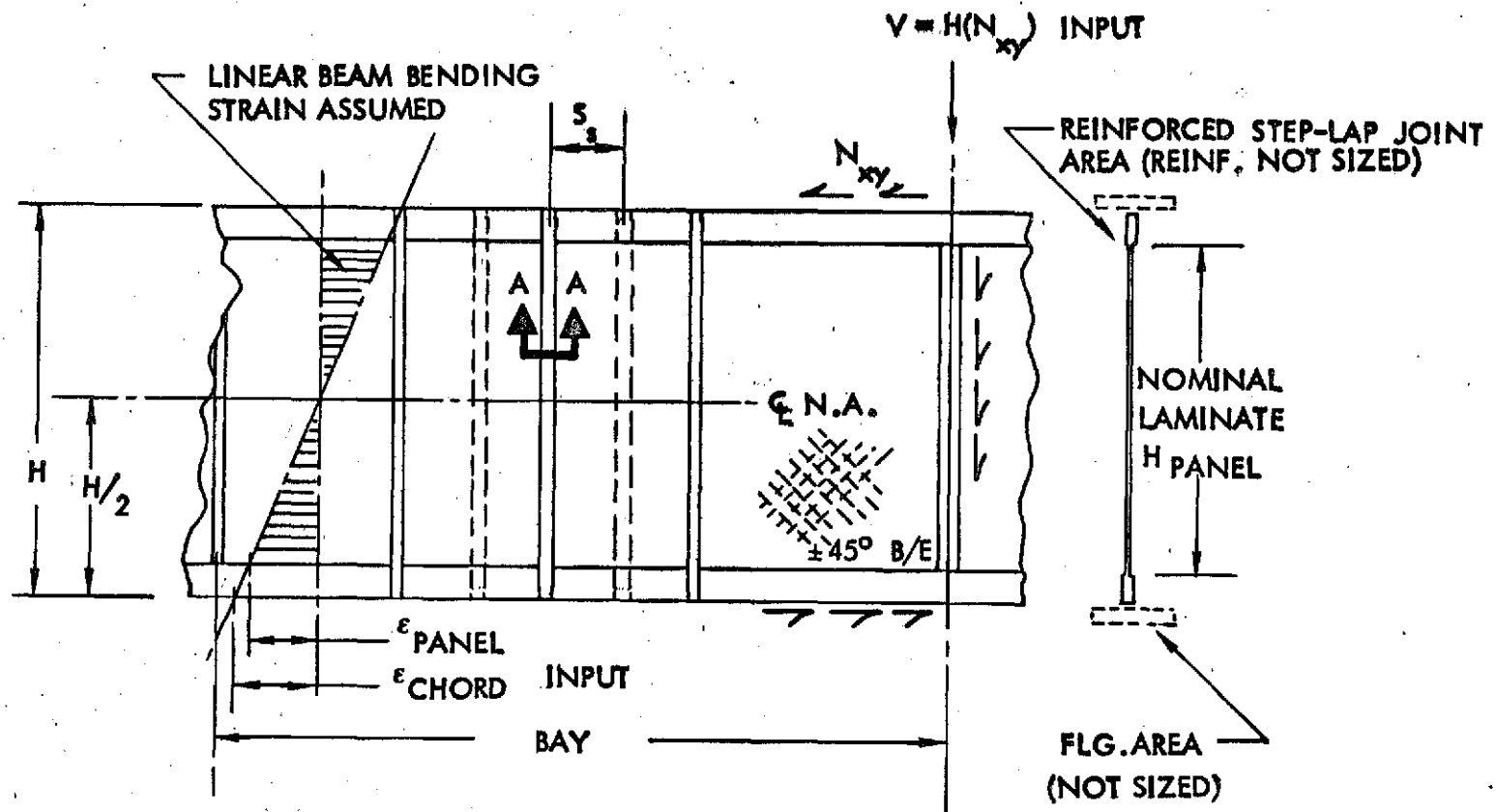
allowance for edge reinforcements, in all buckling analyses. Where combined normal and shear in-plane loads were considered, a load interaction relation of the form given in Appendix A was used (squared-type).

The buckling failure modes were constrained in the OPTRAN runs to be equal to or greater than ultimate design loadings. This constraint enforces the designs to have shear resistant behavior and yields lower-bound optimum structure weights. While it is recognized that nonlinear buckling response can occur because of initial imperfections or out-of-plane secondary loads, suitable rational "knock down" factors or rapidly executable analysis methods are not currently available in the literature for incorporation of nonlinear response in a structural synthesis code. Therefore, the approach taken in the Phase I design studies is to employ classical buckling analyses in the OPTRAN coding and then improve the buckling constraint analyses based on the results of the component tests in Phase III. The initial weight trades obtained in this manner are believed to be realistic on a relative weight basis. The design synthesis approach is also believed to define designs that are close to true optimum weight and shear resistant for loads above limit design loads.

3.5 Computer-Aided Detailed Design Definition

Having selected the baseline B/E reinforced web concept, the OPTRAN code for this concept was refined to include the discrete web laminate variables shown in Figures 9a and 9b. The discrete ply variable is chosen to be number of ply-sets having 8 $\pm 45^\circ$ B/E plies; this ply set configuration selection is based on fabrication considerations given in Section 3.6. Also, allowances were made for differences in local nominal laminate panel depth and the overall web depth defined by the beam flange area separation; these allowances result in calculation of correct beam bending loads for local panel strength analysis and general instability analysis. A constant nominal thickness, as treated in the screening studies, was maintained in order to simplify structural analysis and fabrication. The structural analyses that pertain to the OPTRAN model presented in Figures 9a and 9b are given in Appendix A. Structural dimensions that are treated as constants are shown with their respective assumed values. The results from OPTRAN weight trades for this model provide a definition for detailed design of the baseline B/E reinforced web and a comparative all-metal web.

Idealized OPTRAN weight versus load trades are shown in Figure 10 for the baseline B/E reinforced design concept and the baseline titanium shear resistant web concept having aluminum stiffeners. The definition of nominal weight is given in Appendix A. The trades were generated by starting the OPTRAN cases at high shear load and incrementing the load downward as successive optimum designs were found. (The optimum weight for a case was treated as a weight constraint for the following case. Also, convergence was aided by conducting a global search cycle only on the first high load case.) The optimum baseline titanium web designs were obtained by considering the special case of zero web



TOTAL NUMBER OF VARIABLES = 6 ($S_s, H_s, T_{sr}, T_{cl}, T_{clr}, T_{co}$)

Figure 9a: OPTRAN SHEAR WEB MODEL

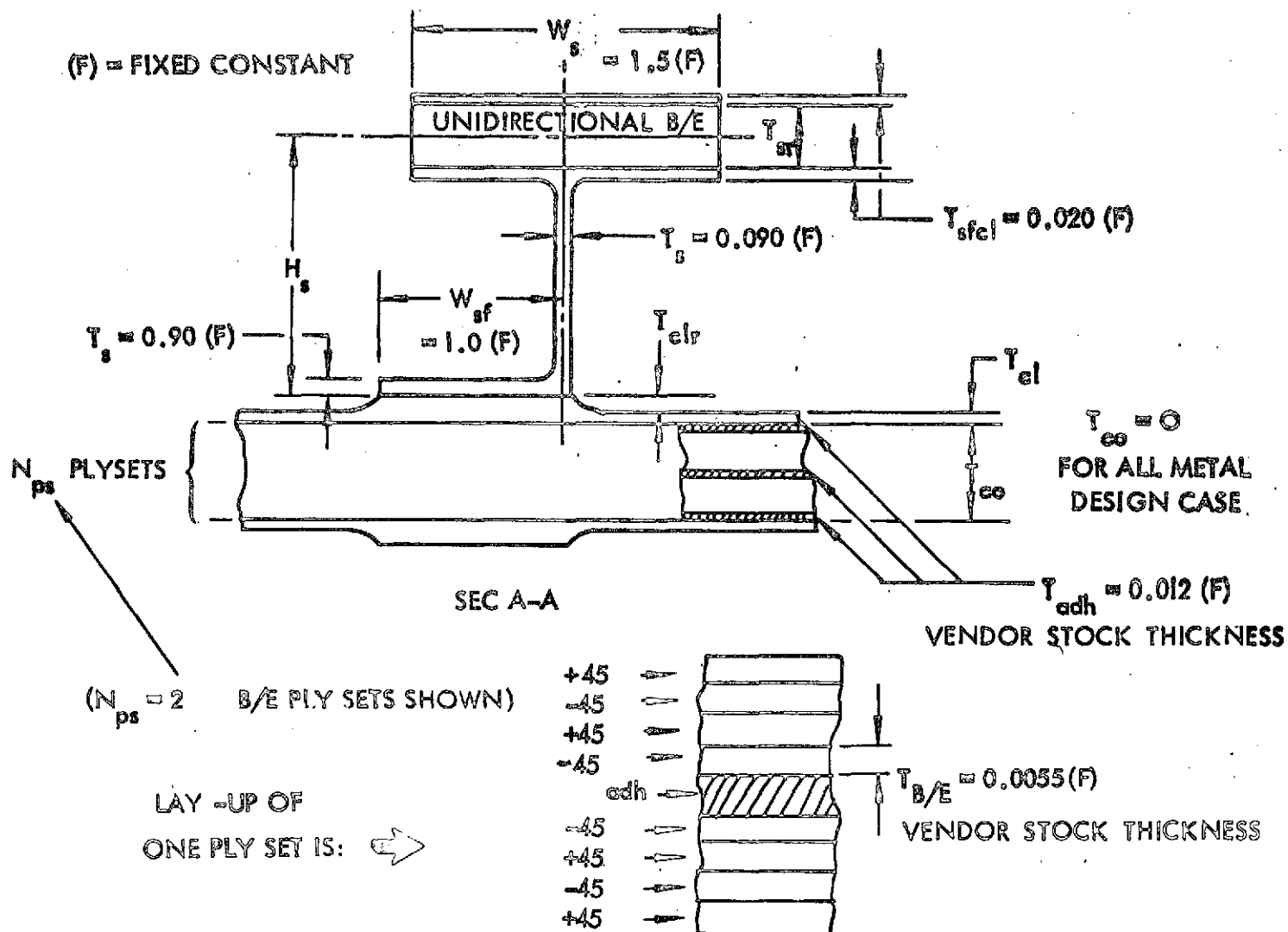


Figure 9b - OPTRAN SHEAR WEB MODEL

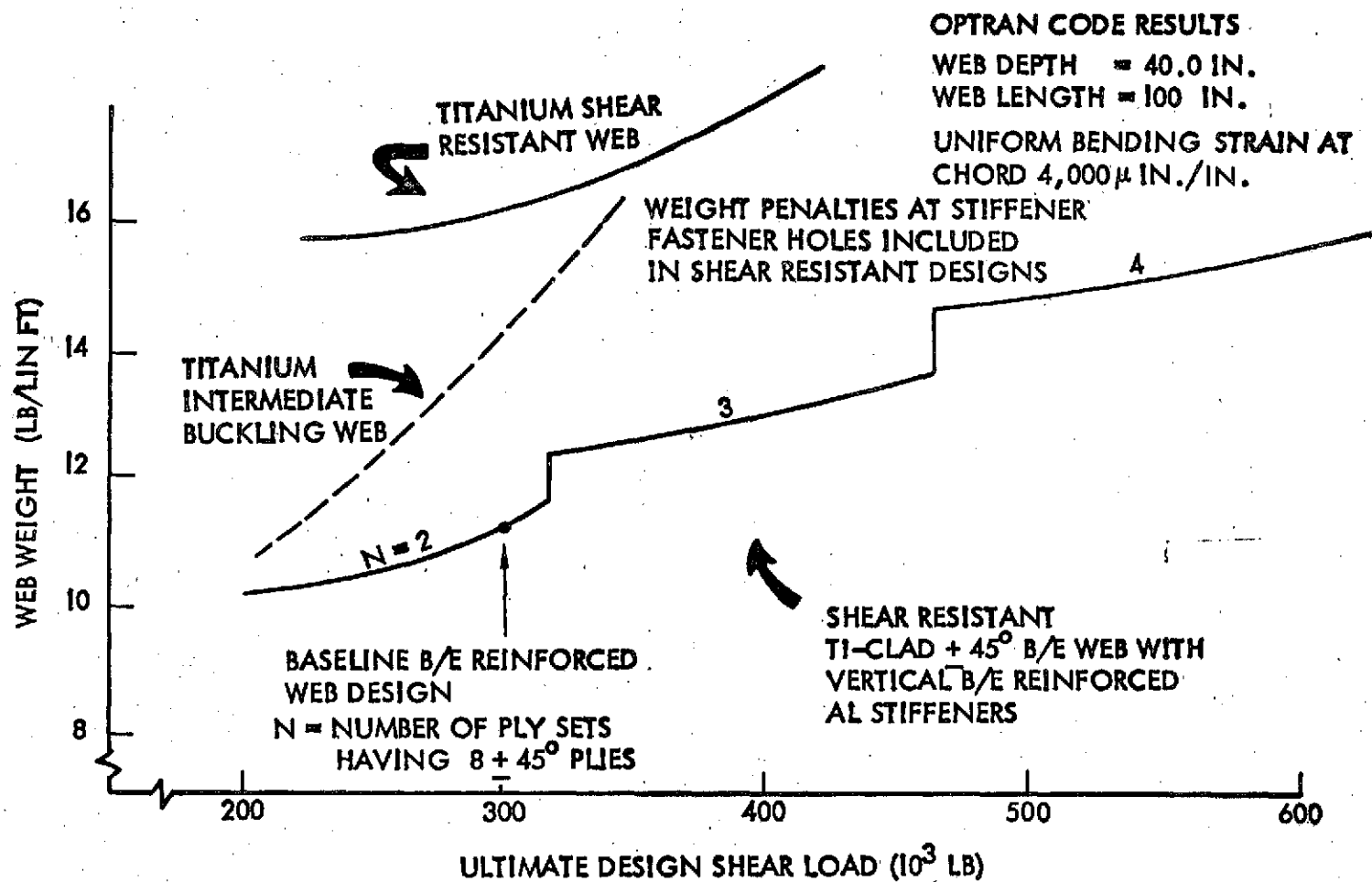


Figure 10 : SHEAR WEB WEIGHT TRADES

plate composite thickness and replacement of B/E stiffener flange reinforcement with aluminum material.

Titanium intermediate buckling web designs are also represented in Figure 10 for weight comparison purposes and were generated by an OPTRAN code utilizing the analysis methods presented in Reference 13. (The intermediate buckling web has single T-type stiffeners, 1.16 in² area, at 20.7 in. spacing with a 0.135 in. web gage at the ultimate design shear load of 305000 lb.)

The idealized weight saving indicated by Figure 10 is 31% for the B/E reinforced web relative to the baseline titanium shear resistant web at the ultimate design shear load requirement of 305000 lb. This weight saving increases with increasing load. The discontinuous plot for the B/E reinforced web reflects the changes in the optimum value for the discrete ply set variable defined in Figure 9.

The data generated in the weight trade OPTRAN runs are tabulated in Table 1. This data, together with tables of stiffness, constitutes a design data bank for the specific design conditions shown in the table. The special baseline B/E reinforced and all-metal web design cases are cases 14 and 20, respectively. It is noteworthy that three failure modes out of a possible five governed the baseline B/E reinforced design and that B/E ultimate strain is not a critical failure mode. In all cases, the assumed minimum stiffener gage ($T_s = 0.090$ in.) exceeds the design constraint given in Appendix A.

Data banks such as Table 1 which include additional load cases and configurations can be incorporated in large finite element structural system optimization codes such as described in References 14 and 15. The system optimization codes would

Table 1a: OPTIMUM SHEAR WEB DESIGN DATA BANK

OPTRAN RESULTS FOR SHEAR RESISTANT DESIGN CRITERIA

H = 40.0 IN BAY = 100.0

MATERIALS:

LAMINATE CLADDING

LAMINATE COMPOSITE

STIFFENER METAL PARTS

STIFFENER REINFORCEMENT

6AL - 4V M.A. TITANIUM

$\pm 45^\circ$ B/E 0.0055 IN. PLIES

0.012 IN ADHESIVE FILLER PLIES

7075-T6 ALUMINUM

0° B/E

NOTES:

CASE 14 IS THE
BASE LINE B/E
REINFORCED
WEB DESIGN

CASE 20 IS THE ALL-METAL
BASELINE DESIGN CASE

| CASE | V _{ULT} LB | ϵ_{CHORD} $\mu\epsilon$ | WT LB/LIN FT | MARGINS OF SAFETY | | | | |
|------|------------------------|-------------------------------------|-----------------|----------------------|---------------------|-------------------|------------------------|--|
| | | | | CLADDING YIELDING | COMPOSITE STRAIN | PANEL BUCKLING | GENERAL INSTABILITY | FAILURE AT STIFFENER FASTENER HOLES |
| 1 | 630000 | 0.0040 | 15.6939 | 0.0804 | 0.1072 | 0.0000 | 0.0020 | 0.0000 |
| 2 | 605000 | 0.0040 | 15.5202 | 0.1159 | 0.1481 | 0.0000 | 0.0001 | 0.0000 |
| 3 | 580000 | 0.0040 | 15.3725 | 0.1534 | 0.1921 | 0.0000 | 0.0000 | 0.0000 |
| 4 | 555000 | 0.0040 | 15.2252 | 0.1931 | 0.2399 | 0.0002 | 0.0001 | 0.0000 |
| 5 | 530000 | 0.0040 | 15.0819 | 0.2352 | 0.2914 | 0.0000 | 0.0002 | 0.0000 |
| 6 | 505000 | 0.0040 | 14.9420 | 0.2798 | 0.3474 | 0.0001 | 0.0001 | 0.0000 |
| 7 | 480000 | 0.0040 | 14.8037 | 0.3271 | 0.4085 | 0.0000 | 0.0001 | 0.0001 |
| 8 | 455000 | 0.0040 | 13.3532 | 0.1614 | 0.1879 | 0.0002 | 0.0000 | 0.0000 |
| 9 | 430000 | 0.0040 | 13.1833 | 0.2130 | 0.2484 | 0.0000 | 0.0003 | 0.0001 |
| 10 | 405000 | 0.0040 | 12.9804 | 0.2685 | 0.3155 | 0.0000 | 0.0001 | 0.0000 |
| 11 | 380000 | 0.0040 | 12.8541 | 0.3284 | 0.3902 | 0.0000 | 0.0002 | 0.0001 |
| 12 | 355000 | 0.0040 | 12.6241 | 0.3929 | 0.4738 | 0.0001 | 0.0001 | 0.0001 |
| 13 | 330000 | 0.0040 | 12.4518 | 0.4623 | 0.5678 | 0.0002 | 0.0004 | 0.0000 |
| 14 | 305000 | 0.0040 | 11.2044 | 0.2479 | 0.2656 | 0.0001 | 0.0001 | 0.0001 |
| 15 | 280000 | 0.0040 | 10.9380 | 0.3291 | 0.3618 | 0.0001 | 0.0003 | 0.0001 |
| 16 | 255000 | 0.0040 | 10.6918 | 0.4192 | 0.4735 | 0.0003 | 0.0000 | 0.0001 |
| 17 | 230000 | 0.0040 | 10.4536 | 0.5190 | 0.6056 | 0.0001 | 0.0002 | 0.0000 |
| 18 | 205000 | 0.0040 | 10.2287 | 0.6291 | 0.7637 | 0.0000 | 0.0002 | 0.0001 |
| 19 | 180000 | 0.0040 | 10.0713 | 0.7496 | 0.9557 | 0.0000 | 0.0001 | 0.0880 |
| 20 | 305000 | 0.0040 | 16.2891 | 0.0786 | - | 0.0000 | 0.0000 | - |

Table 1b

| CASE | COMPOSITE THICKNESS T_{CO} in. | NET B/E THICKNESS T_{CN} | CLADDING THICKNESS T_{CL} | STIFFENER HEIGHT H_S | STIFFENER GAGE T_S | STIFFENER REINFORCEMENT THICKNESS T_{SR} | STIFFENER SPACING S_S | CLADDING REINFORCEMENT THICKNESS T_{CLR} |
|------|---|----------------------------------|-----------------------------------|------------------------------|----------------------------|---|-------------------------------|---|
| 1 | 0.2840 | 0.1760 | 0.0200 | 2.3065 | 0.0900 | 0.0562 | 9.5401 | 0.072 |
| 2 | 0.2840 | 0.1760 | 0.0200 | 1.9933 | 0.0900 | 0.0753 | 9.7314 | 0.0673 |
| 3 | 0.2840 | 0.1760 | 0.0200 | 1.9002 | 0.0900 | 0.0806 | 9.9337 | 0.0627 |
| 4 | 0.2840 | 0.1760 | 0.0200 | 1.9008 | 0.0900 | 0.0773 | 10.1473 | 0.0581 |
| 5 | 0.2840 | 0.1760 | 0.0200 | 1.9964 | 0.0900 | 0.0663 | 10.3745 | 0.0535 |
| 6 | 0.2840 | 0.1760 | 0.0200 | 1.7965 | 0.0900 | 0.0800 | 10.6149 | 0.0489 |
| 7 | 0.2840 | 0.1760 | 0.0200 | 1.7652 | 0.0900 | 0.0792 | 10.8711 | 0.0444 |
| 8 | 0.2160 | 0.1320 | 0.0200 | 1.8354 | 0.0900 | 0.0671 | 8.0447 | 0.0464 |
| 9 | 0.2160 | 0.1320 | 0.0200 | 1.6026 | 0.0900 | 0.0862 | 8.2580 | 0.0418 |
| 10 | 0.2160 | 0.1320 | 0.0200 | 1.8328 | 0.0900 | 0.0604 | 8.4865 | 0.0372 |
| 11 | 0.2160 | 0.1320 | 0.0200 | 1.4148 | 0.0900 | 0.1007 | 8.7327 | 0.0326 |
| 12 | 0.2160 | 0.1320 | 0.0200 | 1.6624 | 0.0900 | 0.0669 | 8.9975 | 0.0281 |
| 13 | 0.2160 | 0.1320 | 0.0200 | 1.7434 | 0.0900 | 0.0558 | 9.2825 | 0.0236 |
| 14 | 0.1480 | 0.0880 | 0.0200 | 1.7412 | 0.0900 | 0.0511 | 6.3800 | 0.0253 |
| 15 | 0.1480 | 0.0880 | 0.0200 | 1.6583 | 0.0900 | 0.0526 | 6.6135 | 0.0207 |
| 16 | 0.1480 | 0.0880 | 0.0200 | 1.5391 | 0.0900 | 0.0582 | 6.8702 | 0.0162 |
| 17 | 0.1480 | 0.0880 | 0.0200 | 1.5949 | 0.0900 | 0.0488 | 7.1525 | 0.0117 |
| 18 | 0.1480 | 0.0880 | 0.0200 | 1.4089 | 0.0900 | 0.0600 | 7.4614 | 0.0072 |
| 19 | 0.1480 | 0.0880 | 0.0200 | 1.4291 | 0.0900 | 0.0519 | 7.7977 | 0.0064 |
| 20 | 0 | 0 | 0.0676 | 2.4838 | 0.0900 | 0.1291 | 5.0000 | 0.0185 |

then enter the data banks to establish an interpolated, approximately optimum element designs as required for optimization iteration of the system finite element model.

Table 2 presents the web laminate properties associated with the optimum B/E reinforced web cases having 2, 3 and 4 ply sets and other future cases having up to 10 ply sets.

Structural analysis data that was computed by OPTRAN for the baseline B/E reinforced web design case 14 are given in Figures 11 (a and b) and 12. The nomenclature and analyses related to this data may be found in Appendix A. It should be noted that the total weight figure is higher than obtained in the screening study (Figure 8) due to additional allowance for adhesive ply weight penalties.

Table 2: LAMINATE ANALYSIS DATA BANK (BASELINE-TYPE LAMINATE WITH 0.020 IN. TI-CLADDING)

* BASELINE NOMINAL LAMINATE

| NUMBER OF PLY SETS N | B/E CONTRT FACTOR (% B/E X 0.01) | PROPERTIES RELATIVE TO EQUAL THICKNESS 6AL-4V M.A. TITANIUM | | | | | | |
|-------------------------------|--|---|---------------------|---------------------|---------------------|--------------------|--------------------|-------------------|
| | | BENDING | | | | MEMBRANE | | |
| | | REL D ₁₁ | REL D ₁₂ | REL D ₂₂ | REL D ₃₃ | REL E | REL G | REL ν |
| 0 | 0.0 | 1.0000 | 1.0000 | 1.0000 | 1.0000 | 1.0000 | 1.0000 | 1.0000 |
| 1 | 0.66666 | 0.76107 | | 0.76107 | 0.83427 | 0.45357 | 0.79591 | 1.5596 |
| 2 * | 0.78723 | 0.63965 | 0.8304 | 0.63965 | 0.81180 | 0.35458 | 0.80126 | 1.8190 |
| 3 | 0.84375 | 0.57114 | | 0.57114 | 0.80621 | 0.30557 | 0.80377 | 1.9697 |
| 4 | 0.97654 | 0.52771 | | 0.52771 | 0.80461 | 0.27614 | 0.80522 | 2.0680 |
| 5 | 0.89796 | 0.49783 | | 0.49783 | 0.80426 | 0.25646 | 0.80617 | 2.1373 |
| 6 | 0.91314 | 0.47604 | | 0.47604 | 0.80435 | 0.24237 | 0.80684 | 2.1887 |
| 7 | 0.92424 | 0.45947 | | 0.45947 | 0.80459 | 0.23177 | 0.80733 | 2.2283 |
| 8 | 0.93288 | 0.44644 | | 0.44644 | 0.80490 | 0.22350 | 0.80772 | 2.2598 |
| 9 | 0.93976 | 0.43594 | | 0.43594 | 0.80522 | 0.21687 | 0.80802 | 2.2855 |
| 10 | 0.94535 | 0.42728 | | 0.42728 | 0.80552 | 0.21144 | 0.80827 | 2.3068 |

Optimum Variable Values

| | | | |
|---------------------------------------|-----------|---|----------|
| Number of Ply Sets | N_{PS} | = | 2 |
| Cladding Thickness | T_{CL} | = | 0.020 In |
| Stiffener height | H_S | = | 1.74 |
| B/E Stiffener Reinforcement thickness | T_{SR} | = | 0.051 |
| Stiffener Spacing | S_S | = | 6.38 |
| Cladding Reinforcement thickness | T_{CLR} | = | 0.025 |

Net Percentage of B/E in Nominal Laminate

$$\xi = 78.7\%$$

Maximum Composite Strain

$$\epsilon = 4741 \mu\epsilon$$

von Mises Effective Cladding Stress

$$F_e = 100969 \text{ Lb/In}^2$$

Critical Panel Buckling Loads

$$\text{Bending } N_{2CRPI} = -7553 \text{ Lb/In}$$

$$\text{Shear } N_{3CRPI} = 8358 \text{ Lb/In}$$

Stiffener Discrete Stiffnesses

$$EA = 5.29E6 \text{ Lb}$$

$$EI = 1.06E7 \text{ Lb-In}^2 \text{ about web laminate centerline}$$

$$GJ = 3120 \text{ Lb-In}^2$$

Stiffened Web Stiffnesses

$$D_{11} = 1673041. \text{ In-Lb}$$

$$D_{22} = 6230.$$

$$D_{33} = 3277.$$

Critical General Instability Loads

$$\text{Bending } N_{2CRGI} = -9187. \text{ Lb/In}$$

$$\text{Shear } N_{3CRGI} = 8611. \text{ Lb/In}$$

Figure 11a Structural Analysis Data for Baseline
B/E Reinforced Web

Net Percentage of B/E in Reinforced Laminate at Stiffener Fasteners

$$\epsilon_R = 49.2\%$$

Diagonal Tension Strain in Reinforced laminate at Stiffener Fastener Holes

$$\bar{\epsilon}_R = 3734 \mu\epsilon$$

Margins of Safety

| | |
|---|------|
| Cladding yielding | 0.25 |
| Composite strain | 0.27 |
| Local Panel Buckling | 0.00 |
| General Instability | 0.00 |
| Material Failure at Stiffener Fastener Holes | 0.00 |

Idealized OPTRAN Weights

Web Laminate:

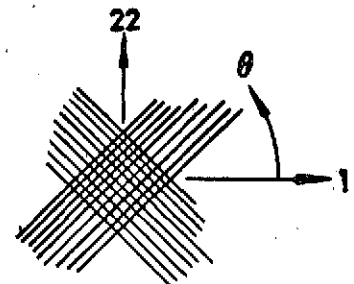
| | |
|---|--------------------------|
| <u>+45°</u> B/E | 3.06 Lb/Lin. Ft. of Beam |
| Nominal Cladding (.020 in.) | 3.07 |
| Cladding Reinforce- ment at Stiffeners | 0.61 |
| Adhesive Plies | 1.83 |

Stiffeners:

| | |
|-------------------------------------|-------|
| Metal parts | 2.21 |
| Unidirectional B/E Reinforcement | 0.42 |
| Total | 11.20 |

Figure 11b Structural Analysis Data for Baseline
B/E Reinforced Web

0.020 IN 6AL-4V M.A. TITANIUM CLADDING
 16 $\pm 45^\circ$ B/E PLIES
 5 0.012 IN ADHESIVE PLIES
 (REF. DWG SK-2-5085-117)



| FIRST B/E PLY θ ORIENTATION | -45° | | | 90° | | |
|---|--|---|---|---------------------------------|---------------------------------|--------------------------|
| MEMBRANE STIFFNESS MATRIX (A_{ij}) LB/IN. | 1.5189E 06 8.2885E 05 4.1321E 02 | 8.2885E 05 1.5189E 06 -4.1321E 02 | 4.1321E 02 -4.1321E 02 9.3395E 05 | 2.1059E 06 2.4732E 05 0.0 | 2.4732E 05 2.1059E 06 0.0 | 0.0 0.0 3.4800E 05 |
| BENDING STIFFNESS MATRIX (D_{ij}) IN.-LB | 6.2275E 03 2.4254E 03 6.0693E 01 | 2.4254E 03 6.2274E 03 5.8772E 01 | 6.0698E 01 5.8772E 01 2.7870E 03 | 6.9796E 03 1.5617E 03 0.0 | 1.5617E 03 7.2187E 03 0.0 | 0.0 0.0 1.9168E 03 |

Figure 12: BASELINE NOMINAL LAMINATE STIFFNESS PROPERTIES

3.6 Detailed Design of B/E Reinforced and All-Metal Shear Webs

Detailed designs were prepared for the baseline B/E reinforced and all-metal shear web designs established by OPTRAN and are included as Dwgs. SK2-5085-101 and SK2-5085-102, respectively, in Appendix B. These drawings serve as a basis for comparative weight and cost analyses.

Features of the B/E reinforced web design are shown in Figures 13a through 13d. The webs are attached to the bulkheads (with integral beam flange material) and side body longerons by simple angle connections. Diaphragm structure which is required for support of propulsion system components can be attached at appropriate stiffener fastener lines. In addition, means are illustrated of providing for a cutout and structural diaphragm interfaces. The web plate laminate contains two precured bonded ply set subassemblies complete with step-lap joint details. Each ply set has a balanced lay-up of 8 $\pm 45^\circ$ B/E plies and a center adhesive filler ply; this configuration results in a reasonably short step-lap joint length (lower joint weight penalty) with an acceptable weight penalty associated with adhesive filler and bondline plies.

The subassembly panels can be secondarily bonded to the titanium sheets which are chem-milled to produce local reinforcement in joint and fastener hole areas and predrilled in the B/E areas. Accurate positioning of the laminate lay-up parts can be accomplished with temporary tooling. After curing, the B/E material can be drilled out with conventional drills using the predrilled holes as guides. Edge joint fastener holes can be drilled after laminate curing and reamed to fit interfacing assemblies.

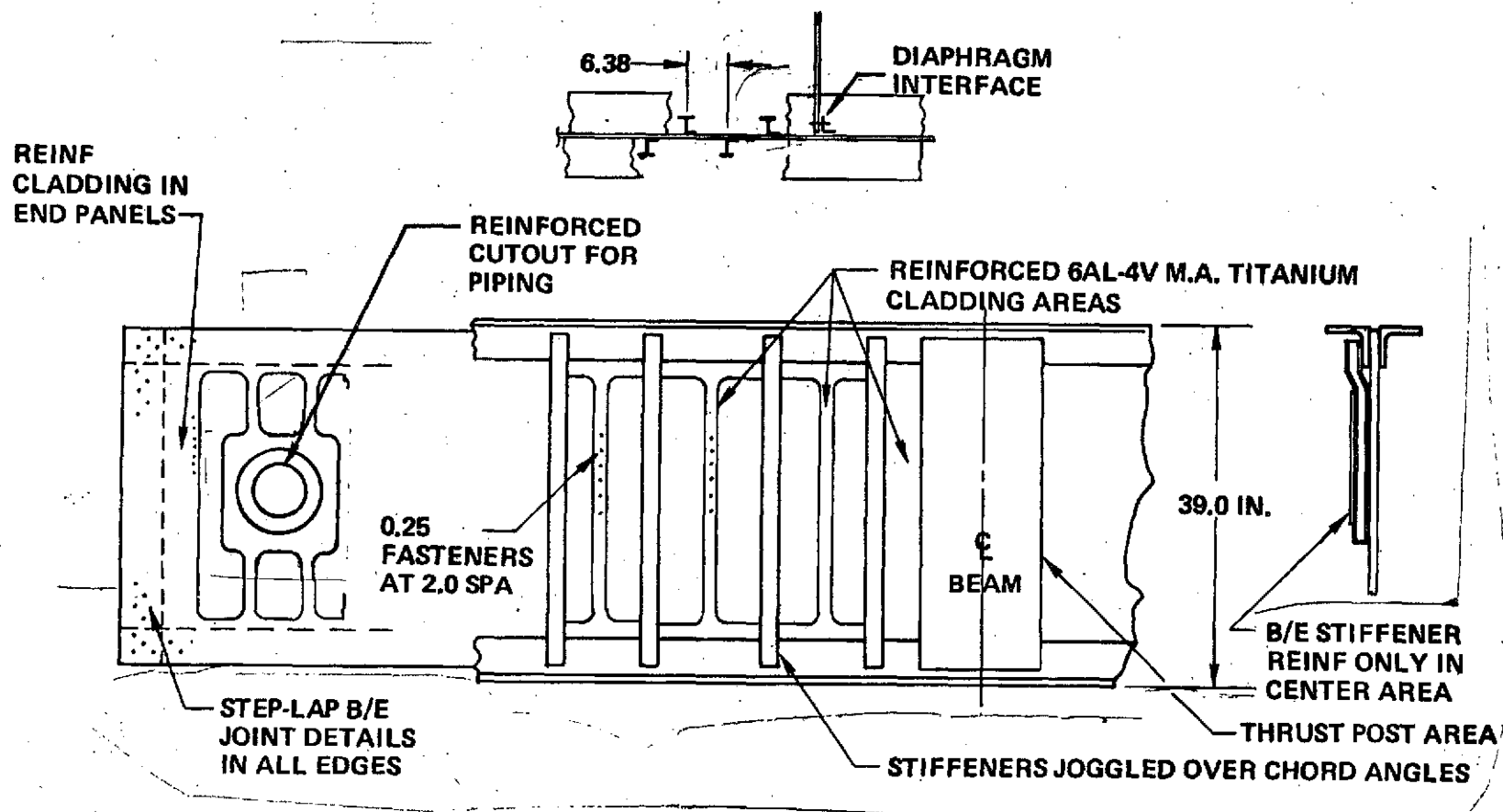


Figure 13a: B/E REINFORCED SHEAR WEB DESIGN DETAILS

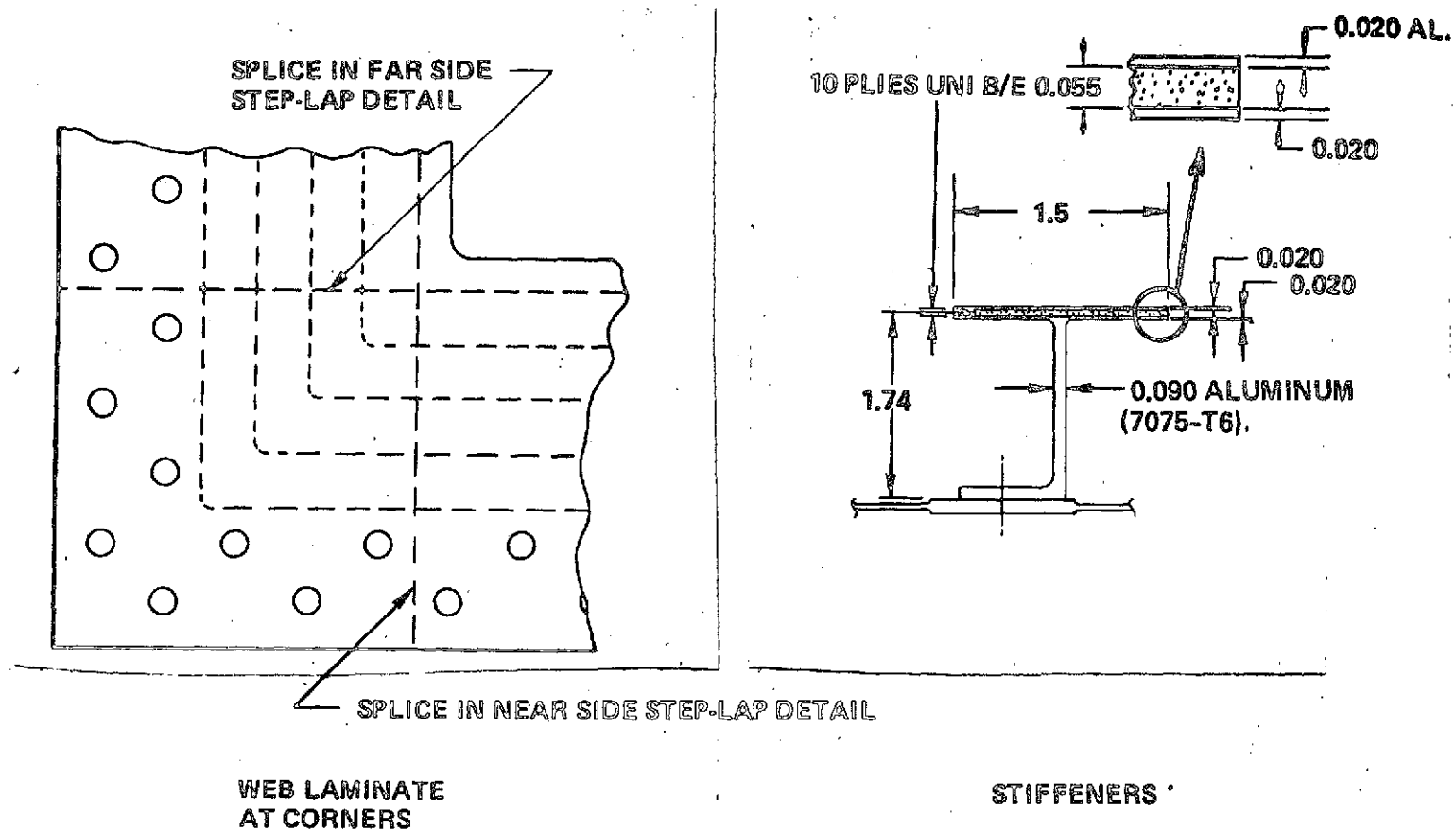


Figure 13b: B/E REINFORCED SHEAR WEB DESIGN DETAILS

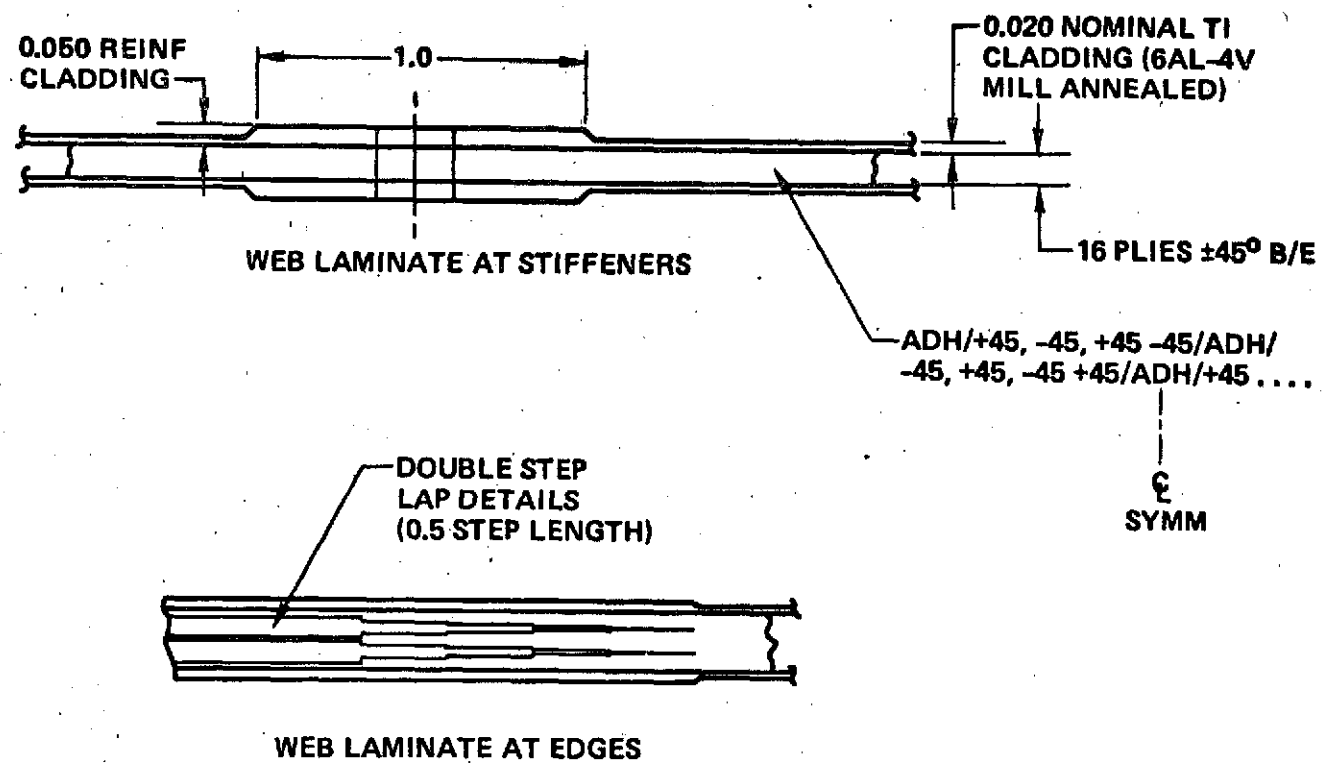


Figure 13c: B/E REINFORCED SHEAR WEB DESIGN DETAILS

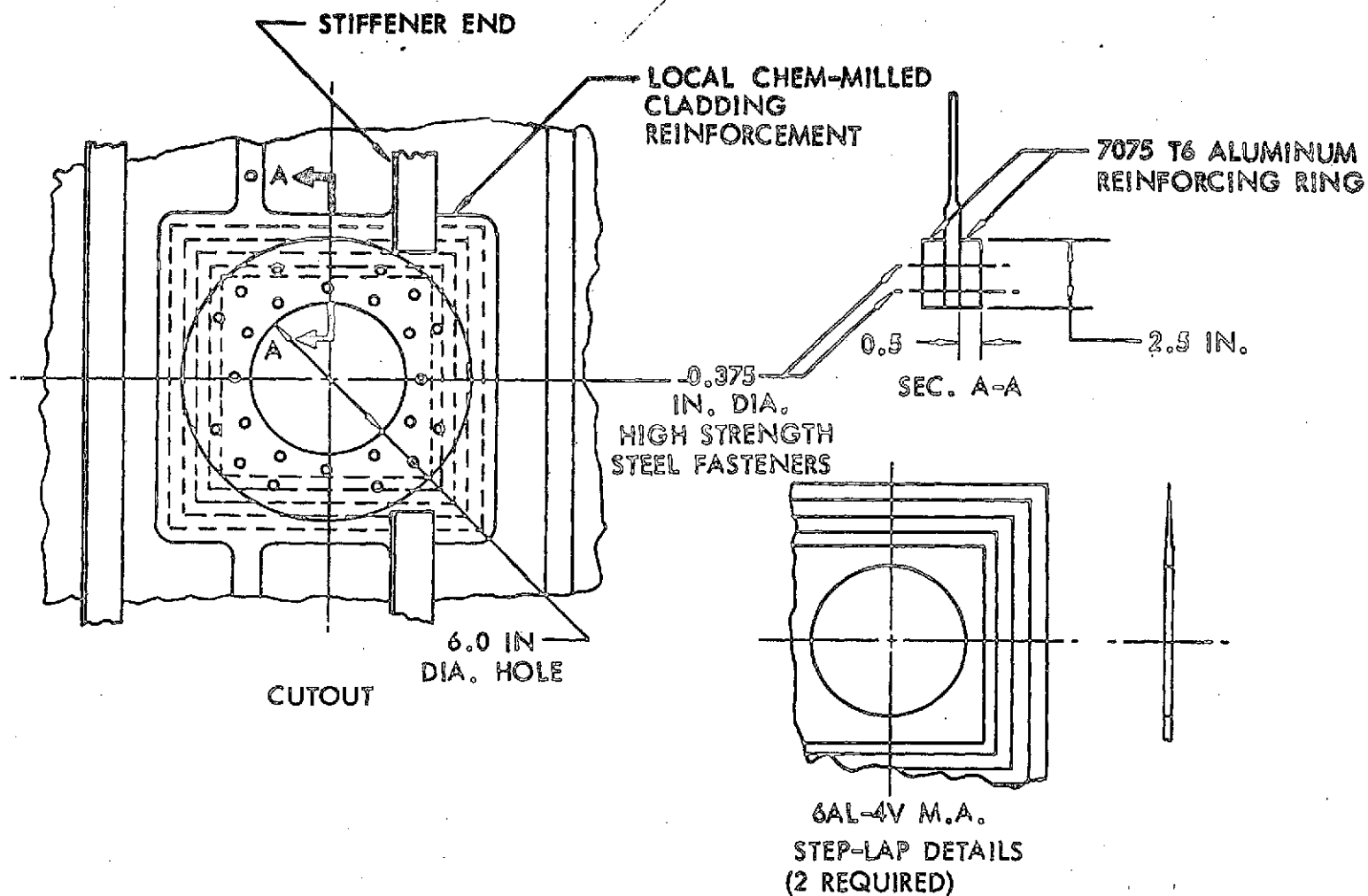


Figure 13d: B/E REINFORCED SHEAR WEB DESIGN DETAILS

The stiffener B/E reinforcement can be precured with step-lap end joint details. The B/E reinforcement, adhesive strips and cladding would then be fastened to the jogged stiffeners at room temperature to minimize residual distortion after elevated temperature curing of the adhesive. Aluminum cladding is applied to the exterior surface of stiffener reinforcement to provide a balanced laminate together with the 0.020 in. portion of the chem-milled stiffener section.

The stiffener attachment leg gage of 0.090 in. was treated as a fixed dimension in the OPTRAN weight trades. This gage exceeds the design requirement given in Appendix A when the titanium land material is assumed to act effectively with the stiffener leg in precluding web crippling between stiffener fasteners.

In order to simplify fabrication of the web step-lap edge joint details, the details are chem-milled in strips and machined to butt-fit at the web corners as shown in Figure 13b. This detailing precludes chem-milling large picture frame step-lap joint details and results in cost savings. The butt splice continuity is provided by B/E ply lapping and the secondary laminate bondlines since the splices are staggered. This simple splice detailing is made possible because strains in the splice areas are significantly reduced by presence of the reinforced titanium cladding which is illustrated in Figure 13c.

The cutout shown in Figure 13d is detailed in Dwg. SK2-5085-124 in Appendix B and was established from design charts given in Reference 16 which are based on charts given in Reference 17. The use of available metal structure design charts for sizing the hole reinforcement rings is believed to be justified in this case because the cutout area is essentially all-metal. A cutout diameter of 6.0 in. and an effective ultimate tensile strength of the shear web of $100,000 \text{ lb/in}^2$

were assumed in entering the design charts. The titanium reinforcement ring area specified by the design charts for the ultimate design shear loading of 7625 lb/in. was factored by the ratio of titanium/aluminum elastic moduli to transform the area to an equal stiffness aluminum section. The fasteners are sized to have excess margin with respect to shear flow around the bolt circles.

3.7 Detailed Design Comparisons

The detailed web designs have weights that are above the OPTRAN weights computed for the idealized nominal web. It is important to recognize weight penalties as they may occur and to use corrected weights in computing cost-benefit assessments. What details are charged as weight penalties against the idealized OPTRAN weights is a function of how the webs would actually be integrated into the adjacent structure. In this study, it is assumed that the reinforced web material located under the flange connection angles and in the end panels function as effective flange areas, load post area or longeron areas (end panels are usually reinforced as a matter of good design practice), as the case may apply. Therefore, the only chargeable weight penalties are considered to be the exposed reinforced step-lap joint areas along the beam flanges, stiffener end details, and cutout reinforcement areas. Slight weight penalties are also produced by having an integer ply count for B/E reinforcement and adhesive plies in the stiffener flanges. These penalties, applied to the net web depth of 34.5 in. for the detailed design drawings in Appendix B, alter the OPTRAN web weights given in Table 1 to 11.8 lb/lin.ft. for the baseline B/E reinforced web and 15.6 lb/lin.ft. for the baseline all-metal web design. The resultant weight saving then becomes 24% for the B/E reinforced web relative to the all-metal design. With the 6 in. diameter cutout shown in SK2-5085-124 (Appendix B) the weight saving for the net web changes to 20% compared to the all-metal design having an identical cutout.

In terms of cost, the web designs compare as shown in Figure 14. The web design costs were estimated on the basis of CY1973 one unit fabrication cost; the costs include quality assurance surveillance under production

conditions. Current material prices were applied to arrive at direct material cost. The costs are for the full gross web sizes shown in the detailed drawings. The weights are based on the net web dimensions (depth = 34.5 in.).

The cost per pound of weight saving associated with the net B/E reinforced web is \$247 by this analysis which is an acceptable figure when the benefits to the Space Shuttle are taken into account. It should be noted that cost analyses of this type are very dependent on the assumptions made and the final hardware details; for example, if the idealized OPTRAN weights are used, the cost per pound of weight saving reduces to \$160.

In a separate analysis, the titanium sheets of the B/E reinforced web were hypothetically substituted with an equivalent stiffness quasi-isotropic lay-up of B/E (12 extra plies of $0 \pm 60^\circ$ B/E). In this case, the net web weight savings for the B/E reinforced web changes to 36%, the web cost increases to \$34,000 and the cost per pound of weight saving increases to \$400. In general, this design concept would require more technology development (e.g. fastening stiffeners to web) and would therefore have significantly higher developmental risk, both in cost and in meeting service conditions.

| | OPTRAN IDEALIZED WEB | | | | NET WEB ▷ | |
|------------------------------|----------------------|------------|--------------|------------|--|----------------------------|
| | B/E REINFORCED TI | | TITANIUM | | B/E REINFORCED TI (SK2-5085-101) | TITANIUM (SK2-5085-102) |
| | d = 34.5" | d = 40" | d = 34.5" | d = 40" | | |
| SHEAR WEB WEIGHT (LB/FT) | 9.7 | 11.2 | 14.1 | 16.3 | 11.8 | 15.6 |
| WEIGHT SAVINGS | 31% | | REF | | 24% | REF |
| LB B/E PER LB WEIGHT SAVING | 0.600 | | - | | 0.676 | - |
| DIRECT MATERIAL COSTS ▷ | | | | | \$6500 | \$1750 |
| ESTIMATED FABRICATION COST ▷ | | | | | \$25,000 | \$18,000 |
| COST/LB OF WEIGHT SAVING | \$190 | \$160 | REF. | REF. | \$247 | REF |

▷ NET WEB DEPTH = 34.5 IN.

▷ CY 1973 ONE UNIT COST. BASED ON GROSS WEB DIMENSIONS (40 IN. X 98.00 IN.)

Figure 14: SHEAR WEB DESIGN COST COMPARISONS

4.0 STRUCTURAL ELEMENT TEST PROGRAM

The B/E reinforced shear web design contains unique details which must be substantiated by testing before the concept can be considered as a candidate for production hardware. Initial testing was conducted on structural test elements simulating eight areas in the design concept where design data was judged to have been needed:

- Stiffener fastener holes
- Step-lap edge joint splices
- Stiffener-to-web plate attachment
- Net section laminate strength
- Laminate bending stiffness
- Stiffener crippling
- Laminate bearing strength
- Flaw growth in titanium cladding

These element tests were completed in Phase I; the results, described in the following sections, substantiate the design concept with respect to local behavior of the details and allow structural testing to proceed to large scale assemblies which will be tested in Phase III of the program. The element tests were conducted to simulate the cyclic load and temperature design environments. Testing in other environments, such as the acoustic and thrust oscillation environments given in Section 3.2, were not considered to be necessary for design substantiation.

4.1 Tension Element Testing

The most critical aspect of the B/E reinforced design is the amount of titanium that is required at stiffener fastener holes. In order to establish a basis for design, a number of drilled tension specimens were tested having various cladding thicknesses and a basic 0-90° B/E lay-up simulating the tension component of principal strain conditions in the shear resistant web laminate. Photographs of the type of specimens that were tested are shown in Figures 15 and 16; the various cladding thicknesses shown were produced by chem-milling the 6AL-4V mill annealed titanium. Some specimens, such as the simulated web strain specimen, had nominal 0.020 inch titanium sections together with reinforced step-lap end joints. In all specimens, the holes were made using conventional high speed steel drills with care taken not to burr the cladding nor to overheat the laminate material.

Figure 17 illustrates several different types of laminates that were tested in addition to the baseline (BL) design laminate. The lay-up variations produced marked differences in the test results as will be discussed later.

Table 3 presents a summary of the tension element tests. The 1.5 inch wide (W) specimens with a B lay-up, and the E lay-up specimens have the simulated web strain specimen configuration shown in Figure 15; all other specimens have the coupon configuration depicted in Figure 16. The % B/E factor is based on the structural laminate thickness (less adhesive plies) and the summed ET factor represents the gross specimen stiffness in the hole-out area, unless otherwise noted. The ϵ_{ULT} item is the gross ultimate strain at failure computed in the vicinity of the hole, unless otherwise noted.

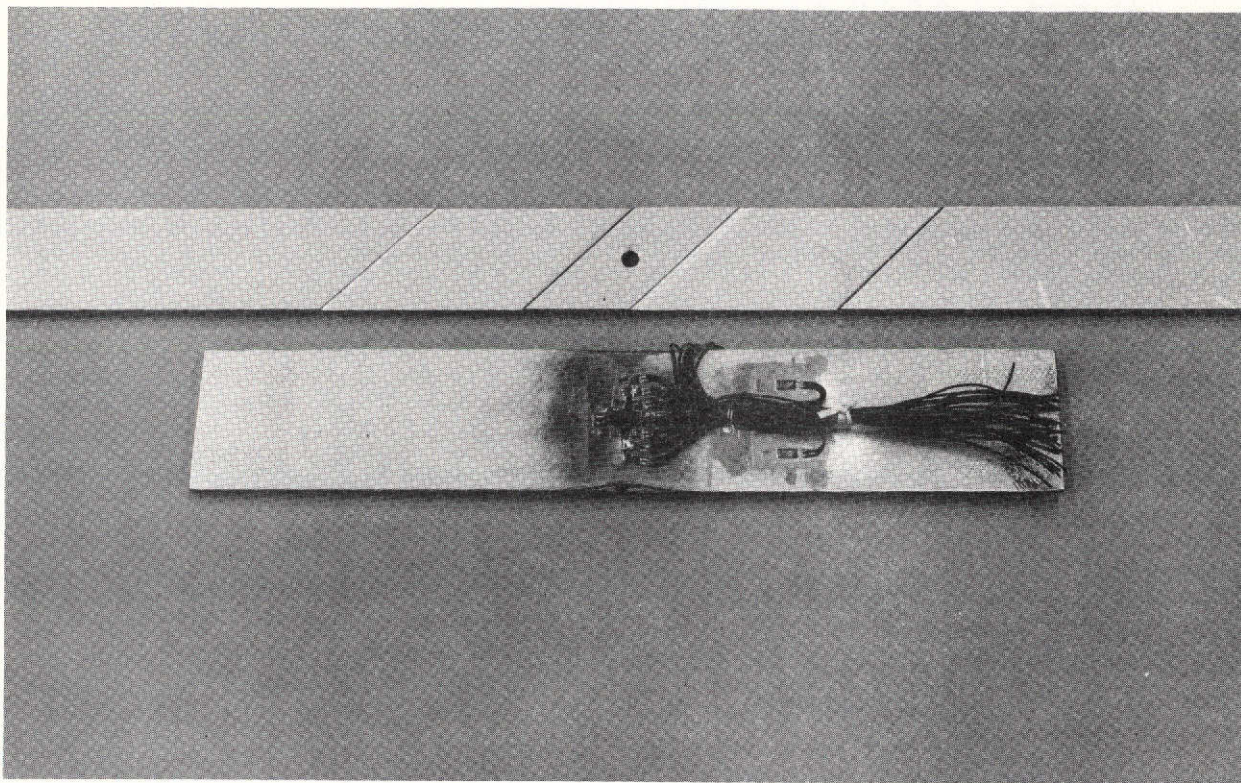


Figure 15: TENSION TEST ELEMENTS

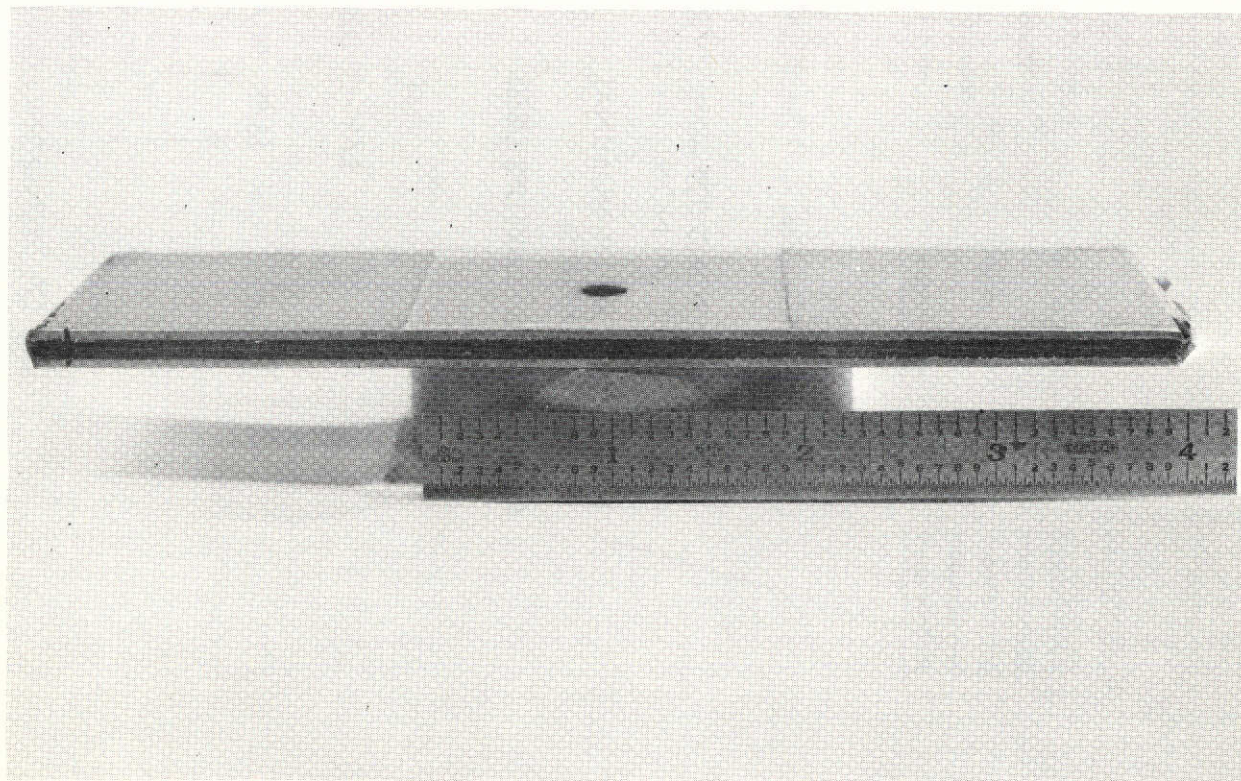
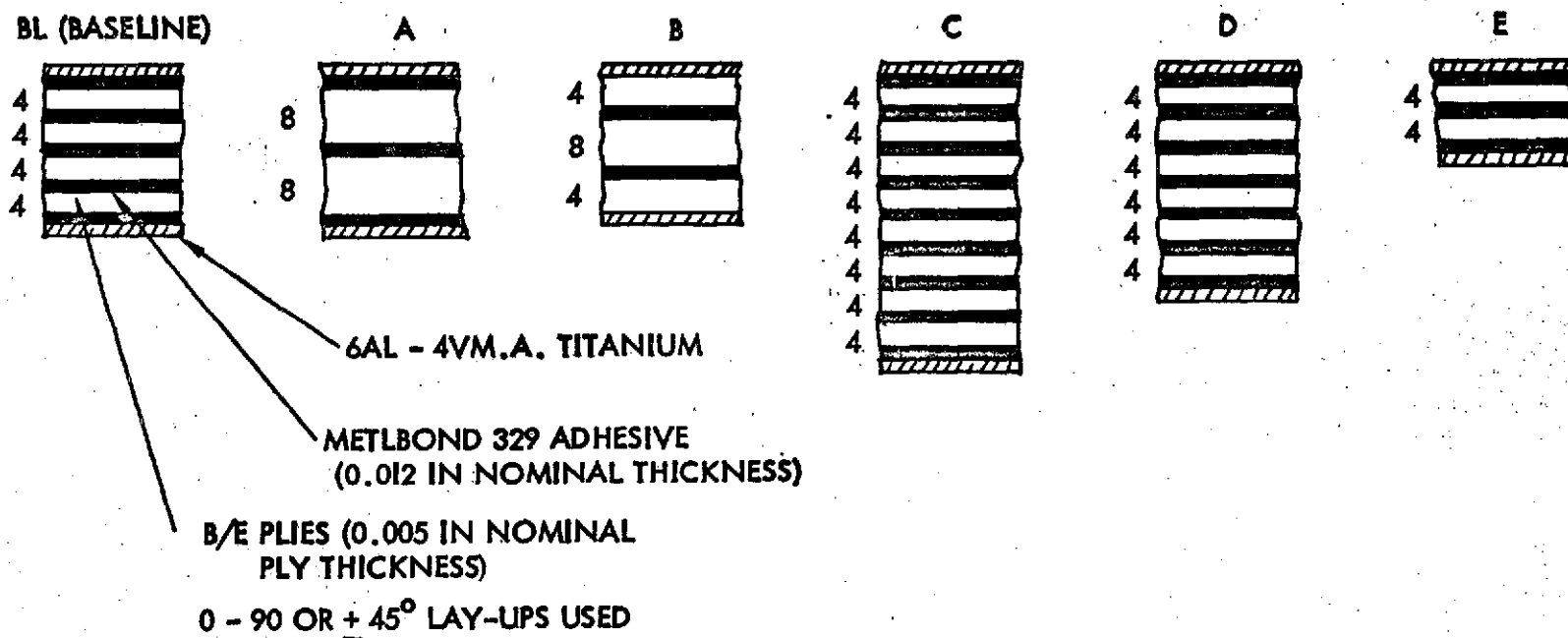


Figure 16: TENSION TEST ELEMENT



LAY-UP DESIGNATION USED IN DATA TABLES

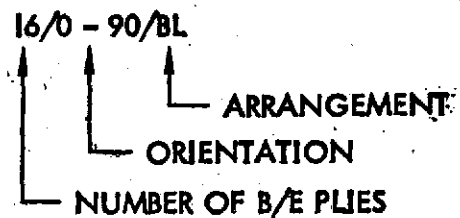





Figure 17: TENSION ELEMENT LAY-UP ARRANGEMENTS

Table 3: TENSION ELEMENT TEST DATA
COUPON SPECIMENS

| SPECIMEN NUMBER | LAY-UP | LOAD LB | W IN | N _x LB/IN | T _{CL} AT HOLE IN | % B/E | Σ _{ET} (10 ⁶) LB/IN | ε _{ULT} με | CYCLED 400~TO (LB) | HOLE DIA | NOTES |
|--------------------|----------------|------------|---------|-------------------------|----------------------------------|-------|--|------------------------|--------------------------|-------------|-------|
| 1 | 16/0-90/A ↓ | 22600 | 1.95 | 11600 | .0535 | 45.1 | 3.07 | 3776 | — | 0.25 | |
| 2 | | 22900 | 1.95 | 11700 | .054 | 44.9 | 3.09 | 3789 | 13300 | | |
| 3 | | 23360 | 1.95 | 12000 | .055 | 44.5 | 3.12 | 3850 | 16600 | | |
| 4 | | 20500 | 1.95 | 10500 | .051 | 46.6 | 2.98 | 3528 | | | |
| 5 | | 21200 | 1.92 | 10900 | .050 | 47.1 | 2.94 | 3702 | 13300 | | |
| 6 | | 22100 | 1.95 | 11300 | .050 | 47.1 | 2.94 | 3840 | 13300 | | |
| 7 | | 24600 | 1.95 | 12600 | .052 | 46.1 | 3.00 | 4189 | 13300 | | |
| 8 | | 22000 | 1.95 | 11300 | .051 | 46.3 | 3.00 | 3775 | 16600 | | |
| 9 | | 21700 | 1.95 | 11100 | .052 | 46.1 | 3.00 | 3690 | 16600 | | |
| 10 | | 21080 | 1.95 | 11200 | .049 | 47.6 | 2.91 | 3846 | 13300 | | |
| 11 | | 19660 | 1.95 | 10100 | .046 | 49.4 | 2.80 | 3607 | — | | |
| 12 | | 20520 | 1.95 | 10500 | .046 | 48.9 | 2.83 | 3708 | 13300 | | |
| 13 | | 18080 | 1.95 | 9250 | .041 | 51.8 | 2.67 | 3570 | 13300 | | |
| 14 | | 19240 | 2.0 | 9850 | .041 | 51.8 | 2.67 | 3689 | 16600 | | |
| 15 | | 17320 | 1.95 | 8900 | .036 | 55.0 | 2.51 | 3550 | 13300 | | |
| 16 | | 17500 | 1.87 | 9000 | .037 | 54.3 | 2.54 | 3538 | 16600 | | |
| 17 | | 20000 | 1.95 | 10200 | .052 | 46.1 | 3.00 | 3400 | 13300 | 0.1875 | |
| 18 | | 23200 | 1.98 | 11700 | .052 | 46.1 | 3.00 | 3900 | 13300 | 0.1875 | |
| 19 | | 24100 | 1.93 | 12500 | .052 | 45.8 | 3.00 | 4170 | 13300 | 0.125 | |
| 20 | | 24500 | 1.95 | 12600 | .052 | 46.1 | 3.00 | 4200 | 13300 | 0.125 | |
| SG-1 | | 22800 | 1.94 | 11800 | .050 | 47.1 | 2.94 | 4000 | — | 0.25 | |

Table 3 : (Continued)
TENSION ELEMENT TEST DATA
SIMULATED WEB STRIP SPECIMENS

| SPECIMEN NUMBER | LAY-UP | LOAD LB | W IN | N _x LB/IN | T _{CL} AT HOLE IN | % B/E | ΣET (10 ⁶) LB/IN | E _{ULT} μE | CYCLED 400~TO (μE) | HOLE DIA | NOTES |
|--------------------|-----------|------------|---------|-------------------------|----------------------------------|--------------|------------------------------------|------------------------|------------------------------|-------------|---|
| 21 | 16/0-90/B | 20080 | 1.50 | 13850 | .049 | 47.3 | 2.93 | 4730 | 3530 3530 4450 4450 | .25 |  |
| 22 | | 19980 | | 13320 | .047 | 48.4 | 2.86 | 4651 | | | |
| 23 | | 18580 | | 12387 | .043 | 50.6 | 2.74 | 4527 | | | |
| 24 | | 16940 | | 11293 | .044 | 50.4 | 2.75 | 4104 | | | |
| 25 | | 17200 | | 11467 | .040 | 52.7 | 2.62 | 4370 | | | |
| 26 | | 17100 | | 11400 | .041 | 51.8 | 2.67 | 4266 | | | |
| 27 | | 15440 | | 10293 | .035 | 55.8 | 2.48 | 4158 | | | |
| 28 | | 17320 | | 11547 | .043 | 50.6 | 2.73 | 4225 | | | |
| 29 | | 15840 | | 10560 | .041 | 51.9 | 2.66 | 3966 | | | |
| 30 | | 18560 | | 12373 | .046 | 48.9 | 2.83 | 4374 | | | |
| 31 | | 15260 | | 10173 | .040 | 52.1 | 2.65 | 3835 | | | |
| 32 | | 14220 | | 9480 | .035 | 55.7 | 2.48 | 3823 | | | |
| 33 | | 22000 | | 14667 | .056 | 44.0 | 3.15 | 4653 | | | |
| 34 | | 3920 | 1.99 | 1976 | 0 | 100 | 1.36 | 1450 | | | |
| SG-2 | | 16300 | 1.98 | 8230 | .020 | 68.9 | 1.96 | 4250 | | | |
| SG-3 | | 3720 | 1.98 | 1800 | 0 | 100 | 1.36 | 1380 | | | |
| SG-4 | | 21700 | 1.50 | 14450 | .060 .029 | 42.2 60.2 | 3.38 2.19 | 4270 6600 | | |   |

1. E_{ULT} CALCULATED FOR REINFORCED SECTION

2. E_{ULT} MEASURED IN UNREINFORCED SECTION (T_{CL} = 0.020)

3. FAILED IN UNREINFORCED SECTION, ALL OTHERS FAILED AT THE HOLE

Table 3: (Continued)
TENSION ELEMENT TEST DATA
COUPON SPECIMENS

| SPECIMEN NUMBER | LAY-UP | LOAD LB. | W IN | N _x LB/IN | T _{CL} AT HOLE IN | % B/E | Σ _{ET} (10 ⁶) LB/IN | ε _{ULT} με | CYCLED 400~TO (LB) | HOLE DIA | NOTES |
|--------------------|------------|-------------|---------|-------------------------|----------------------------------|-------|--|------------------------|--------------------------|-------------|-------|
| 35 | 32/0-90/C | 66240 | 2.0 | 33080 | .125 | 41.3 | 6.82 | 4840 | | .25 | |
| SG-5 | ↓ | 66500 | | 33325 | .125 | 41.3 | 6.82 | 4860 | | ↓ | |
| 36 | 24/0-90/D | 37500 | | 18750 | .063 | 51.0 | 4.06 | 4620 | | | |
| 37 | 16/0-90/BL | 66600 | | 33300 | .125 | 26.0 | 5.41 | 6150 | | | |
| 38 | ↓ | 34000 | | 17000 | .060 | 35.5 | 3.28 | 5180 | | | |
| 39 | | 29700 | | 14850 | .050 | 46.8 | 2.96 | 5020 | 16600 | | |
| 40 | | 29600 | | 14800 | .050 | ↓ | ↓ | 5000 | 16600 | | |
| 41 | | 28800 | | 14400 | .050 | | | 4860 | 16600 | | |
| 42 | | 41300 | | 20650 | .063 | 41.2 | 2.44 | 8450 | | None | |
| 43 | | 41100 | | 20500 | ↓ | ↓ | ↓ | 8400 | 28500 | | |
| 44 | | 40200 | | 20100 | | | | 8200 | 28500 | | |
| 45 | 16/+45/BL | 36600 | | 18300 | ↓ | ↓ | ↓ | 7500 | | | |
| 46 | ↓ | 38800 | | 19400 | ↓ | ↓ | ↓ | 7950 | 28700 | | |
| 47 | ↓ | 39600 | | 19800 | ↓ | ↓ | ↓ | 8100 | | | |
| SG-6 | 16/0-90/BL | 27500 | | 13750 | .050 | 46.8 | 2.96 | 4650 | | 0.25 | |

Table 3: (Continued)
TENSION ELEMENT TEST DATA
SIMULATED WEB STRIP SPECIMENS

| SPECIMEN NUMBER | LAY-UP | LOAD LB | W IN | N _x LB/IN | T _{CL} AT HOLE IN | % B/E | 1 Δ Σ ET (10 ⁶) LB/IN | e _{ULT} μ e | 2 Δ CYCLED 400-TO | HOLE DIA | NOTES |
|--------------------|----------|------------|---------|-------------------------|----------------------------------|-------|---|-----------------------------|-----------------------------|-------------|------------|
| 48 | 8/0-90/E | 8000 | 1.0 | 8000 | .012 | 64.7 | 1.03 | 7800 | | NONE | |
| 49 | | 8260 | | 8260 | | | | 8250 | 4450 | | |
| 50 | | 8060 | | 8060 | | | | 8100 | 4450 | | |
| 51 | | 7260 | | 7260 | | | | 7650 | | | 3 Δ |
| 52 | | 7160 | | 7160 | .063 | 24.7 | | 6950 | 4450 | 5/32 | 5 Δ |
| 53 | | 6080 | | 6080 | .012 | 64.7 | | 5200 | 3525 | | |
| 54 | | 7320 | | 7320 | .043 | 33.5 | | 7120 | 4450 | | 5 Δ |
| 55 | | 5220 | | 5220 | .012 | 64.7 | | 4450 | 4450 | | 4 Δ |
| 56 | | 7000 | | 7000 | .033 | 44.3 | | 7325 | 3525 | | 5 Δ |
| 57 | | 7380 | | 7380 | .027 | 46.8 | | 7300 | 3525 | | 5 Δ |

1 Δ NOMINAL UNREINFORCED SECTION STIFFNESS (T_{CL} = 0.012)

2 Δ e CALCULATED FOR UNREINFORCED SECTION

3 Δ LOADED 43 HRS TO 3525 μ e PRIOR TO FAILURE

4 Δ FAILED ON 15th LOAD CYCLE

5 Δ FAILED IN UNREINFORCED SECTION

Cyclic loading simulating the design requirements and temperatures were applied to the specimens as noted. Two cyclic load levels were applied; a level simulating the gross diagonal tension load at limit load (13,300 lb.) and a higher load (16600 lb.) which increases the peak elastic hole strain to the theoretical elastic level for the tension-compression diagonal strain field existing in a pure shear web. Cyclic loads and temperatures did not have a significant effect on the ultimate strain results.

Hole diameters of 0.25 in. and smaller were tested. However, insufficient data was obtained for diameters other than the baseline 0.25 in. to support any conclusions. Some specimens were tested without holes and these sustained very high strain levels prior to failure. All specimens, except for specimen 45 having $\pm 45^\circ$ B/E, exhibited essentially linear behavior up to failure. It is noteworthy that in all cases the specimens failed either in hole-out sections or in unreinforced laminate areas. No failures occurred in end areas having reinforced titanium even though conventional mechanical grips were used; this demonstrates the effectiveness of the reinforcement lands in alleviating joint strain.

Figure 18 is a plot of ultimate strain versus net B/E content for all tension elements that failed in the hole-out section. The data is the basis for the preliminary reinforcement design function included in the OPTRAN code analyses described in Appendix A. The function is chosen to be conservative, as discussed later. The data scatter is attributed to different behavior of the layups that were tested and appears to increase as the B/E content increases. The two specimens tested without cladding (100% B/E content) failed at remarkably low strains in a manner indicating rapid, brittle crack growth. A data point from the shear web element testing which will be discussed in Section 4.2 is shown to correlate with the tension element test data.

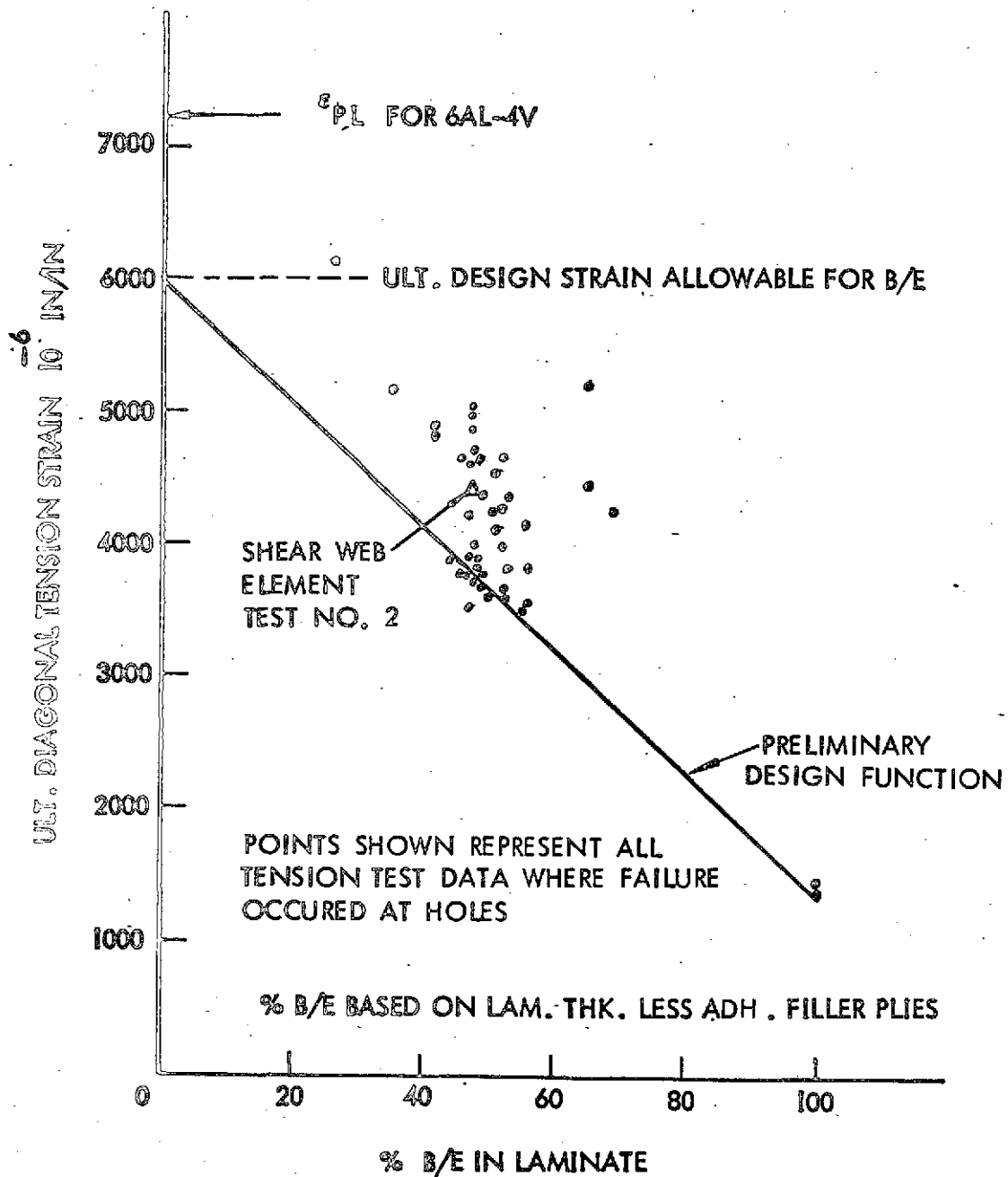


Figure 18: DATA USED IN OPTRAN TO ESTABLISH
TI-CLADDING REINFORCEMENT REQUIREMENT

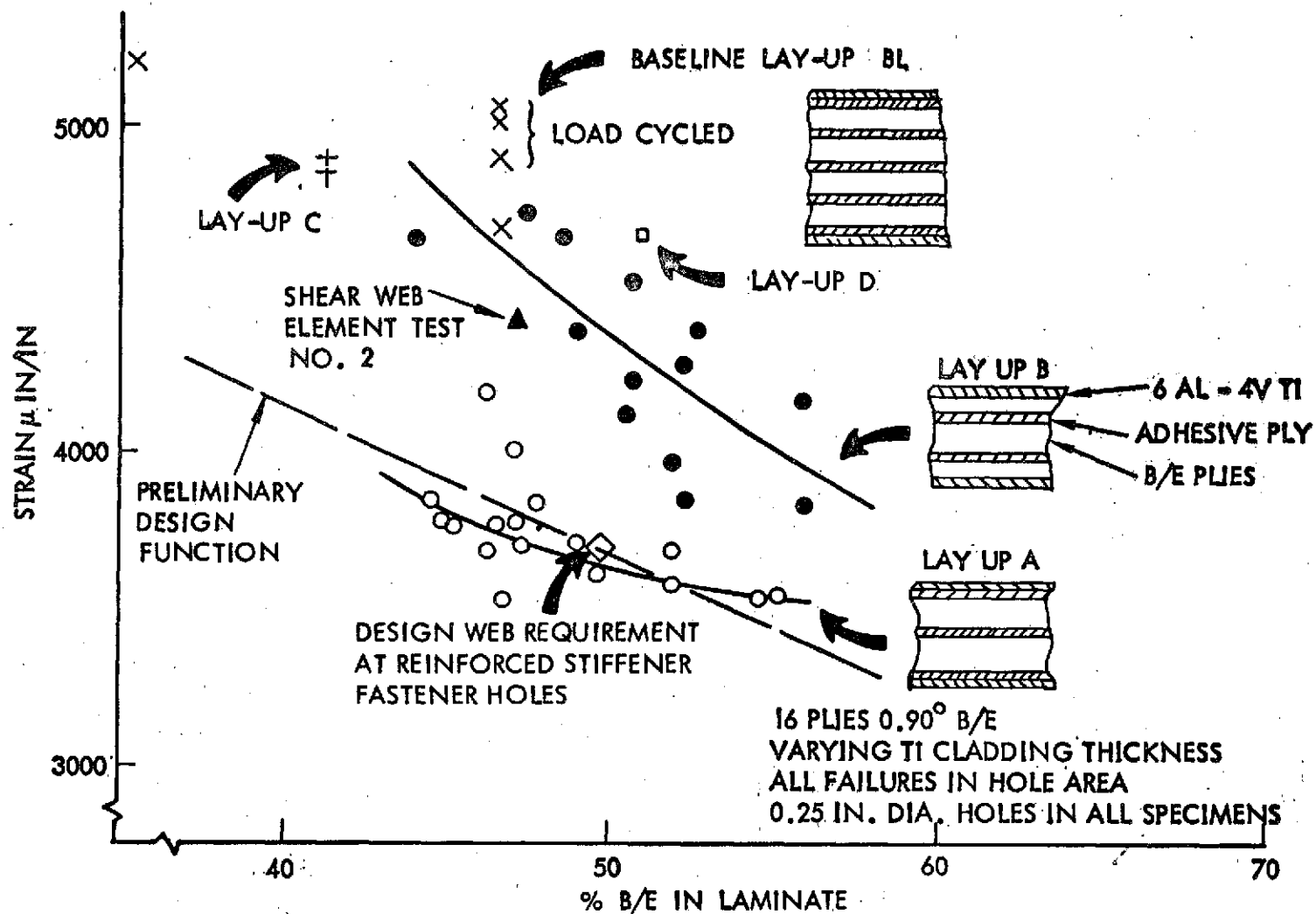


Figure 19: SHEAR WEBS TENSION ELEMENT TEST DATA COMPARISON

The data in Figure 18 is replotted in Figure 19 for the region of interest for titanium reinforcement lands. Data from layup A were typically below the other layups because this layup has higher strain concentration, as discussed later, and no division of the B/E ply groups on each side of the centerline adhesive ply. Division of the B/E ply groups apparently retards crack growth propagation to ply groups adjacent to the center groups, where initial fracturing occurs. The baseline (BL) laminate has high performance because of its high degree of ply group divisioning. The preliminary design function is located well below the baseline laminate data and the shear web element test point. The baseline laminate specimens which were load cycled have slightly higher strengths than the uncycled specimen. Other load cycled specimens have lower strengths than comparable uncycled specimens; however, the differences in strengths are small.

Six specimens were strain gaged as shown in Figures 20, 21 and 22 so that the laminate strain response could be better understood. In addition to gages placed on the titanium, cladding gages were located inside the holes on the titanium and on the laminate centerline as shown in Figure 23. The gages used in the holes were small single element gages oriented in the plane of the laminate.

Figure 24 presents strain gage and acoustic emission results for specimen SG-1, which is a layup B specimen. The peak B/E strains at the center of the laminate are essentially linear up to the ultimate strain capability of boron filaments. In the elastic range the strain concentration factor is 4.66 compared to the theoretical plane stress value of 3.4, based on classical orthotropic strain concentration analysis (18). This indicates a definite deviation from plane stress elastic response in the hole area. The strain

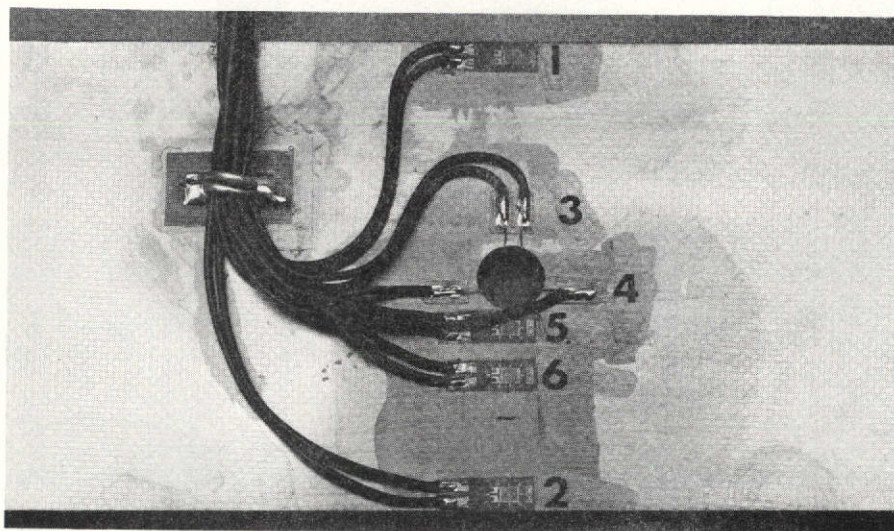


Figure 20: STRAIN GAGED TENSION SPECIMEN SG-2

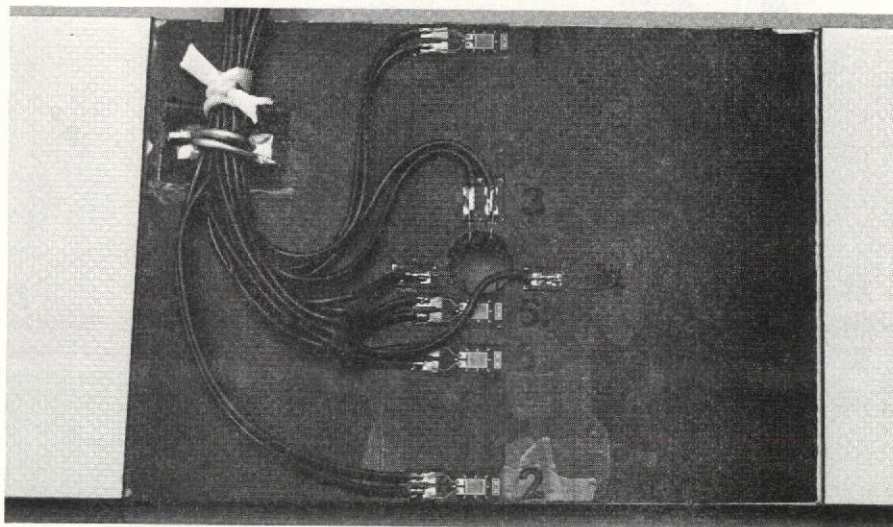


Figure 21: STRAIN GAGED TENSION SPECIMEN SG-3

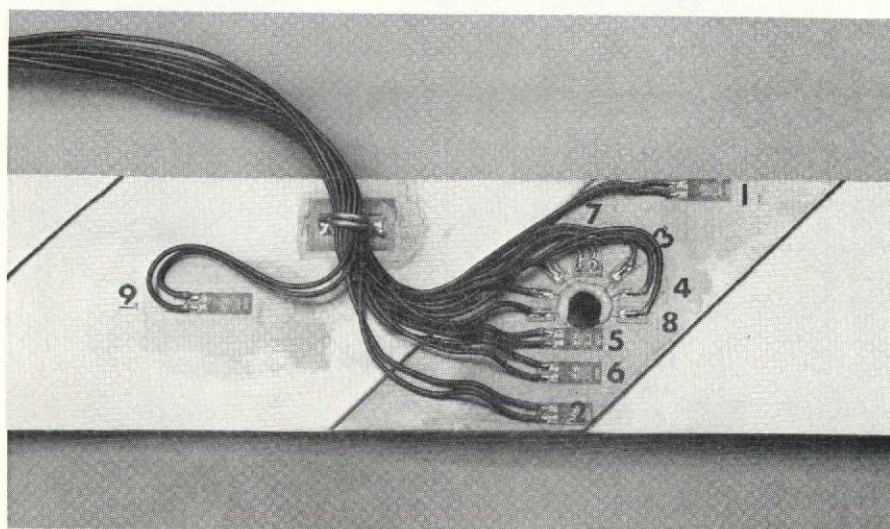


Figure 22: STRAIN GAGED TENSION SPECIMEN SG-4

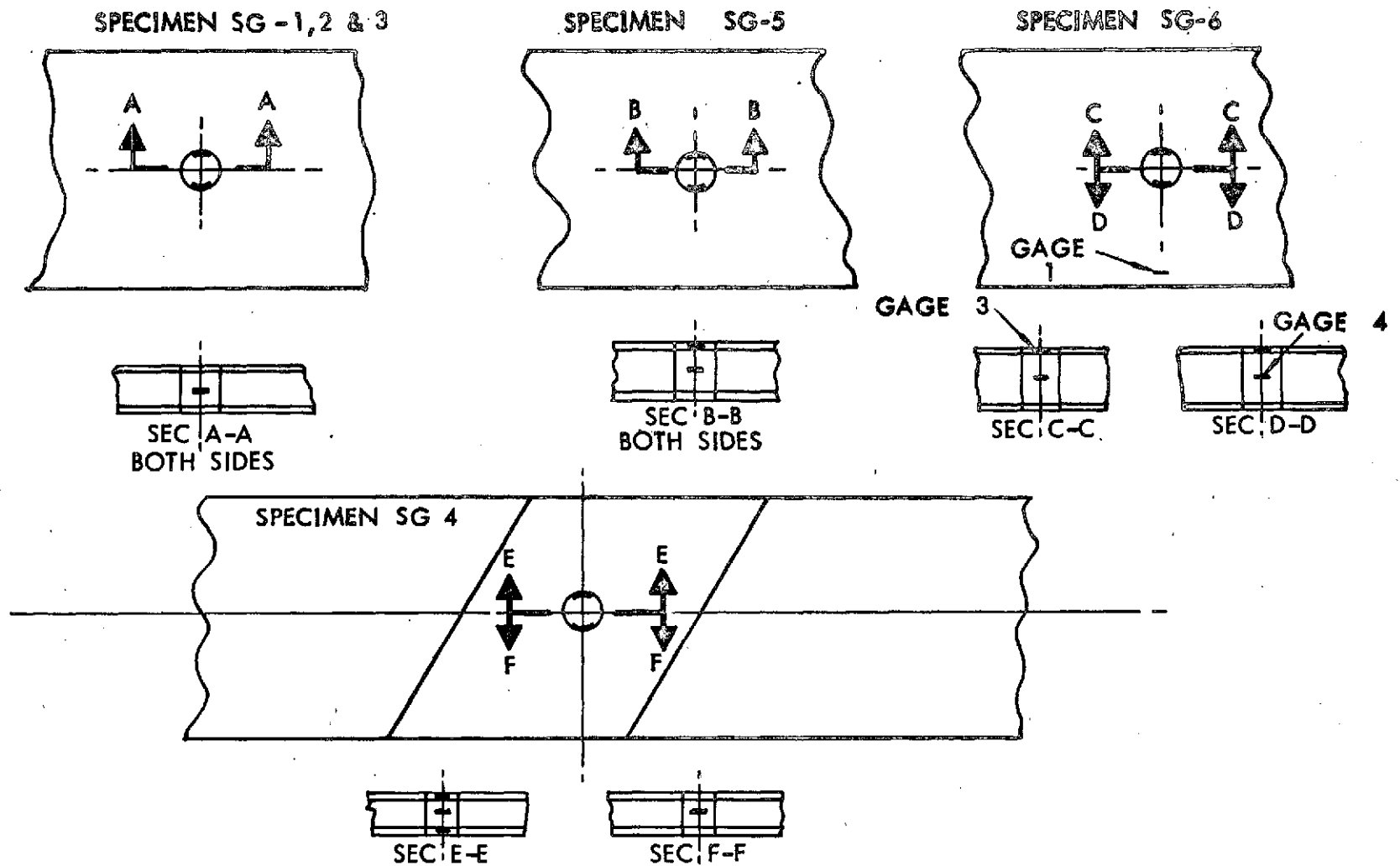


Figure 23: HOLE STRAIN GAGE LOCATIONS

SIGNIFICANT ACOUSTIC EMISSION EVENTS

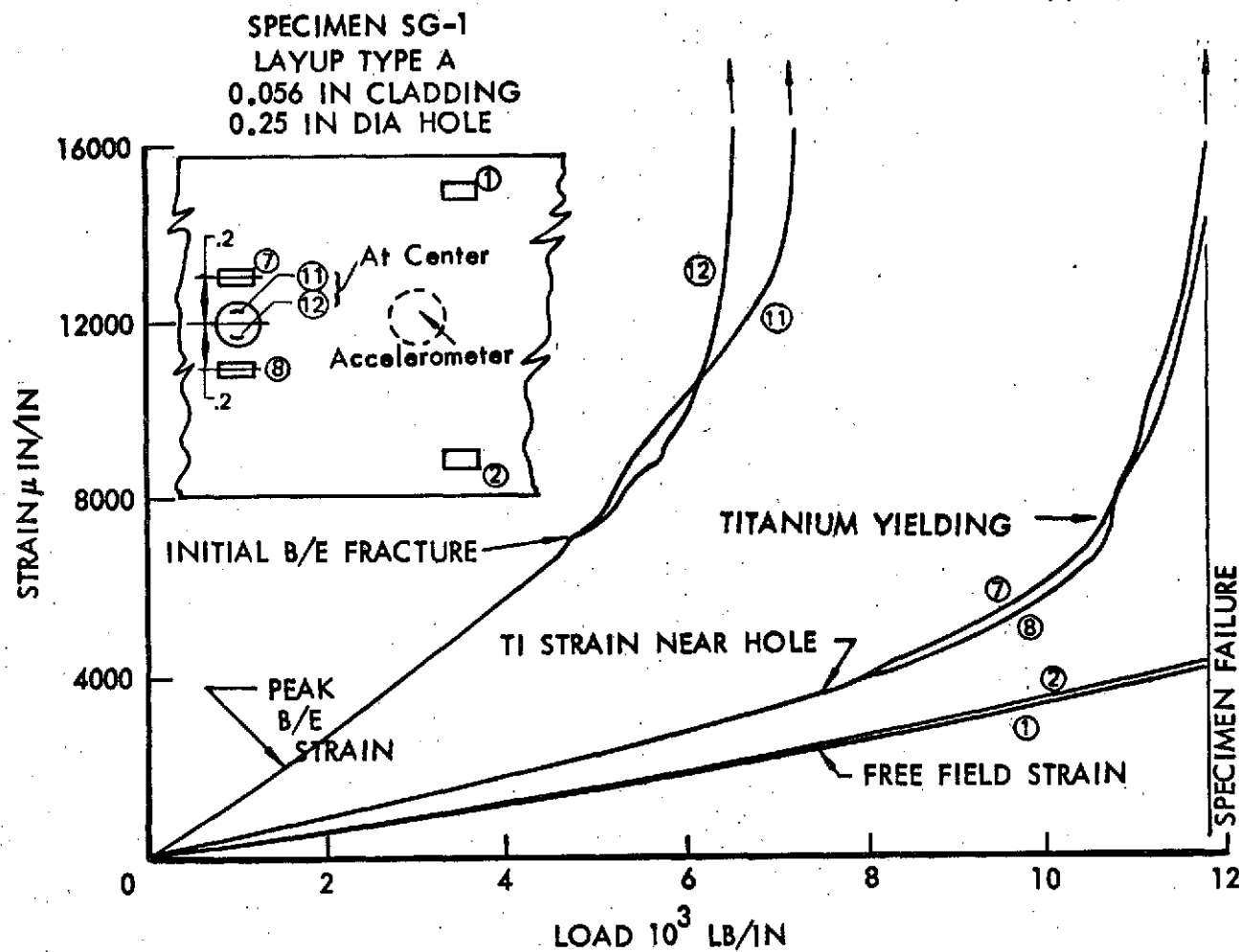
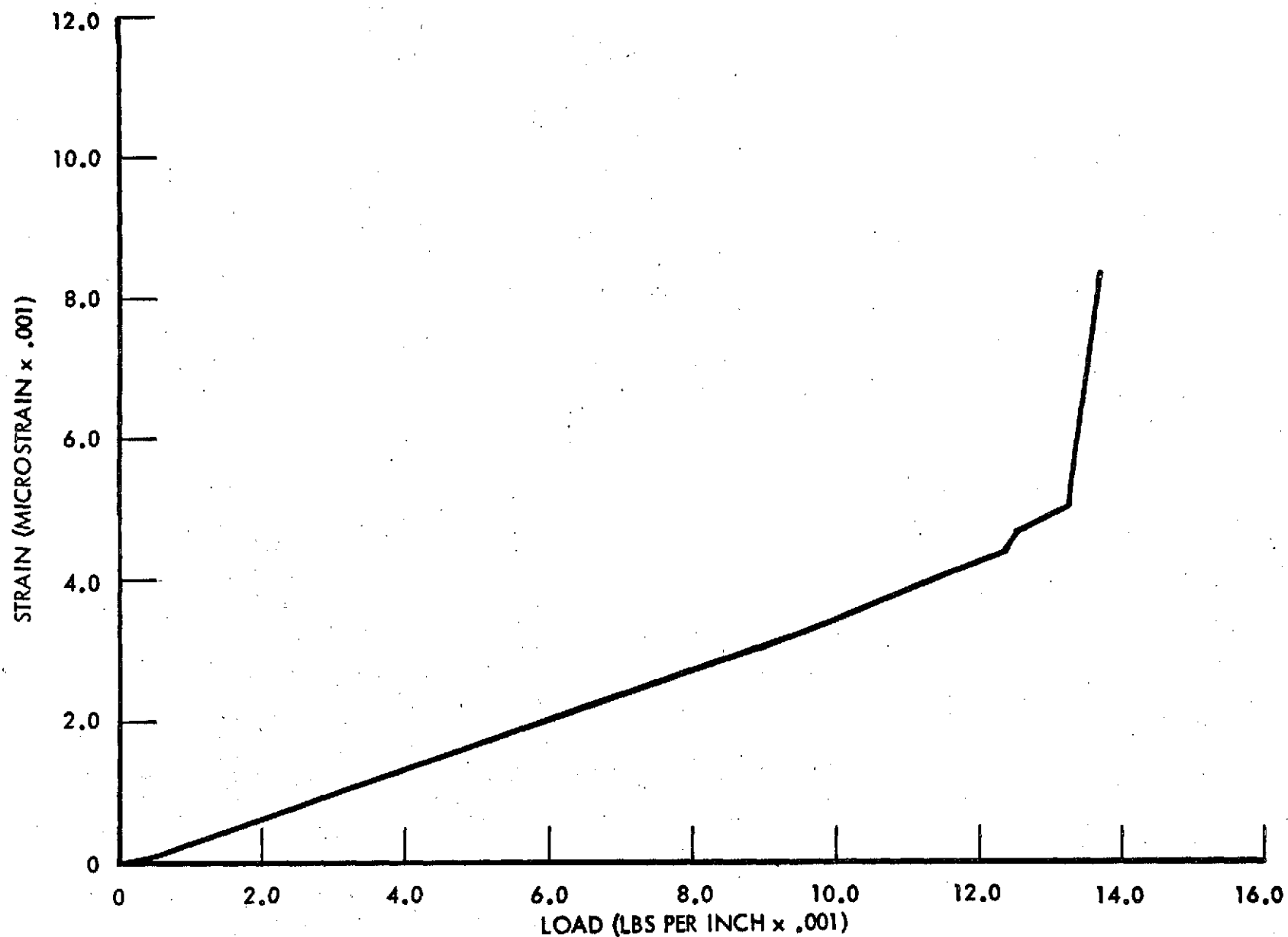


Figure 24: TENSION TEST STRAIN/ACOUSTIC EMISSION RESULTS

concentration in the titanium appears to be very localized at the hole. After initial B/E fracture, the titanium begins to behave non-linearly indicating fracture zone growth. The gages on the B/E failed due to local crack growth at loads which are approximately the same as the limit load level in the baseline B/E reinforced web. Other strain gages not shown in the figure indicated that the yield zone in the titanium progressed past gages 7 and 8 to about 3 radii out from the hole center at specimen failure. The acoustic emission recording, represented in Figure 24, shows little activity until titanium yielding at the hole edge allows large laminate strain increments. The acoustic signature is relatively low during initial B/E fracturing compared to the events near specimen failure.

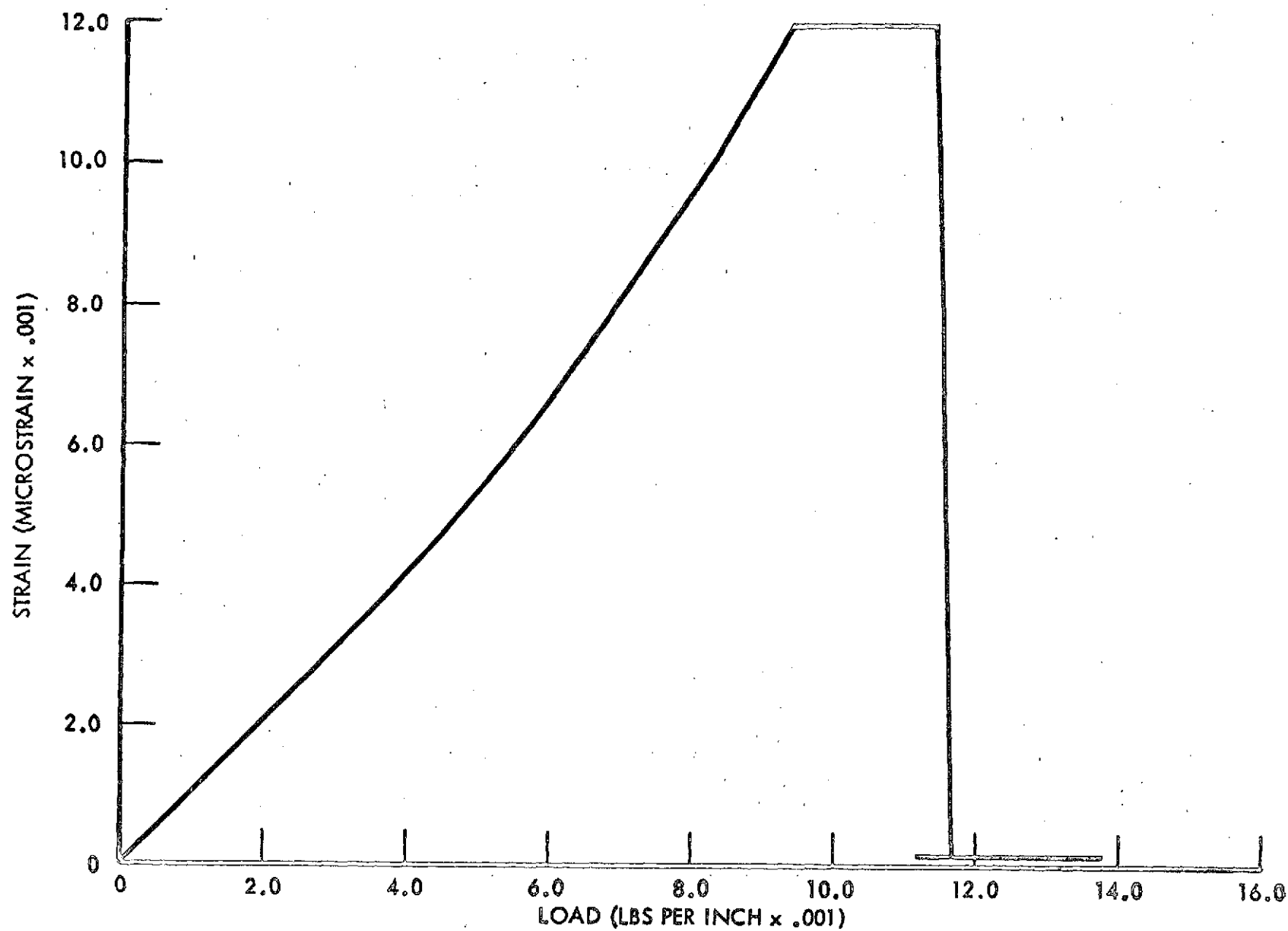
Figures 25, 26, and 27 present additional load-strain plots corresponding to the baseline layup specimen SG-6. The computer plotting instructions limited the strains to a maximum of 12,000 $\mu\epsilon$ in order to enhance the curve resolution in the region of interest. The data is similar to the other specimens except for the initial peak strain concentration factors (K_I). These factors are given in Figure 28 and were obtained by dividing the initial slope of the hole centerline gage by the average slope of the free-field gages. The data for the SG-1, 5 and 6 specimens, which have titanium reinforcement lands on the order of what is specified in the web design, indicates that the layup A specimens have the highest K_I . This partially explains why the layup A specimens have lower ultimate strains in Figure 19. The K_I factor for the baseline layup specimen is closest to the theoretical plane stress value of 3.4; however, definite deviation from plane stress response is noted in comparing the B/E and metal K_I differences. The metal K_I factors approach the classical value of 3.0 given by isotropic plate theory.

59



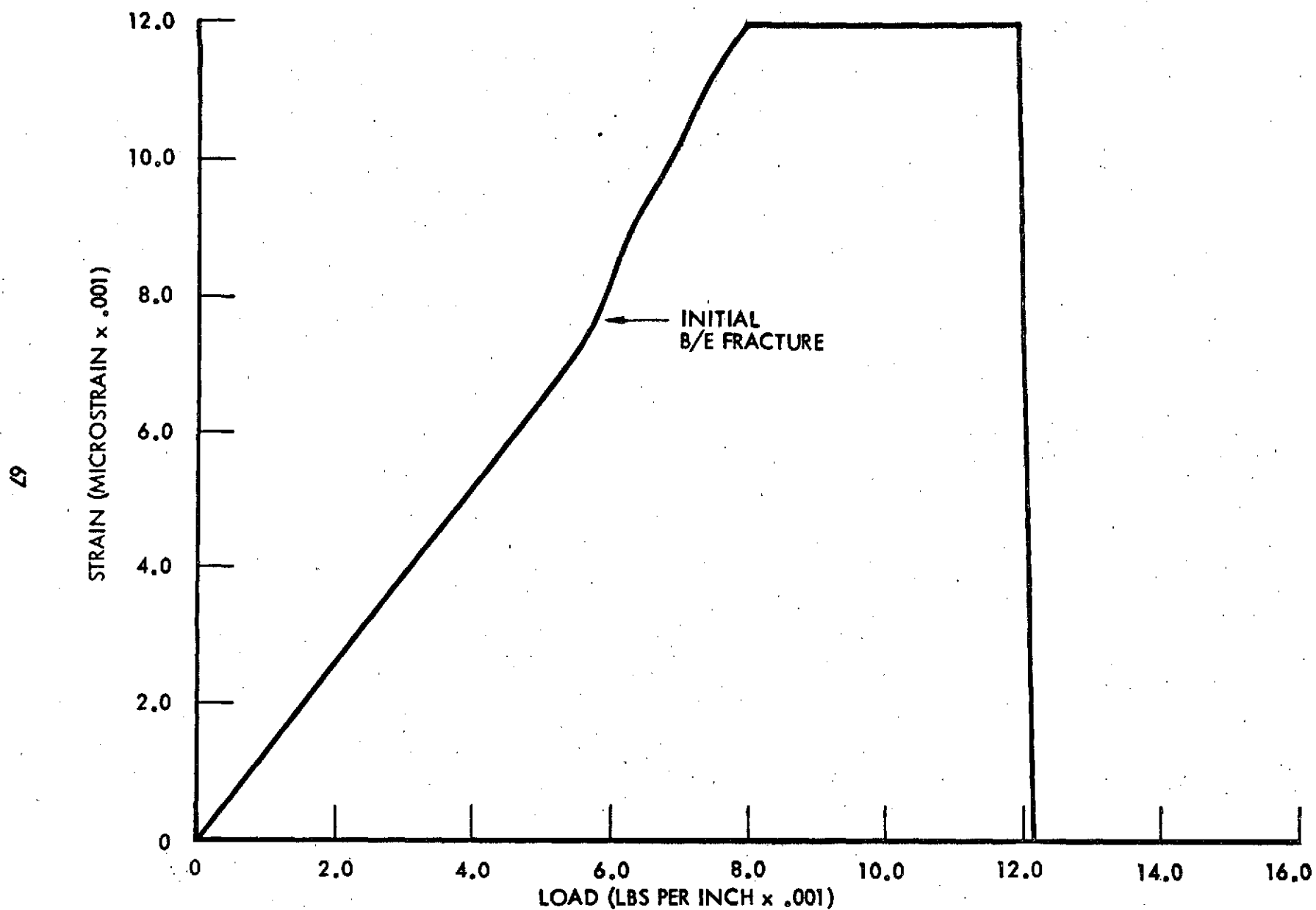
GAGE 1
(FREE FIELD)

Figure 25: TITANIUM CLAD BORON COMPOSITE TESTS SPECIMEN NO. SG-6



GAGE 3
(HOLE ON TITANIUM)

Figure 26: TITANIUM CLAD BORON COMPOSITE TESTS SPECIMEN NO. SG-6



GAGE 4
(IN HOLE ON B/E)

Figure 27: TITANIUM CLAD BORON COMPOSITE TESTS SPECIMEN NO. SG-6

| SPECIMEN | LAY - UP | % B/E AT HOLE | MAXIMUM INITIAL K ₁ | | B/E FRACTURE STRAIN $\mu\epsilon$ | FREE FIELD ULTIMATE $\mu\epsilon$ | NOTES |
|----------|-------------|------------------|--------------------------------------|------|--|---|---|
| | | | B/E | TI | | | |
| SG-1 | 16/0 - 90/A | 47.1 | 4.66 | -- | 7700 | 4000 | FAILURE OCCURED AT THE HOLE |
| SG-2 | 16/0-90/B | 68.9 | 5.13 | -- | 6800 | 4250 | FAILURE OCCURED AT THE HOLE |
| SG-3 | 16/0-90/B | 100 | 6.75 | -- | 6750 | 1380 | NO TI CLADDING. FAILURE OCCURED AT THE HOLE |
| SG-4 | 16/0-90/B | 42.2 | 4.0 | 3.53 | 6300 | 4270 | SPECIMEN WITH CHEM-MILLED CLADDING FAILURE OCCURED IN THIN SECTION WITH 0.020 CLADDING |
| SG-5 | 32/0-90/BL | 41.3 | 3.95 | 3.00 | 7400 | 4860 | FAILURE OCCURED AT THE HOLE |
| SG-6 | 16/0-90/BL | 46.8 | 3.72 | 3.12 | 7400 | 8100 | FAILURE OCCURED AT THE HOLE |

Figure 28: STRAIN CONCENTRATION DATA COMPARISONS

Strain data from specimen SG-4 (Figure 22) indicates that the strains measured by SG-1 (at the edge of the specimen on the reinforcement land) are 70% of the free-field values given by SG-9. The SG-1 strain can be treated as the average strain in the reinforced land section and is 9% higher than predicted by the relation given in Appendix A.

4.2 Shear Web Element Testing

Two tests of shear web elements (18 by 25 in.) were conducted to substantiate the design web with respect to edge joint details, stiffener-to-web attachment and laminate strength. The two web elements were placed in one side of a center-loaded test beam and loaded to failure at 345,000 lb. and 334,000 lb., respectively. In both tests, 400 load cycles to 195,000 lb., which corresponds to the limit shear loading in the design web, were applied prior to loading to failure. Details of the shear web element are given on Dwg. SK-25085-112 in Appendix B. The web elements are identical to the full-scale baseline design web except for plan configuration and stiffener details. The chem-milled nominal laminate panels are visible in the photographs that follow. The stiffeners are not reinforced with B/E but have identical web and attachment leg gages (.090 in.) as in the baseline design web.

Figures 29 and 30 illustrate the failed web element number 1. The stiffeners appear to have functioned properly in precluding buckle propagation past the stiffeners in both tests. Failure of the element occurred by tearing at the stiffener fastener holes along a diagonal line as shown by Figure 31 which is a view of the web element with the titanium chem-milled off.

Figures 32 to 35 are close-up views of the respective corners marked in Figure 31; these views demonstrate that in no case did the step-lap joint corner splice details fail to function properly; there is no evidence of bondline or B/E failure in these areas. In corner B (Figure 33), the step-lap butt splices are intact in spite of large yield deformations visible in Figure 31. In corner D (Figure 35) the B/E ply is shown to be unfractured where it crosses the step-lap butt splice (a resin ridge appears in the photograph).

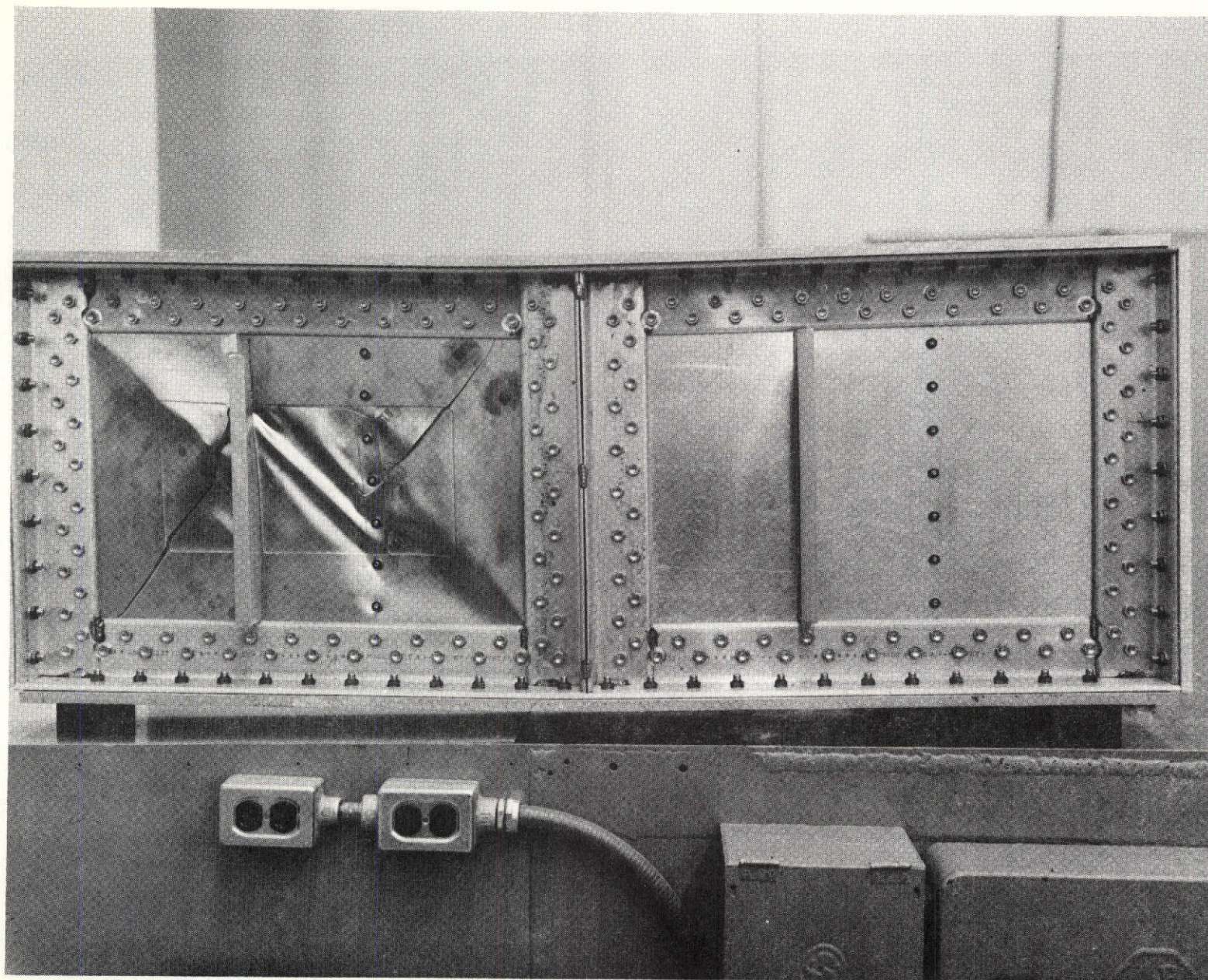


Figure 29: FAILED SHEAR WEB ELEMENT 1 IN TEST FRAME

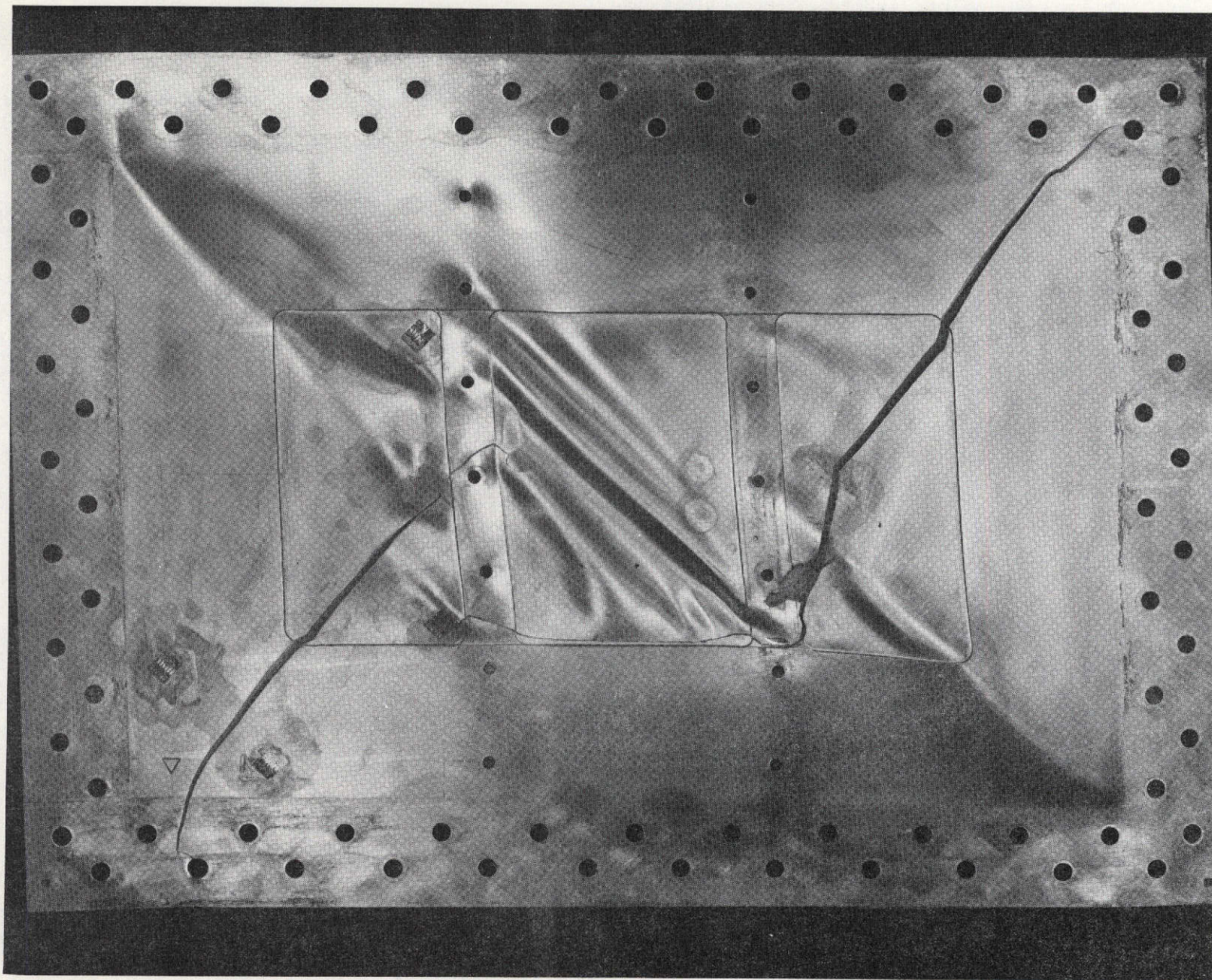


Figure 30: WEB ELEMENT NO. 1

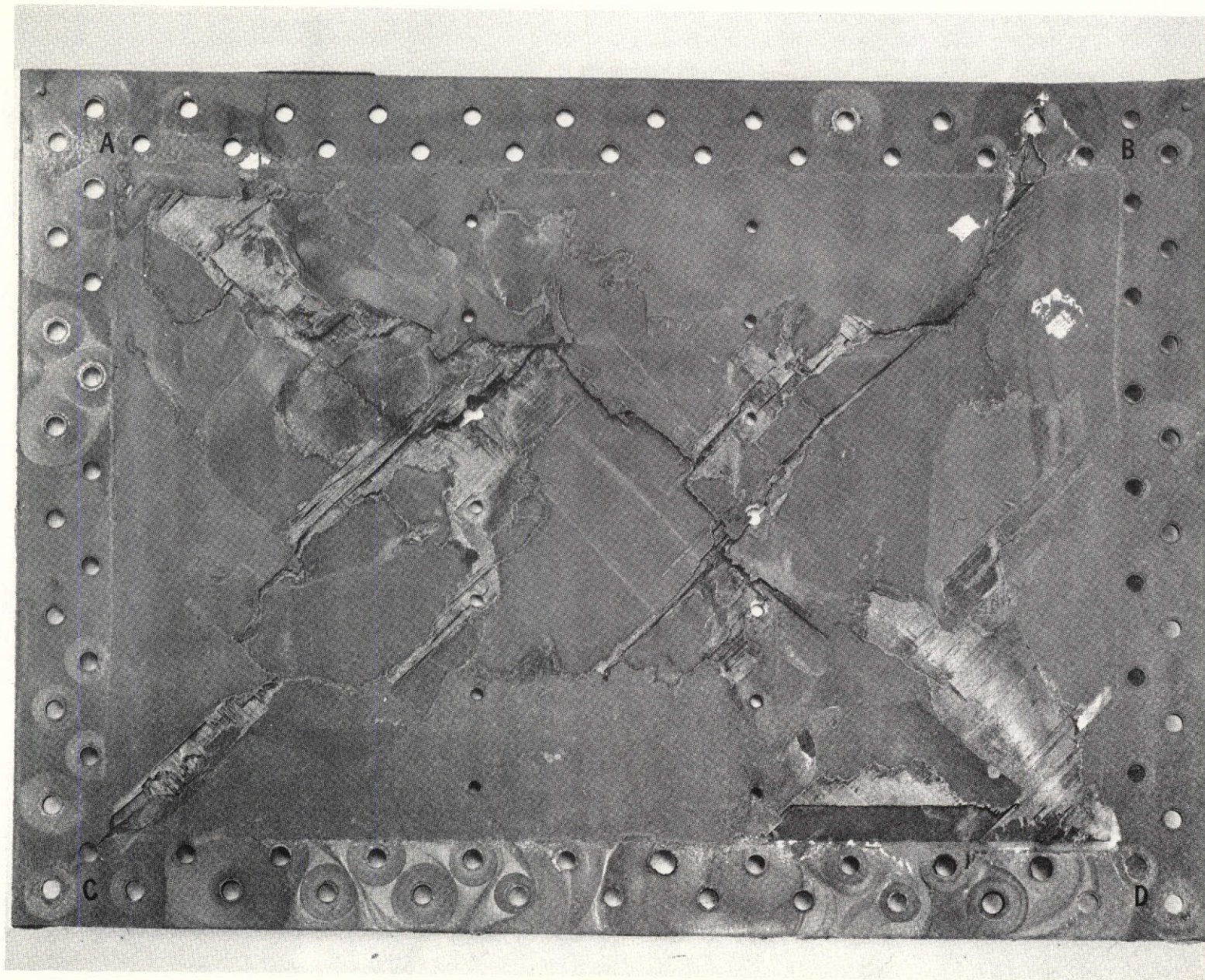


Figure 31: TEST WEB ELEMENT NO. 1 (Ti-CLADDING CHEM-MILLED OFF)

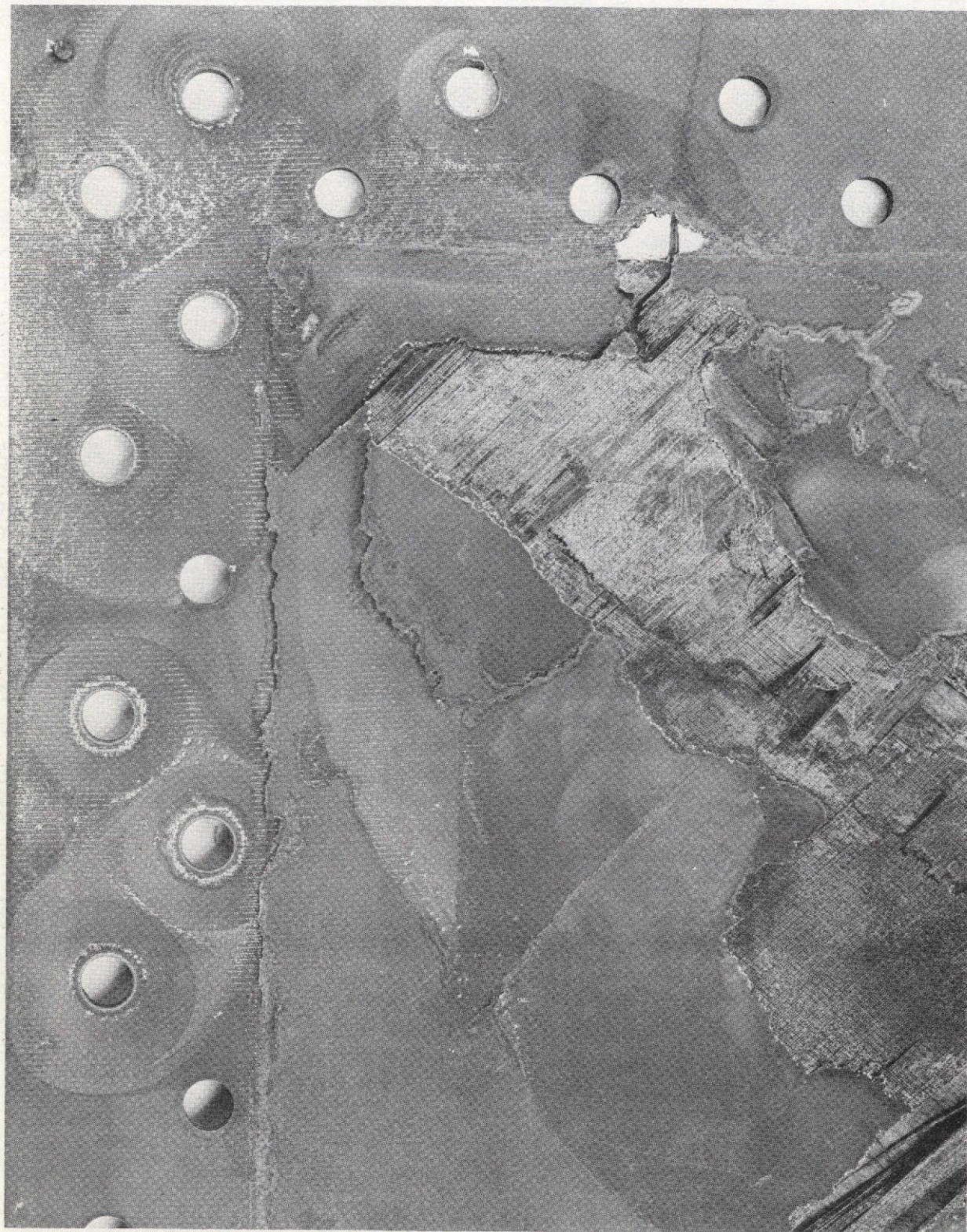


Figure 32: CORNER A

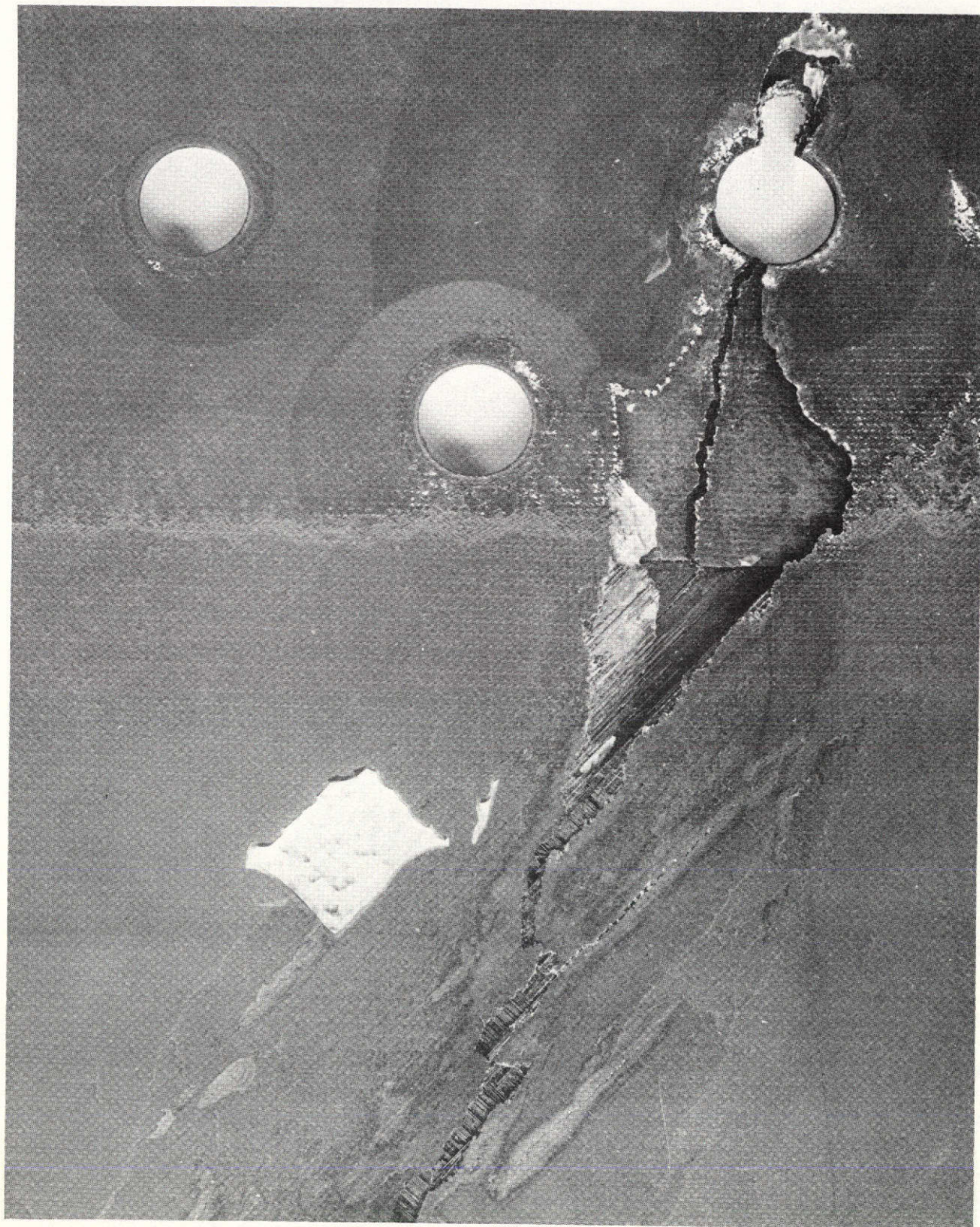


Figure 33: CORNER B

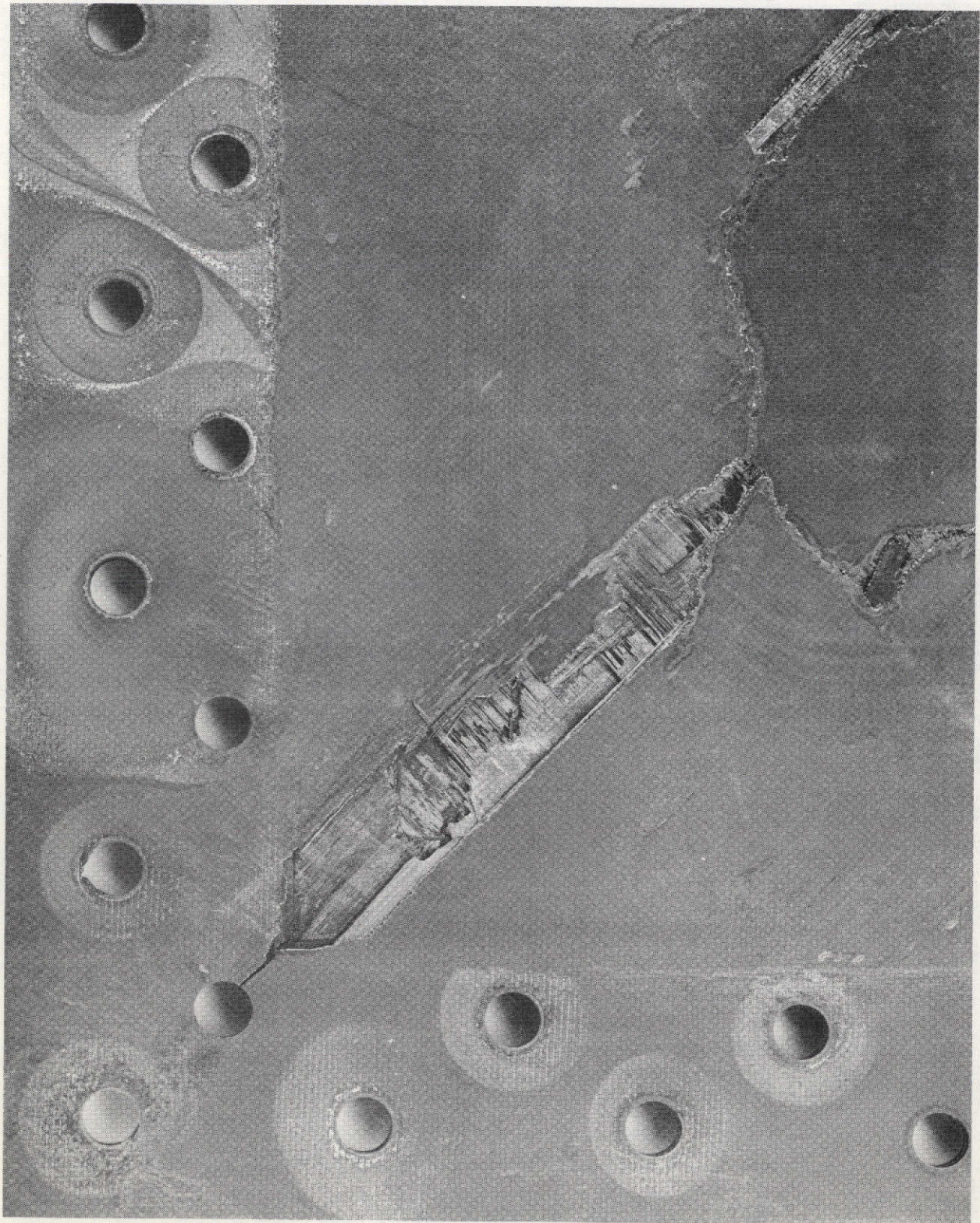


Figure 34: CORNER C

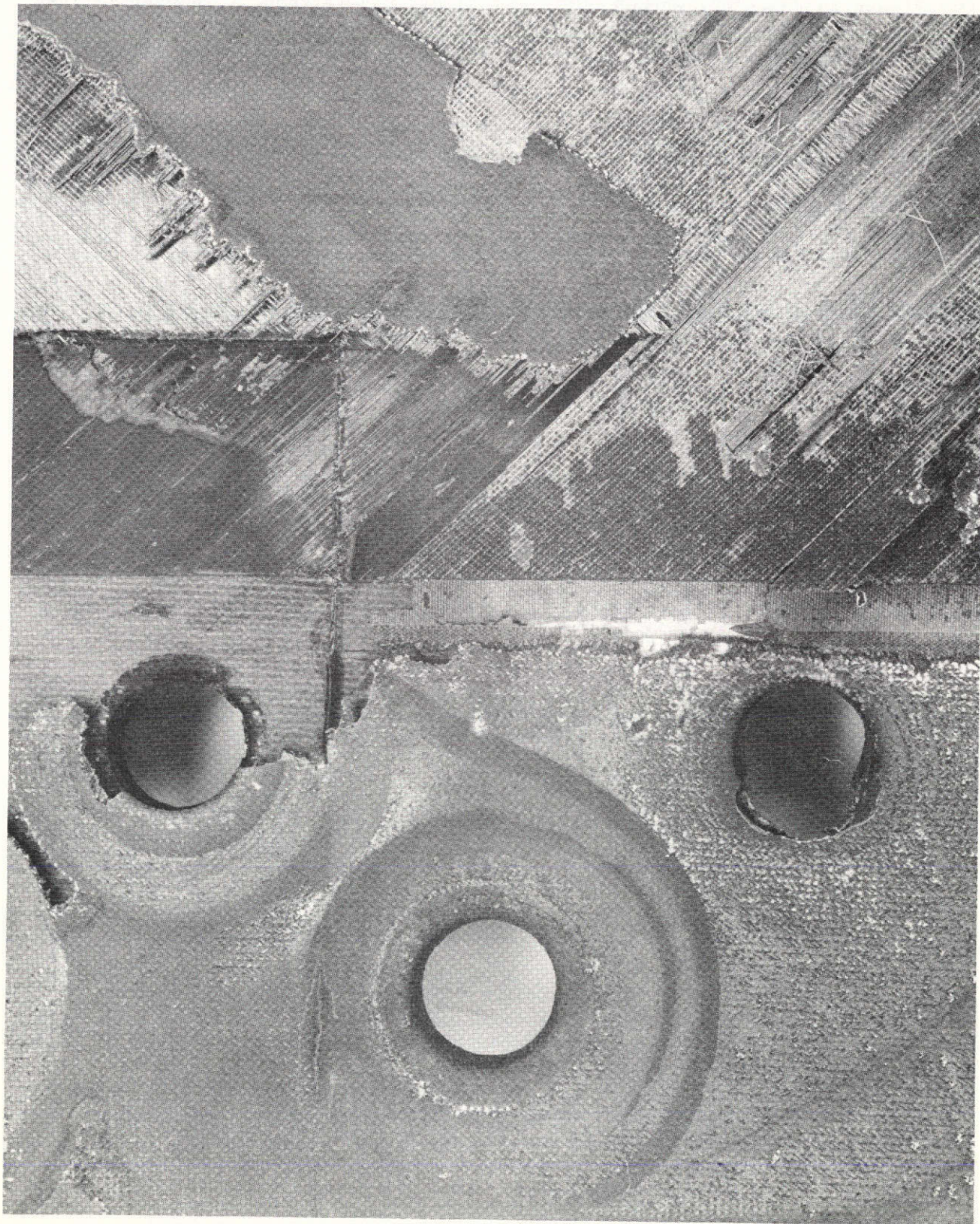


Figure 35: Corner D

Figure 36 shows the second web element that was tested. Less post-failure deformation was produced because of less load machine head travel after fracture of the B/E material. An x-ray of the web element taken after failure is shown in Figure 37; the B/E tension fracture patterns are clearly visible and intersect the holes along a diagonal line. Figure 38 is a typical x-ray of a corner step-lap detail after testing which indicates that no failure occurred in the step-lap splice areas.

The peak principal strain conditions experienced by the web elements are shown in Figure 39. These principal strains were computed from strains measured by the rosette strain gages that are indicated as SG-8, etc. The tension strains shown, while probably not the highest tension strains existing in the nominal laminate area, are above the baseline design web requirement of 4741 $\mu\epsilon$ given in Figure 11. The peak principal compression and shear strains also have high magnitudes. On a shear loading basis, the average ultimate shear load is 9400 lb/in. which is 23.5% above the design requirement. However, the average flange strain due to beam bending is calculated to be 1740 $\mu\epsilon$ at the beam quarter point compared to the design requirement of 4000 $\mu\epsilon$, which allows the higher shear loading. The tests demonstrated the capability of the reinforced baseline design laminate to carry the required diagonal tension load.

Figure 40 presents the strain gage locations for web element number 1. Also shown is the finite element grid employed in the NASTRAN analysis to be discussed later. In this test, rosette gages were located in the nominal laminate areas and on the reinforced step-lap joint areas. Figures 41 to 46 are plots of the principal strains and angles computed from digitalized strain data

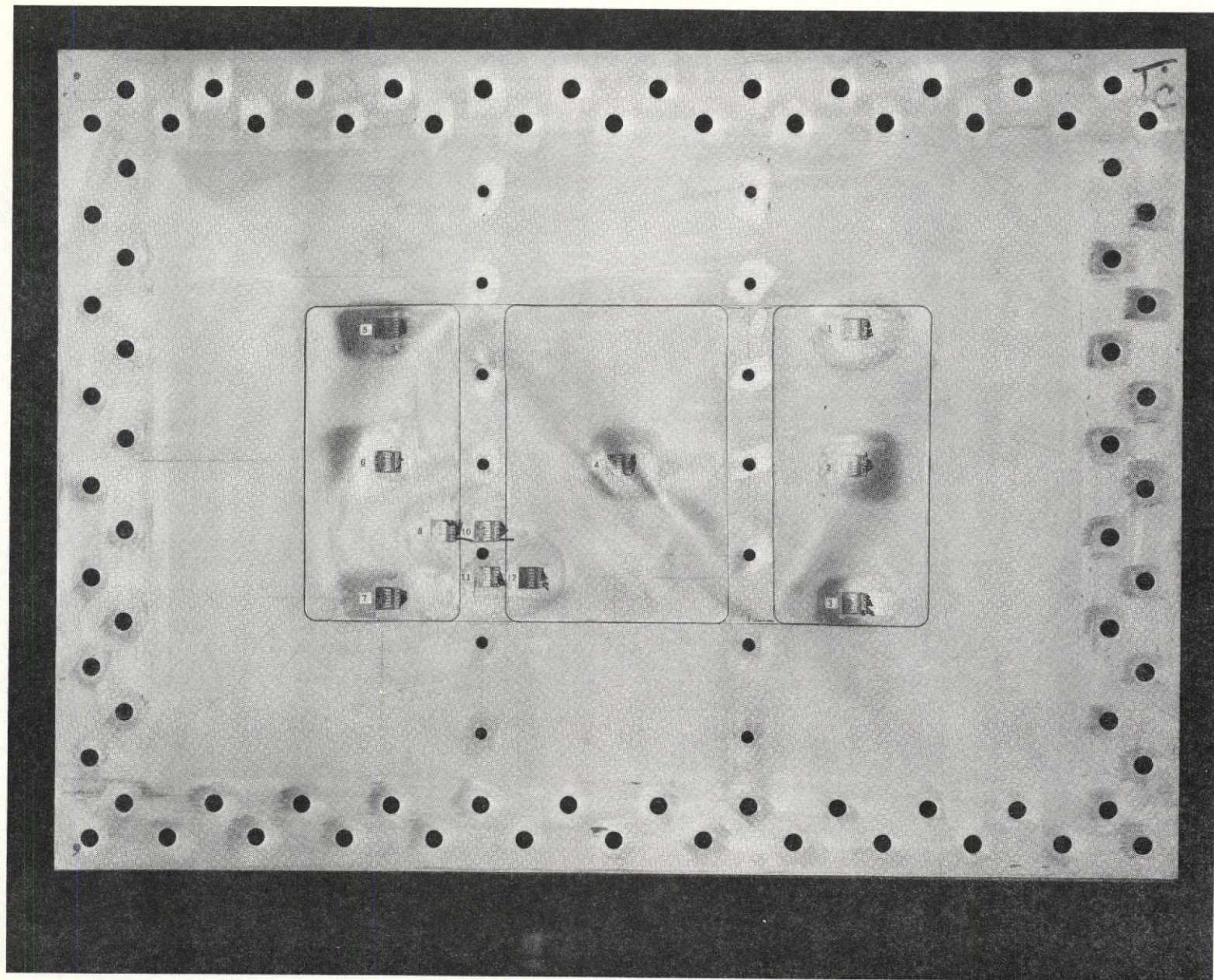


Figure 36: WEB ELEMENT NO. 2

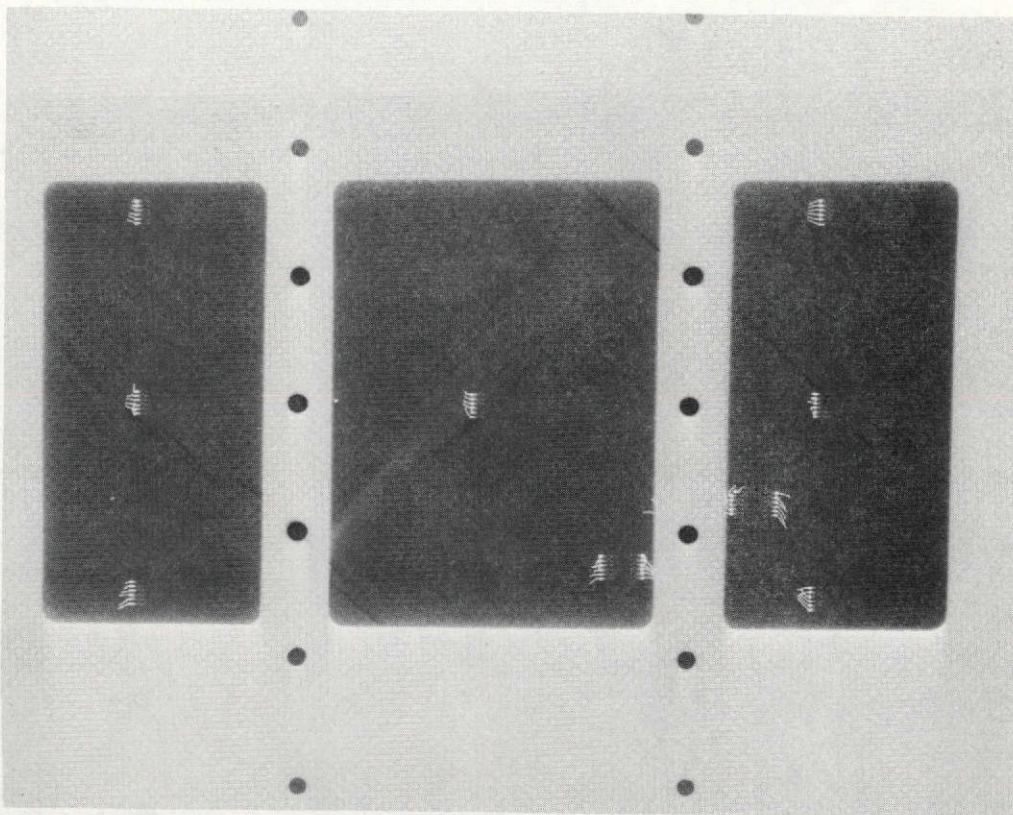


Figure 37: X-RAY OF SHEAR WEB ELEMENT NO. 2 AFTER TEST

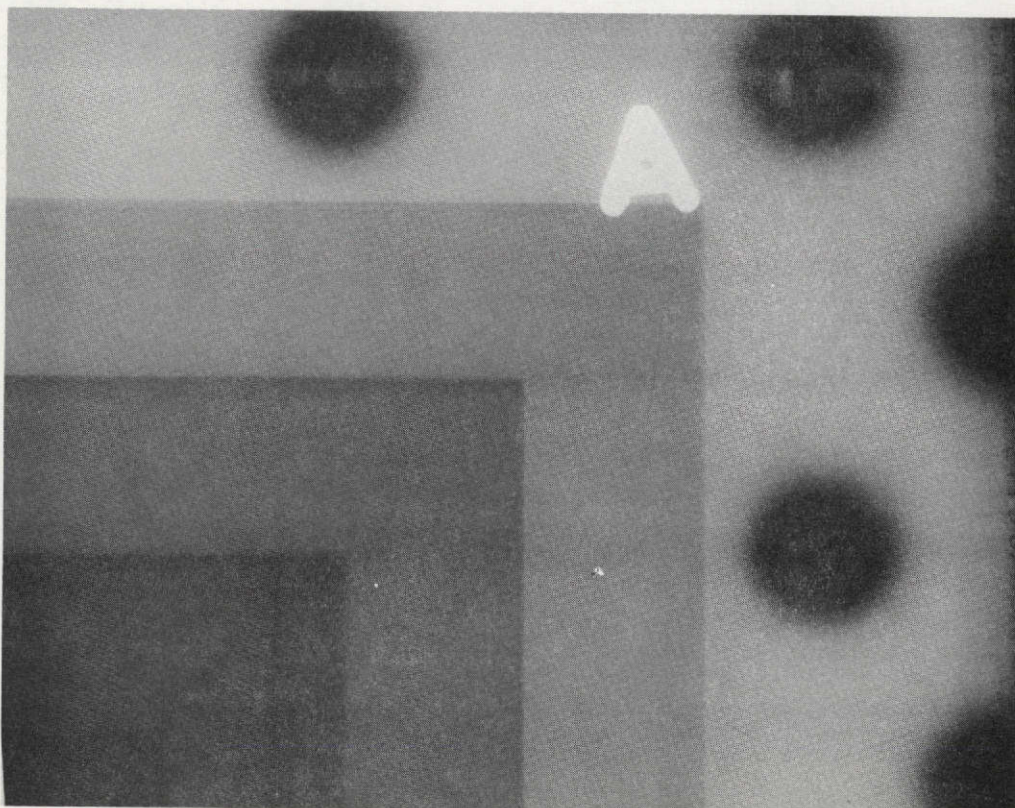
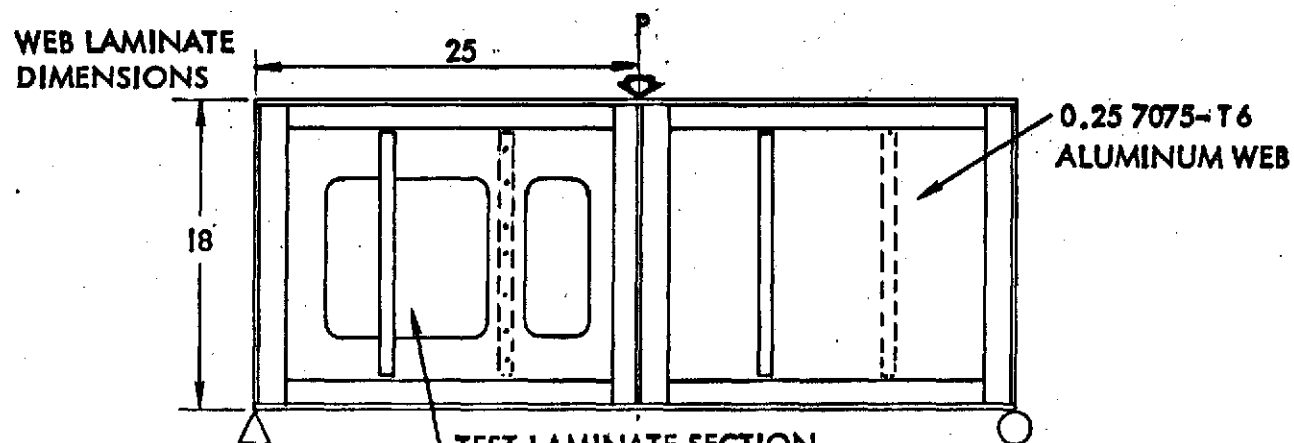


Figure 38: X-RAY OF SHEAR WEB ELEMENT AT REACTION CORNER AFTER TEST



TEST LAMINATE SECTION
(REF. DWG. SK2-5085-112)
BASE LINE NOMINAL LAMINATE SECTION

$16 \pm 45^\circ$ B/E plies
0.020, 6AL - 4V M.A. TI CLADDING

STEP - LAP EDGE DETAILS AND CLADDING REINFORCEMENT
SIMILAR TO LARGE SCALE TEST WEB LAMINATE
(REF. DWG 2-5085-117).

ELEMENTS CYCLED 400 CYCLES 0 TO 195000 LB PRIOR TO FAILURE

| WEB LAMINATE SPECIMEN | P_{ULT} | MAXIMUM PRINCIPAL STRAINS IN NOMINAL LAMINATE SECTION (CALCULATED FROM STRAIN GAGE DATA) $\mu\epsilon$ | | |
|-----------------------|-----------|---|--------------|--------------|
| | | TENSION | COMPRESSION | SHEAR |
| 1 | 345000 | 5300 (SG-8) | -7200 (SG-7) | 11500 (SG-7) |
| 2 | 334000 | 5200 (SG-13) | -7200 (SG-6) | 11600 (SG-8) |

Figure 39: SHEAR WEB ELEMENT TEST BEAM

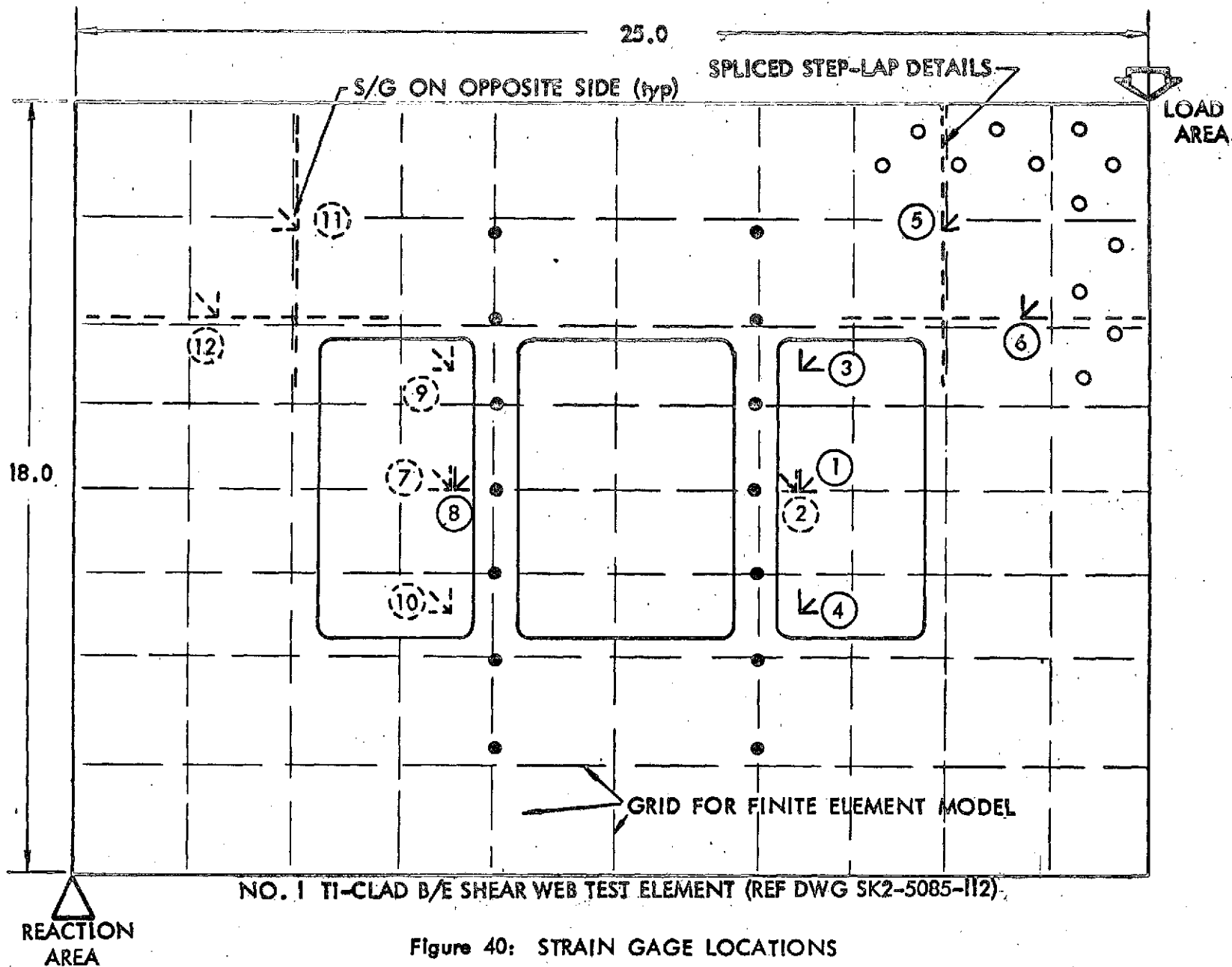


Figure 40: STRAIN GAGE LOCATIONS

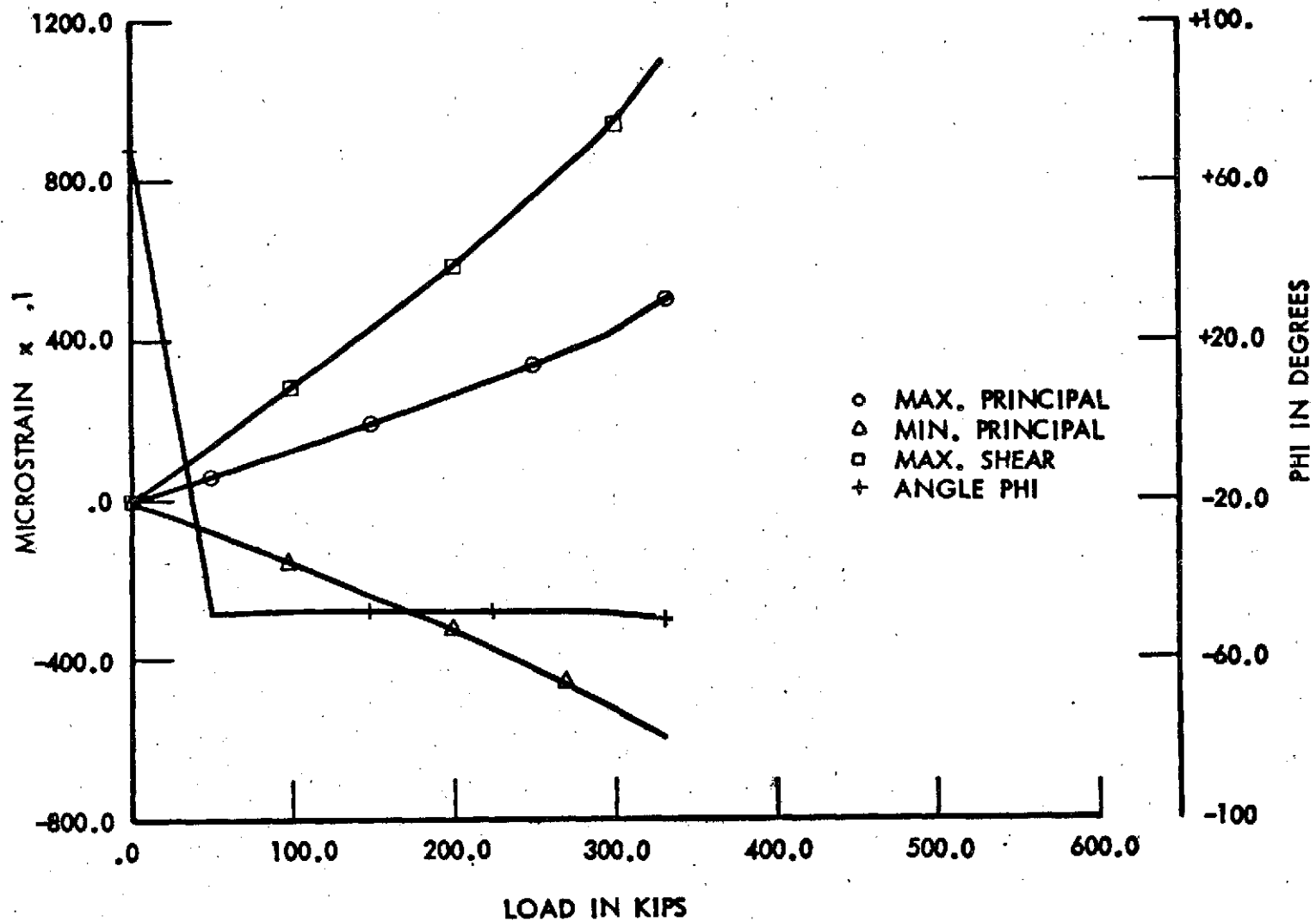


Figure 41: PRINCIPAL STRAIN DATA FOR WEB ELEMENT 1 ROSETTE NO. 1

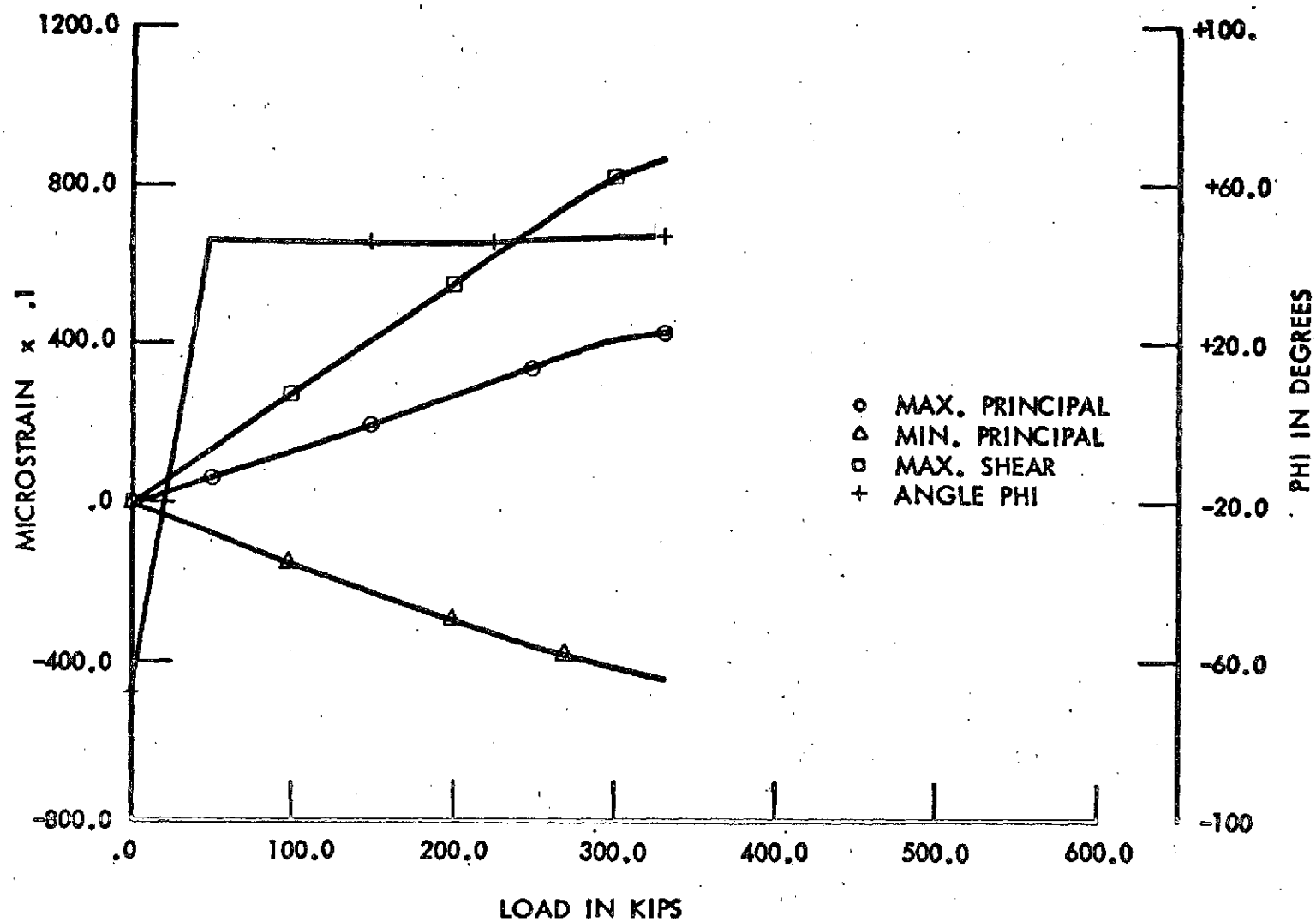


Figure 42: PRINCIPAL STRAIN DATA FOR WEB ELEMENT 1 ROSETTE NO. 2

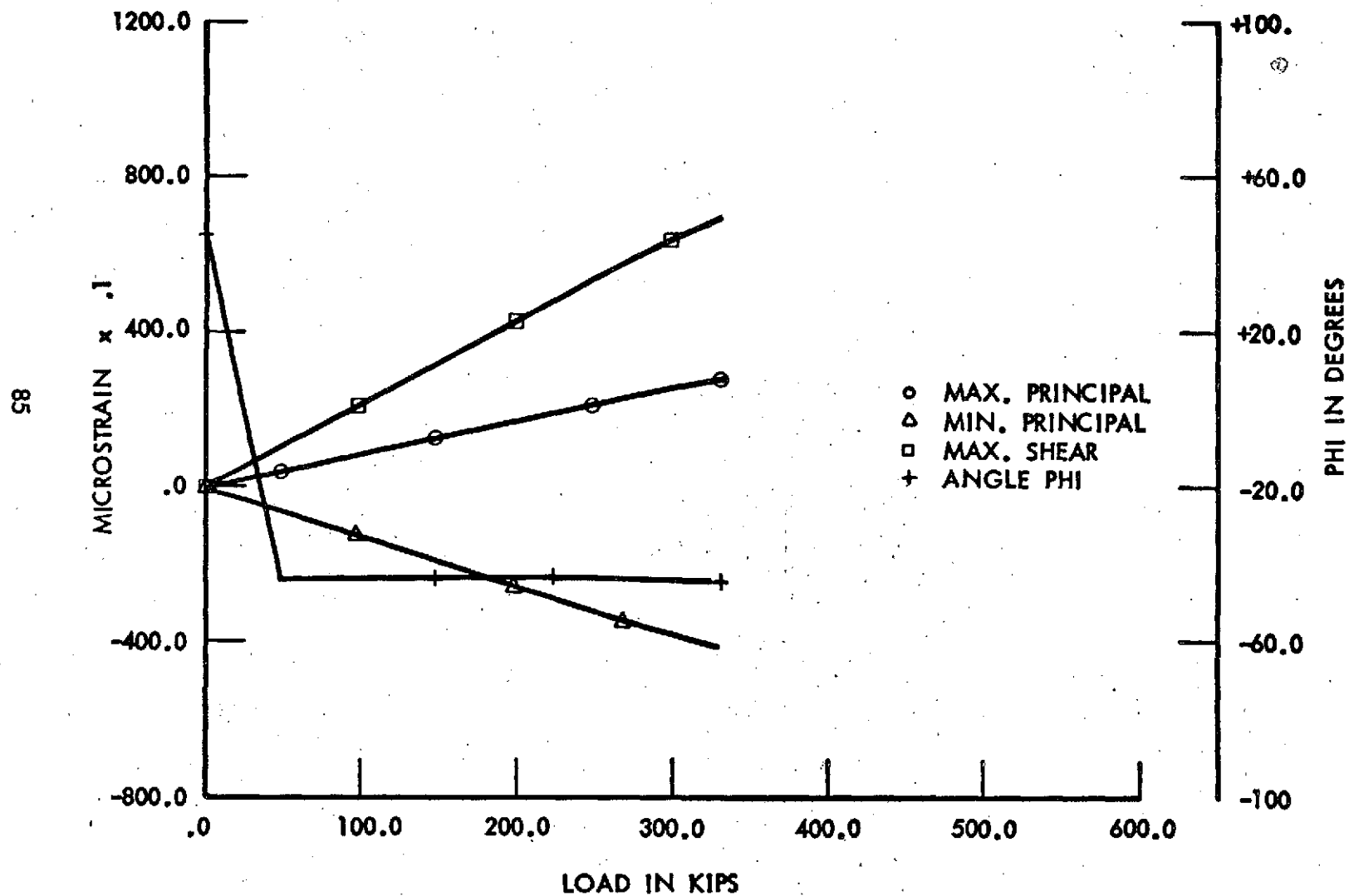


Figure 43: PRINCIPAL STRAIN DATA FOR WEB ELEMENT 1 ROSETTE NO. 5

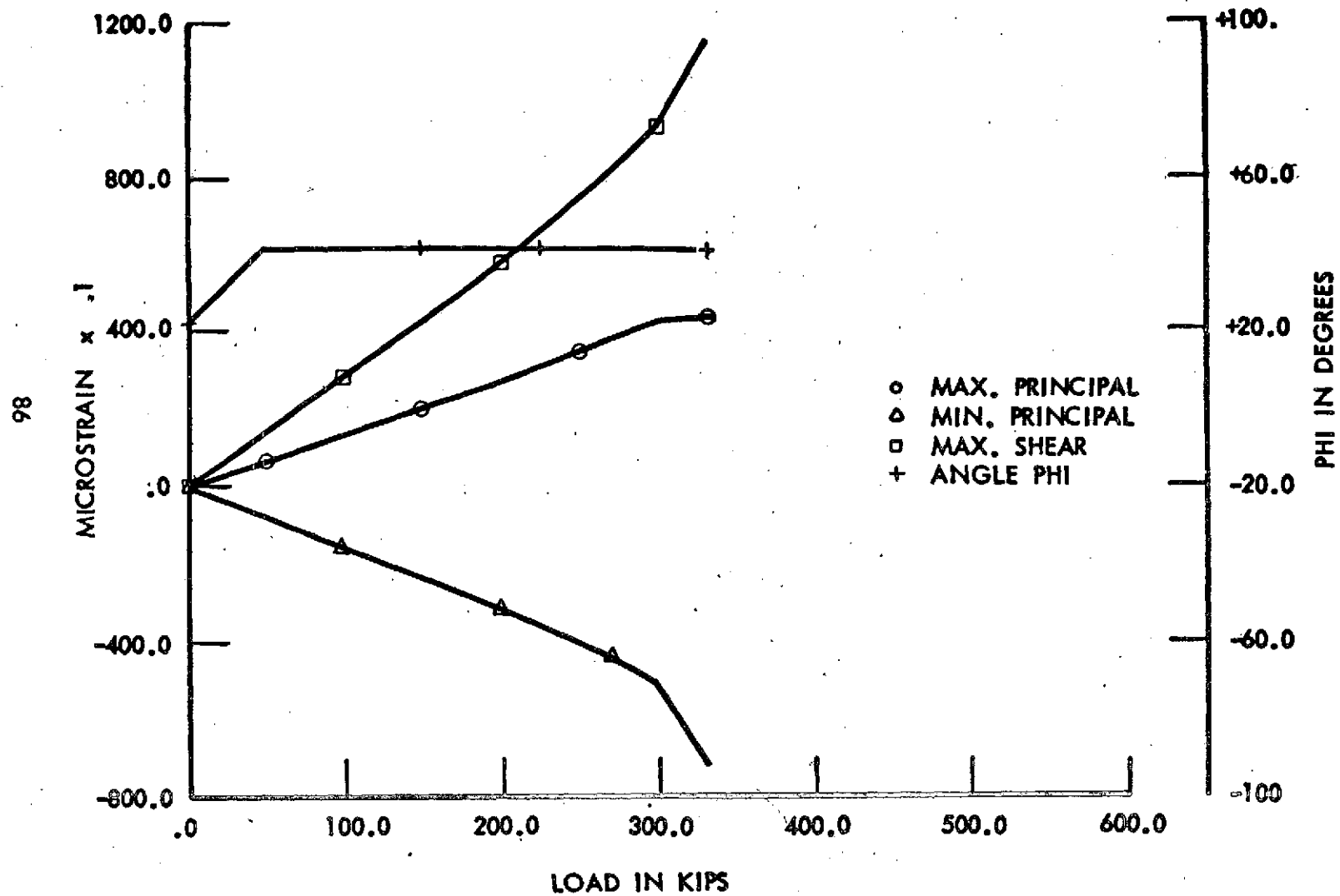


Figure 44: PRINCIPAL STRAIN DATA FOR WEB ELEMENT 1 ROSETTE NO. 7

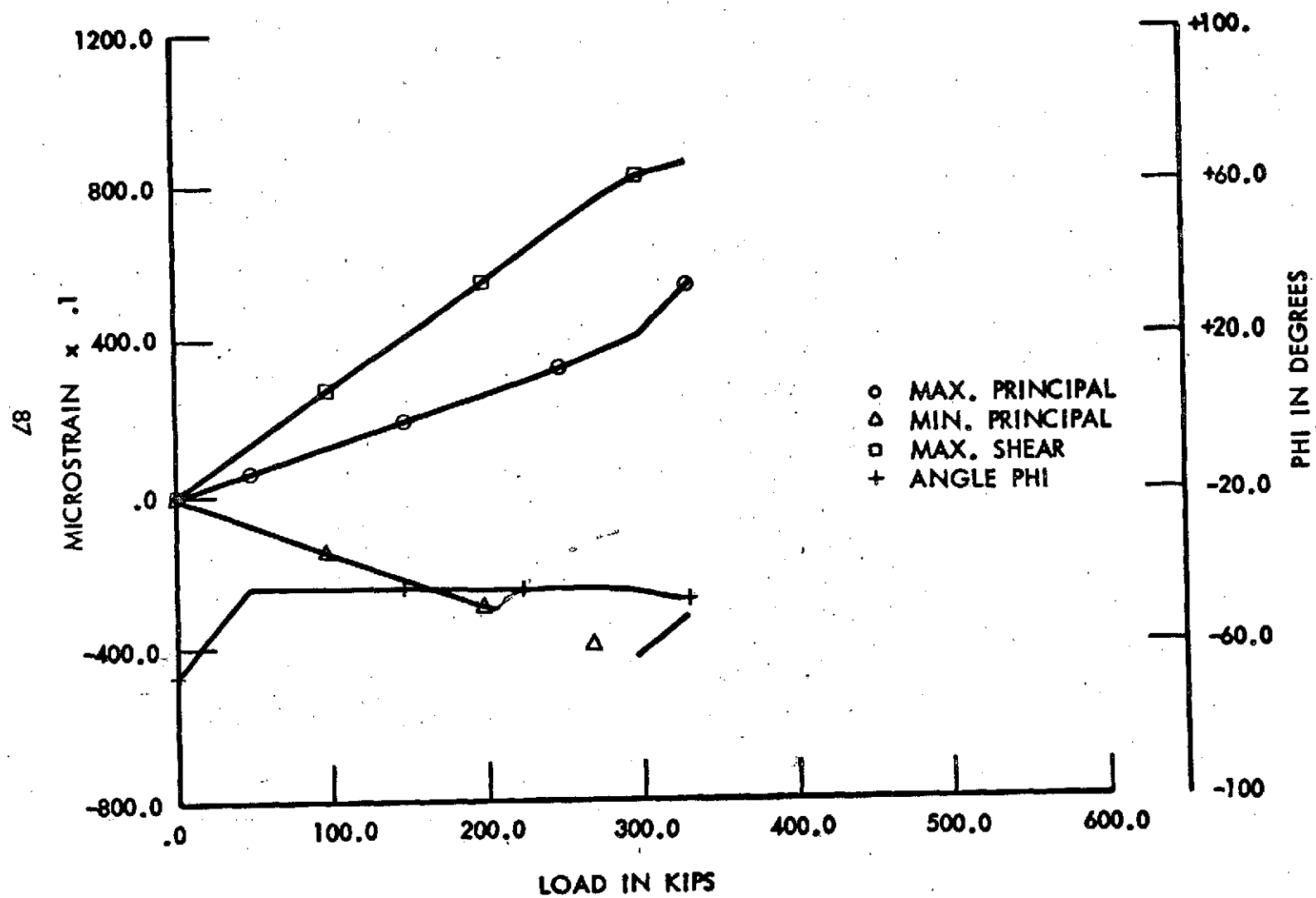


Figure 45: PRINCIPAL STRAIN DATA FOR WEB ELEMENT 1 ROSETTE NO. 8

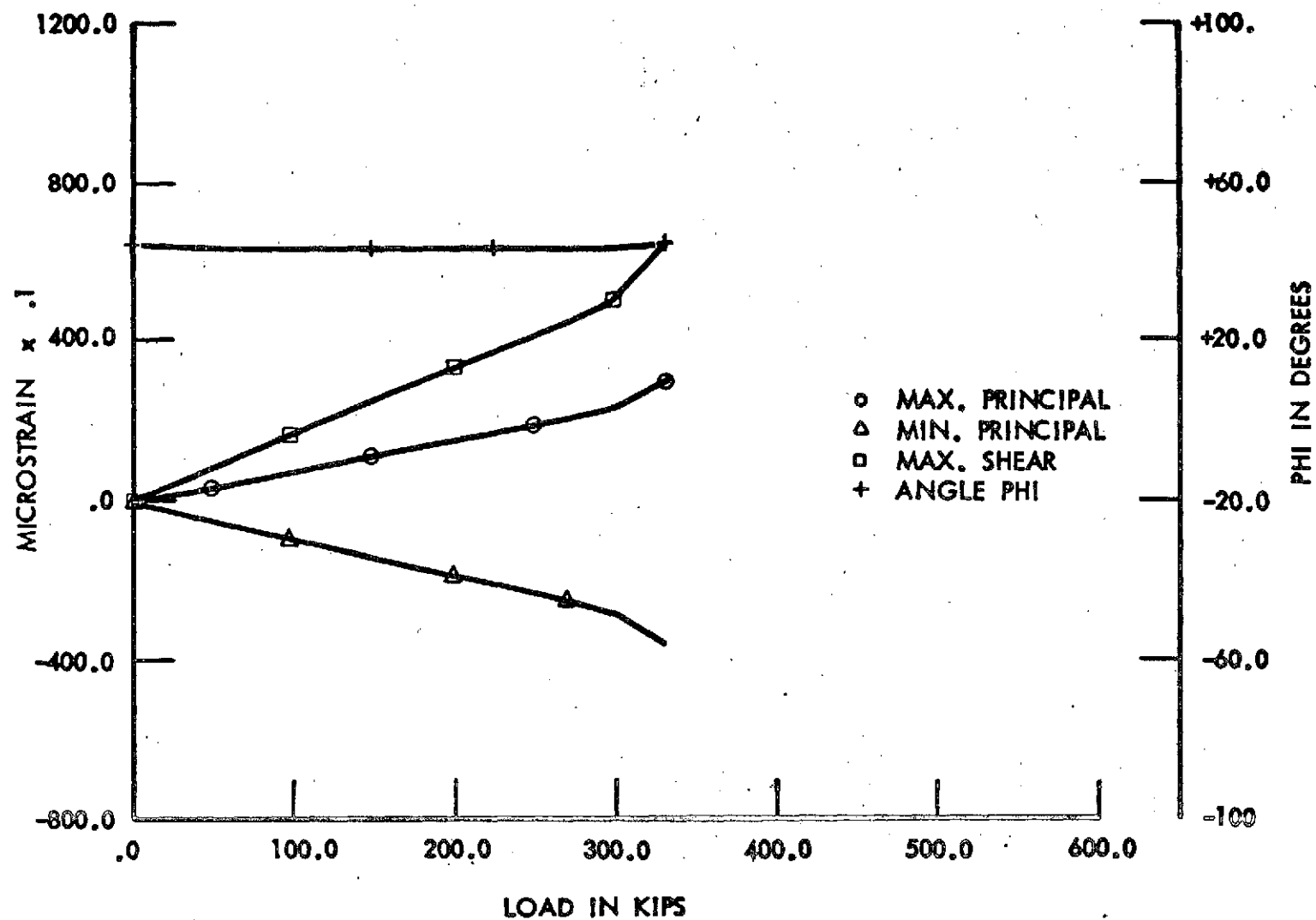


Figure 46: PRINCIPAL STRAIN DATA FOR WEB ELEMENT 1 ROSETTE NO. 12

recorded for the gages noted. The principal tension angle is with respect to the vertical axis and is correctly plotted above 50,000 lb. load. Significantly reduced strain levels exist in the reinforced joint areas as indicated by gages SG-5 and SG-12.

The peak strains are associated with the back-to-back gages SG-7 and 8 with a definite display of buckling response. At the failure load, the SG-7 strains give an effective von Mises stress in the cladding that is $125,000 \text{ lb/in.}^2$ which is close to the titanium allowable yield stress ($126,000 \text{ lb/in.}^2$) and well past the proportional limit. Therefore, inelastic buckling deformations were occurring which testifies to the toughness of the laminate. Since the response is linear considerably past the limit shear load level of 195,000 lb., the web-element laminate is considered to be shear resistant.

The gage locations for web element number 2 are shown in Figure 47. Gages were placed in this test on the nominal laminate and reinforced stiffener land areas. Figure 48 presents the measured tension and compression strains for the stiffener land gages SG-10 and SG-11, which very nearly are principal strains. The data plot discontinuities which occurred at 200,000 lb load are a result of machine loading control switchover from manual to a function (ramp) generator. This switchover inadvertently resulted in a change in loading rate from the 300 kips/min rate followed to the limit load (195,000 lb), to 1,500 kips/min from limit load to the failure load (320,000 lb). By extrapolating the linear portion of the tension data out to the failure load and treating the resulting strain of 4400 $\mu\epsilon$ as the middle surface strain, a value for maximum tension strain is obtained which is plotted with the tension element data in Figures 18 and 19. The correlation between the tension element and the shear element test data is

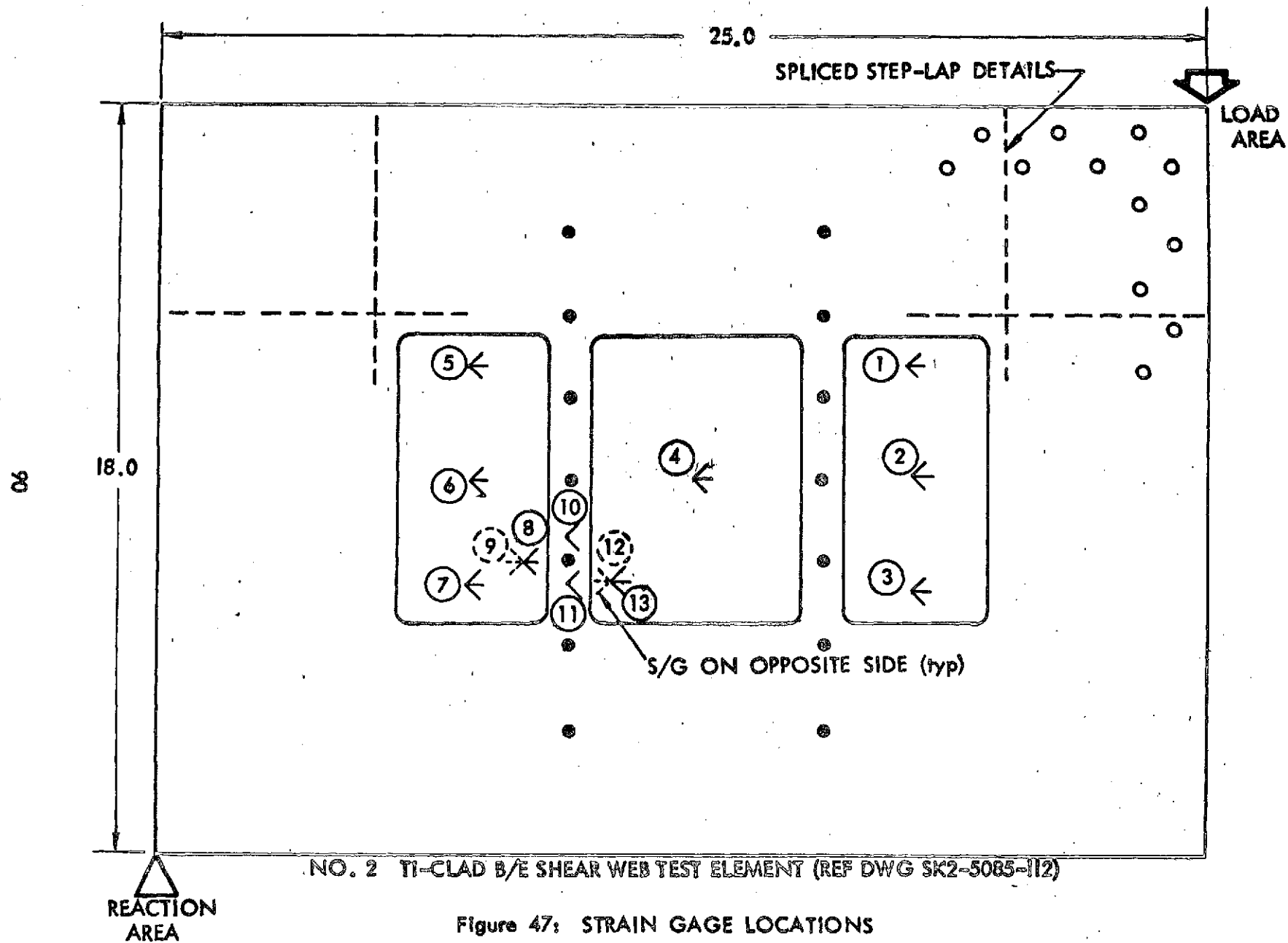


Figure 47: STRAIN GAGE LOCATIONS

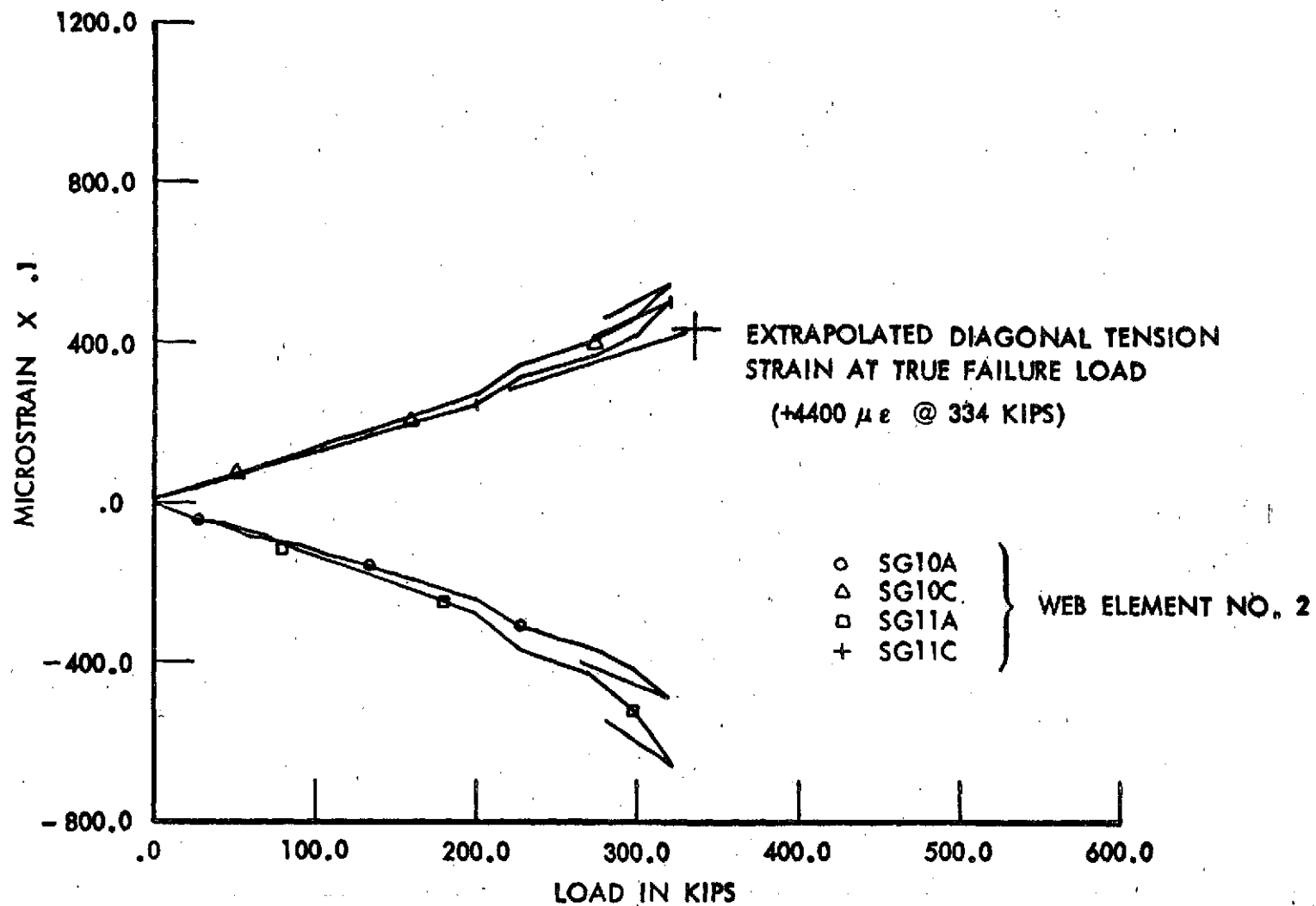


Figure 48: REINFORCED CLADDING STRAIN DATA USED IN TENSION ELEMENT DATA CORRELATION

good. The measured strains from SG-10 and SG-11 (on stiffener land) are almost as high as the strains in the adjacent unreinforced titanium area which indicates bending effects are present in these strains. Plots of principal strains and angles for other selected gages are shown in Figures 49 to 52. The data appears to be similar to data from the first web element test.

A finite element model of the shear web element and the test beam framework was established using the NASTRAN code (19) for test data evaluation purposes. The orthotropic plate elements in this model are shown in Figure 53; the orthotropic material properties that pertain to these elements are given in Figure 75 and were derived from the classical laminate analysis results for the respective reinforced and nominal laminate parts (the nominal laminate stiffness data appears in Figure 12). The test structure was load modeled as a symmetric half-span and was analyzed for the ultimate test load condition for web element number 1.

The principal strains and angles given in Figures 54 through 57 were calculated from the results of a NASTRAN static stress analysis. The principal strains are calculated by a separate computer code using classical orthotropic strain analysis and principal strain transformations. The NASTRAN stress data is automatically obtained from the checkpoint/restart tape generated during the NASTRAN run (NASTRAN normally does not place stresses on the checkpoint/restart tape, so a simple "Alter" to checkpoint file OES1 is made).

The principal strain output is printed in a grid format simulating the finite element model grid as shown in Figures 54 to 57. This format, which simulates the plate model given in Figure 53, is convenient in correlating data from strain gage instrumentation.

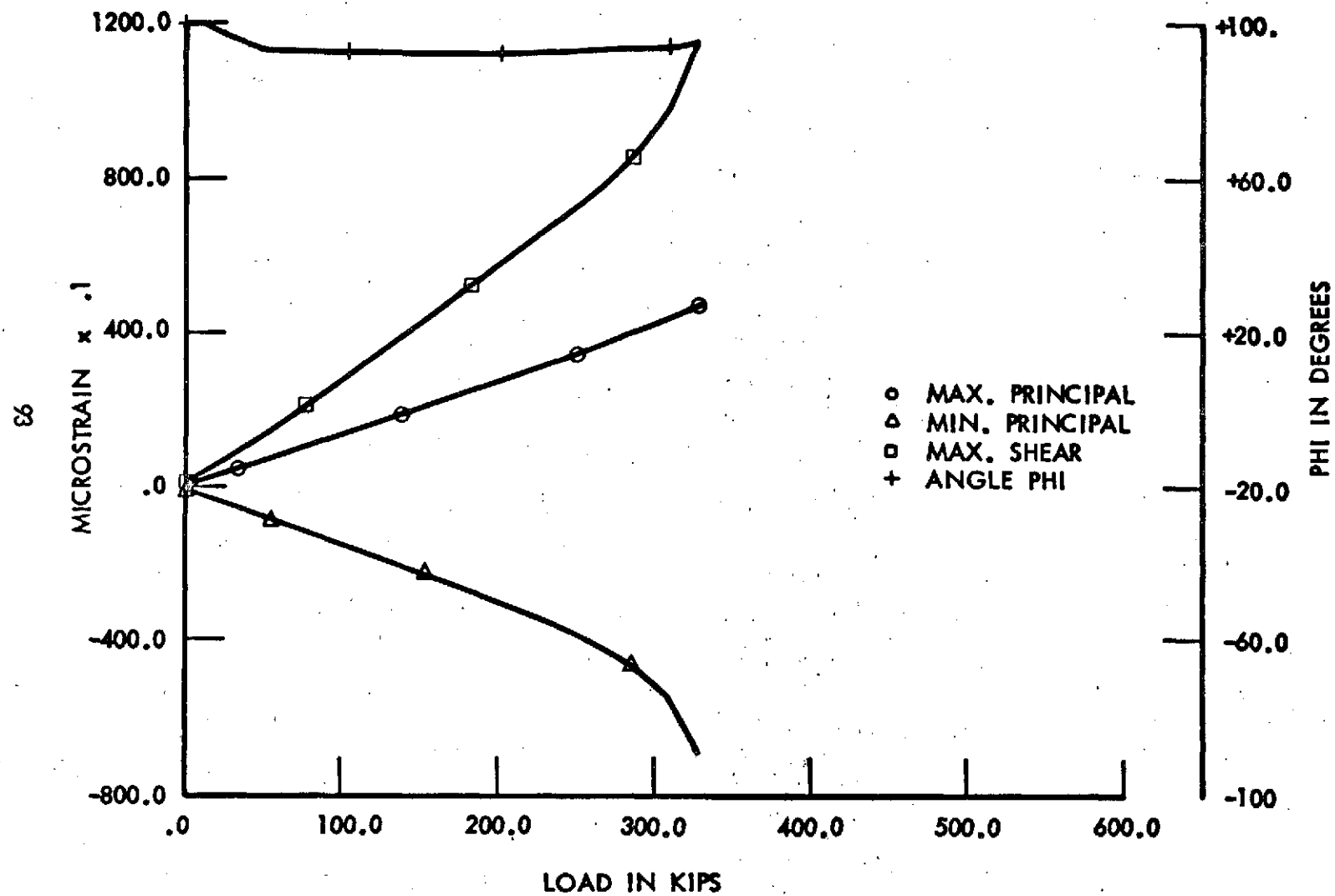


Figure 49: PRINCIPAL STRAIN DATA FOR WEB ELEMENT 2 ROSETTE NO. 8

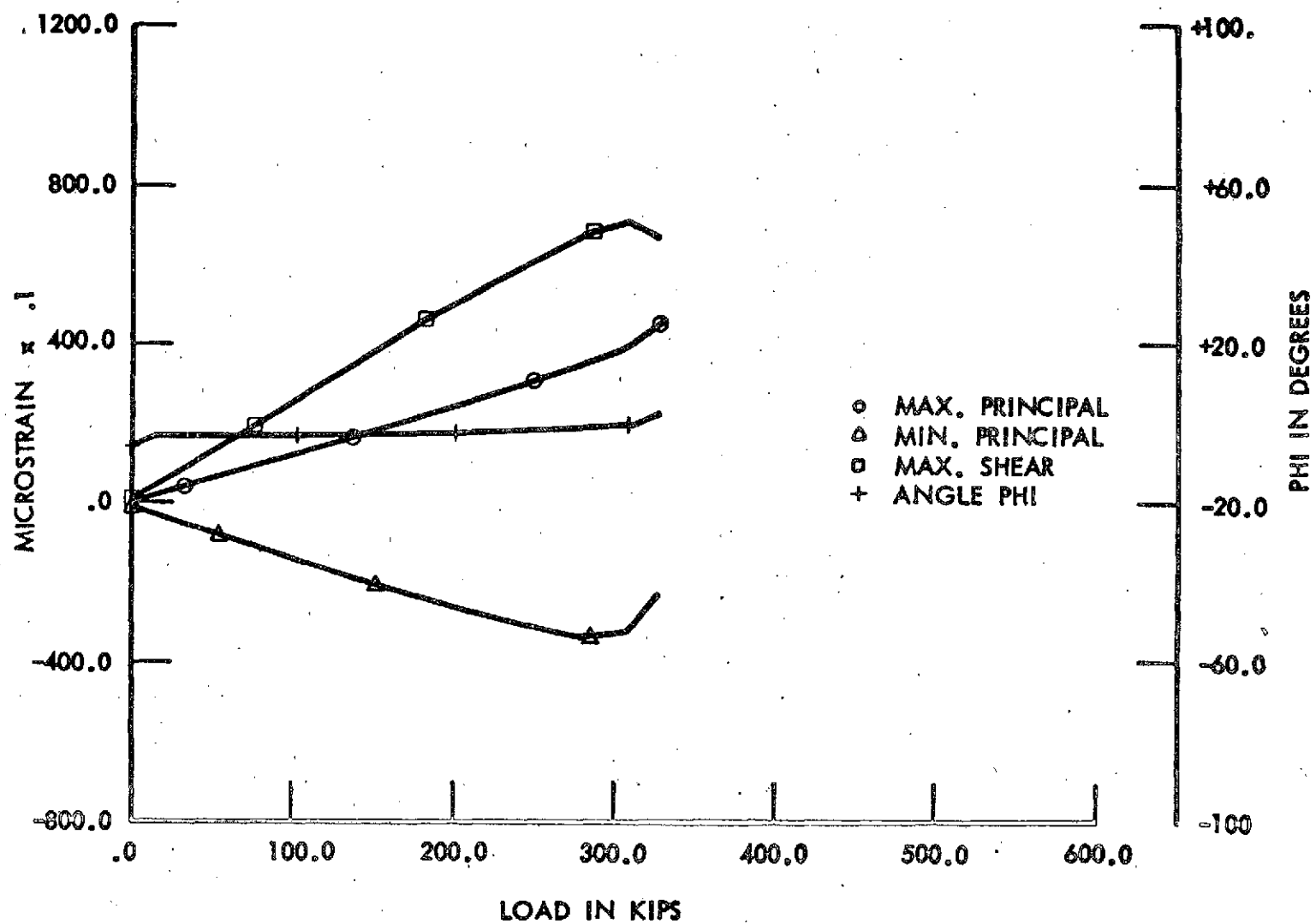


Figure 50: PRINCIPAL STRAIN DATA FOR WEB ELEMENT 2 ROSETTE NO. 9

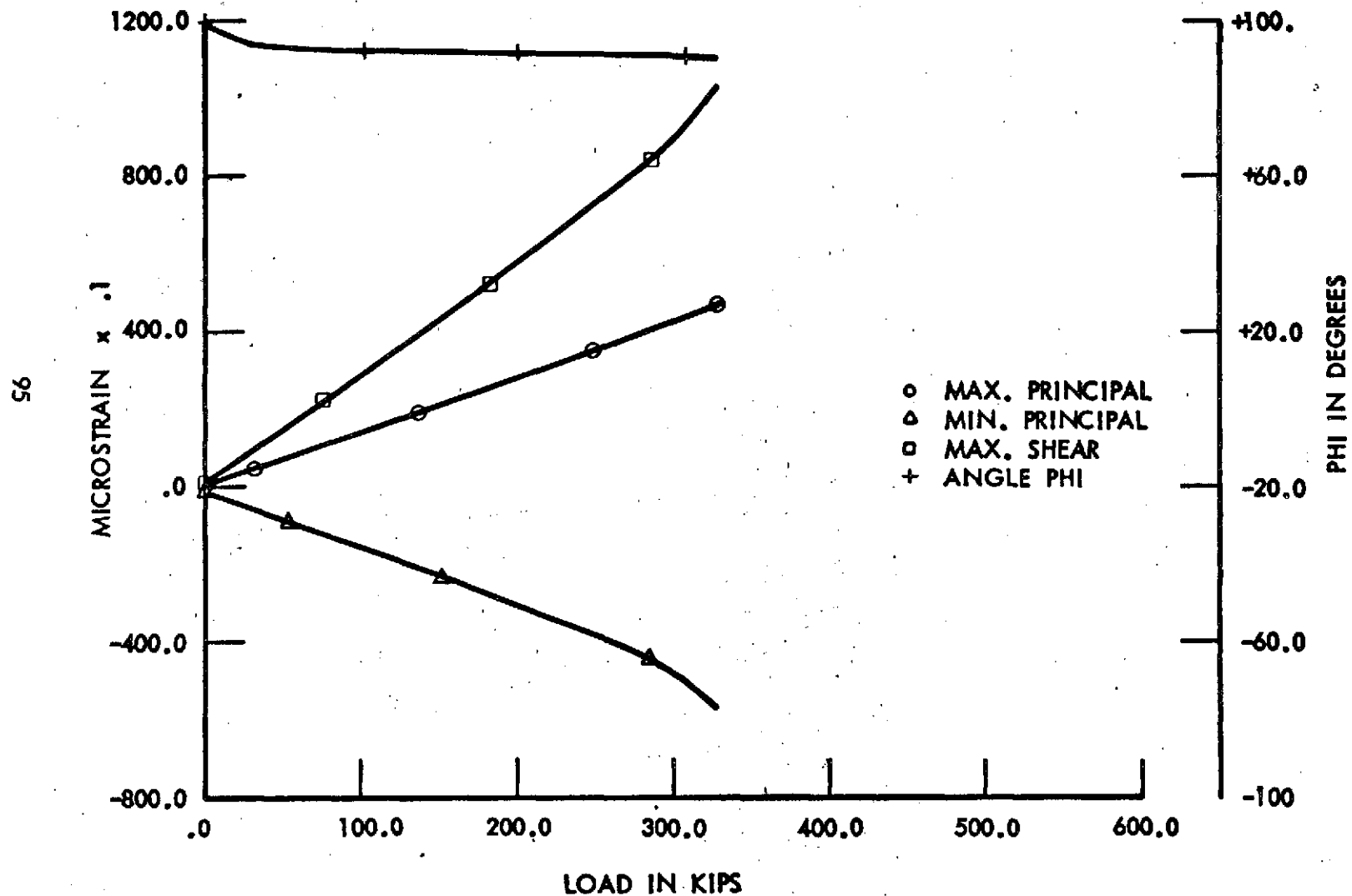


Figure 51: PRINCIPAL STRAIN DATA FOR WEB ELEMENT 2 ROSETTE NO. 12

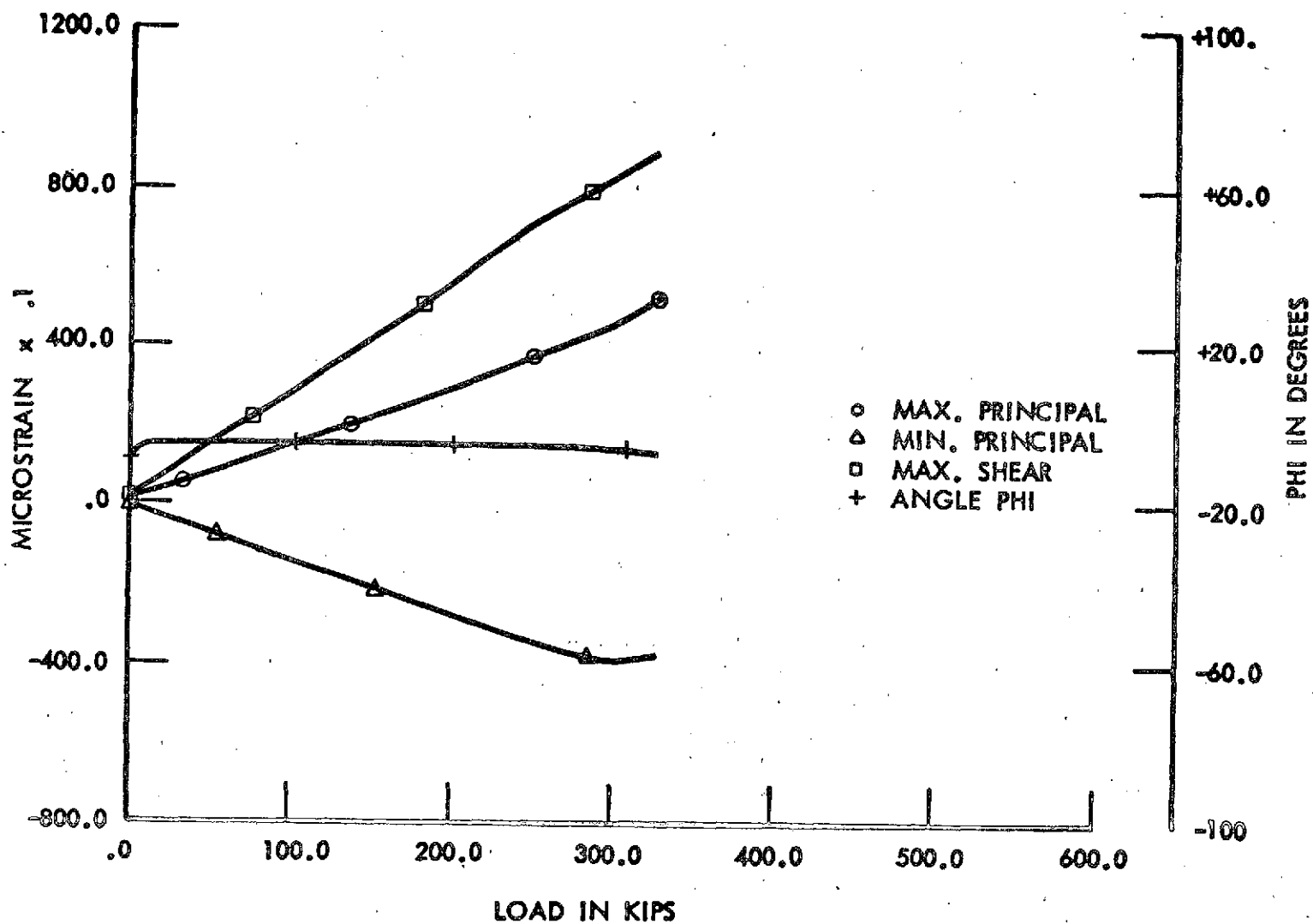


Figure 52: PRINCIPAL STRAIN DATA FOR WEB ELEMENT 2 ROSETTE NO. 13

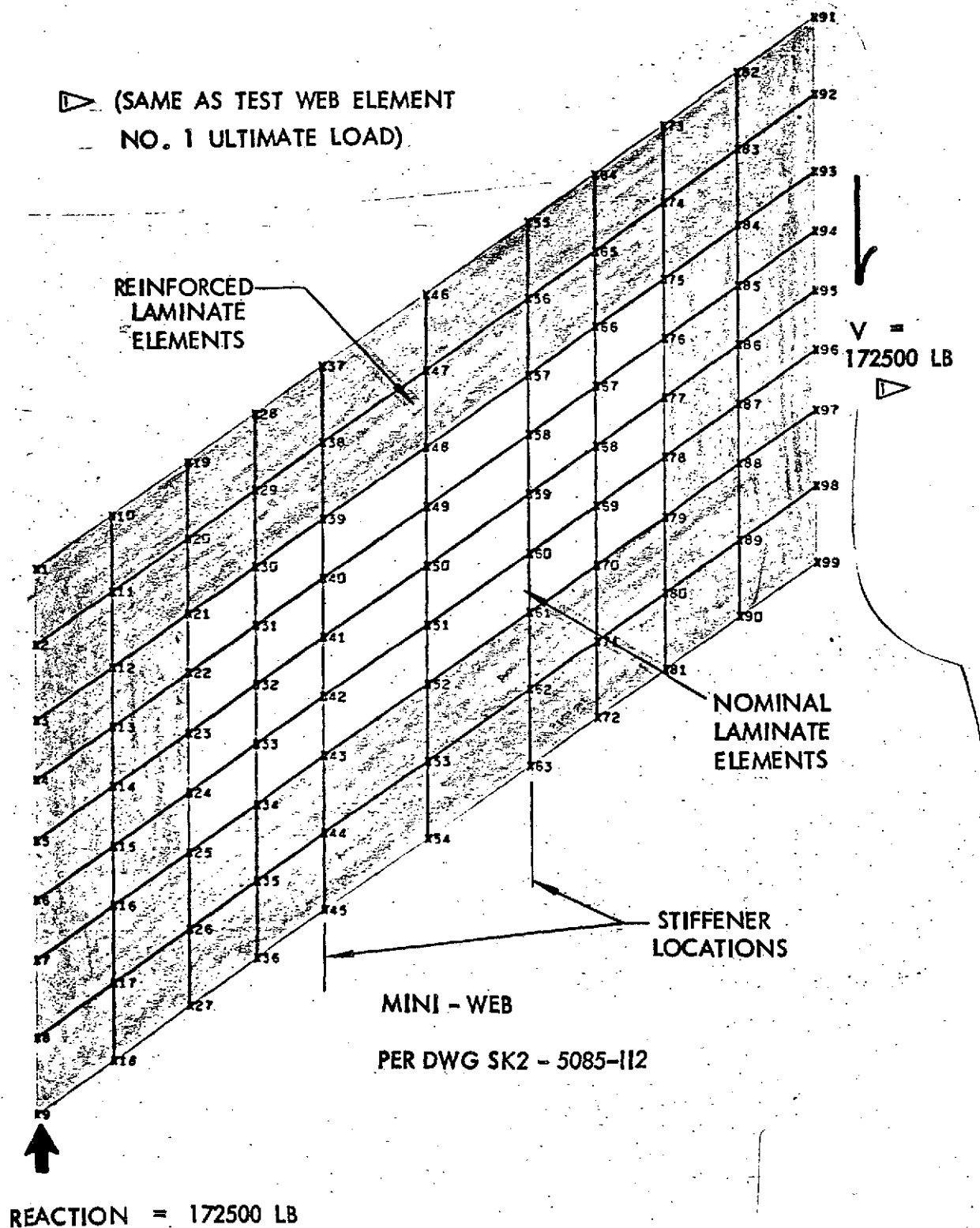
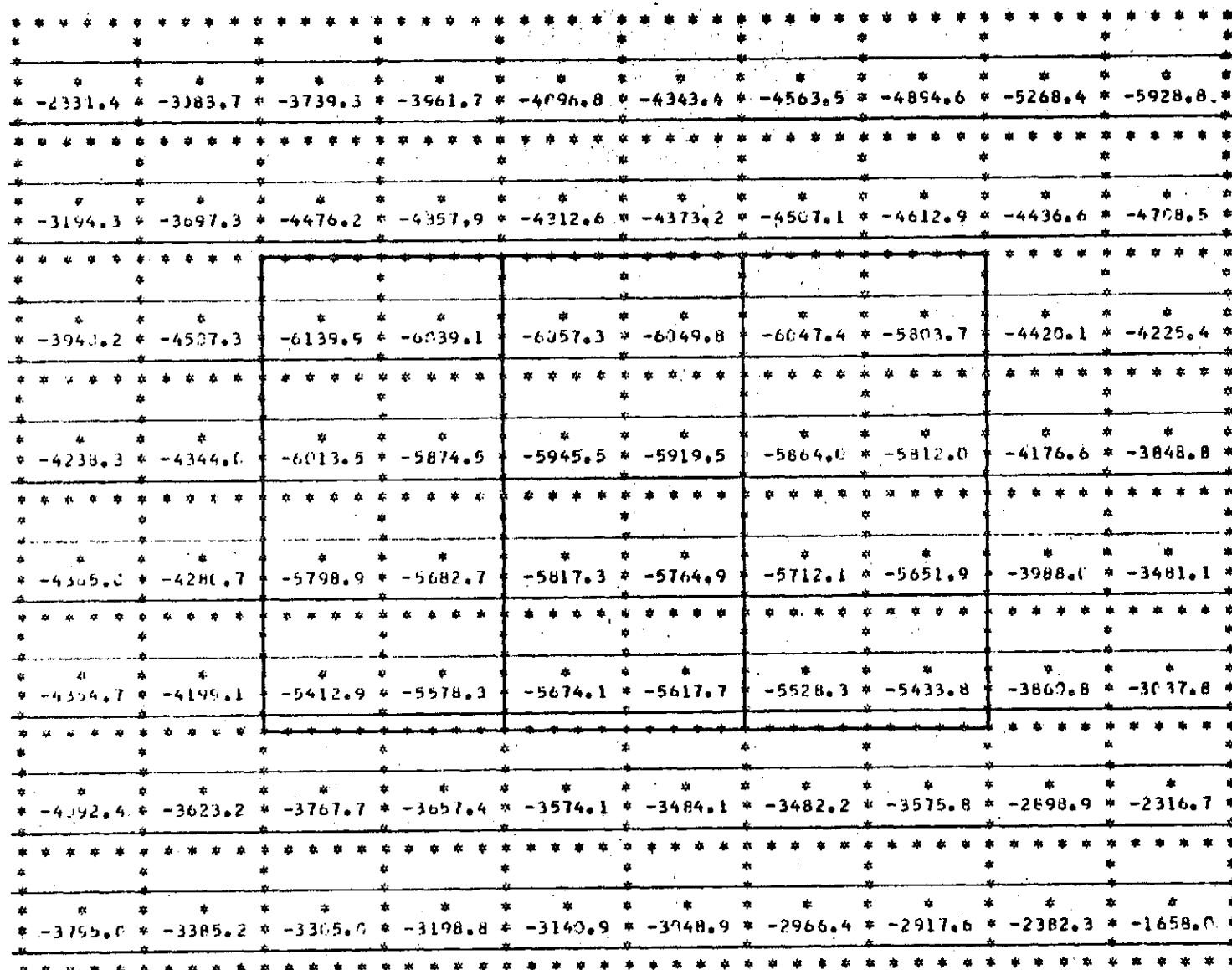


Figure 53: NASTRAN PQUAD ELEMENT MODEL
(HALF SPAN MODELED)

Figure 54: PRINCIPAL TENSION STRAIN DISTRIBUTION (MICROSTRAIN)



BOEING-MODIFIED NASTRAN OUTPUT DATA ELEMENTS ARE NOT - TO - SCALE

Figure 55: PRINCIPAL COMPRESSION STRAIN DISTRIBUTION (MICROSTRAIN)

| | | | | | | | | | |
|--------|--------|---------|---------|---------|---------|---------|---------|--------|--------|
| 4582.1 | 5857.1 | 6853.8 | 7133.5 | 7272.3 | 7476.4 | 7717.4 | 8055.3 | 7927.7 | 7834.3 |
| 6093.7 | 6645.1 | 7374.4 | 7811.5 | 7770.0 | 7812.4 | 8081.4 | 8302.5 | 7425.4 | 7183.7 |
| 7553.2 | 8120.5 | 11084.0 | 11296.8 | 11501.0 | 11446.1 | 11382.2 | 11034.3 | 8053.9 | 7129.8 |
| 7677.9 | 8138.9 | 11326.5 | 11177.7 | 11453.2 | 11365.5 | 11227.0 | 11092.4 | 7659.9 | 6776.3 |
| 8096.8 | 8240.4 | 11378.7 | 11165.9 | 11418.9 | 11299.2 | 11073.9 | 10907.7 | 7408.7 | 6350.7 |
| 8019.7 | 8413.3 | 11161.7 | 11260.8 | 11409.3 | 11281.1 | 10971.3 | 10499.1 | 7286.8 | 5865.7 |
| 7293.3 | 7248.4 | 8091.3 | 7653.0 | 7641.7 | 7539.8 | 7496.3 | 7526.6 | 6235.0 | 5265.1 |
| 6412.0 | 6591.4 | 7052.0 | 7103.6 | 7150.5 | 7245.5 | 7224.1 | 7259.2 | 6500.1 | 5330.9 |

BOEING-MODIFIED NASTRAN OUTPUT DATA ELEMENTS ARE NOT - TO - SCALE

Figure 56: PRINCIPAL SHEAR STRAIN DISTRIBUTION (MICROSTRAIN)

| | | | | | | | | | |
|-------|-------|-------|-------|-------|-------|-------|-------|-------|-------|
| ***** | | | | | | | | | |
| ***** | | | | | | | | | |
| 44.2 | 42.3 | 41.5 | 39.9 | 38.5 | 37.3 | 36.6 | 36.6 | 39.3 | -44.7 |
| ***** | | | | | | | | | |
| ***** | | | | | | | | | |
| -44.4 | 43.3 | 41.3 | 39.9 | 39.6 | 39.8 | 40.6 | 41.9 | -44.3 | -37.9 |
| ***** | | | | | | | | | |
| ***** | | | | | | | | | |
| -43.4 | -44.9 | 42.9 | 41.6 | 41.8 | 42.6 | 44.2 | -44.5 | -41.1 | -35.8 |
| ***** | | | | | | | | | |
| ***** | | | | | | | | | |
| -42.1 | -43.6 | 44.2 | 43.0 | 43.1 | 43.5 | 45.0 | -43.7 | -40.5 | -36.3 |
| ***** | | | | | | | | | |
| ***** | | | | | | | | | |
| -41.0 | -43.2 | -44.8 | 44.8 | 44.4 | 44.7 | -44.4 | -42.8 | -40.4 | -37.2 |
| ***** | | | | | | | | | |
| ***** | | | | | | | | | |
| -39.7 | -42.4 | -43.4 | -43.4 | -43.9 | -44.0 | -43.8 | -42.4 | -40.5 | -37.8 |
| ***** | | | | | | | | | |
| ***** | | | | | | | | | |
| -38.5 | -41.3 | -42.2 | -41.7 | -41.6 | -41.2 | -41.0 | -39.9 | -38.0 | -35.2 |
| ***** | | | | | | | | | |
| ***** | | | | | | | | | |
| -37.3 | -40.4 | -41.4 | -40.2 | -38.8 | -37.3 | -36.0 | -34.5 | -32.8 | -29.4 |
| ***** | | | | | | | | | |

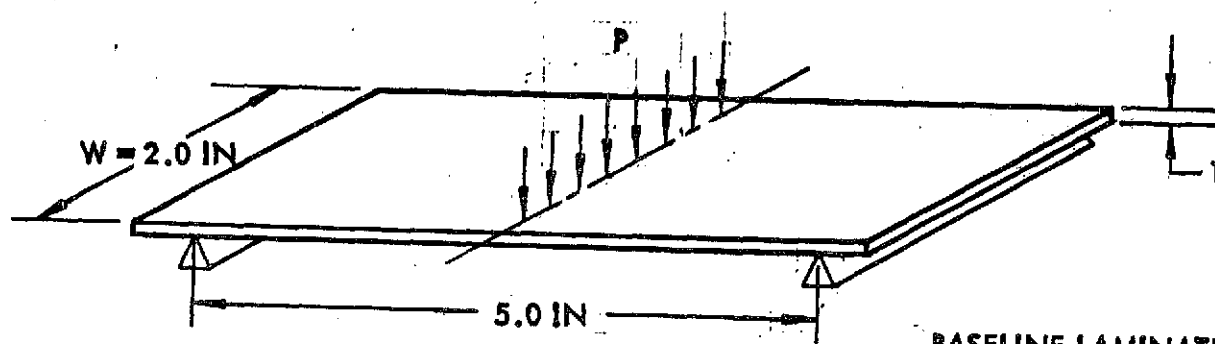
BOEING-MODIFIED NASTRAN OUTPUT DATA ELEMENTS ARE NOT - TO - SCALE

Figure 57: PRINCIPAL STRAIN AXIS ANGLE DISTRIBUTION (DEGREES)

Principal strain axis angles, as given in Figure 57, are relative to the vertical axis, counterclockwise being negative; the positive and negative angles refer to the principal tension and compression axes, respectively. The correlation between the NASTRAN and linearized test strain data is good considering the coarse finite element grid layout. For example, the linearized principal tension strain response at failure for SC-7, web element 1, is 4800 $\mu\epsilon$; the NASTRAN value in this location is approximately 5400 $\mu\epsilon$.

4.3 Bending Stiffness Element Testing

Several bending stiffness tests of the nominal baseline laminate were conducted to evaluate the classical laminate analysis coding incorporated in the OPTRAN code for the baseline B/E reinforced web. The bending stiffness correlation presented in Figure 58 is good for a 0-90° specimen layup. For a $\pm 45^\circ$ layup, the analytical predictions are high due to non-uniform strain distributions at the specimen edges which is a characteristic of angle-ply specimens. The laminate analyses were conducted with nominal laminate thicknesses corrected for adhesive bleed-out. Separate measurement tests have indicated that the METLBOND 329 (a high flow adhesive system) nominal cured thickness in a large panel is 0.012 in. and within a 2 in. edge distance high bleed-out occurs. All of the specimen thickness deviation from nominal was assumed to have occurred in the adhesive plies for the predictions shown.



BASELINE LAMINATE

16 B/E PLIES (0.0055 IN. THK. EACH)

5 ADHESIVE PLIES (0.012 IN. THK. EACH LESS BLEED-OUT)

0.020 NOMINAL TI CLADDING

| SPECIMEN | PLY SET LAY-UP | T_{avg} IN | ACTUAL CLADDING THK T_{cl} | ASSUMED ADHESIVE PLY THK. AFTER BLEED-OUT IN | P LB | CENTER DEFL IN | BENDING STIFFNESS (IN LB) TEST BEAM DEFL. EQ. | CLASSICAL ANALYSIS BENDING STIFFNESS |
|----------|----------------|-----------------|------------------------------|--|---------|-------------------|---|--------------------------------------|
| 1A | 0-90° | .170 | 0.021 | .008 | 890. | 0.2 | 5800 | 5656 |
| 1B | 0-90° | .171 | 0.021 | .0082 | 445. | 0.1 | 5775 | 5733 |
| 2A | +45° | .170 | 0.021 | .008 | 910. | 0.25 | 4725 | 5081 |
| 2B | +45° | .169 | 0.021 | .0078 | 355. | 0.1 | 4620 | 5013 |

Figure 58: BENDING ELEMENT TEST DATA

4.4 Stiffener Element Testing

Stiffener crippling tests were performed to substantiate the integrity of the bonded stiffener assembly detailed in Dwg. SK2-5085-118. These tests were conducted on straight and jogged sections, illustrated in Figure 59, in simple end compression. The straight sections tested to an order-of-magnitude above the actual loads in a shear resistant web (based on the finite element analysis results described in Section 5.2). Buckling predictions furnished by the BUCLASP code (20) show good correlation with the critical test loads for two of the three straight stiffener elements as shown in Figure 60. The BUCLASP model consisted of 2, 1, and 1 longitudinal elements for the laminate flange, the web and the metal flange, respectively. Loading of the jogged section was terminated after yielding of the metal joggle area initiated; the bonded areas were undamaged.

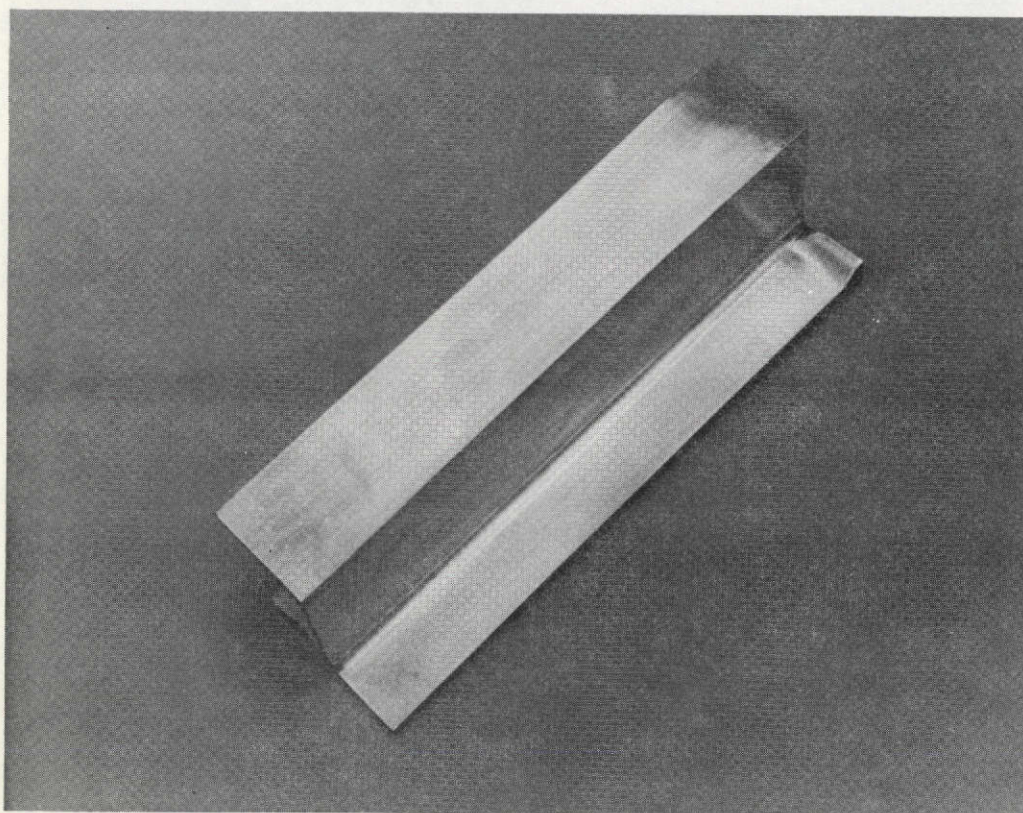
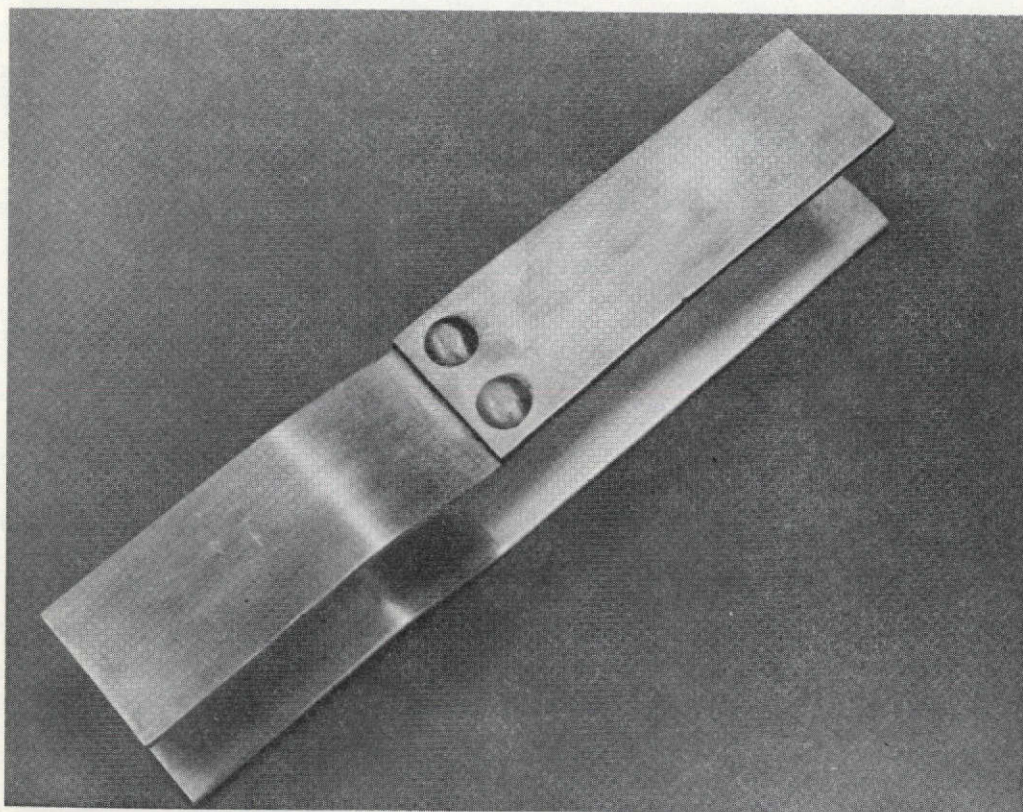
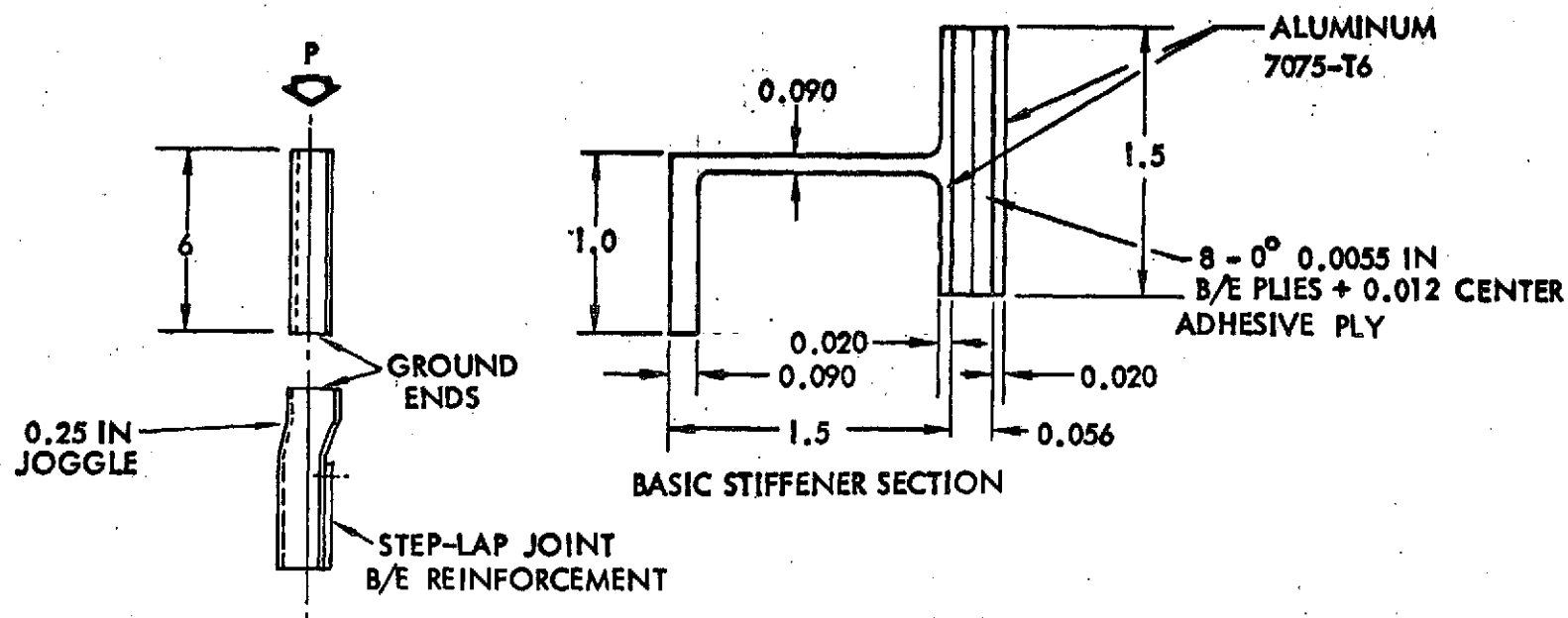


Figure 59: STIFFENER TEST ELEMENT



| SPECIMEN | TEST P _{CR} LB | BUCLASP PREDICTION | NOTES |
|----------|----------------------------|-----------------------|-----------------------------------|
| 1 | 27,600 | 28,100 | STRAIGHT SECTION |
| 2 | 25,800 | 28,100 | STRAIGHT SECTION |
| 3 | 28,200 | 28,100 | STRAIGHT SECTION |
| 4 | 14,000 | — | JOGGLED END SECTION |
| | | | REF. DWG. SK2-5085-118 |
| | | | CRITICAL BUCLASP MODE SHAPE m = 3 |

Figure 60: STIFFENER ELEMENT TEST DATA

4.5 Corner Element Testing

Figure 61 shows corner test elements, with and without loading fixture plates. The corner elements simulate the corner areas in the baseline design web with respect to titanium thickness, 16 ply $\pm 45^\circ$ B/E layup, and step-lap detail butt splices under diagonal tension loading condition. Figure 62 presents the ultimate strength results after initial thermal and load cycling. The specimens failed in the B/E area away from the corner step-lap details (the cracks in the cladding that are visible in the photograph occurred after the cladding debonded from the fractured B/E). Figures 63 and 64 are x-rays of the second test specimen, before and after testing; there is no apparent damage sustained in the spliced corner step-lap joint details.

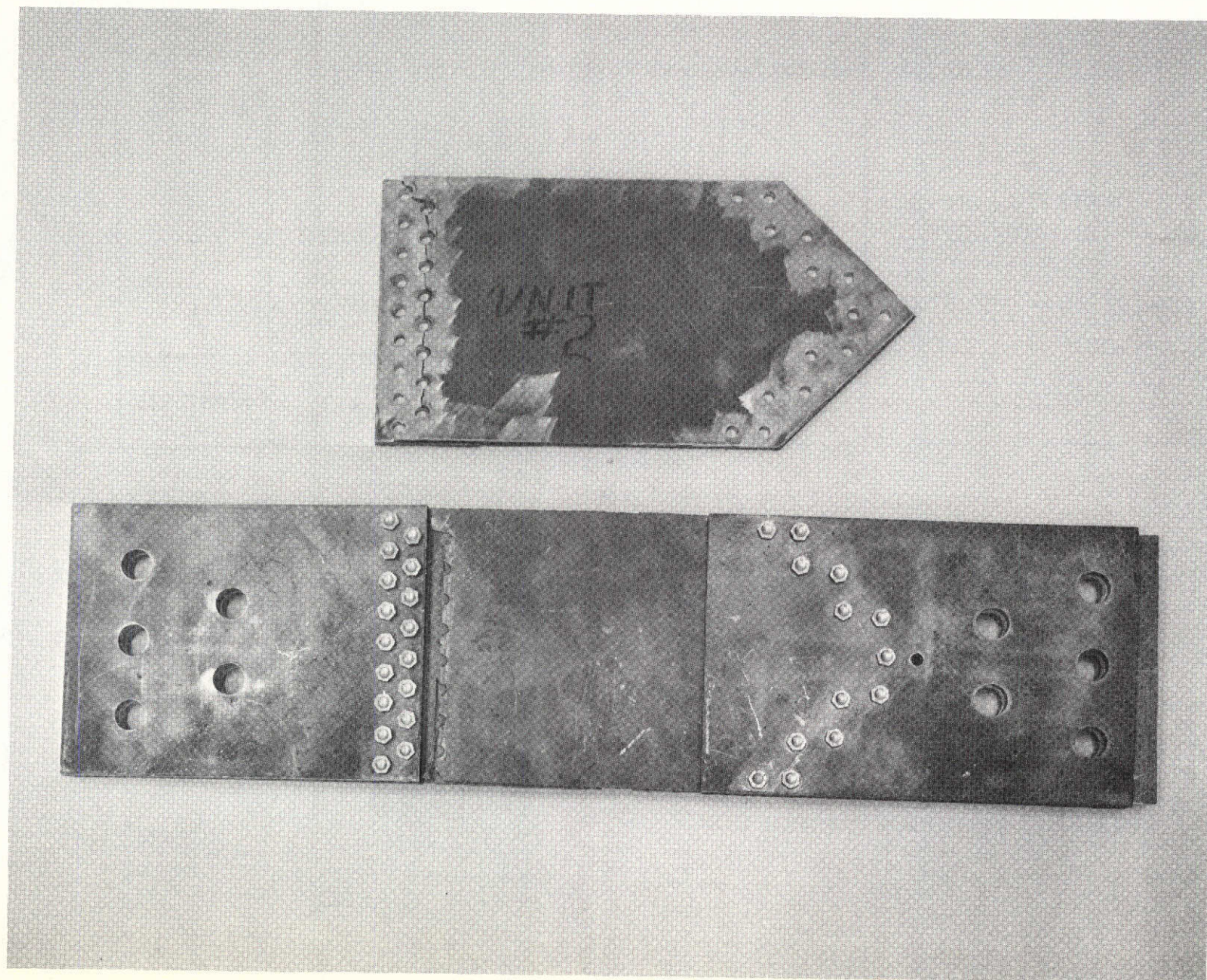
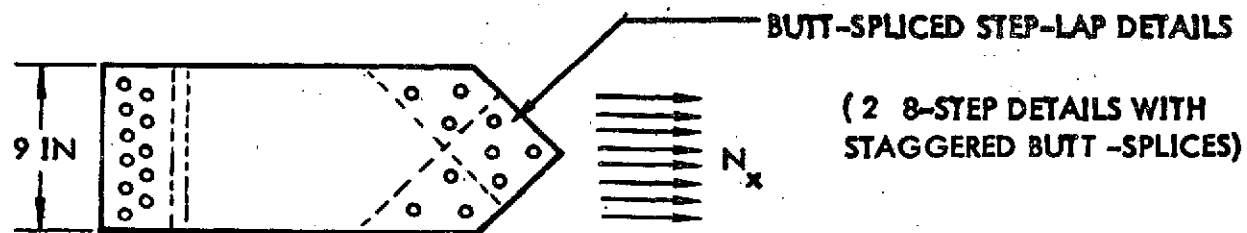


Figure 61: CORNER TEST ELEMENT WITH AND WITHOUT LOADING PLATES ATTACHED



BASELINE LAY-UP

16/ 0-90/BL

0.063 TI 6Al-4V M.A. CLADDING

| SPECIMEN | P_{ULT} LB | N_x LB/IN | ΣET 10^6 LB/IN | ϵ_{ULT} | NOTES |
|----------|-----------------|----------------|-----------------------------|------------------|--|
| 1 | 205000 | 22400 | 3.38 | 6620 | CYCLED 400 ~ 0 to 63000 LB |
| 2 | 215000 | 23900 | 3.38 | 7050 | CYCLED 400 ~ -100 to + 250° AND 400 ~ 0 to 63000 LB |

Figure 62: SPLICED STEP-LAP DETAIL ELEMENT TEST DATA

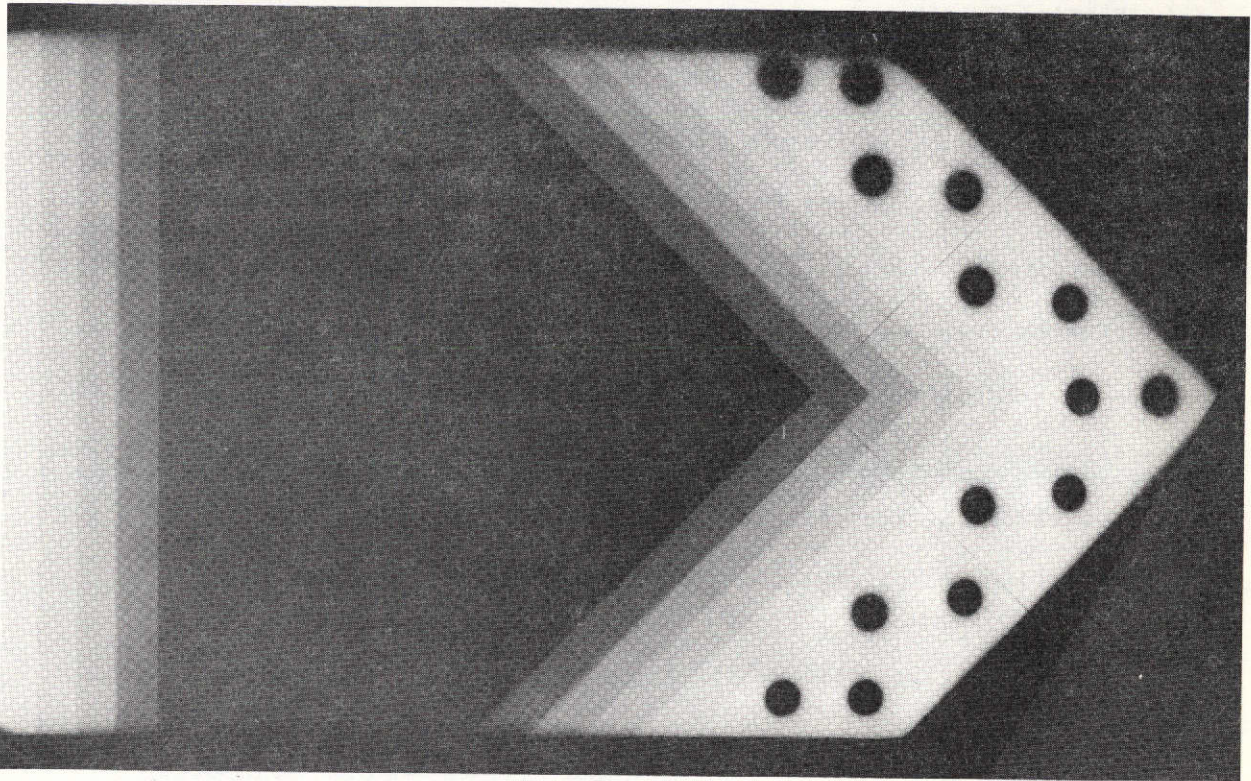


Figure 63: X-RAY OF CORNER TEST ELEMENT NO. 2 BEFORE TEST

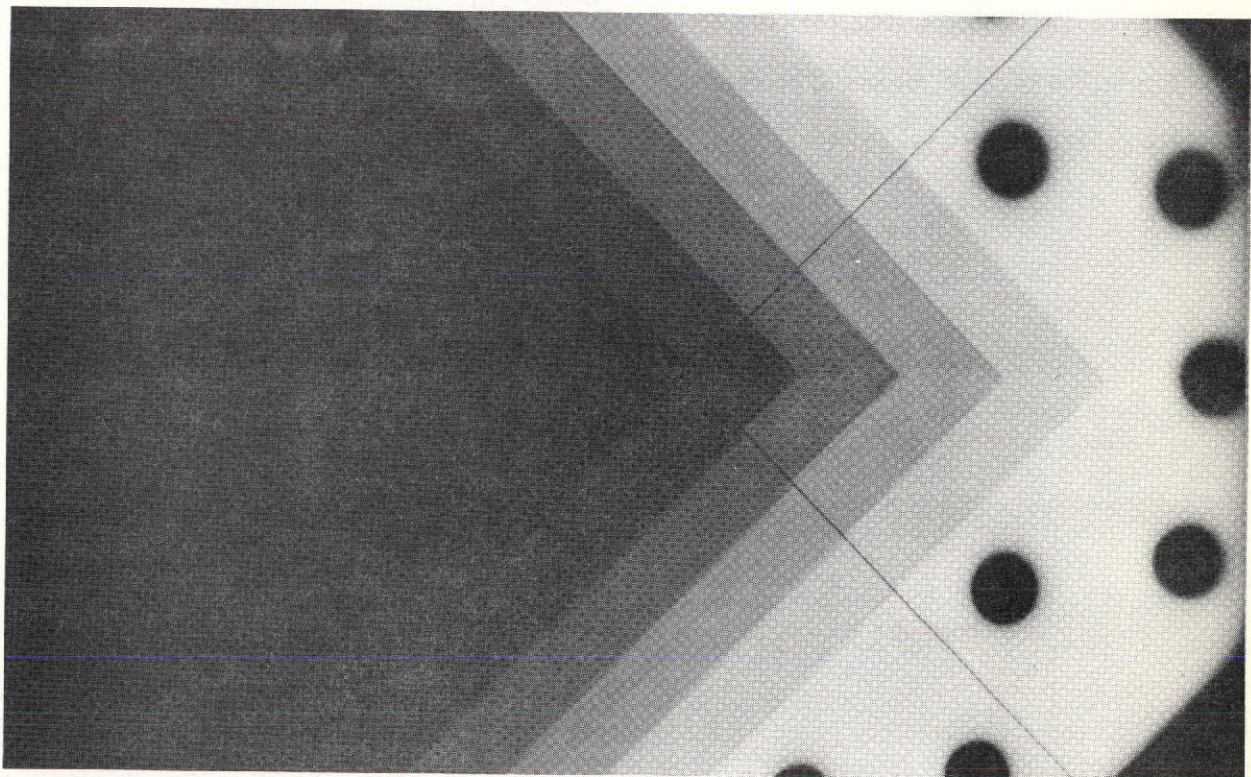


Figure 64: X-RAY OF CORNER TEST ELEMENT NO. 2 AFTER TESTING

4.6 Bearing Specimen Testing

Conventional fastener bearing tests were conducted on specimens of the type shown in Figure 65. The tests demonstrate bearing load capability of the reinforced baseline design laminate which is on the order of 6Al-4V mill annealed titanium alone. The tests were conducted with a large edge distance to represent isolated fasteners located away from the shear web edges, such as would be required for miscellaneous brackets too small to require special titanium step-lap joint inserts in the laminate. No significant differences in the ultimate bearing stresses are apparent due to load cycling, thermal cycling or long duration loading prior to static loading to failure.

The ultimate bearing stresses, as reported above, are interpreted as shown on Figure 66. The $\pm 45^\circ$ layup specimens typically behave differently than the $0-90^\circ$ specimens as illustrated by the respective plots (Figure 67). The $\pm 45^\circ$ specimens exhibit greater ductility which is characteristic of angle-ply layups. In both cases, loading was terminated before net-section tension failure. The high bearing strengths achieved in these tests indicate the effectiveness of the titanium lands in reinforcing hole areas having complex strain distributions.

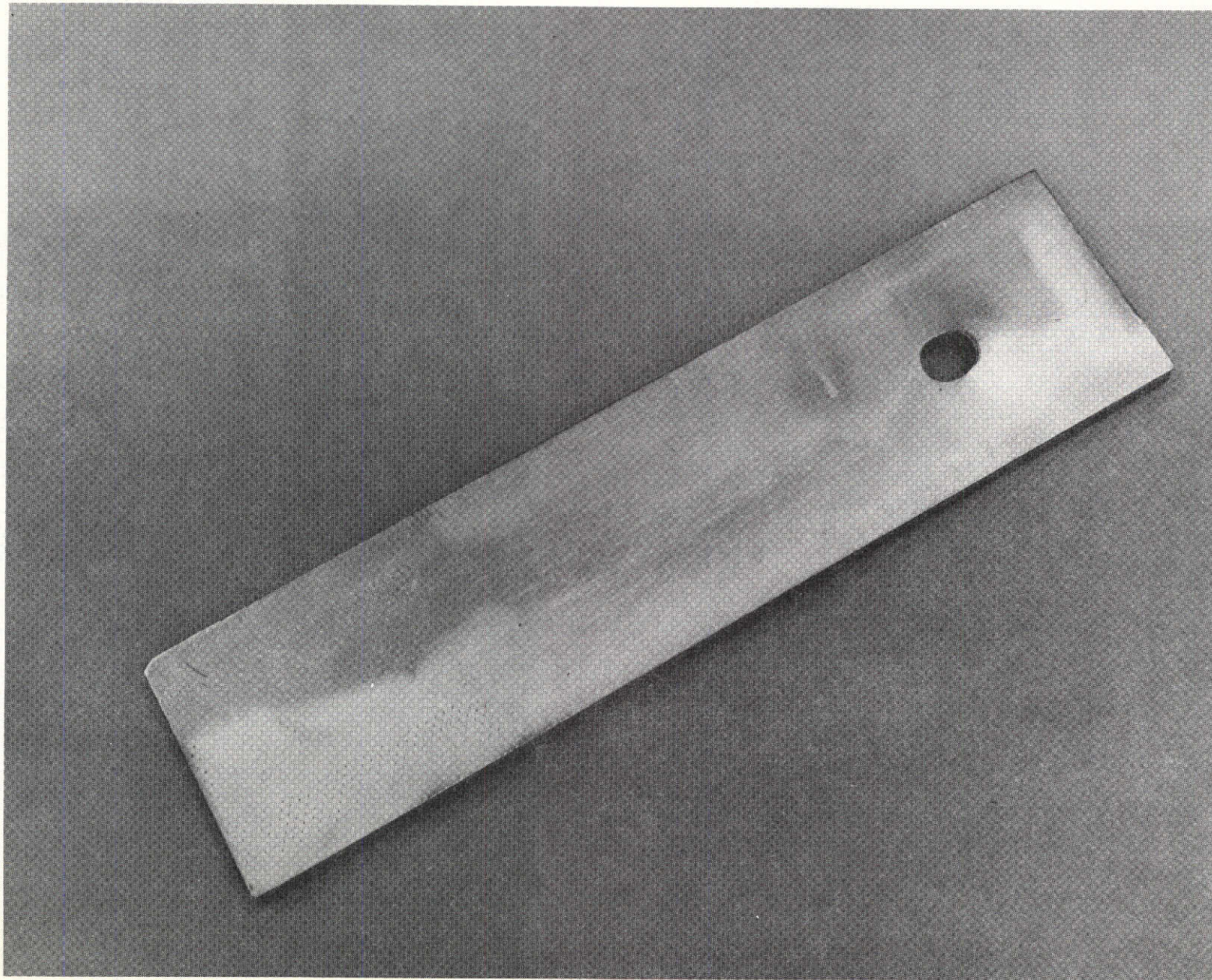


Figure 65: BEARING TEST SPECIMEN

ALL FAILURES ARE BEARING FAILURES

























| SPECIMEN | PLY-SET LAY-UP | P _{ULT} | \bar{P} AVG. | F _{BRU} | NOTES: |
|--|-------------------|------------------|-------------------|------------------|---|
| 1  | 16/0-90/BL ↓ | 20.0 | 0.270 | 197 |  THERMAL CYCLED 400~-100° to 250° F  LOAD CYCLED 400~ 0 TO 12300 LBS  LOAD CYCLED 400~ 0 TO 15800 LBS  LOADED 30 HRS TO 12300 LBS  LOADED 30 HRS TO 14700 LBS  0.0035 IN OVERSIZE HOLE |
| 2  | | 17.2 | 0.261 | 172.5 | |
| 3  | | 19.0 | 0.256 | 198 | |
| 4  | | 17.3 | 0.263 | 182 | |
| 5  | | 20.7 | 0.256 | 215 | |
| 6  | | | | | |
| 7  | 16/± 45/BL ↓ | 22.0 | 0.257 | 228 |  THERMAL CYCLED 400~-100° to 250° F  LOAD CYCLED 400~ 0 TO 12300 LBS  LOAD CYCLED 400~ 0 TO 15800 LBS  LOADED 30 HRS TO 12300 LBS  LOADED 30 HRS TO 14700 LBS  0.0035 IN OVERSIZE HOLE |
| 8  | | 20.6 | 0.260 | 212 | |
| 9  | | 20.0 | 0.261 | 204 | |
| 10  | | 19.8 | 0.257 | 206 | |
| 11  | | 18.6 | 0.256 | 194 | |
| 12  | | | | | |

Figure 66: BEARING ELEMENT TEST DATA

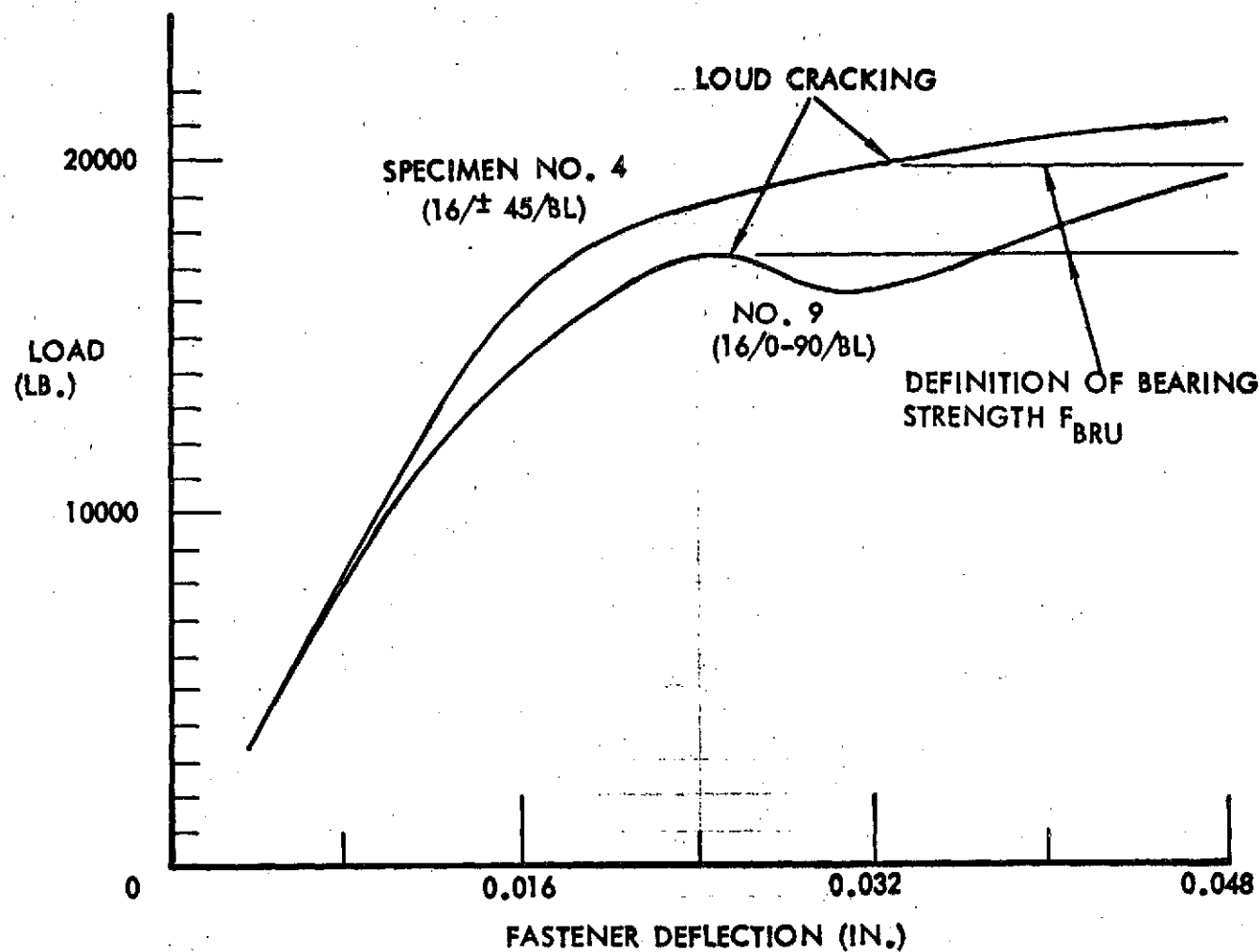
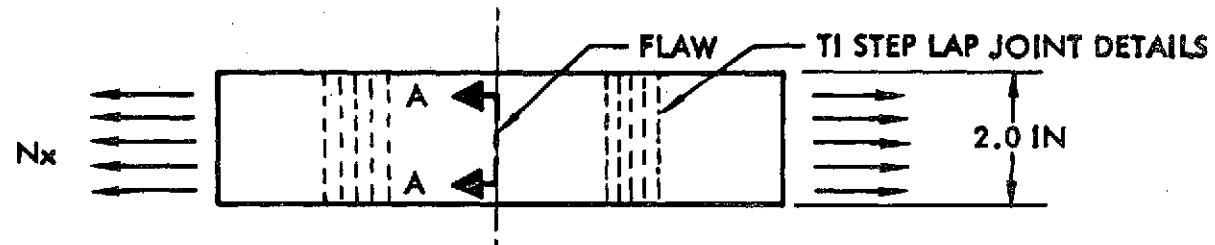


Figure 67: BEARING TEST LOAD-DEFLECTION DATA

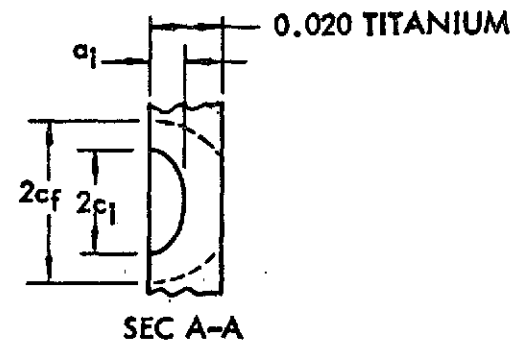
4.7 Flaw Growth Element Testing

A preliminary investigation of the flaw growth behavior of the baseline nominal titanium cladding was performed because undetectable flaws can exist after fabrication. Flaws can also be produced by impacting objects in service because of the vulnerable position of the titanium on the laminate surfaces. Flaw growth tests were conducted on the specimens shown in Figure 68 having single small flaws in the titanium.

The first test was performed on a 0.020 in. titanium skin alone, as shown in Figure 69. The flaw grew from an initial width ($2C_i$) of 0.057 in. to a final width ($2C_f$) of 0.087 in., after 1504 high tension strain cycles were applied. The specimen was cycled at $2/3$ yield stress until the flaw grew through the thickness. This occurred at 1104 cycles. Another 400 cycles were then applied to determine flaw growth. In the two laminated specimens (Figure 10 typical), the average $2C_i$ of 0.058 in. grew to 0.079 in. in the same number of strain cycles which indicates that cladding flaw growth is somewhat retarded in the laminated form. The cyclic loading was adjusted to give the same titanium strain level in the laminate specimen as that in the titanium skin alone. For the all titanium specimen, flaw growth occurred at the rate of 1.99×10^{-6} in./cycle while in the laminate form this growth was reduced to 1.40×10^{-6} in./cycle. This is believed to be due to the restraint offered by the underlying material to crack opening displacements in the titanium. In no case did the titanium flaw propagate into the underlying composite material. A similar retardation of flaw growth has been observed in laminates consisting of all-titanium plies (21). In addition to reduced crack tip stresses due to crack displacement restraint, the cladding may have a higher K_{cr} factor than would an all metal plate having the same thickness as the laminated plate because it responds more in plane stress than in plane strain (21).



INITIAL FLAW IN CLADDING SKIN FORMED
BY HIGH CYCLE/LOW STRESS FATIGUE CYCLING



| SPECIMEN | LAY-UP | NUMBER OF CYCLES FOR FLAW GROWTH THRU CLADDING THICKNESS | INITIAL a_i IN | INITIAL $2c_l$ IN | FLAW WIDTH $2c_f$ AFTER 1504 ~ TO 5450 μe | N_{xULT} LB/IN | ϵ_{ULT} (μe) | |
|----------|-----------------|---|------------------------|-------------------------|---|---------------------|------------------------------|----------------------|
| | | | | | | | BONDED CLADDING | DEBONDED CLADDING |
| 1 | TI SKIN ONLY | 1104 | .014 | .057 | 0.087 | — | — | — |
| 2 | 16/0 - 90/BL | NOT DETERMINED | .012 | .056 | 0.074 | 11300 | 5780 | 6800 |
| 3 | 16/0-90/BL | NOT DETERMINED | .014 | .060 | 0.084 | 11200 | 5700 | 6820 |

Figure 68: FLAW GROWTH ELEMENT TEST DATA

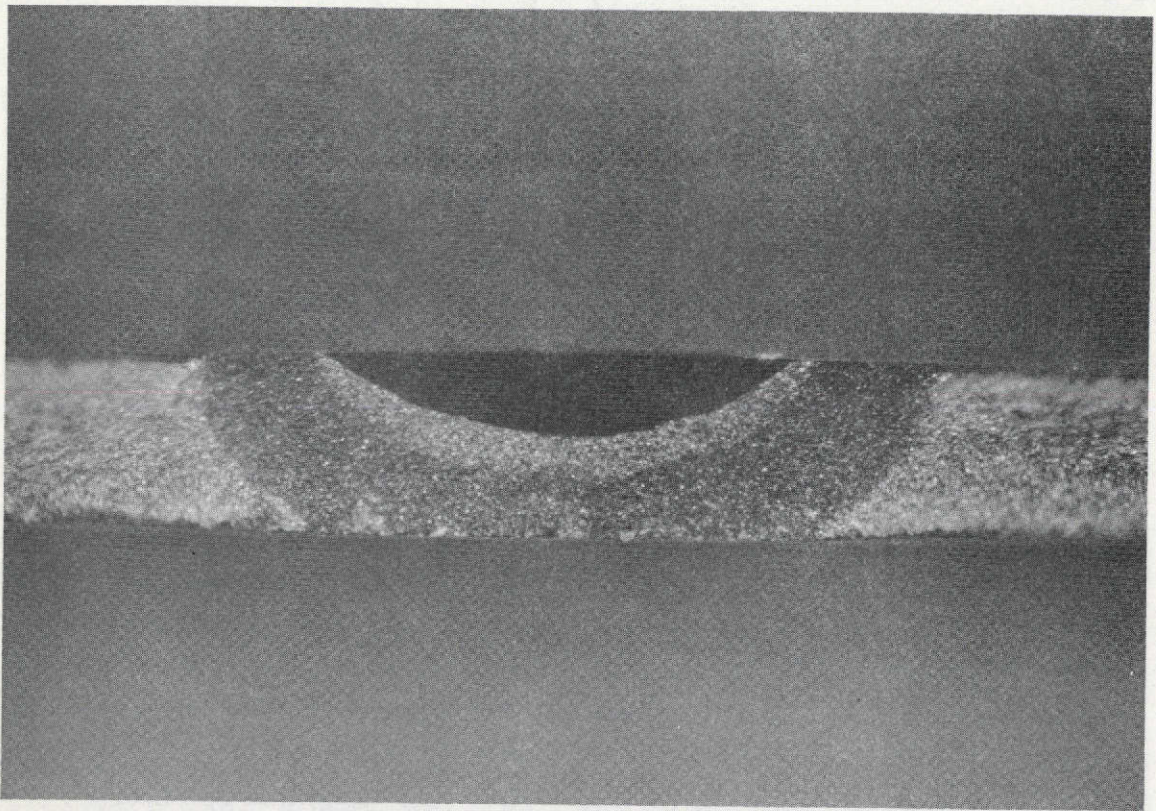


Figure 69: FRACTOGRAPH - Titanium

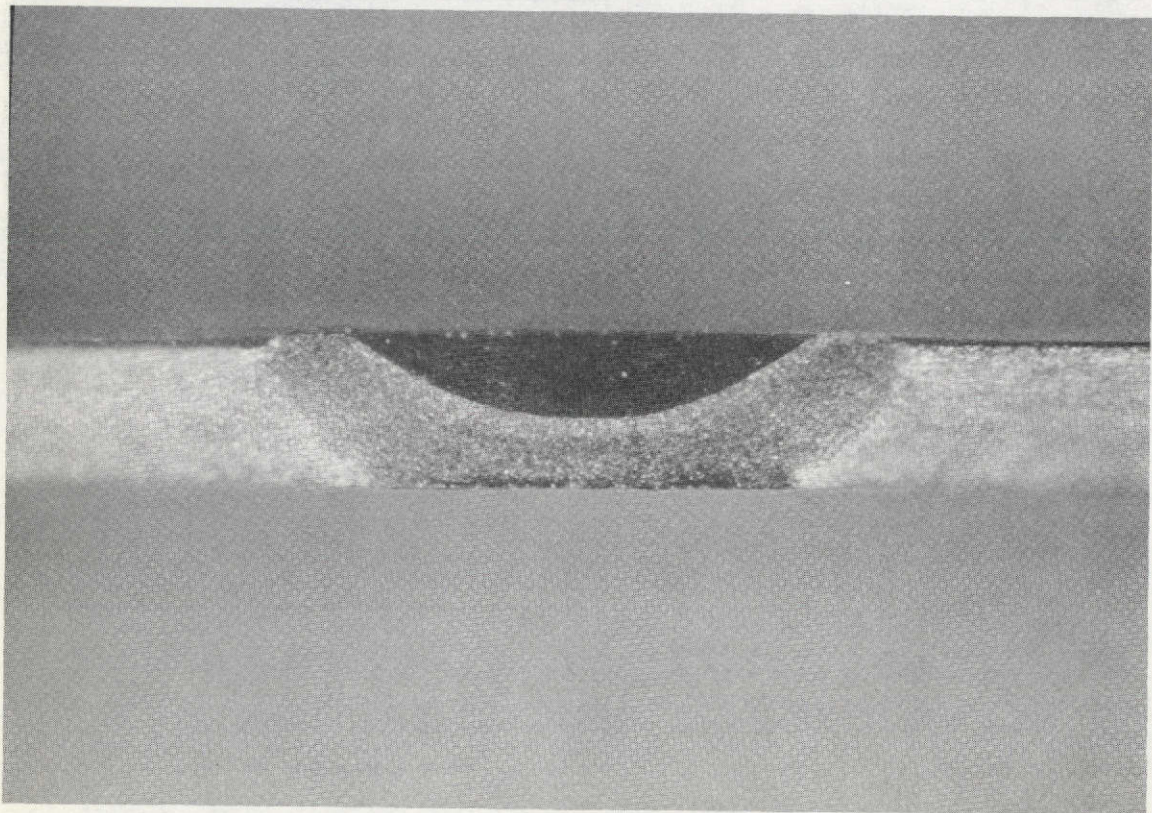


Figure 70: FRACTOGRAPH - B/E Reinforced Titanium

After load cycling, the laminated specimens were failed in tension. The resulting ultimate strains are somewhere between the values shown in Figure 68, assuming the flawed cladding is either bonded or unbonded. In either case, the ultimate strain is above the baseline web design requirement of 4741 μ s in spite of the applied strain load cycles being above the design requirement.

These test results coupled with titanium having critical crack length for the cyclic design limit load conditions which is of normally detectable size, assure that the nominal ti-clad B/E laminate is not susceptible to critical growth of undetectable flaws in the design load conditions. Resistance to flaw growth in the joint and hole-out areas of the baseline laminate has been indirectly verified in the other element test categories. In particular, the drilled tension elements, all having conventionally drilled holes with some amount of internal burring of the titanium developed no apparent flaw growth during cyclic limit load applications.

5.0 SHEAR WEB TEST COMPONENT DESIGN AND ANALYSIS

The three large scale shear web component tests in Phase III of the program are planned to demonstrate the structural performance of the assembled B/E reinforced shear web structure under cyclic and static loads at room temperature. The first two web tests are planned to be conducted on components having similar design details; these tests are intended to verify structural analysis methods. The final test will be conducted on an optimized web component based on the preceding test/analysis correlation results and optimum design definition from an up-dated OPTRAN code. The final web component will be designed as part of Phase III activities.

5.1 Shear Web Test Component Design

The design details established for the initial test components are shown in Dwg. SK2-5085-117 and 118 in Appendix B; the details are identical to the baseline B/E reinforced design web except for overall size, stiffener section, stiffener spacing and edge detail dimensions. Cutout and miscellaneous attachment details are not considered to be strength critical details and so are not included in the test web components. Based on the analysis relationships given in Appendix A and finite element analysis results, the test web component design is close to being simultaneously critical in three failure modes. This indicates that the web test component design is a reasonable simulation of an optimum design configuration.

A 36 by 47 in. web size was selected to allow cutting the titanium cladding from a single sheet available in stock (36 x 96 in) with allowance for material test coupons. The resulting web has six stiffeners and five nominal laminate panels. The central panels are isolated from the reinforced end panels. The laminate design is the baseline 16 ply $\pm 45^\circ$ B/E layup with 0.020 inch 6AL-4V mill annealed titanium cladding. As indicated by the OPTRAN weight trades, Figure 10, this nominal laminate is optimum over a range of loading and has excess margins of safety with respect to B/E strain in the design web.

A thickness of 0.050 in. in the reinforced stiffener land areas was chosen to provide a slight excess in the final chem-milled thickness. The edge cladding thickness of 0.063 was dictated by available stock sheet sizes and furnishes the necessary reinforcement in the edge joint areas. The edge fastening is designed to preclude net section, bearing or bolt shear failures. A stiffener spacing of 6.0 in. was selected, rather than the baseline design

web value of 6.38 in., to simplify fabrication layout. Design of the stiffener details and fabrication techniques for both the web laminate and stiffeners are discussed in Section 3.6.

The test web fixture framework, which is nearly full depth but is half the span of the design web, is shown in Figure 71 and is detailed in Dwg. SK2-5085-114 in Appendix B. Aluminum (7075-T6) was selected for the beam frame material in order to minimize fabrication cost. Figures 72 and 73 show the B/E reinforced web components parts. The beam flange material is sized to have an average strain of $1500 \mu\epsilon$, at a loading of 550000 lb. which produces an average web shear of 7625 lb/in (equal to the baseline web design requirements). A low flange strain level is required because the beam will be subjected to numerous high-level cyclic loads. Because of the differences in beam flange strains in the test beam and the baseline web design requirements, the test web will require a higher shear load than the baseline design load of 7625 lb/in in order to experience the same maximum principal strains.

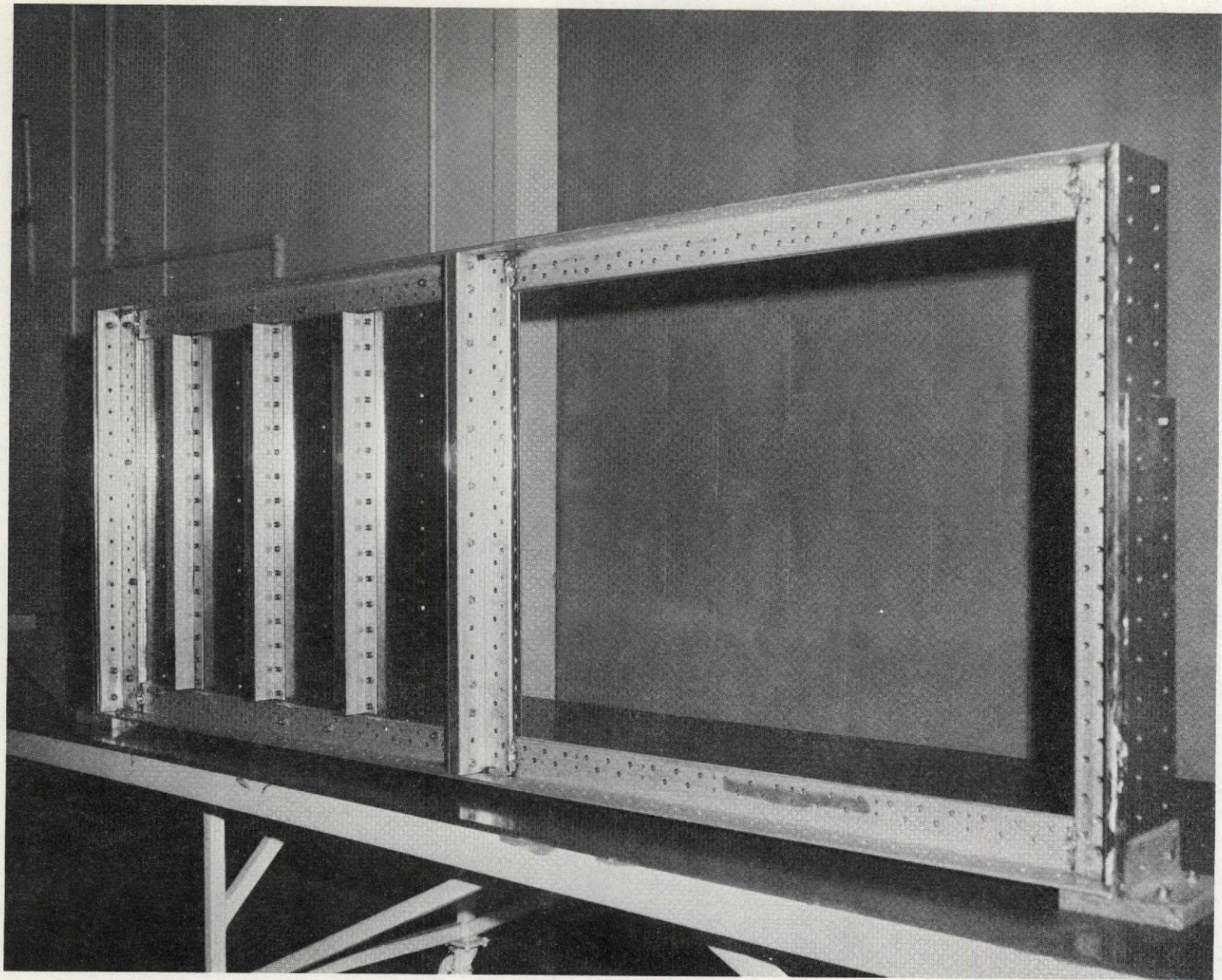


Figure 71: TEST BEAM ALUMINUM FRAME WORK

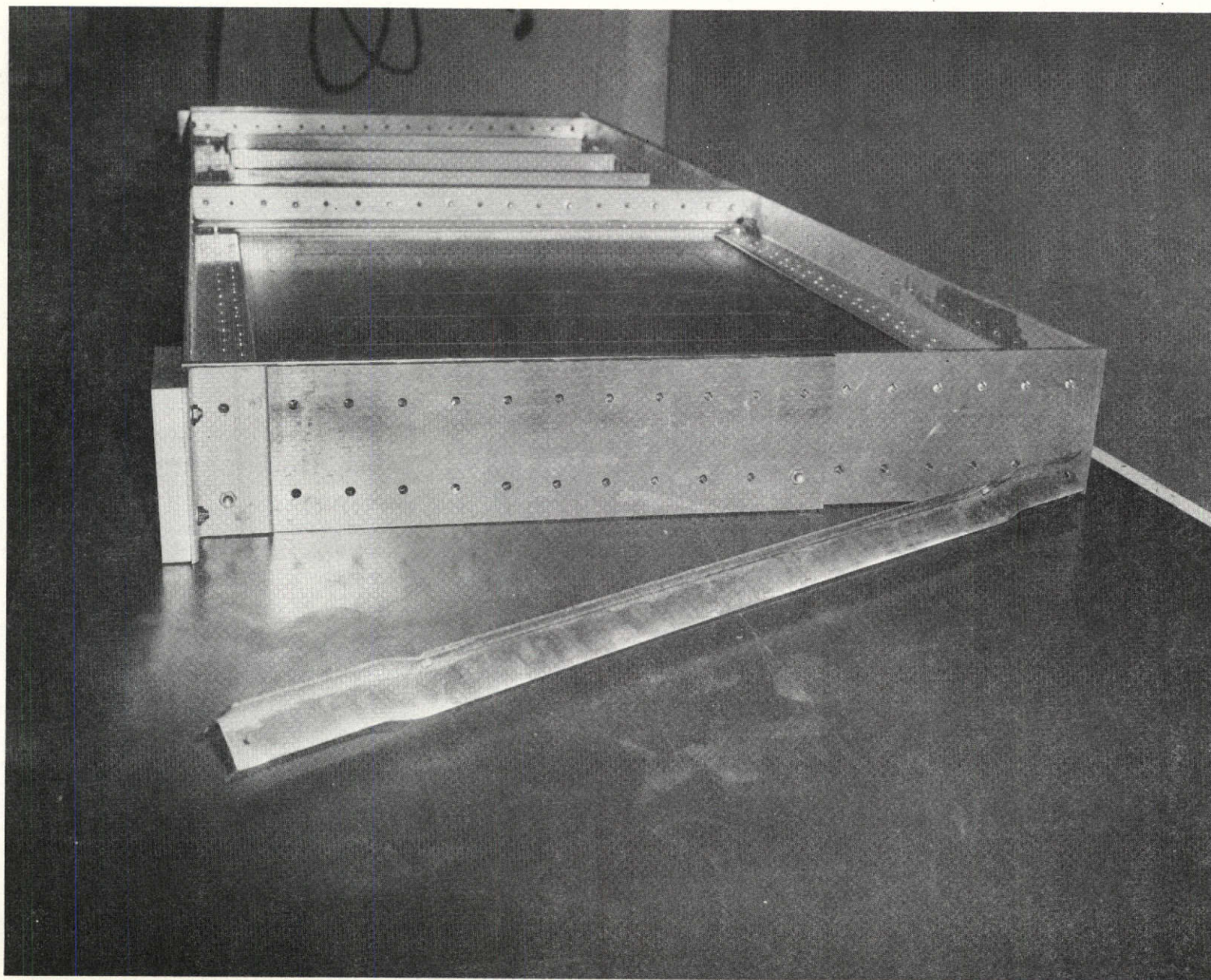


Figure 72: B/E REINFORCED JOGGLED STIFFENER

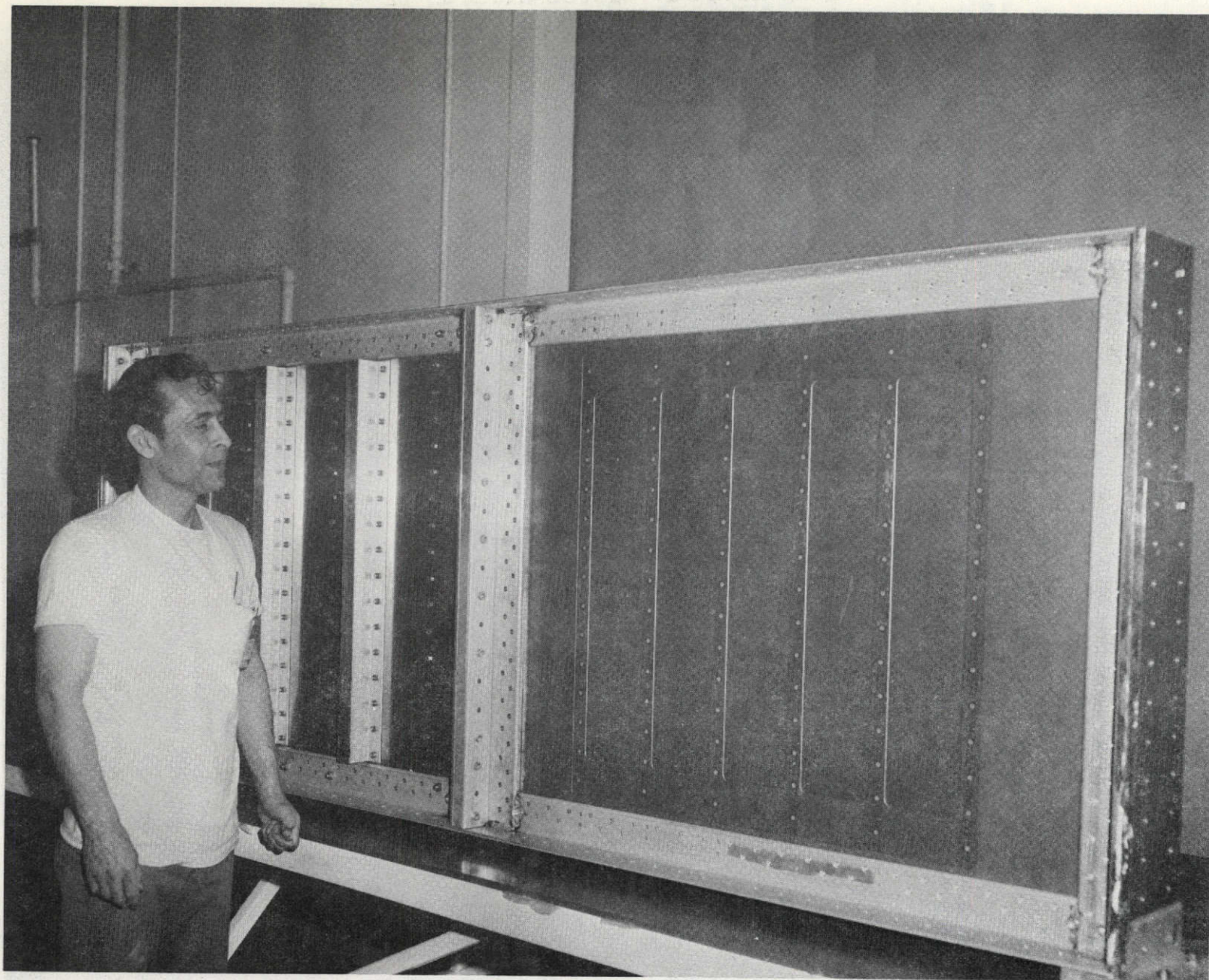


Figure 73: TEST WEB BEAM ASSEMBLY (WITHOUT B/E REINFORCED STIFFENERS)

5.2 Shear Web Test Component Analysis

Computation of the principal strains and critical general instability load for the test web was accomplished with the detailed NASTRAN model illustrated in Figures 74, 75 and 76. The web laminate is modeled with orthotropic plate elements having properties determined by classical laminate analysis. The nominal laminate properties shown correspond to the baseline nominal laminate properties given in Figure 12. The B/E reinforced stiffener elements have their minor bending and torsional stiffnesses set to zero to obtain a conservative instability analysis. The stiffeners are terminated short of the flange angle plate elements in order to discount the stiffnesses offered by the joggled extensions that ride over the flange connection angle legs.

The static deflection solution for the applied load of 550000 lb is shown in Figure 77. The loci (neutral axis) of transition in sign of the web element stresses in the x-direction is indicated on the figure; the loci sweeps high near the point of loading and is slightly below the beam centerline in the other areas which is characteristic of low aspect ratio webs.

Principal strain and angle distributions, which were processed from the NASTRAN static solution as described in Section 4.2, are reproduced in Figures 78 to 93 for the four quadrants in the B/E reinforced web component area. The principal strain data will be employed in the evaluation of the test strain data recorded during testing. The effects of reinforcing the laminate in the edge areas is seen to be effective in reducing the strains in these areas. In spite of the low web aspect ratio, the resulting principal shear strain distribution is essentially uniform.

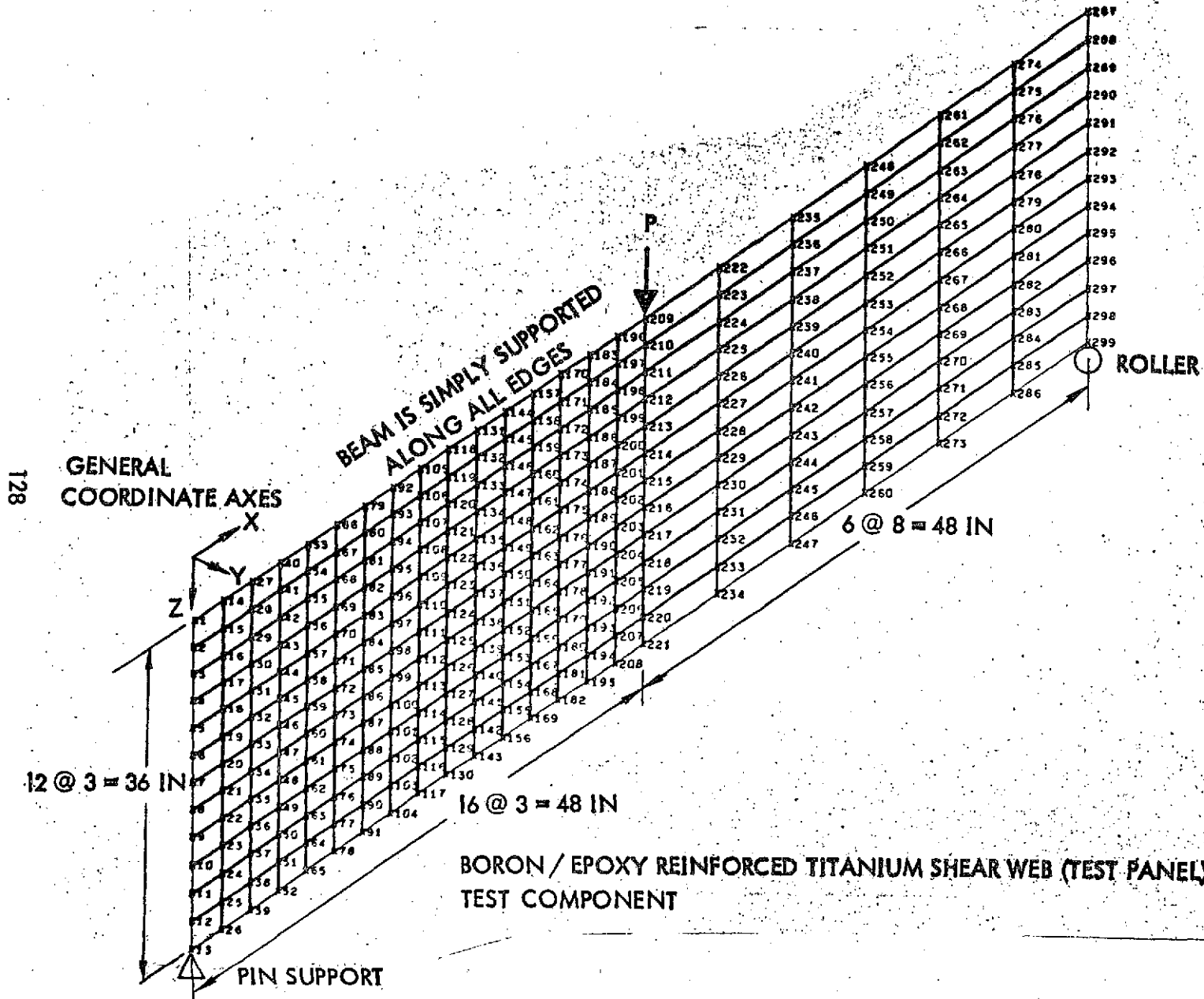


Figure 74: NASTRAN FINITE ELEMENT MODEL NODES

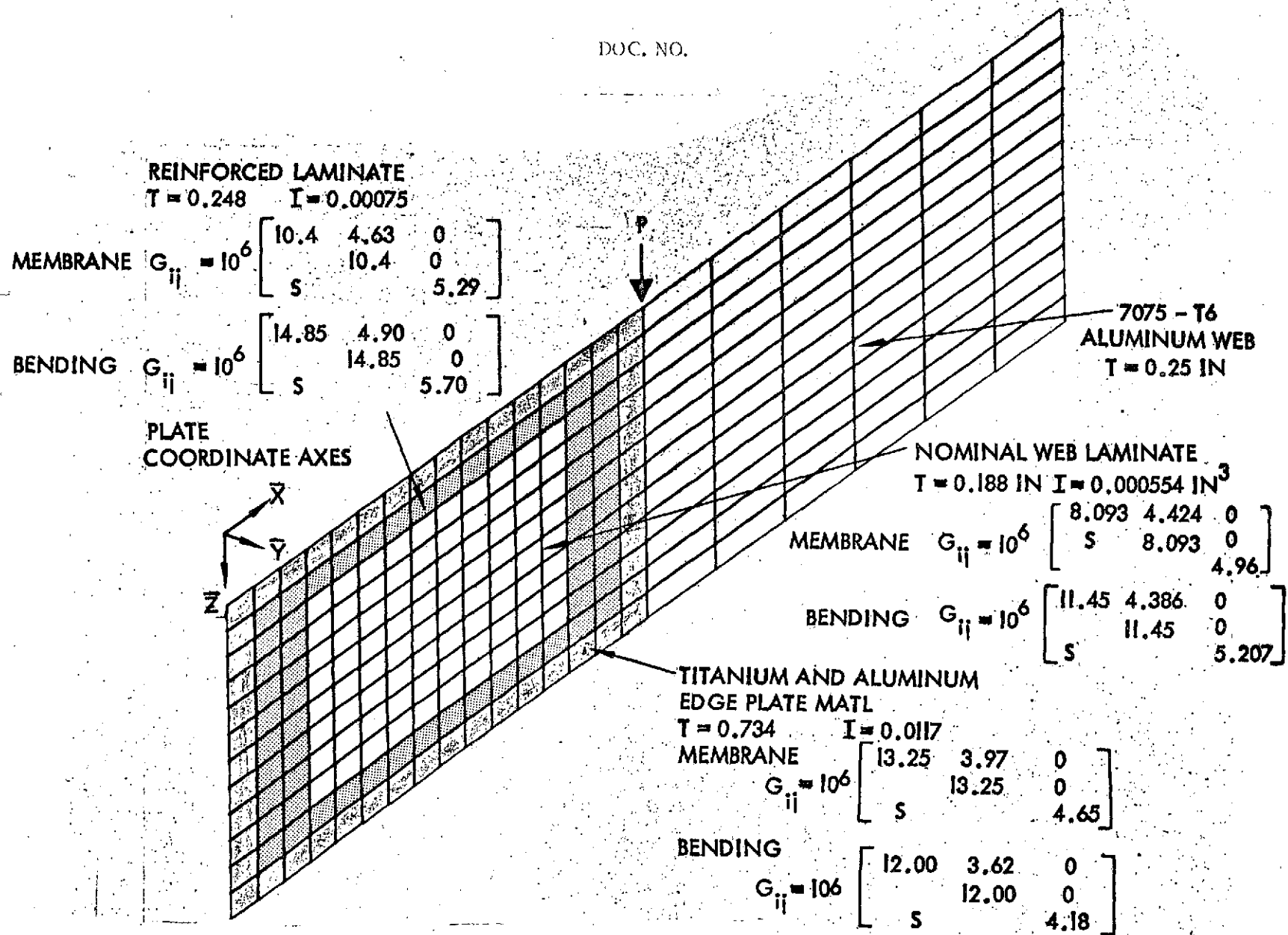


Figure 75: WEB PLATE ELEMENTS (NASTRAN PQUAD ELEMENTS)

ALL BEAM ELEMENTS HAVE THEIR WEBS
PERPENDICULAR TO THE SHEAR WEBS

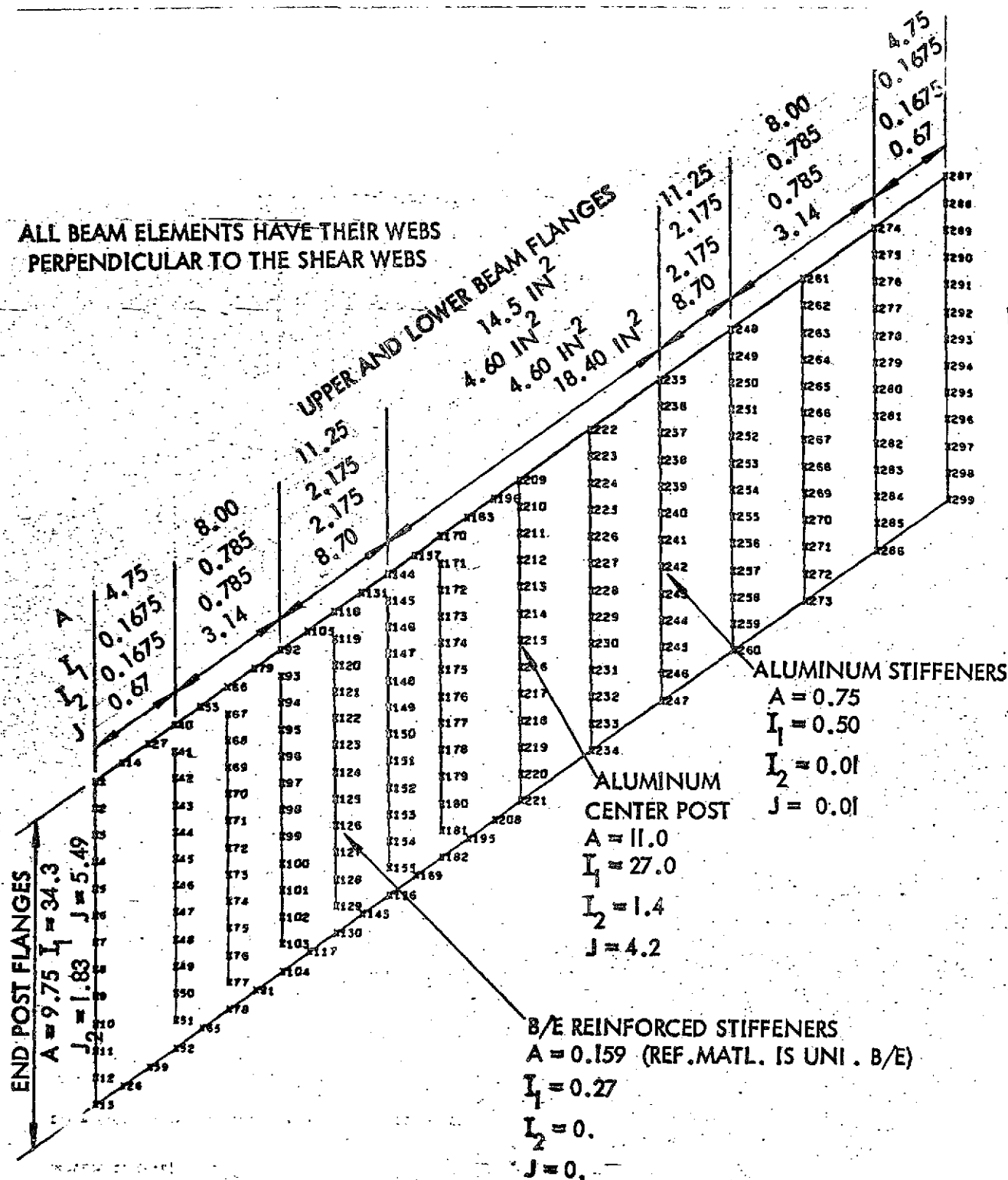


Figure 76: BEAM ELEMENTS (CBAR NASTRAN ELEMENTS)

DOC. NO.

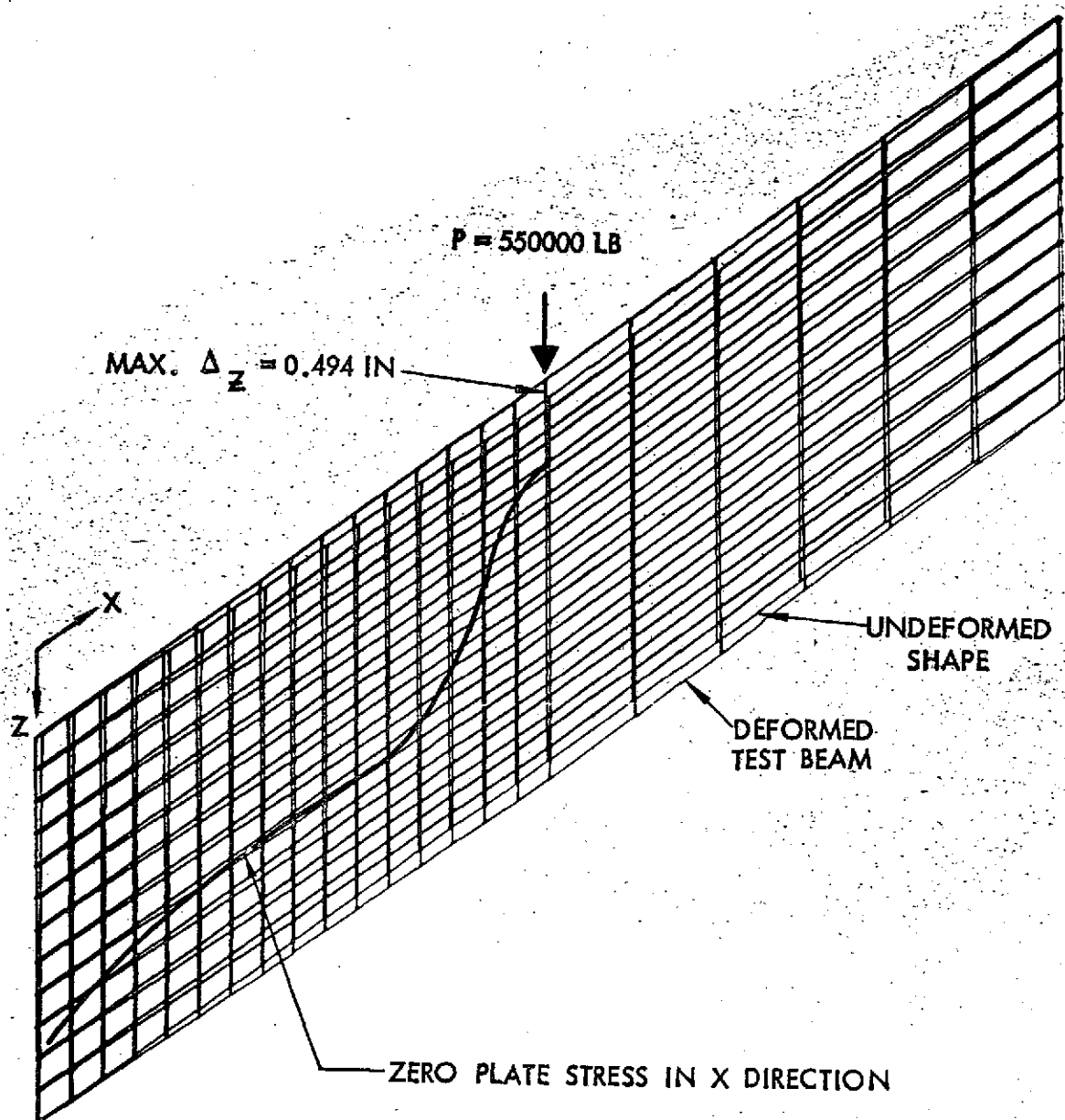


Figure 77: NASTRAN STATIC SOLUTION DATA

| | | | | | | | |
|--------|--------|--------|--------|--------|--------|--------|--------|
| 123.1 | 520.7 | 719.7 | 886.3 | 912.0 | 909.0 | 916.6 | 926.1 |
| 655.8 | 1762.8 | 2070.1 | 2553.1 | 2747.5 | 2791.2 | 2830.5 | 2803.6 |
| 884.2 | 2287.8 | 2358.6 | 3272.8 | 3579.9 | 3747.1 | 3834.7 | 3924.6 |
| 956.4 | 2615.8 | 2556.1 | 3497.8 | 3569.0 | 3737.9 | 3786.1 | 3832.3 |
| 988.0 | 2805.7 | 2733.0 | 3709.0 | 3680.8 | 3769.9 | 3784.0 | 3836.6 |
| 1013.3 | 2923.5 | 2868.2 | 3879.4 | 3812.8 | 3837.4 | 3818.2 | 3860.4 |

Figure 78: PRINCIPAL TENSION STRAINS IN TEST WEB QUADRANT 1

| | |
|---|---|
| 1 | 3 |
| 2 | 4 |

| | | | | | | | |
|--------|--------|--------|--------|--------|--------|--------|--------|
| 1044.4 | 3005.2 | 2966.5 | 4004.4 | 3925.3 | 3922.0 | 3680.5 | 3911.8 |
| 1085.6 | 3065.9 | 3039.3 | 4089.0 | 4011.0 | 4014.3 | 3965.0 | 3992.0 |
| 1134.6 | 3101.5 | 3106.4 | 4147.1 | 4086.2 | 4119.8 | 4058.1 | 4098.2 |
| 1185.0 | 3061.1 | 3241.6 | 4229.0 | 4180.8 | 4257.0 | 4176.8 | 4232.5 |
| 1298.4 | 2848.2 | 3082.5 | 3466.0 | 3384.2 | 3369.3 | 3333.6 | 3328.2 |
| 886.8 | 1397.4 | 1421.5 | 1418.1 | 1550.6 | 1588.7 | 1739.6 | 1620.8 |

Figure 79: PRINCIPAL TENSION STRAINS IN TEST WEB QUADRANT 2

| | | | | | | | | |
|--------|--------|--------|--------|--------|--------|--------|--------|--|
| | | | | | | | | |
| 915.5 | 932.7 | 968.6 | 1070.3 | 1124.1 | 1195.5 | 1136.0 | 149.0 | |
| | | | | | | | | |
| 2827.8 | 2797.0 | 2806.3 | 2895.2 | 3038.9 | 2804.6 | 2527.0 | 1188.4 | |
| | | | | | | | | |
| 3846.6 | 3792.5 | 3772.6 | 3754.7 | 3766.4 | 2960.7 | 2787.1 | 1075.0 | |
| | | | | | | | | |
| 3812.6 | 3755.7 | 3740.8 | 3724.4 | 3702.4 | 2740.2 | 2709.3 | 967.5 | |
| | | | | | | | | |
| 3303.6 | 3788.6 | 3727.8 | 3695.0 | 3563.1 | 2593.4 | 2575.1 | 874.9 | |
| | | | | | | | | |
| 3816.2 | 3753.1 | 3726.1 | 3672.4 | 3632.6 | 2499.2 | 2452.5 | 798.6 | |
| | | | | | | | | |

| | |
|---|---|
| 1 | 3 |
| 2 | 4 |

Figure 80: PRINCIPAL TENSION STRAINS IN TEST WEB QUADRANT 3

| | | | | | | | | |
|--------|--------|--------|--------|--------|--------|--------|--------|--|
| | | | | | | | | |
| 3856.7 | 3820.2 | 3740.4 | 3657.8 | 3611.2 | 2444.6 | 2275.4 | 739.3 | |
| | | | | | | | | |
| 3929.6 | 3879.6 | 3779.1 | 3653.4 | 3595.8 | 2423.4 | 2324.8 | 697.8 | |
| | | | | | | | | |
| 4034.0 | 3983.8 | 3854.8 | 3671.5 | 3570.5 | 2432.6 | 2298.1 | 678.6 | |
| | | | | | | | | |
| 4152.7 | 4151.3 | 3974.8 | 3780.7 | 3484.6 | 2465.3 | 2271.0 | 695.6 | |
| | | | | | | | | |
| 3323.9 | 3336.2 | 3239.8 | 3123.2 | 2952.4 | 2466.9 | 2152.6 | 756.3 | |
| | | | | | | | | |
| 1741.4 | 1799.1 | 1915.0 | 1786.2 | 1838.6 | 1762.5 | 1710.3 | 1352.2 | |
| | | | | | | | | |

Figure 81: PRINCIPAL TENSION STRAINS IN TEST WEB QUADRANT 4

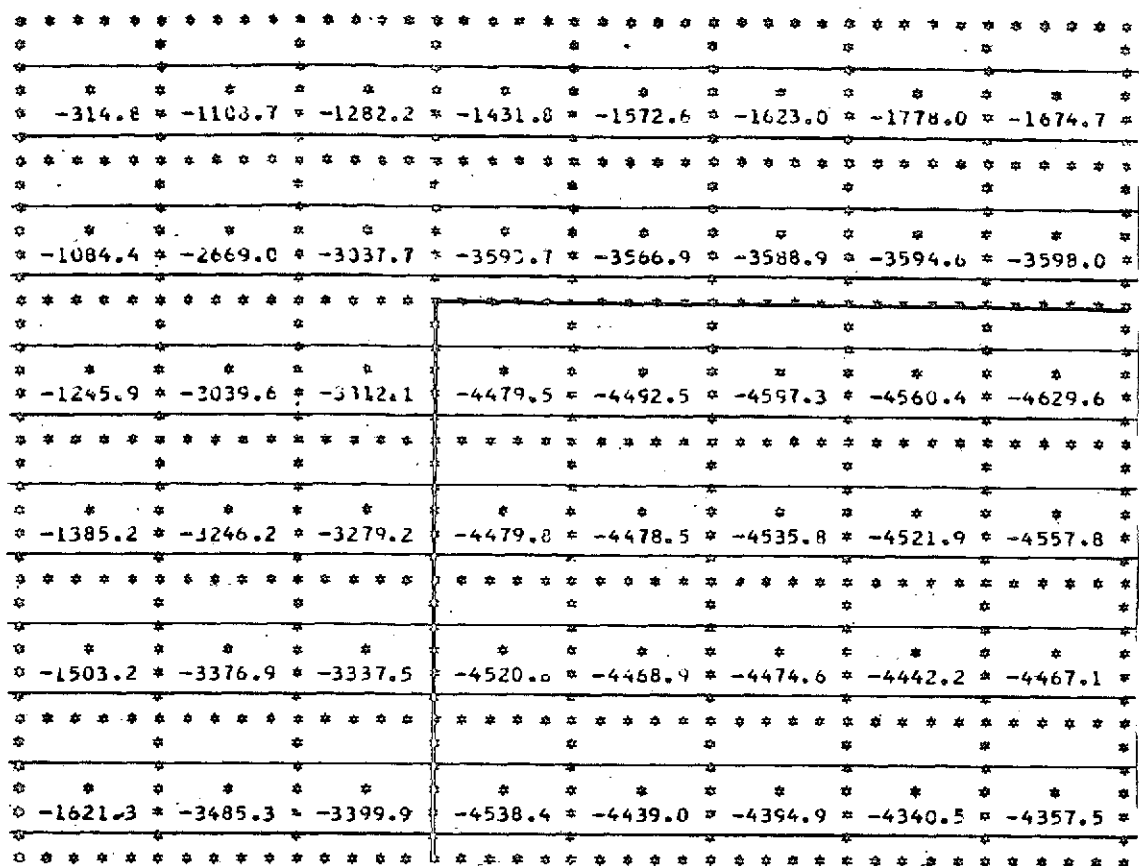


Figure 82: PRINCIPAL COMPRESSION STRAINS IN TEST WEB QUADRANT 1

| | |
|---|---|
| 1 | 3 |
| 2 | 4 |

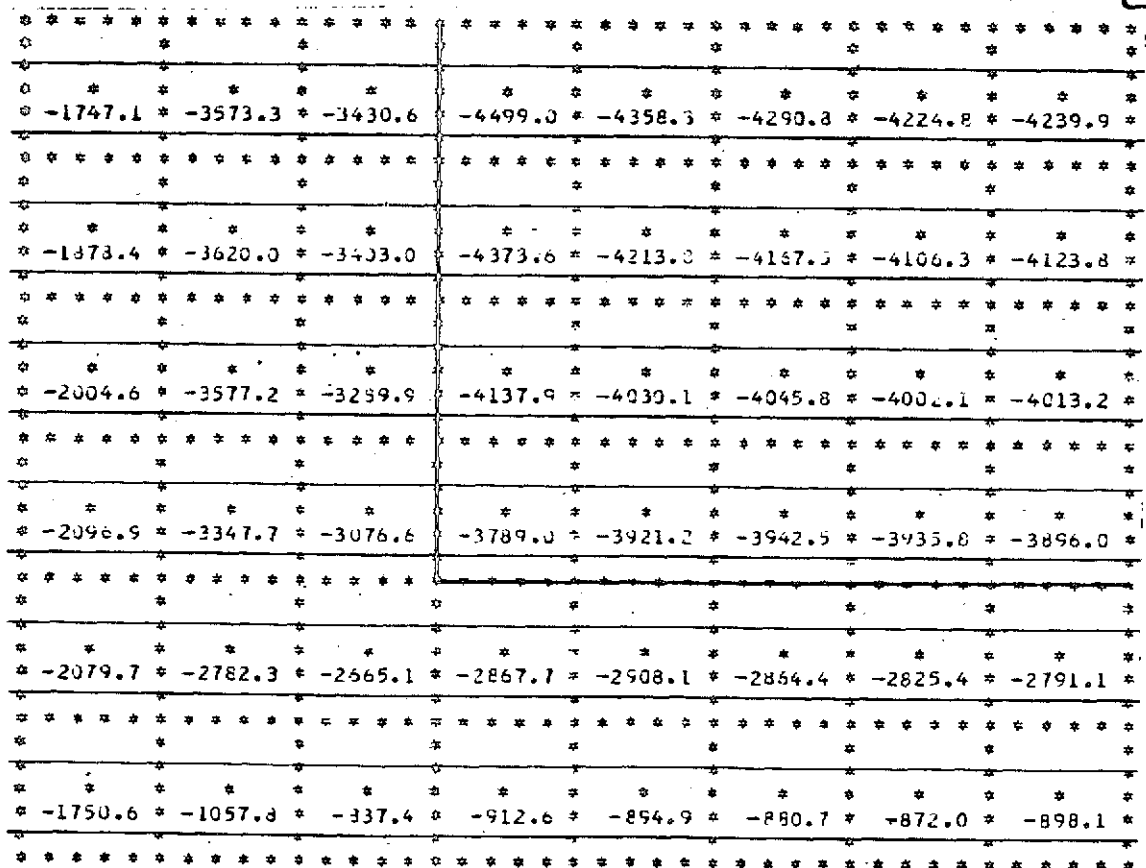


Figure 83: PRINCIPAL COMPRESSION STRAINS IN TEST WEB QUADRANT 2

| | | | | | | | | |
|--------|--------|--------|--------|--------|--------|--------|--------|--|
| | | | | | | | | |
| 437.9 | 1729.3 | 2001.8 | 2318.6 | 2484.6 | 2532.0 | 2694.6 | 2600.8 | |
| | | | | | | | | |
| 1740.1 | 4431.8 | 5107.8 | 6146.7 | 6314.5 | 6380.1 | 6425.0 | 6401.6 | |
| | | | | | | | | |
| 2130.2 | 5327.4 | 5670.7 | 7752.4 | 8072.4 | 8344.4 | 8395.2 | 8454.1 | |
| | | | | | | | | |
| 2341.7 | 5862.0 | 5835.3 | 7977.6 | 8047.4 | 8273.7 | 8308.1 | 8390.0 | |
| | | | | | | | | |
| 2491.2 | 6182.6 | 6070.5 | 8229.8 | 8149.7 | 8244.5 | 8226.2 | 8303.7 | |
| | | | | | | | | |
| 2634.6 | 6408.8 | 6268.1 | 8417.8 | 8251.8 | 8232.3 | 8158.7 | 8217.9 | |

Figure 86: PRINCIPAL SHEAR STRAINS IN TEST WEB QUADRANT 1

| | |
|---|---|
| 1 | 3 |
| 2 | 4 |

| | | | | | | | | |
|--------|--------|--------|--------|--------|--------|--------|--------|--|
| | | | | | | | | |
| 2791.5 | 6578.5 | 6397.1 | 8503.4 | 8283.6 | 8212.7 | 8105.4 | 8151.6 | |
| | | | | | | | | |
| 2964.1 | 6685.9 | 6442.3 | 8462.6 | 8224.8 | 8182.3 | 8071.3 | 8115.8 | |
| | | | | | | | | |
| 3139.2 | 6678.7 | 6398.2 | 8285.0 | 8116.3 | 8165.6 | 8070.2 | 8111.4 | |
| | | | | | | | | |
| 3281.9 | 6408.8 | 6318.1 | 8018.0 | 8102.0 | 8199.0 | 8112.6 | 8126.4 | |
| | | | | | | | | |
| 3378.1 | 5630.5 | 5747.7 | 6333.6 | 6292.3 | 6233.7 | 6158.9 | 6119.3 | |
| | | | | | | | | |
| 2637.4 | 2455.3 | 2258.9 | 2330.0 | 2445.5 | 2469.3 | 2611.7 | 2519.0 | |

Figure 87: PRINCIPAL SHEAR STRAINS IN TEST WEB QUADRANT 2

| | | | | | | | |
|--------|--------|--------|--------|--------|--------|--------|--------|
| 2711.6 | 2792.6 | 2994.3 | 3052.6 | 3254.1 | 3494.4 | 3766.2 | 2975.7 |
| 6462.4 | 6507.9 | 6538.3 | 6734.2 | 6912.5 | 6721.8 | 6623.1 | 3574.0 |
| 8448.1 | 8457.4 | 8418.9 | 8486.0 | 8221.1 | 6736.6 | 6609.1 | 3558.3 |
| 8350.4 | 8367.4 | 8266.4 | 8259.6 | 8205.9 | 6239.1 | 6247.5 | 3171.2 |
| 8235.5 | 8229.1 | 8116.8 | 8074.0 | 8011.3 | 5852.7 | 5840.1 | 2824.4 |
| 8126.7 | 8098.2 | 7973.1 | 7884.3 | 7795.6 | 5555.4 | 5484.0 | 2517.5 |

13
24

Figure 88: PRINCIPAL SHEAR STRAINS IN TEST WEB QUADRANT 3

| | | | | | | | |
|--------|--------|--------|--------|--------|--------|--------|--------|
| 8342.6 | 7990.0 | 7843.1 | 7696.3 | 7588.6 | 5331.3 | 5193.0 | 2249.2 |
| 7995.0 | 7920.4 | 7741.5 | 7523.1 | 7359.8 | 5175.5 | 4976.1 | 2018.4 |
| 7993.6 | 7904.7 | 7839.0 | 7336.7 | 7219.4 | 5090.2 | 4792.4 | 1828.9 |
| 8036.5 | 7752.2 | 7711.2 | 7363.0 | 7015.1 | 5075.6 | 4562.1 | 1695.8 |
| 6115.3 | 6062.8 | 5922.0 | 5747.1 | 5649.3 | 4725.7 | 4104.3 | 1657.7 |
| 2635.7 | 2699.8 | 2825.7 | 2730.0 | 2758.0 | 2617.6 | 2518.1 | 1814.7 |

Figure 89: PRINCIPAL SHEAR STRAINS IN TEST WEB QUADRANT 4

| | | | | | | | | |
|-------|-------|-------|------|------|------|------|------|--|
| | | | | | | | | |
| 40.3 | 36.0 | 31.9 | 33.1 | 30.8 | 29.1 | 27.6 | 28.2 | |
| | | | | | | | | |
| -41.4 | 42.8 | 40.3 | 39.2 | 38.3 | 37.9 | 37.9 | 37.9 | |
| | | | | | | | | |
| -37.4 | -43.6 | 44.1 | 41.5 | 40.2 | 39.5 | 39.8 | 39.7 | |
| | | | | | | | | |
| -35.7 | -41.9 | -43.6 | 43.2 | 41.2 | 40.3 | 40.1 | 40.4 | |
| | | | | | | | | |
| -34.2 | -41.4 | -43.0 | 44.1 | 42.2 | 41.3 | 40.9 | 41.1 | |
| | | | | | | | | |
| -32.9 | -41.4 | -43.2 | 44.4 | 43.0 | 42.2 | 41.9 | 42.1 | |

Figure 90: PRINCIPAL STRAIN AXIS ANGLES IN TEST WEB QUADRANT 1

| | |
|---|---|
| 1 | 3 |
| 2 | 4 |

| | | | | | | | | |
|-------|-------|-------|-------|-------|-------|-------|-------|--|
| | | | | | | | | |
| -31.8 | -41.6 | -43.6 | 44.4 | 43.7 | 43.3 | 43.1 | 43.2 | |
| | | | | | | | | |
| -31.0 | -41.9 | -44.1 | 44.6 | 44.5 | 44.5 | 44.4 | 44.5 | |
| | | | | | | | | |
| -30.6 | -42.1 | -44.2 | -44.7 | -44.3 | -44.1 | -44.2 | -44.2 | |
| | | | | | | | | |
| -30.2 | -41.5 | -43.0 | -42.9 | -42.6 | -42.4 | -42.8 | -42.6 | |
| | | | | | | | | |
| -29.5 | -39.3 | -40.2 | -40.7 | -40.2 | -40.1 | -40.2 | -40.0 | |
| | | | | | | | | |
| -24.2 | -33.6 | -31.1 | -32.7 | -30.3 | -29.7 | -27.1 | -28.2 | |

Figure 91: PRINCIPAL STRAIN AXIS ANGLES IN TEST WEB QUADRANT 2

| | | | | | | | | |
|------|------|------|-------|-------|-------|-------|-------|--|
| | | | | | | | | |
| 27.0 | 26.6 | 26.7 | 29.3 | 30.4 | 34.2 | 41.6 | -33.2 | |
| | | | | | | | | |
| 38.3 | 38.6 | 39.7 | 41.0 | 43.1 | -42.4 | -36.5 | -21.6 | |
| | | | | | | | | |
| 40.5 | 41.1 | 42.5 | 43.8 | -44.1 | -39.9 | -34.8 | -19.4 | |
| | | | | | | | | |
| 41.0 | 41.9 | 43.2 | 44.7 | -43.4 | -38.9 | -34.5 | -19.0 | |
| | | | | | | | | |
| 41.7 | 42.7 | 43.9 | -44.5 | -42.6 | -38.2 | -34.5 | -19.4 | |
| | | | | | | | | |
| 42.6 | 43.4 | 44.6 | -43.6 | -41.9 | -37.9 | -34.9 | -20.5 | |
| | | | | | | | | |

13
24

Figure 92: PRINCIPAL STRAIN AXIS ANGLES IN TEST WEB QUADRANT 3

| | | | | | | | |
|-------|-------|-------|-------|-------|-------|-------|-------|
| | | | | | | | |
| 43.6 | 44.2 | -44.7 | -43.2 | -41.3 | -37.9 | -35.6 | -22.0 |
| | | | | | | | |
| 44.7 | -44.9 | -44.1 | -42.7 | -41.0 | -38.1 | -36.4 | -24.2 |
| | | | | | | | |
| -44.1 | -43.9 | -43.5 | -42.4 | -40.8 | -38.6 | -37.4 | -26.8 |
| | | | | | | | |
| -42.9 | -42.8 | -42.9 | -42.2 | -41.3 | -39.6 | -38.4 | -29.5 |
| | | | | | | | |
| -40.1 | -40.1 | -40.3 | -40.2 | -40.0 | -39.4 | -38.3 | -30.1 |
| | | | | | | | |
| -27.1 | -26.6 | -26.1 | -27.5 | -27.0 | -25.7 | -24.9 | -15.3 |
| | | | | | | | |

Figure 93: PRINCIPAL STRAIN AXIS ANGLES IN TEST WEB QUADRANT 4

The failure mode analysis relationships in Appendix A and the strain results from the finite element static solution give the following critical test beam loads (total applied test machine load):

| | |
|---|------------|
| Failure by Tearing at the Stiffener Fastener Holes | 640000 lb. |
| Failure by Local Panel Buckling Interaction | 674000 lb. |
| Failure by Cladding Yielding | 763000 lb. |
| Failure by B/E ultimate strain | 780000 lb. |

The allowable tension strain in the reinforced fastener hole areas is 3845 $\mu\epsilon$ based on the design function in Figure 18. Taken individually, the critical loads defined in Appendix A for local panel buckling in shear and beam bending are 9511 and 8537 lb./in., respectively.

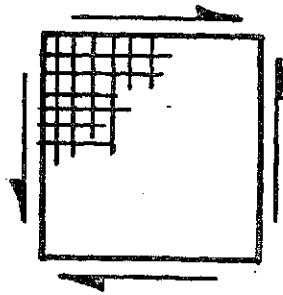
The critical test beam loads for fastener hole tearing and panel buckling are close to the general instability load. It is recognized that some local panel prebuckling deformations can precipitate from initial imperfections which will tend to increase the tension strains that are predicted for shear resistant conditions. The web component could then be expected to fail by tearing at the stiffener fastener holes at a load level less than indicated above.

Prior to determining the general instability load for the test web, NASTRAN runs were made on simple pure shear web models shown in Figure 94 to evaluate modeling quality. The agreement between the NASTRAN solution and Seydel's analysis given in Appendix A is considered to be satisfactory for the model shown, which is the same as the test web (3 x 3 in. plate elements) except for reinforced edge areas, support conditions and overall configuration.

The B/E reinforced test web buckling modes computed by NASTRAN are shown in Figures 95, 96 and 97. The critical mode has an eigenvalue of 1.21 which corresponds to a critical applied load of 665000 lb. The critical mode shape is typical of highly orthotropic stiffened web structure and is quite close in form to the second mode shape. The maximum first mode amplitude occurs at node 83 which is a panel node located between stiffeners. Based on the calculated critical mode shape, considerable stiffener torsion displacements will result if general instability type deflections occur during loading. The stiffener configuration selected for the web component is considered to be resistant to B/E reinforcement debonding under such torsional deflection conditions, particularly since the prebuckling stiffener loads are very low in a shear resistant web and are essentially due to Poisson's strain response at the web edges.

As a fail safe assessment of the baseline design web, the test web model was modified by removing the B/E reinforcement from one stiffener simulating a debonded condition. The resultant critical mode (shown in Figure 98) eigenvalue is 19% lower than the undamaged model which reflects adequate capability of the design to carry limit load in a fail safe manner.

| CONSTRUCTION | NASTRAN N_{XYCR} LB / IN | THEORETICAL N_{XYCR} | <u>NASTRAN</u> THEORY |
|---|-------------------------------|---|--------------------------|
| UNSTIFFENED TITANIUM ($T = 0.156$ IN.) | 429.6 | 406.8 (SEYDEL) | 1.056 |
| UNSTIFFENED TI-CLAD B/E TEST WEB | 535.2 | 443.2 (ISOTROPIC PLATE BUCKLING ANALYSIS ASSUMED BLEICH) | 1.208 |
| STIFFENED TI-CLAD B/E TEST WEB | 9803. | 9354. (SEYDEL) | 1.048 |

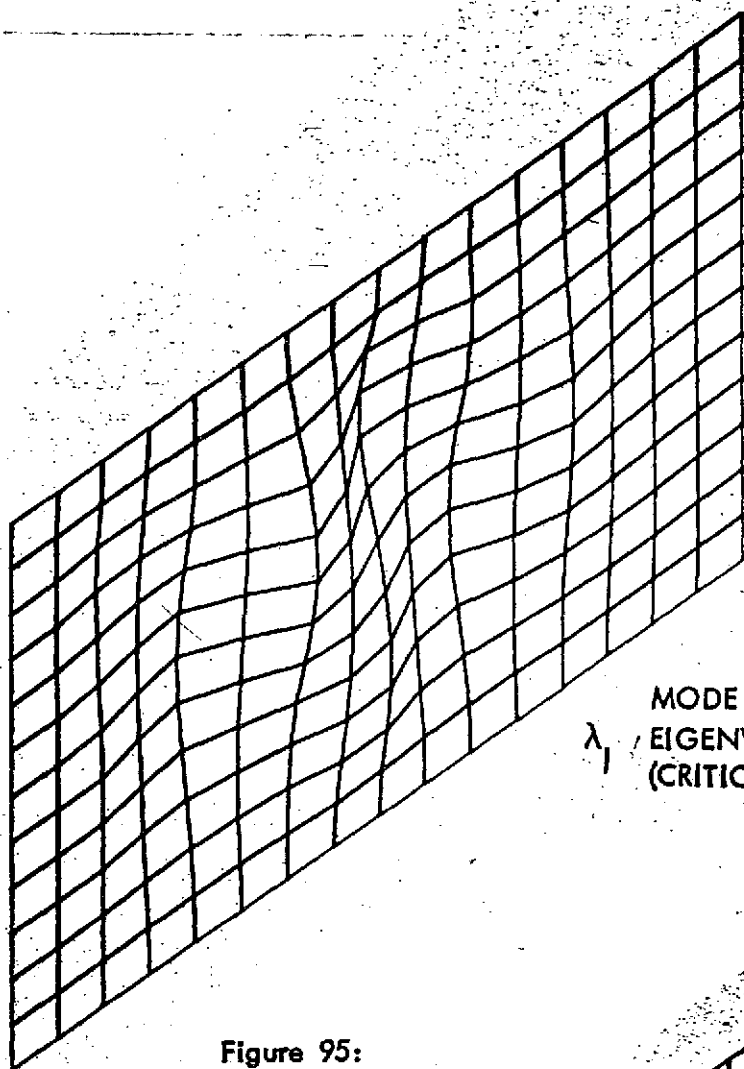


PURE SHEAR WEB MODEL

36 X 36 IN

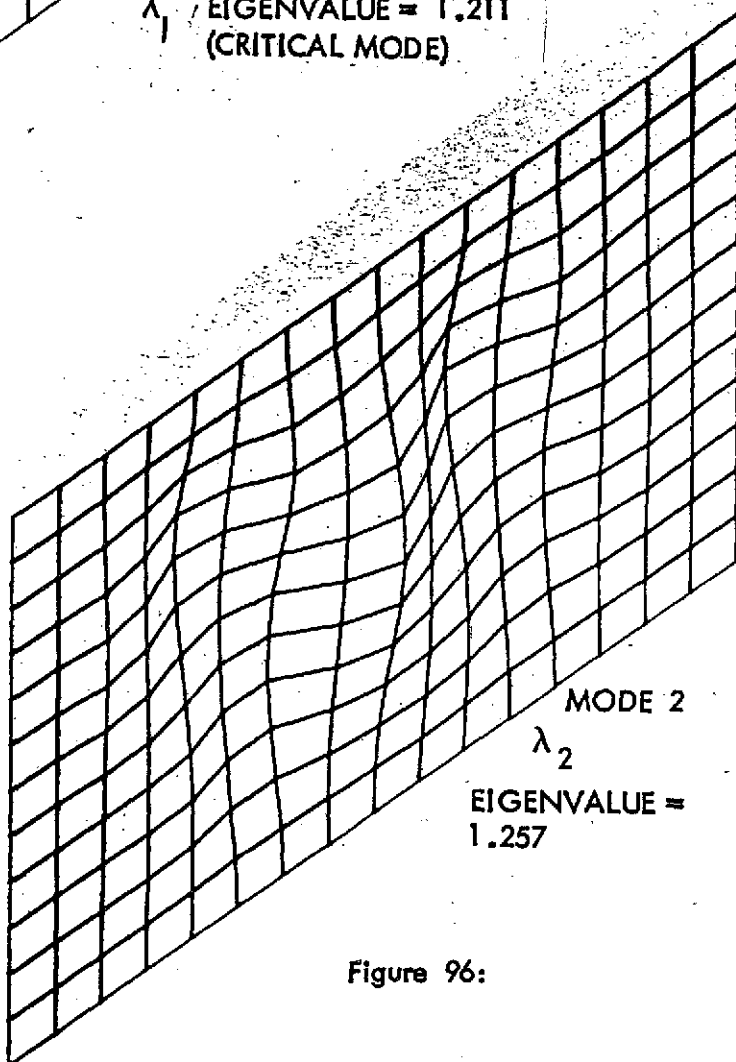
144 SQUARE PLATE
ORTHOTROPIC ELEMENTS

Figure 94: NASTRAN BUCKLING ANALYSIS CORRELATION



MODE 1
 λ_1 EIGENVALUE = 1.211
 (CRITICAL MODE)

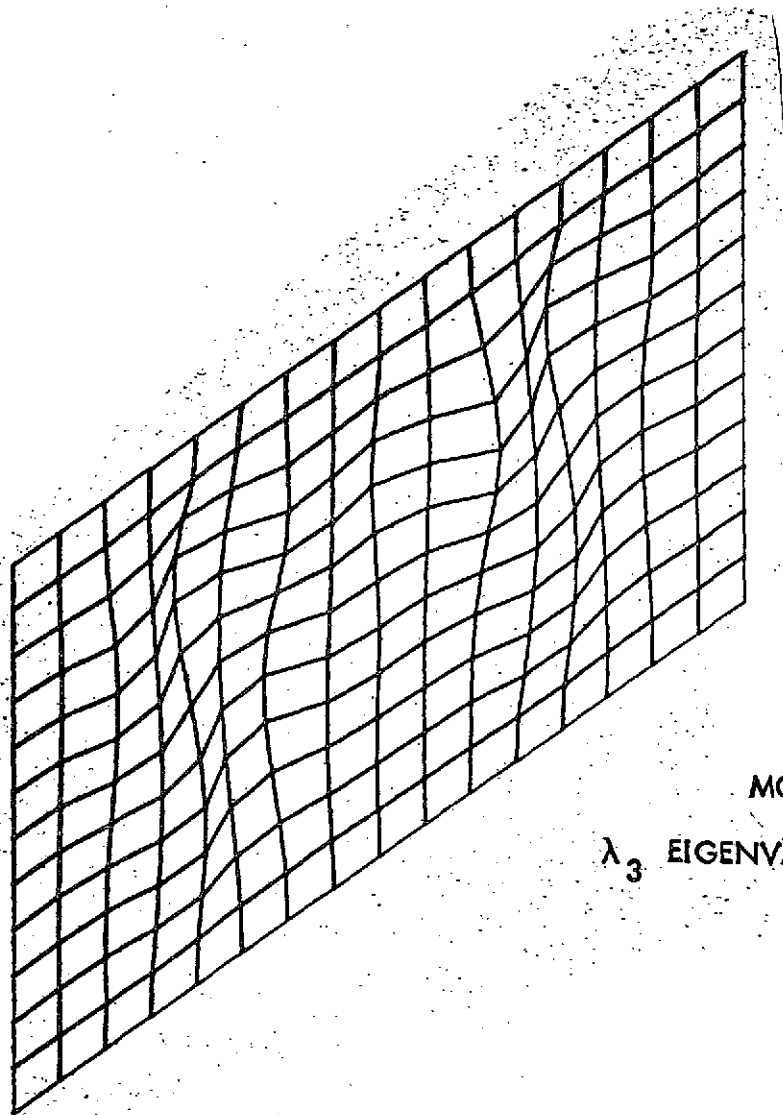
Figure 95:



MODE 2
 λ_2
 EIGENVALUE = 1.257

Figure 96:

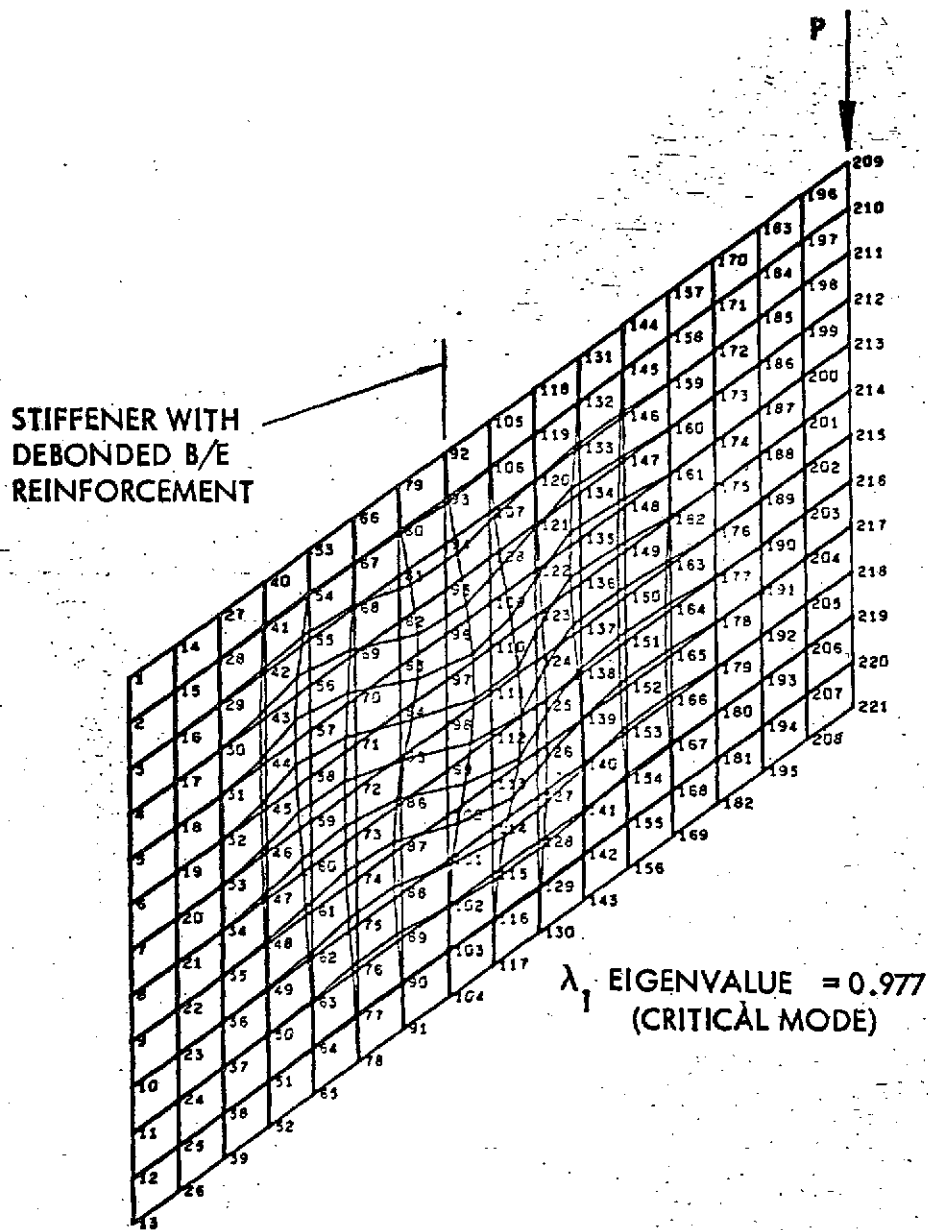
NASTRAN BUCKLING SOLUTION FOR TEST WEB COMPONENT



MODE 3

 λ_3 EIGENVALUE = 1.503

Figure 97: NASTRAN BUCKLING SOLUTION FOR TEST WEB COMPONENT



BORON/EPOXY REINFORCED TITANIUM SHEAR WEB
(TEST PANEL) WITH DEBONDED STIFFENER

BUCKLING SOLUTION
MODAL DEFORMATION - SUBCASE 2 MODE 1

Figure 98: NASTRAN BUCKLING SOLUTION FOR TEST WEB COMPONENT WITH DEBONDED STIFFENER REINFORCEMENT

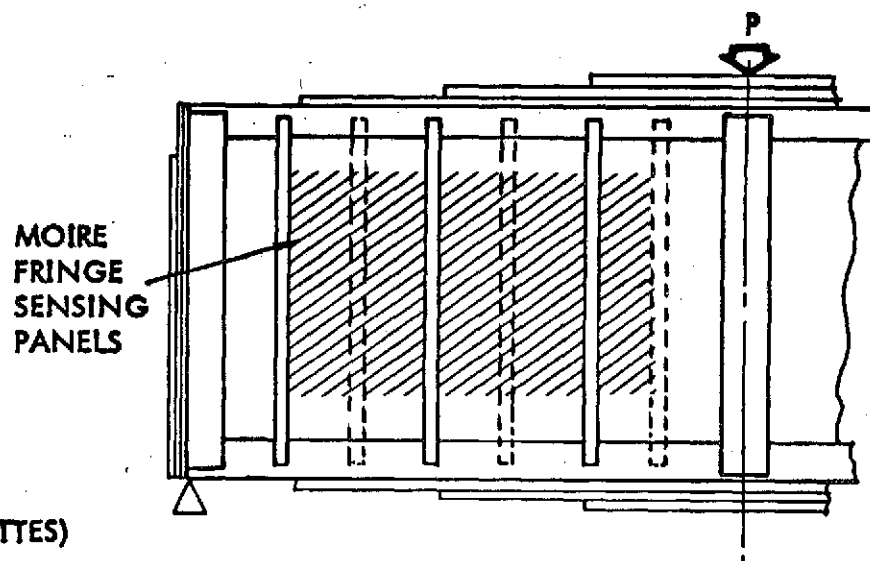
5.3 Component Test Planning

Test procedures and equipment that will be used in the first shear web component test are presented in Appendix C, and are summarized in Figure 99. Data from Moire fringe, strain gage, deflection and acoustic emission data will be recorded in the initial cyclic limit load application simulating orbiter engine operation and during the final loading to failure. The limit load level is established at 400000 lb. which reproduces the limit N_{xy} shear loading experienced by the baseline design web. The test beam will be rigidly restrained to preclude lateral movement of the flanges in the end and center areas.

The rosette strain gages will be placed in areas of the web laminate having the highest principal strains predicted by the NASTRAN static analysis and in areas of reinforced titanium. Rosette strain gages will also be located in areas of the principal diagonal modal line indicated by the NASTRAN buckling solution for the critical general instability mode. The gages in the nominal laminate areas will be back-to-back to sense out-of-plane buckling-type deformations.

The Moire fringe measurements will be accomplished by the basic method described in Reference 22 and will be important in detecting local buckling in the laminate panels. Both nonlinear buckling, precipitated by initial imperfections, and/or classical bifurcation buckling modes can be observed in this manner. In addition, the fringe sensing panels will be placed to overlap the stiffener fastener reinforcement lands so that crippling between fasteners can be detected.

Based on the results of the first web component test, the test procedures and instrumentation will be revised as required to improve data acquisition during the following tests.



PANEL RESPONSE MEASUREMENTS

- . MOIRE FRINGES
- . STRAINS (16 THREE-ELEMENT ROSETTES)
- . DEFLECTIONS (1 VERTICAL AND 1 LATERAL)
- . ACOUSTIC EMISSIONS (HIGH AND LOW FREQUENCY & ACCELEROMETERS)

LOAD PROGRAM

- . LOAD TO LIMIT LOAD- RECORD DATA ON ELECTRONIC DATA RECORDING SYSTEM
- . LOAD 100 CYCLES TO LIMIT LOAD
- . RECORD DATA AT 50th CYCLE
- . LOAD TO FAILURE LOAD-RECORD DATA

DATA PROCESSING

- . PLOT MEASURED STRAIN AND DEFLECTION DATA
- . PLOT COMPUTED PRINCIPAL STRAIN DATA
- . PROCESS MOIRE FRINGE PHOTOGRAPHS AND CALIBRATE FRINGE ORDERS

Figure 99: DATA ACQUISITION REQUIREMENTS FOR THE FIRST WEB COMPONENT TEST

6.0 CONCLUSIONS

The titanium-clad boron-epoxy shear web design concept selected and developed in Phase I offers good weight savings at reasonable cost for a Space Shuttle main engine thrust structure application. The concept is practical to fabricate in production shops and has a high degree of inspectability by non-destructive test methods.

The design synthesis technique utilized allowed an extensive search for the best design concept and optimum design details. The selected composite reinforced shear web design, consisting of a titanium clad $\pm 45^\circ$ boron-epoxy web with boron-epoxy reinforced vertical aluminum stiffeners, provides 24% weight saving compared to a similar web without composite reinforcement. Structural element testing and detailed analyses have substantiated the performance and reliability of the design details on a laboratory basis. From these results, it is concluded that the Phase I studies provide an adequate basis for proceeding to fabrication and test of the shear webs in Phases II and III.

7.0 REFERENCES

1. Grumman Report MSC-03810, "Final Report Alternate Space Shuttle Concepts Study," Part II Technical Summary, Vols. I and II, July 1971.
2. NASA/MSFC Documents: 13M15000B, "Space Shuttle Vehicle/Engine, 550K(SL), Interface Control Document," and "Contract and Item (CEI) Specification, Space Shuttle Main Engine, 550K(SL)," March 1, 1971.
3. AVCO Systems Division, AVCO Corp. Specification sheet BP-200-174-5M "RIGIDITE 5505/4 PREPREG TAPE."
4. NARMCO Material Division, Whittaker Corp., Product Information Sheet, "METLBOND 329 ADHESIVE," September 1970.
5. Adhesives, Coatings And Sealers Division, 3 M Co. Product Specification, "SCOTCH-WELD BRAND STRUCTURAL ADHESIVE PRIMER EC-2333."
6. Boeing Material Specification, BMS 5-51C, "Moderate Temperature Curing Structural Adhesive System," The Boeing Co.
7. NASA CR-224, "Strength Characteristics of Composites," S. W. Tsai, April 1965.
8. Prager, W. and P. G. Hodge, "Theory of Perfectly Plastic Solids," John Wiley, 1951.
9. Timoshenko, S. P., and J. M. Gere, "Theory of Elastic Stability," Second Edition, McGraw-Hill, 1961.
10. NACA TM 705, "The Critical Shear Load of Rectangular Plates," E. Seydel.
11. Yusuff, S., "Theory of Wrinkling in Sandwich Construction," Journal of the Royal Aeronautical Society, pp. 30-36, Vol. 59, January 1955.
12. NASA CR-1457, "Manual for Structural Stability Analysis of Sandwich Plates and Shells," R. T. Sullins, G. W. Smith and E. E. Spier, December 1969.
13. NACA TN 2661 and 2662, "A Summary of Diagonal Tension, Parts I (Methods of Analysis) and II (Experimental Evidence)", P. Kuhn and J. P. Peterson, May 1952.
14. Sobieszcanski, J., and D. Loendorf, "A Mixed Optimization Method for Automated Design of Fuselage Structures," AIAA/ASME/SAE 13th Structures, Structural Dynamics and Materials Conference, San Antonio, Texas, April 10, 12, 1972.
15. AFFDL-TR-70-118, "An Automated Procedure for the Optimization of Practical Aerospace Structures," W. J. Dwyer, R. K. Emerton and I. U. Ojalvo, Grumman Aerospace Corporation, Prepared for the Air Force Flight Dynamics Lab., April 1971.

16. BOEING DESIGN MANUAL, The Boeing Co., "Holes In Webs" Section 318.4.5.3.
17. King, K. M., Article On Shear Web Hole Reinforcement, AERO Digest, pp 24-29, August 1955.
18. Lekhnitskii, S. G., "Anisotropic Plates," (translation by S. W. Tsai and T. Cheron) Gordon and Breach Science Publishers, New York, 1968.
19. NASA SP-222, "The NASTRAN User's Manual," September 1970.
20. Viswanathan, A. V., Soong, Tsai-Chen, and R. E. Miller, Jr., "Buckling Analysis for Axially Compressed Flat Plates -- Structural Sections and Stiffened Plates Reinforced With Laminated Composites," NASA CR-1887, 1971.
21. Boeing Data, to be published.
22. Dykes, B. C., "Analysis of Displacements in Large Plates by the Grid-Shadow Moire Technique," Proceedings 4th International Conference On Experimental Stress Analysis, Inst. Mech. Engrs., Cambridge, Eng., 1970.
23. Bleich, F., "Buckling Strength of Metal Structures," McGraw-Hill, 1952.
24. BOEING DESIGN MANUAL, Section 318.5, "Shear Buckling Resistant Beams," (Unreleased), The Boeing Co.

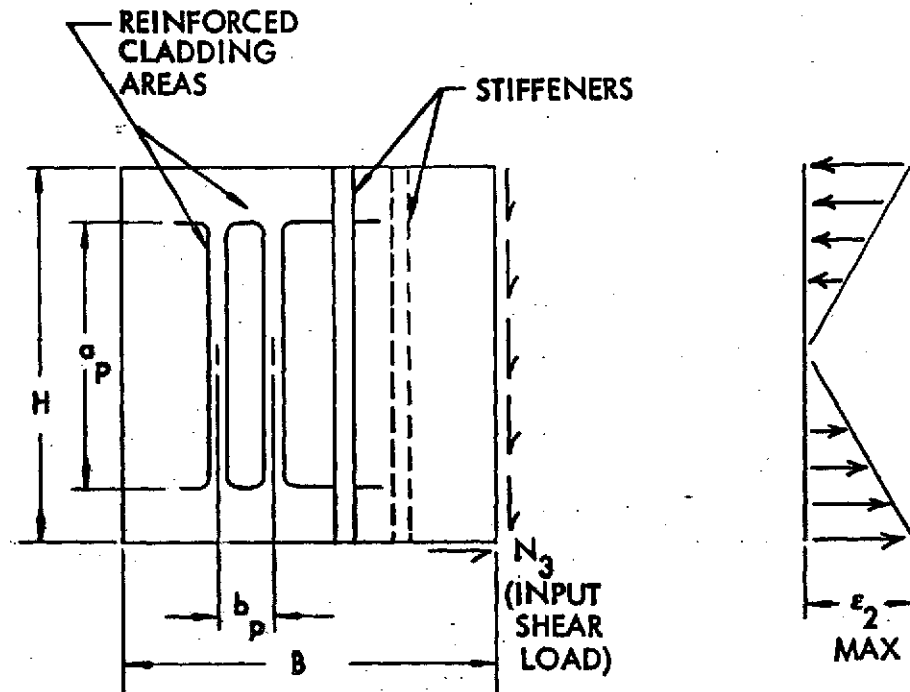
PRECEDING PAGE BLANK NOT FILMED

APPENDICES

- APPENDIX A - Analyses used in OPTRAN Code for Vertically Stiffened Shear Resistant Shear Web
- APPENDIX B - Design Drawings
- APPENDIX C - Test Plan for the Shear Web Test Components

Appendix A - Analyses used in OPTRAN Code for Vertically Stiffened Shear Resistant Shear Web

CONFIGURATION



Laminate and stiffener section details are given in Figure 9 in Section 3.5.

PROPERTIES

The room temperature material properties used in the structural analyses are input as shown in Table A-1.

ELASTIC STIFFNESSES

Web Plate

$$\left. \begin{array}{l} \text{Membrane} \\ \text{Bending} \end{array} \right\} \begin{array}{l} A_{w_{ij}} \\ D_{w_{ij}} \end{array} \quad i, j = 1, 2, 3$$

These stiffnesses are computed by classical laminate analysis (7) & stored in tabular form as shown in Table 2, Section 3.5. The data is stored in terms

| | BORON/EPOXY UNIDIRECTIONAL PLIES (RIGIDITE 5505/4) | ADHESIVE (METLBOND 329) | TITANIUM 6AL-4V MILL ANNEALED | ALUMINUM 7075-T6 |
|---|---|-------------------------------|--|---------------------|
| E_x 10^6 lb/in^2 | 30 | 0.5 | 16 | 10.3 |
| E_y 10^6 lb/in^2 | 1.0 | 0.5 | 16 | 10.3 |
| G_{xy} 10^6 lb/in^2 | 1.0 | 0.2 | 6.2 | 3.9 |
| ν_{xy} | 0.25 | 0.4 | 0.3 | 0.33 |
| PLY THK. In. | 0.0055 | 0.012 | - | - |
| MIN. THK | - | - | 0.020 | 0.020 |
| VOLUME FRACTION % | 50 | - | - | - |
| UNIT. WT. lb/in^3 | 0.0725 | 0.0635 | 0.16 | 0.1012 |
| ϵ_{ULT} 10^{-6} IN/IN | 6000 | - | - | - |
| F_{ty} lb/in^2 | - | - | 126000 | 67000 |

Table A-1:
ROOM TEMPERATURE MATERIAL PROPERTIES USED IN STRUCTURAL ANALYSIS

of stiffnesses relative to respective stiffness as for an equal thickness titanium plate (6Al-4V mill annealed) for various laminate constructions defined by ξ .

ξ is the net filamentary composite fraction in the structural laminate (less adhesive plies).

$$\xi = \frac{t_{CO}}{2t_{CL} + t_{CO} - \sum t_{adh}}$$

These thicknesses are defined in Figure 9, (Section 3.5).

Stiffened Web (Smeared Stiffeners Assumed)

$$\left. \begin{array}{l} \text{Membrane} \\ \text{Bending} \end{array} \right\} \begin{array}{l} A_{ij} \\ D_{ij} \end{array} \quad i, j = 1, 2, 3$$

LOADS

$$\epsilon_{2 \max} = \text{input uniform linear beam bending strain at chord}$$

Maximum beam bending strain in nominal laminate section

$$\epsilon_2 = \frac{a_p}{H} \epsilon_{2 \max}$$

$$N_3 = \text{input shear load}$$

$$\text{Shear strain } \epsilon_3 = \frac{N_3}{A_{33}}$$

Web plate biaxial loads (web assumed to be in plane strain in 1 - Direction to produce a conservative value for N_2):

For general instability analysis:

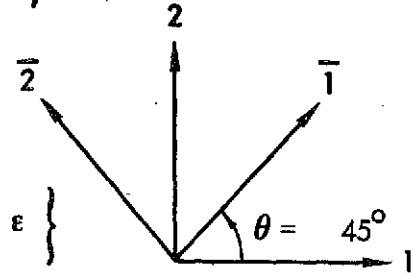
$$\begin{Bmatrix} N_1 \\ N_2 \max \\ N_3 \end{Bmatrix} = [A_{ij}] \begin{Bmatrix} 0 \\ \epsilon_2 \max \\ \epsilon_3 \end{Bmatrix}$$

For nominal laminate panel analyses:

$$\begin{Bmatrix} N_1 \\ N_2 \\ N_3 \end{Bmatrix} = [A_{ij}] \begin{Bmatrix} \epsilon_1 \\ \epsilon_2 \\ \epsilon_3 \end{Bmatrix}$$

Transformed Strains at $\theta = 45^\circ$

$$\begin{Bmatrix} \bar{\epsilon} \end{Bmatrix} = \frac{1}{2} \begin{bmatrix} 1 & 1 & -1 \\ 1 & 1 & 1 \\ -1 & 1 & 0 \end{bmatrix} \begin{Bmatrix} \epsilon \end{Bmatrix}$$



Cladding Stresses

$$\sigma_i = a_{ij} \epsilon_j \quad i, j = 1, 2, 3$$

where a_{ij} are the cladding elastic modulus properties

$$a_{11} = a_{22} = \frac{E}{1 - \nu^2}$$

$$a_{33} = G$$

$$a_{12} = a_{21} = \nu a_{11}$$

$$a_{13} = a_{31} = a_{23} = a_{32} = 0$$

FAILURE MODES

Cladding Yielding

Von Mises yield criterion (8)

$$F_e = \left[\sigma_1^2 + \sigma_2^2 - \sigma_1 \sigma_2 + 3 \sigma_3^2 \right]^{1/2}$$

$$F_e \leq F_{TY}$$

Composite Strain

$$|\bar{\epsilon}_1| \leq \epsilon_{\text{Allowable}}$$

$$|\bar{\epsilon}_2| \leq \epsilon_{\text{Allowable}}$$

Local Panel Instability

Shear (23)

$$K_s = 5.34 + \frac{4}{(a_p/b_p)^2} \quad a_p = H - 11.0 \text{ (Assumed)}$$

$$N_{3\text{CRPI}} = \frac{K_s \pi^2 D_{11w}}{b_p^2} \quad \text{(Critical web load, lb/in)}$$

Bending

$$k_{bp} = 5.0 \text{ (Assumed Minimum Value)}$$

$$N_{2\text{CRPI}} = \frac{k_{bp} \pi^2 D_{22w}}{b_p^2} \quad \text{(Critical web load, LB/IN)}$$

Interaction

$$R_{\text{SPI}} = \frac{N_3}{N_{3\text{CRPI}}} \quad R_{\text{BPI}} = \frac{N_2}{N_{2\text{CRPI}}}$$

$$R_{\text{SPI}}^2 + R_{\text{BPI}}^2 \leq 1.0$$

General Instability

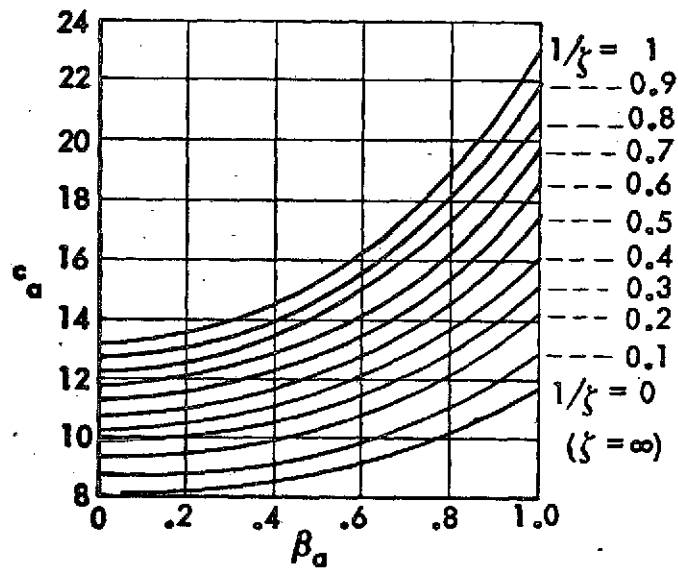
Shear (10)

$$a = H \quad b = B$$
$$N_{3\text{CRGI}} = \frac{4C_a}{b^2} \left[D_{11}^3 D_{22} \right]^{\frac{1}{4}}$$

C_a is a function of

$$\beta_a = \frac{a}{b} \left[\frac{D_{22}}{D_{11}} \right]^{\frac{1}{4}} \quad \text{and} \quad \frac{1}{\xi} = \left[\frac{D_3}{D_{11} D_{22}} \right]^{\frac{1}{2}}$$

$$\text{where } D_3 = \nu_{21} D_{11} + 2D_{33}$$



CRITICAL SHEAR LOAD COEFFICIENT

Bending⁽¹⁸⁾

$$K_{bGI} = 11.1 \left[1.25 + \frac{D_3}{\left[D_{11} D_{22} \right]^{\frac{1}{2}}} \right]$$

$$N_{2CRGI} = \frac{K_{bGI} \pi^2}{a^2} \left[D_{11} D_{22} \right]^{\frac{1}{2}} \quad \text{(Critical Web Load, Lb/in)}$$

Interaction

$$R_{SGI} = \frac{N_3}{N_{3CRGI}} \quad \left| \quad R_{BGI} = \frac{N_{2 \max}}{N_{2CRGI}} \right.$$

$$R_{SGI}^2 + R_{BGI}^2 \leq 1.0$$

The effects of N_1 are omitted from the above interaction equations since this load is actually an order of magnitude less than the shear load. This omission is offset by the conservative value for N_2 resulting from the assumption of plane strain web laminate response.

Failure at Reinforced Holes for Stiffener Fasteners

Allowable Strain:

$$\bar{\epsilon}_{ra} = 6000 - (6000 - 1400) \xi_r \quad (\mu\epsilon)$$

where ξ_r is the net filamentary composite fraction in the reinforced laminate (less adhesive plies). The allowable strain function appears in Figure 19, Section 4.1.

Actual Diagonal Tension Strain:

$$\bar{\epsilon}_r = \frac{\bar{A}_{r11}^{-1}}{\bar{A}_{11}^{-1}}$$

where \bar{A}_{r11}^{-1} and \bar{A}_{11}^{-1} are terms

from the inverted membrane stiffness matrices transformed to the $\theta = 45^\circ$ orientation for the reinforced and nominal laminates, respectively.

For an all-metal design case, the allowable $\bar{\epsilon}_r$ is arbitrarily selected to be 65% of the proportional limit tension strain to produce a slight pad-up in fastener hole areas.

$$\bar{\epsilon}_r \leq \bar{\epsilon}_{ra}$$

Constraint on Stiffener Gage

$$t_s \geq 0.6 (2t_{CL} + t_{CO}) - 2t_{CLR}$$

This relation is based on unpublished design data for shear resistant titanium webs (24) which requires that $t_s \geq 0.6 t_w$. The cladding reinforcement is assumed to act as effective stiffener attachment leg gage.

Weight Analysis

Nominal weights are computed and summed for the following items in terms of lb/lin. ft. of web.

Nominal cladding skins

Adhesive plies

Filamentary composite plies

Cladding reinforcement along stiffener fastener lines

Nominal stiffener section

A depth of H (full web depth) is assumed in the analyses. Weight allowances for fasteners, radii, edge joints, reinforced cladding edge areas, cutouts, stiffener end details and manufacturing tolerances are not made in the OPTRAN weight analyses.

APPENDIX B

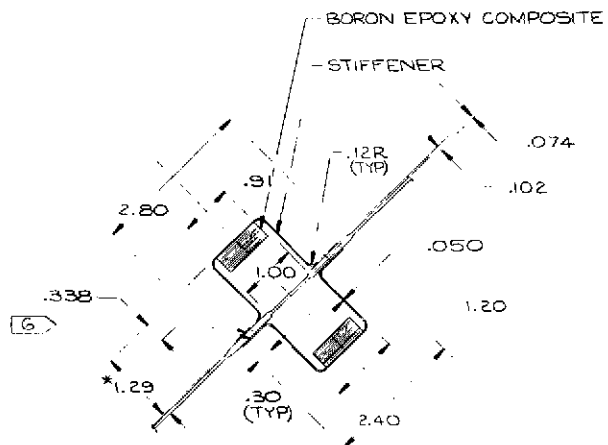
DESIGN DRAWINGS



- SK11-043165

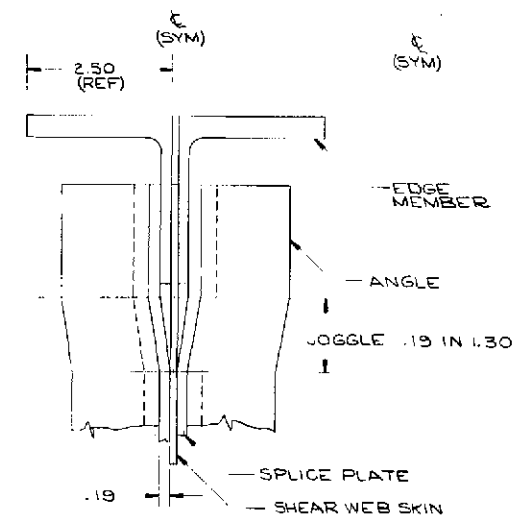
SK11-043162

| REV | DESCRIPTION | DATE | APPROVED |
|-----|-------------|------|----------|
| 1 | | | |

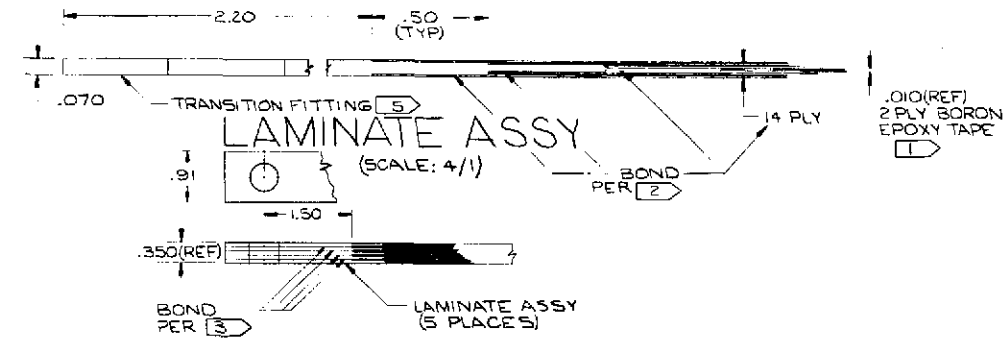


SECTION B-B
(SCALE: 1/1)

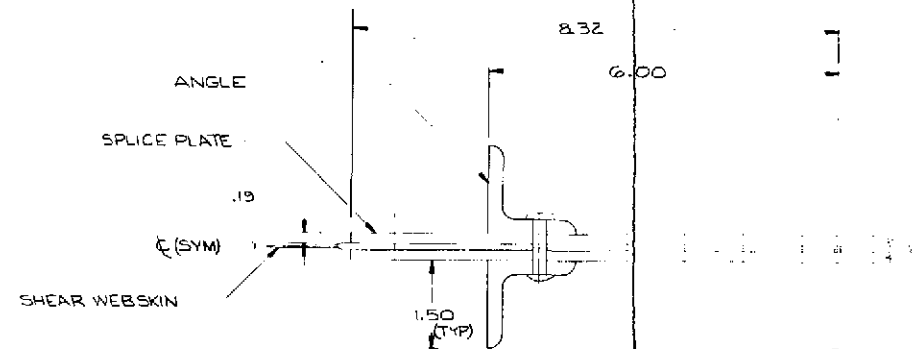
* HEIGHT AT CENTER OF LONG STIFFENER. SEE VIEW C-C FOR TYPICAL END



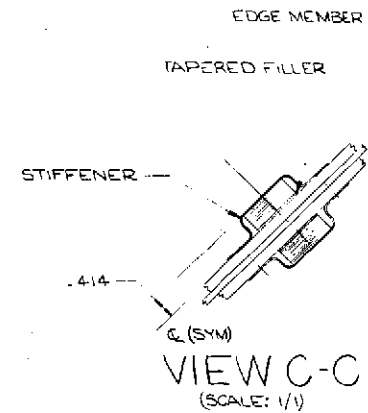
SECTION F-F
(SCALE: 1/1)



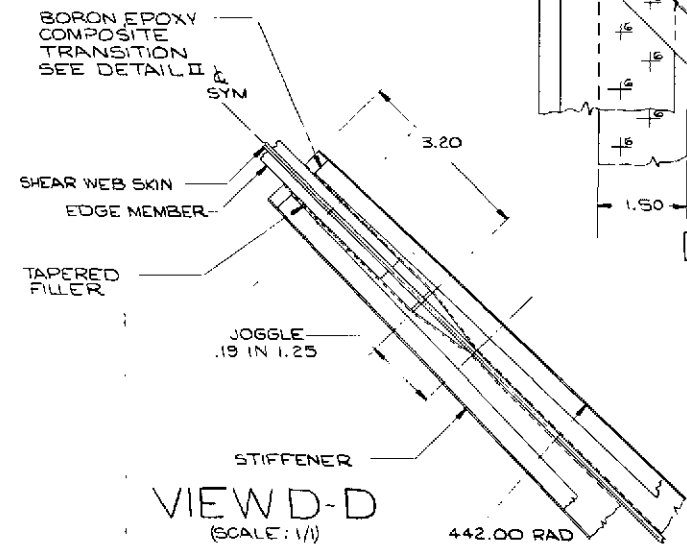
DETAIL II
(BORON EPOXY COMPOSITE)
(SCALE: 1/1)



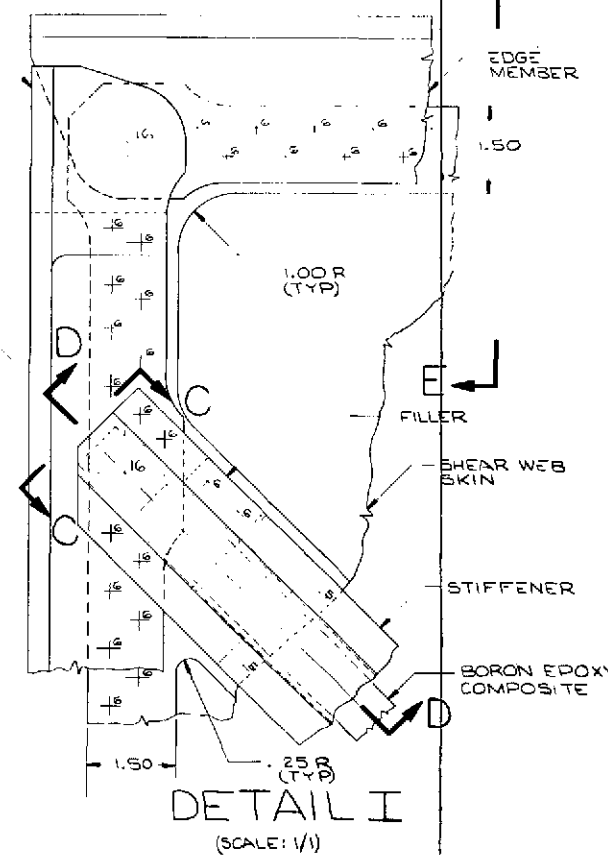
SECTION A-A
(SCALE: 1/1)



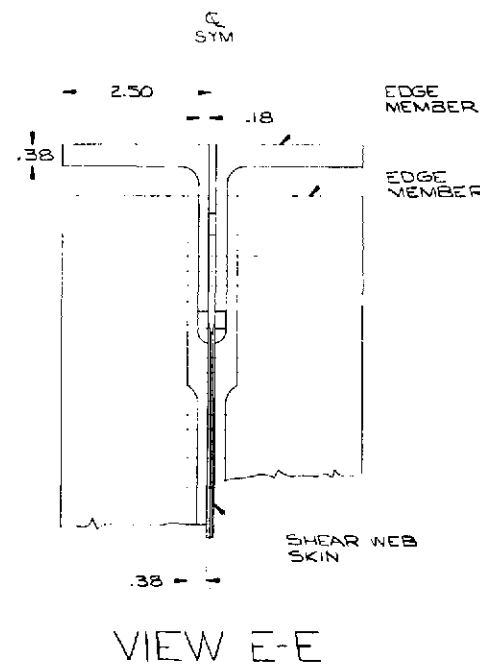
VIEW C-C
(SCALE: 1/1)



VIEW D-D
(SCALE: 1/1)



DETAIL I
(SCALE: 1/1)



VIEW E-E

| | | | | | |
|--------------------------------------|-------------|--------------------------------|----|--|----|
| SEE SHEET 1 FOR PARTS LIST AND NOTES | | CONTRACT NUMBER NAS 1-10860 | | THE BOEING COMPANY SEATTLE WASHINGTON 98148 | |
| DWG ORG | DATA REVIEW | DATE | BY | DATE | BY |
| STRUCT | | | | | |
| MATL & PRG | | | | | |
| ENGR | | | | | |
| ORG | | | | | |
| PROJECT APPROVAL | | | | | |
| CHANGE/ITEM NUMBER | | | | | |
| SHEET CODE IDENT NO J | | | | SK11-043165 | |
| SCALE/NOTED | | | | SH 2 of 2 | |

FOLDOUT FRAME 1

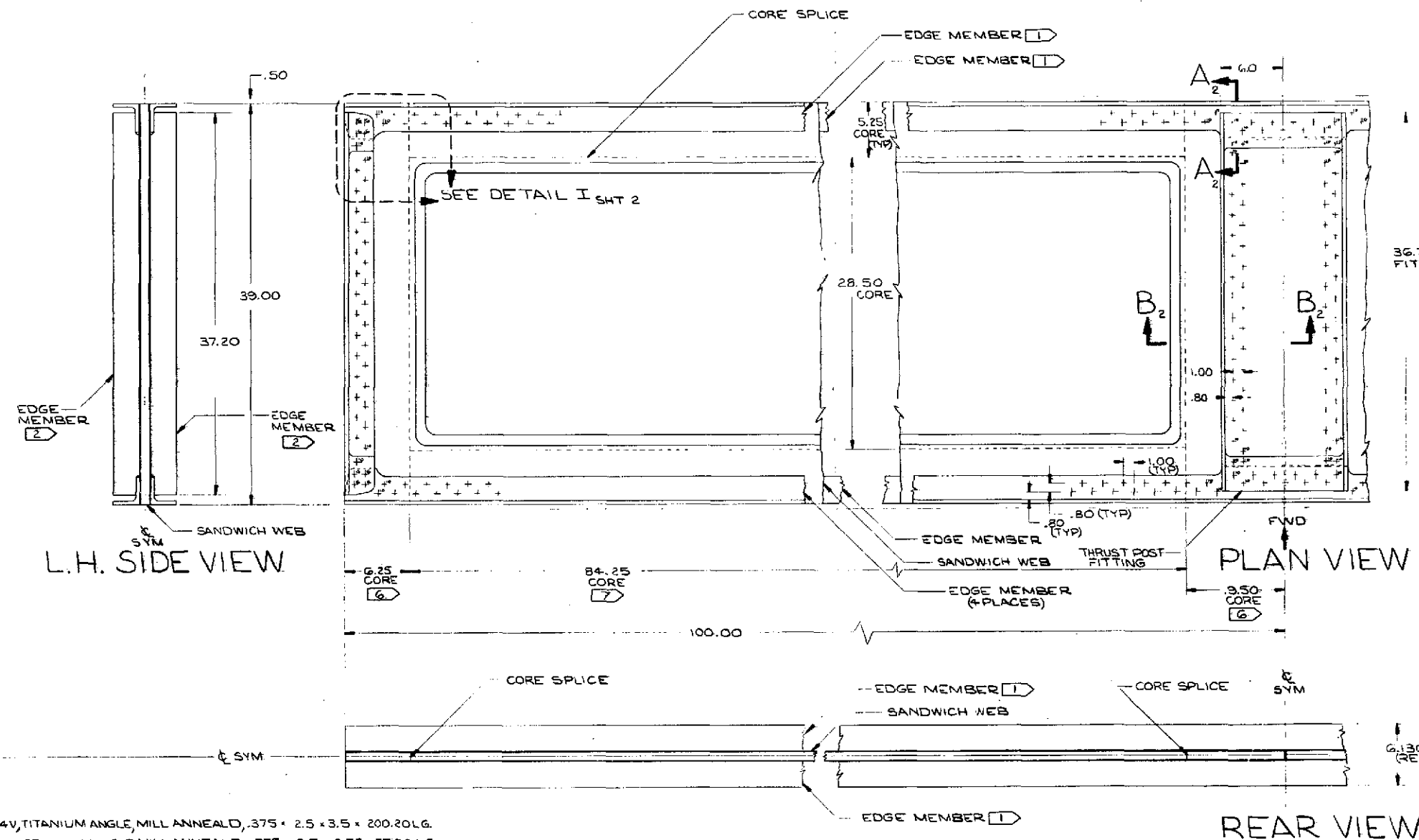
FOLDOUT FRAME 2

B-3

340

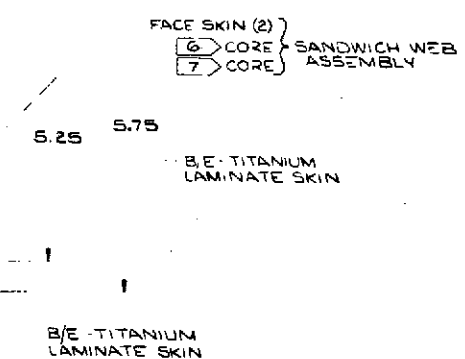
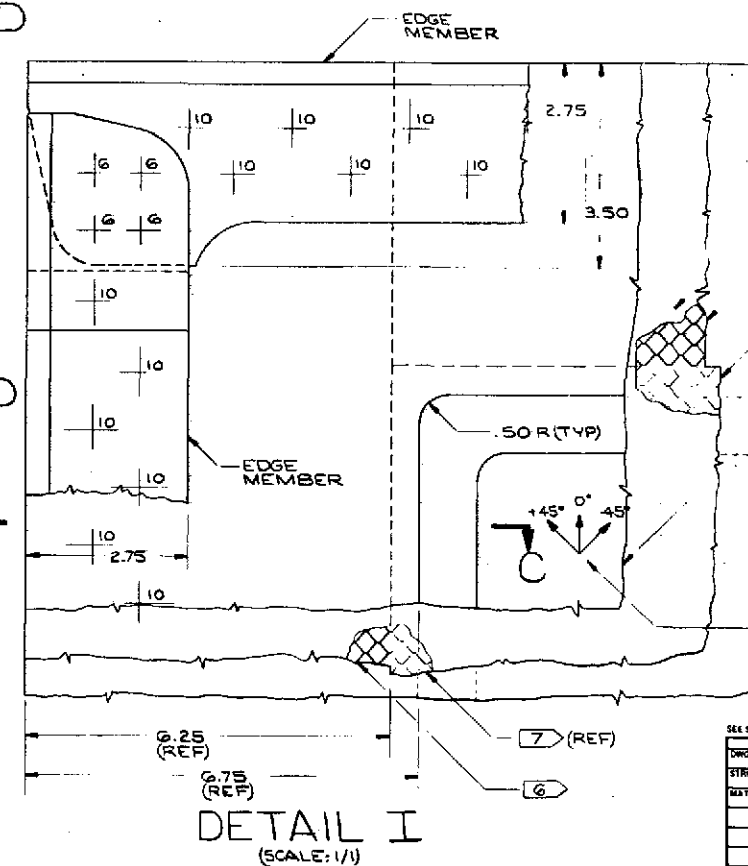
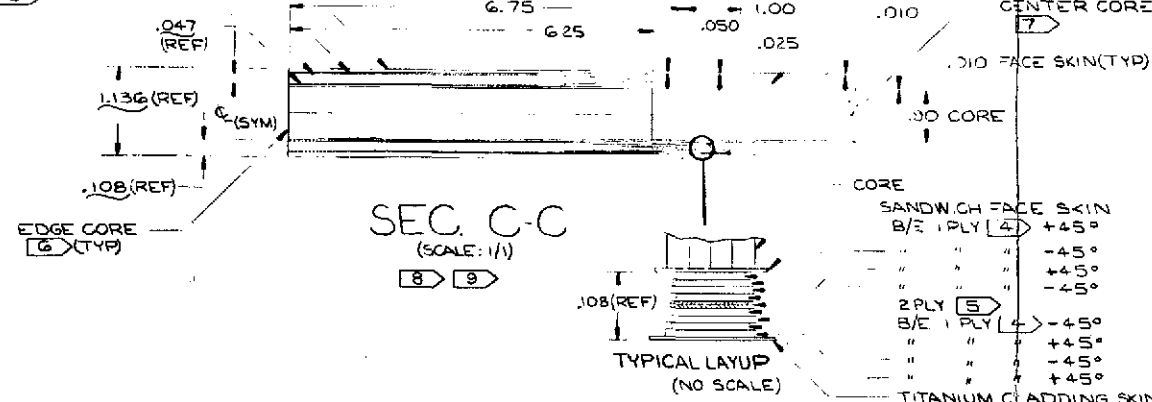
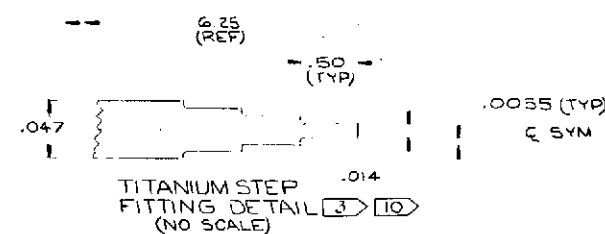
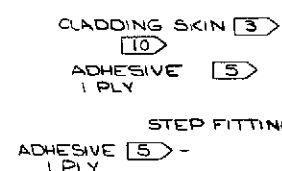
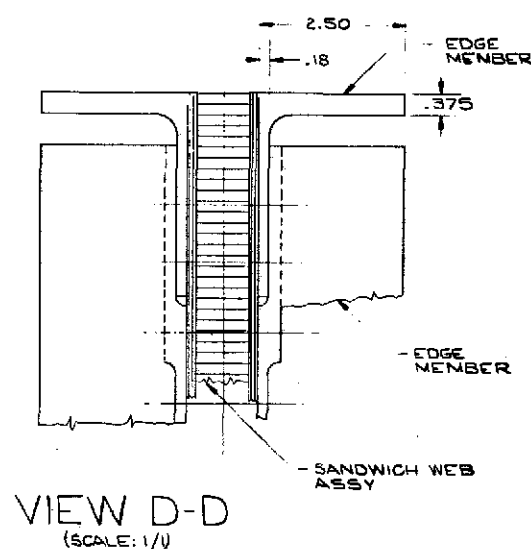
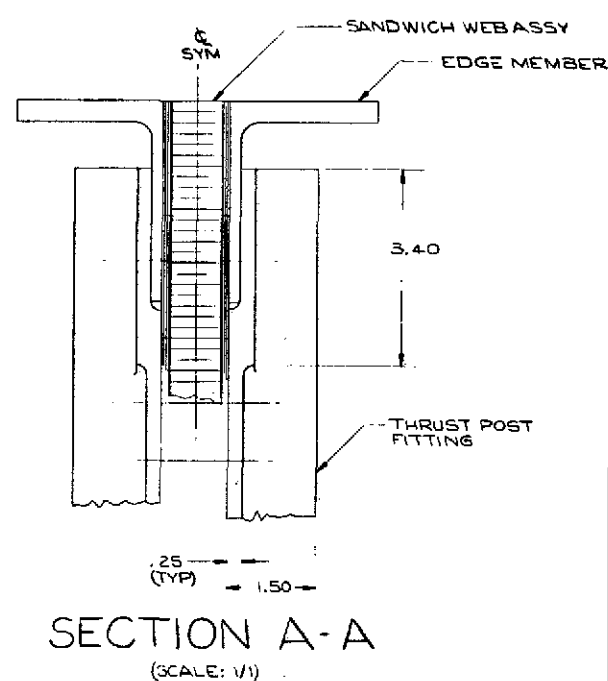
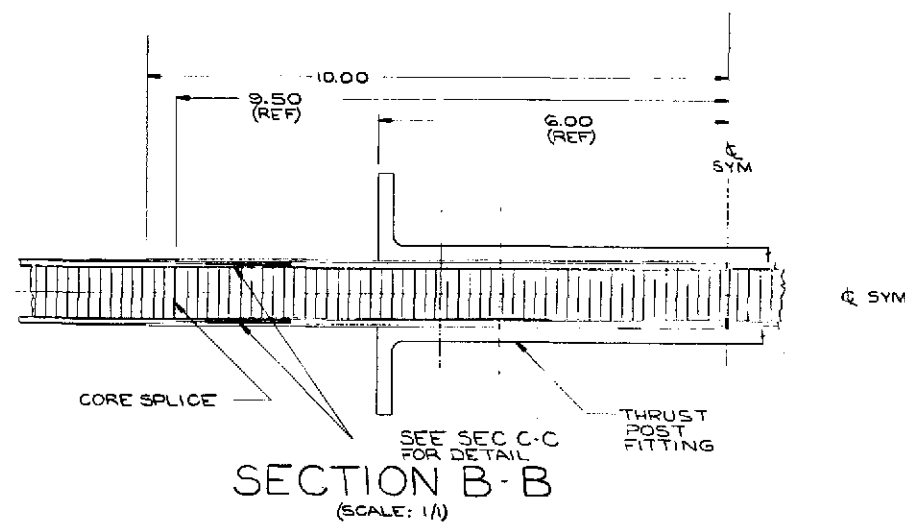
SK11-043165

SK11-043162



- 1 GAL-4V, TITANIUM ANGLE, MILL ANNEALD, .375 x 2.5 x 3.5 x 200.20 LG
- 2 GAL-4V, TITANIUM ANGLE, MILL ANNEALD, .375 x 2.5 x 2.75 x 37.30 LG
- 3 GAL-4V TITANIUM SHEET, MILL ANNEALD, PER BMS 7-174, TYPE B, COND I, OPTIONAL PER MIL-T-9046F, TYPE II, COMP B.
- 4 5505/4 BORON EPOXY TAPE
- 5 NARMCO MB 329 MODIFIED EPOXY ADHESIVE FILM
- 6 TITANIUM WELDED CELL HONEYCOMB CORE, PER YBMS 4-12, TYPE 4-GG, (MATERIAL OPTIONS: 35A(C.P) OR 3AL 2.5V TITANIUM)
- 7 TITANIUM WELDED CELL HONEYCOMB CORE, PER YBMS 4-12, TYPE 4-20, (MATERIAL OPTIONS: 35A(C.P) OR 3AL 2.5V TITANIUM)
- 8 CLEAN & PRIME FAYING SURFACES PER DG-23841 TN SEC 6.4.2d.
- 9 BOND PER DG-23841 TN SEC 6.8.2.2..
- 10 CHEM MILL PER BAC 5842

| | | | | | |
|--------------------|--|------------------------------|--|--|--|
| DATA REVIEW | | CONTRACT NUMBER NAS-10860 | | THE BOEING COMPANY | |
| SHEET | | DRAWN K.W. O'BORNE | | CORPORATE OFFICES SEATTLE, WASHINGTON, 98124 | |
| DATE & PAGE | | CHKD CJR | | SHEAR NEB-TI, CLAD B, F, BRAZED TI, SANDWICH, THRUST STRUCT, SPACE SHUTTLE ORBITER | |
| | | ENGR | | SITE CODE IDENT NO J SK25085-100 | |
| | | DRG | | | |
| CHANGE ITEM NUMBER | | PROJECT APPROVAL | | SCALE: 1/4" = 1' JH 1 OF 2 | |

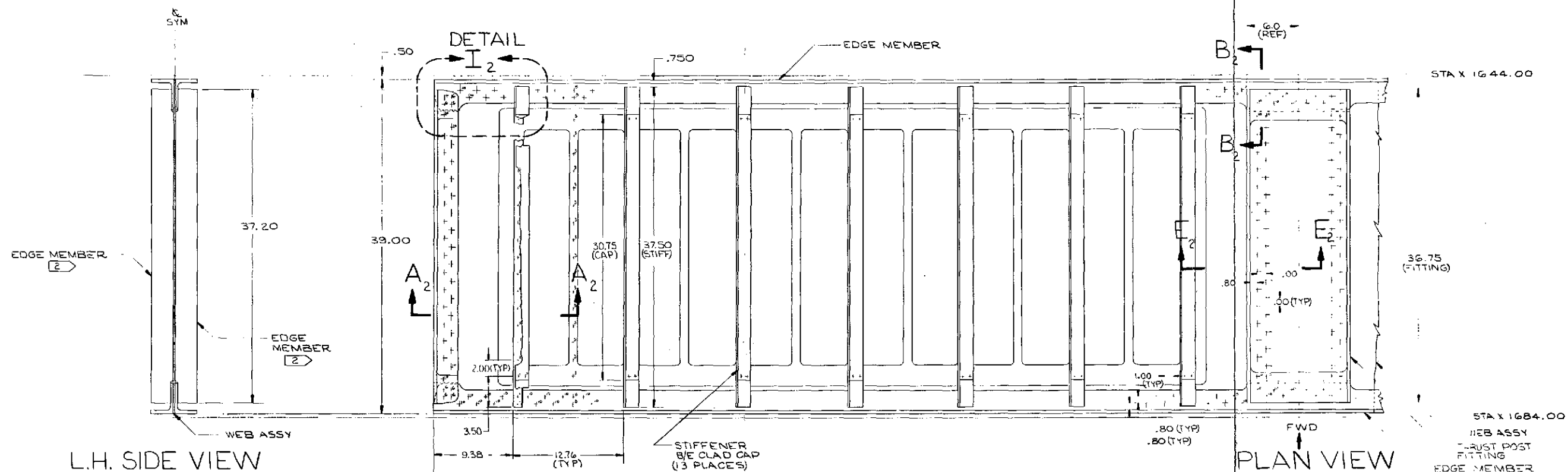


| | | | | | |
|--------------------------------------|--|------------------|--------------|--|-------------|
| SEE SHEET 1 FOR PARTS LIST AND NOTES | | CONTRACT NUMBER | | THIS BOEING COMPANY | |
| DATA REVIEW | | NAS1-10860 | | CORPORATE OFFICES SEATTLE, WASHINGTON 98148 | |
| OWING CO. | | DATE | 02-11-57 | SHEAR WEB-T; CLAD B/E BRAZE T1. SANDW.CH. THRUST STRUCT. SPACE SHUTTLE ORBITER | |
| STRUCT. | | DRW. | CHN. OSBORNE | | |
| MAT'L & PCE | | CHK. | | | |
| | | ENGR. | | | |
| | | ORG. | | | |
| CHANGE ITEM NUMBER | | PROJECT APPROVAL | | SIZE CODE IDENT NO. | SK25085-100 |
| | | | | J | |
| | | | | SCALE NOTED | SH 2 OF 2 |

2KS2082-101

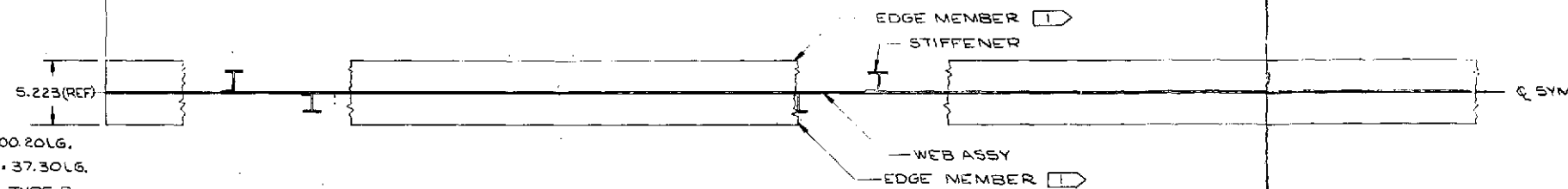
| REVISIONS | | | |
|-----------|-------------|------|----------|
| NO. | DESCRIPTION | DATE | APPROVED |
| 1 | | | |

340



L.H. SIDE VIEW

PLAN VIEW



REAR VIEW

- 1 GAL-4V TITANIUM ANGLE, MILL ANNEALD, .375 x 2.5 x 3.5 x 200.20 LG.
- 2 GAL-4V TITANIUM ANGLE, MILL ANNEALD, .375 x 2.5 x 2.75 x 37.30 LG.
- 3 GAL-4V TITANIUM SHEET, MILL ANNEALD, PER BMS 7-174, TYPE B, COND I, OPTIONAL PER MIL-T-9046, TYPE III, COMP B.
- 4 5505/4 BORON EPOXY TAPE
- 5 NARMCO MB 329 MODIFIED EPOXY ADHESIVE FILM.
- 6 7075-T6 ALUM SHEET, .020 x 1.6 x 30.85 LG
- 7 7075-T6 EXTRUSION, 37.60 LG.
- 8 CLEAN & PRIME FAYING SURFACES PER DG-23841 TN, SEC 6.4.2.4.
- 9 BOND PER DG-23841, TN SEC 6.8.2.2.
- 10 CHEM MILL PER BAC 5842

| | | | |
|---|------------------|--------------------------------|------|
| DATA REVIEW | | CONTRACT NUMBER NAS-1-10860 | |
| DRG QUAL | STRUT | DRG | DATE |
| DATE & PAGE | DATE | DATE | DATE |
| CHANGELIST NUMBER | PROJECT APPROVAL | DATE | DATE |
| THE BOEING COMPANY CORPORATE OFFICES SEATTLE, WASHINGTON 98124 | | SEATTLE, WASHINGTON 98124 | |
| SHEAR WEB, CLAD 3/E-T; BE-AL STIFFENED THRUST STRUCTURE SPACE SHUTTLE ORBITER | | SK2-5085-101 | |
| SCALE 1/4" | | 1 of 2 | |

SK2-5085-101

2KS2082-101

FOLDOUT FRAME

FOLDOUT FRAME

2

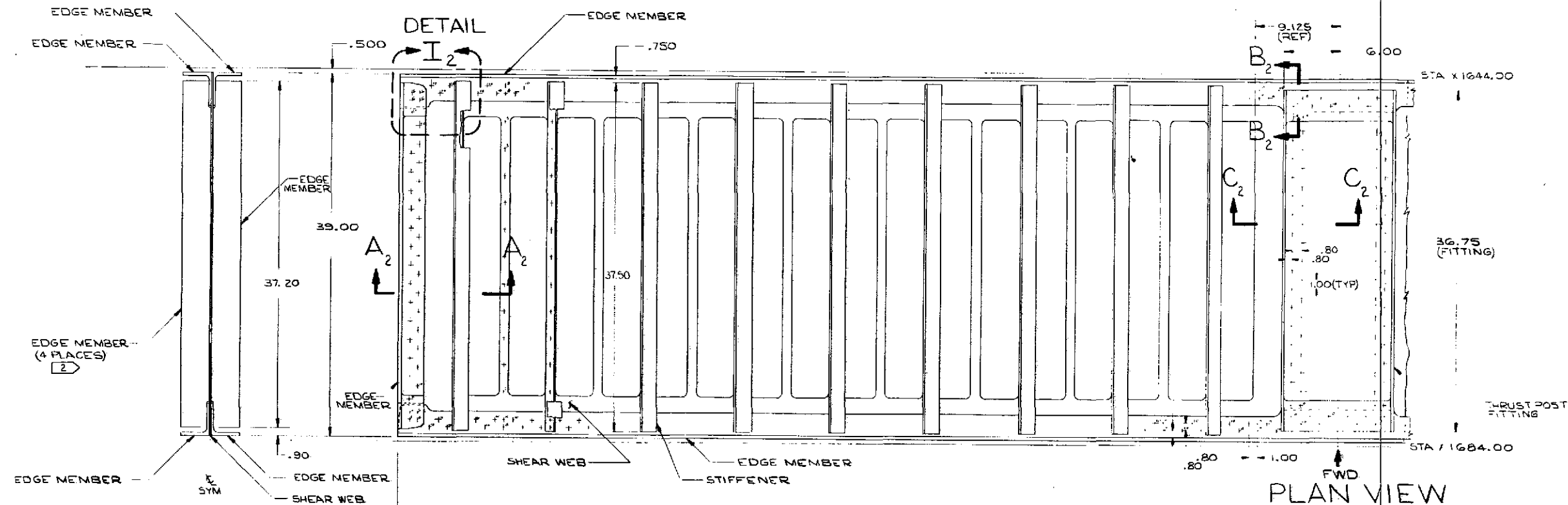
B-6

FOLDOUT FRAME 2

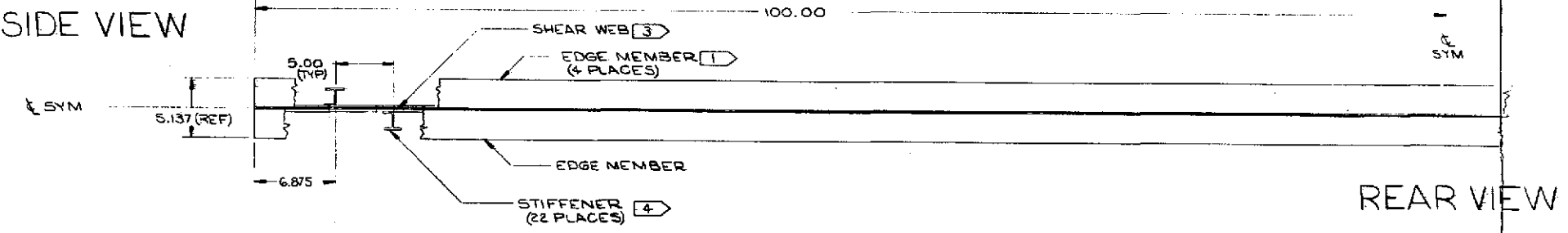
B-7

SK2-5085-102

| REVISIONS | | | |
|-----------|-------------|------|----------|
| NO. | DESCRIPTION | DATE | APPROVED |
| | | | |



L.H. SIDE VIEW



PLAN VIEW

REAR VIEW

- 1 GAL-4V TITANIUM ANGLE, MILL ANNEALD, .375 x 2.5 x 3.5 x 200.20 LG.
- 2 GAL-4V TITANIUM ANGLE, MILL ANNEALD, .375 x 2.5 x 2.5 x 37.30 LG.
- 3 GAL-4V TITANIUM SHEET, MILL ANNEALD, PER BMS 7-174, TYPE B, COND I. OPTIONAL PER MIL-T-9046F, TYPE II, COMP B.
- 4 7075-T6 ALUM EXTRUSION.
- 5 CHEM MILL PER BAC 5842

| | | | | | |
|--------------------|--|------------------|-------|--|---------------------------|
| DATA REVIEW | | CONTRACT NUMBER | | THE BOEING COMPANY | |
| DRG QUAL | | NAS 1-10860 | | CORPORATE OFFICES | SEATTLE, WASHINGTON 98101 |
| STRUCT | | OWN | | SHEAR WEB, TITANIUM, ALUM STIFFENED THRUST STRUCT. SPACE SHUTTLE ORBITER | |
| MAT & PRIC | | ENDORSE | 21-71 | | |
| | | ENGR | | | |
| | | DRG | | | |
| | | PROJECT APPROVAL | | SIZE CODE IDENT NO | |
| CHANGE/ITER NUMBER | | | | J SK2-5085-102 | |
| | | | | SCALE 1/4" = 1" | |
| | | | | ON 1 OF 2 | |

FOLDOUT FRAME

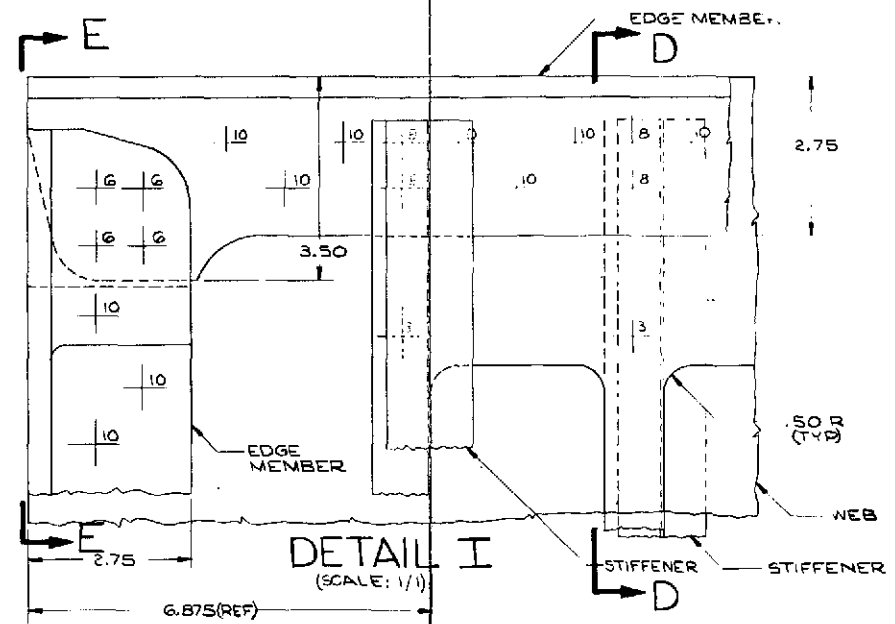
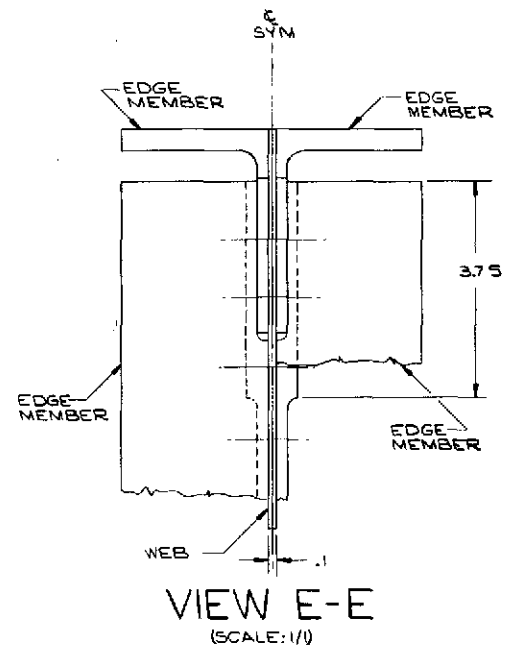
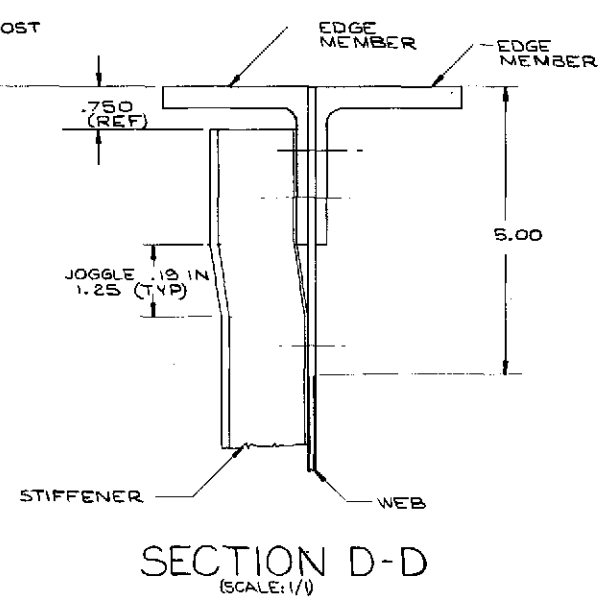
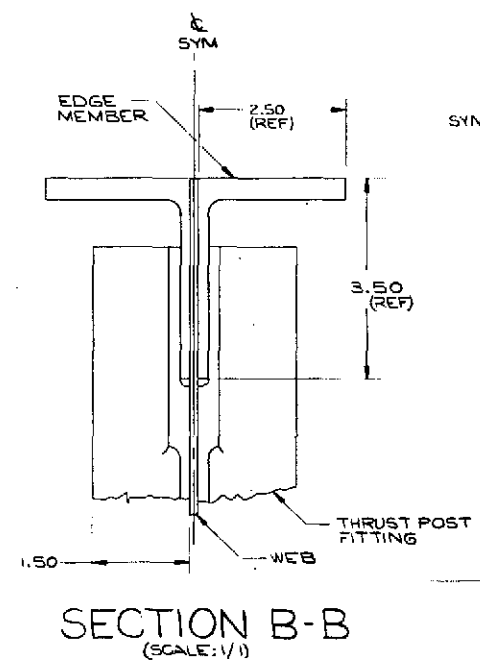
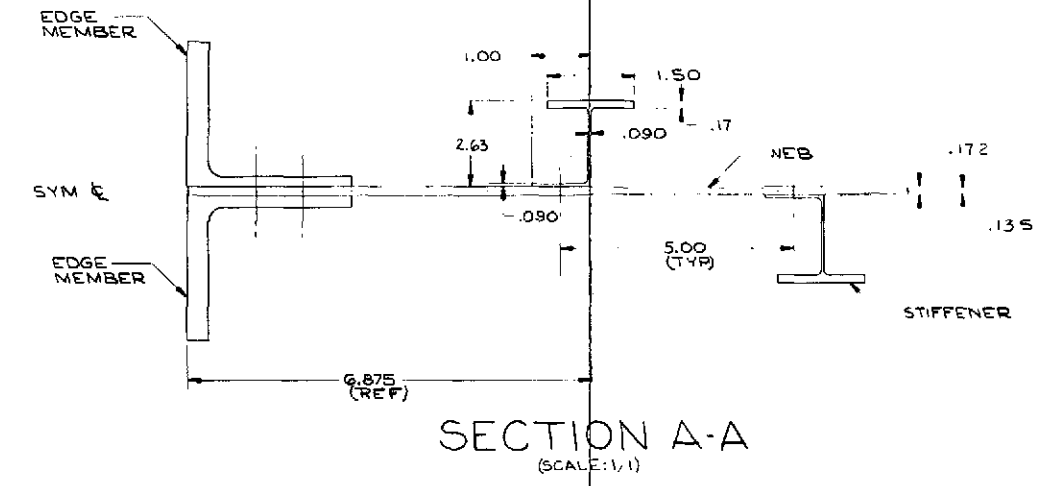
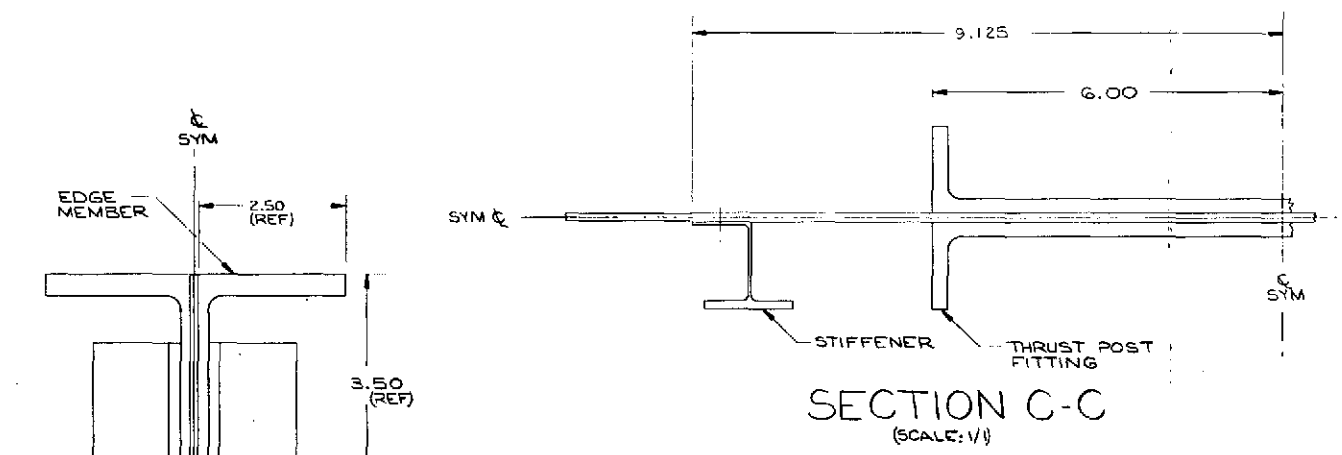
FOLDOUT FRAME

B-8

SK2-5085-102

2KS-2082-105

| REVISIONS | | | |
|-----------|------|-------------|----------|
| ZONE | DATE | DESCRIPTION | APPROVED |
| | | | |



| | | | |
|--------------------|--|---------------------------|--|
| CONTRACT NUMBER | | THE BOEING COMPANY | |
| NAS-10860 | | SEATTLE, WASHINGTON 98144 | |
| DESIGNED BY | | CORPORATE OFFICE | |
| C.W. OSBORNE | | 12-1-21 | |
| CHECKED BY | | ENGINEER | |
| ENG | | PROJECT APPROVAL | |
| ORG | | SHEET IDENT NO | |
| PROJECT APPROVAL | | J | |
| CHANGE/ITEM NUMBER | | SK2-5085-102 | |
| DWG ORG | | SCALE NOTED | |
| 2-5085 | | SH 2 OF 2 | |

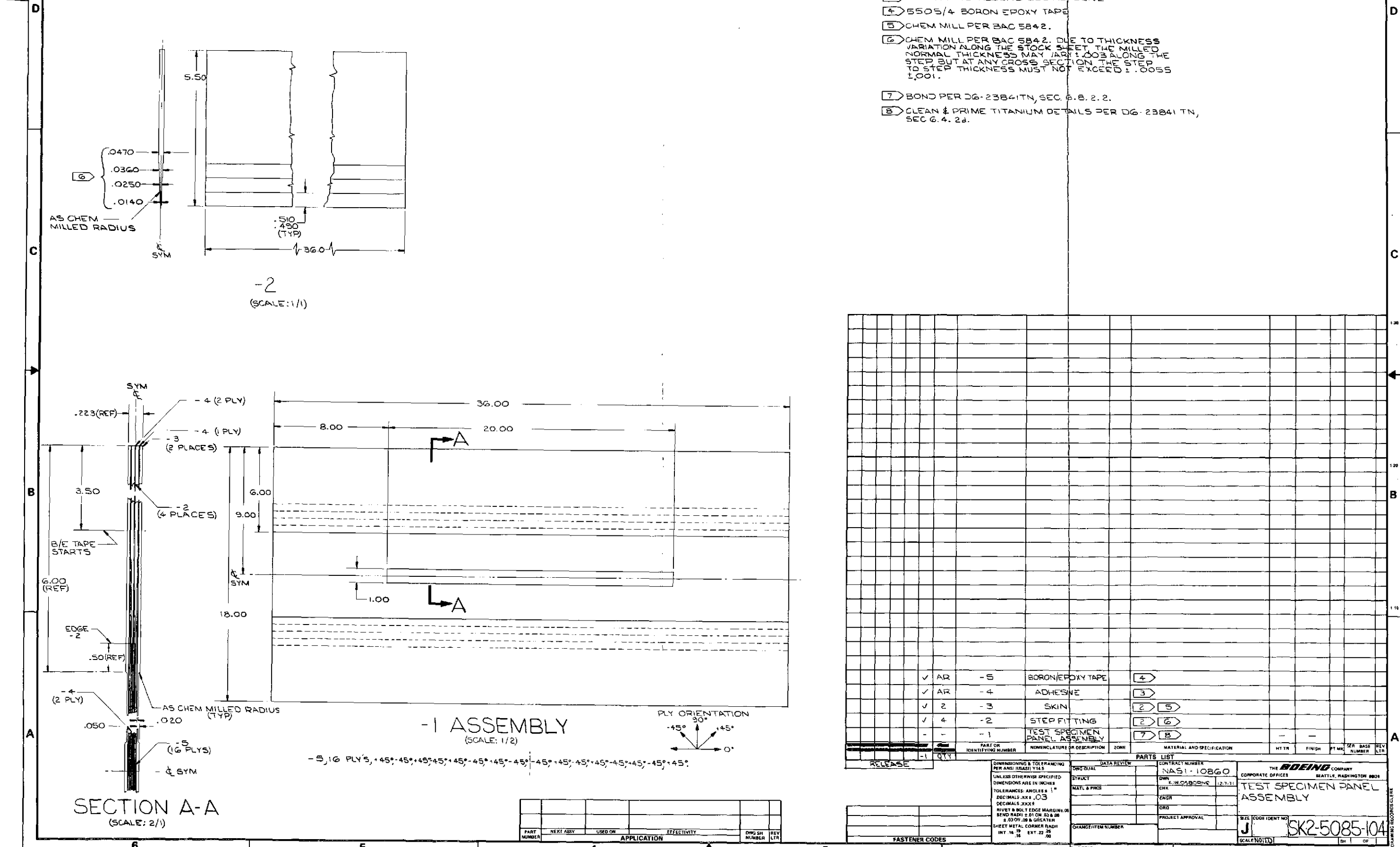
FOLDOUT FRAME

FOLDOUT FRAME 2

B-9

2KS-2082-105
SK2-5085-102
340

SK2-5085-104

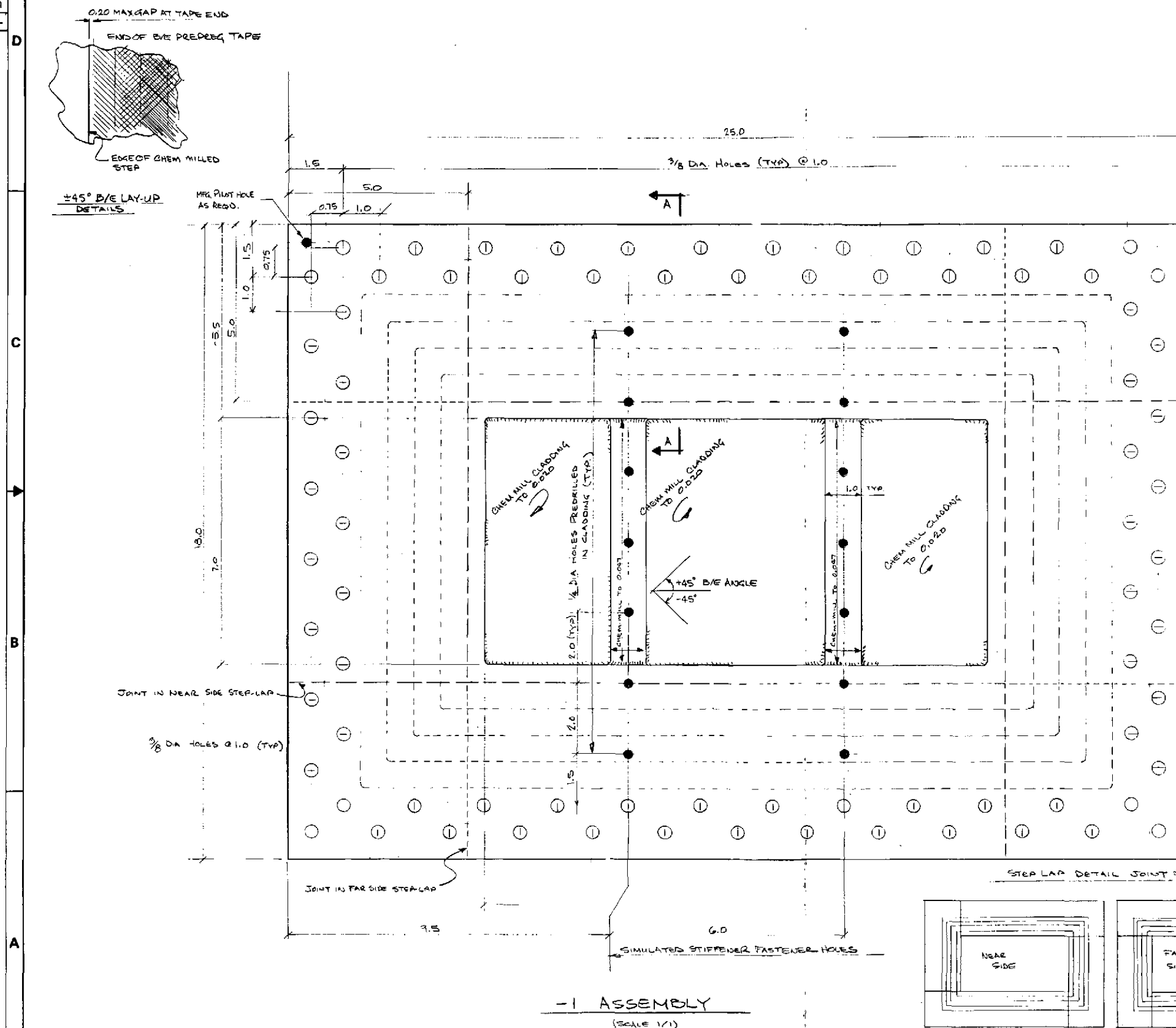


FOLDOUT FRAME

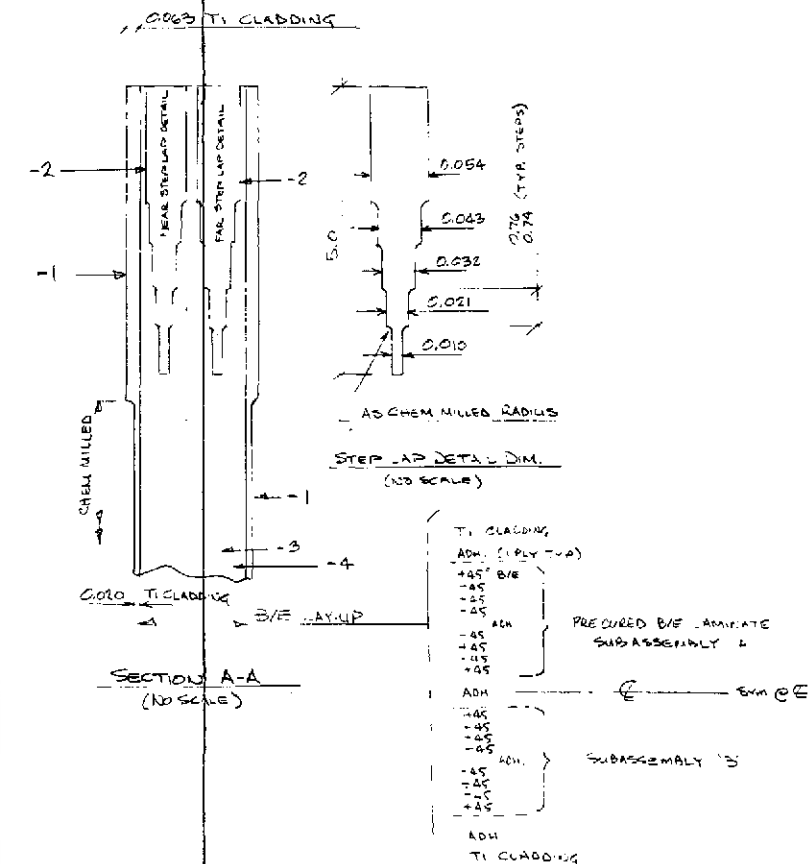
FOLDOUT FRAME 2

B-10

SK2-5085-104

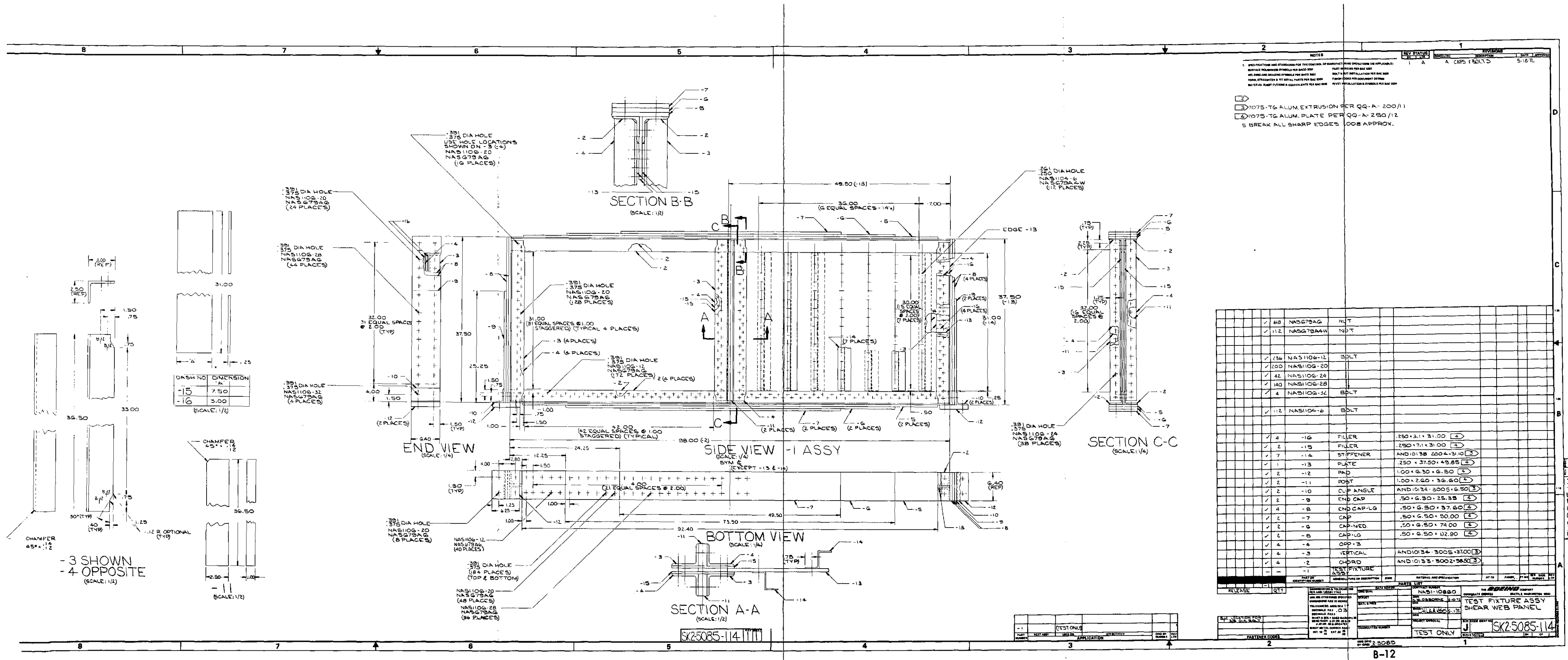


2. GALVAL TITANIUM SHEET M.A. 7063 ± 0.01X0.0
3. NARMCO METABOND D99 ADHESIVE
4. 3505/4 B/E TAPE PREPREG
5. CHEM MILL PER BAC 5842
6. CHEM MILL PER BAC 5842 DUE TO THICKNESS VARIATION ALONG THE STOCK SHEET, THE MILLED NOMINAL THICKNESS MAY VARY 0.003 ALONG THE STEP BUT AT ANY CROSS SECTION THE STEP-TO-STEP THICKNESS MUST NOT EXCEED 0.0055 ± 0.001
7. CLIZE LAMINATE PER ENG INSTRUCTIONS
8. CLEAN AND PRIME TITANIUM DETAILS PER DG-73841 TN SER 3.4.2d



| | | | |
|-----|------|-----------------|-------------|
| AR | 4 | B/E PREPARE | 5 |
| AR | 3 | ADHESIVE | 5 |
| B | 2 | STEPLAP DETAILS | 5 16 |
| 2 | 1 | TI SCAFFOLD | 3 5 |
| QTY | UNIT | DESCRIPTION | MATL. SPEC. |

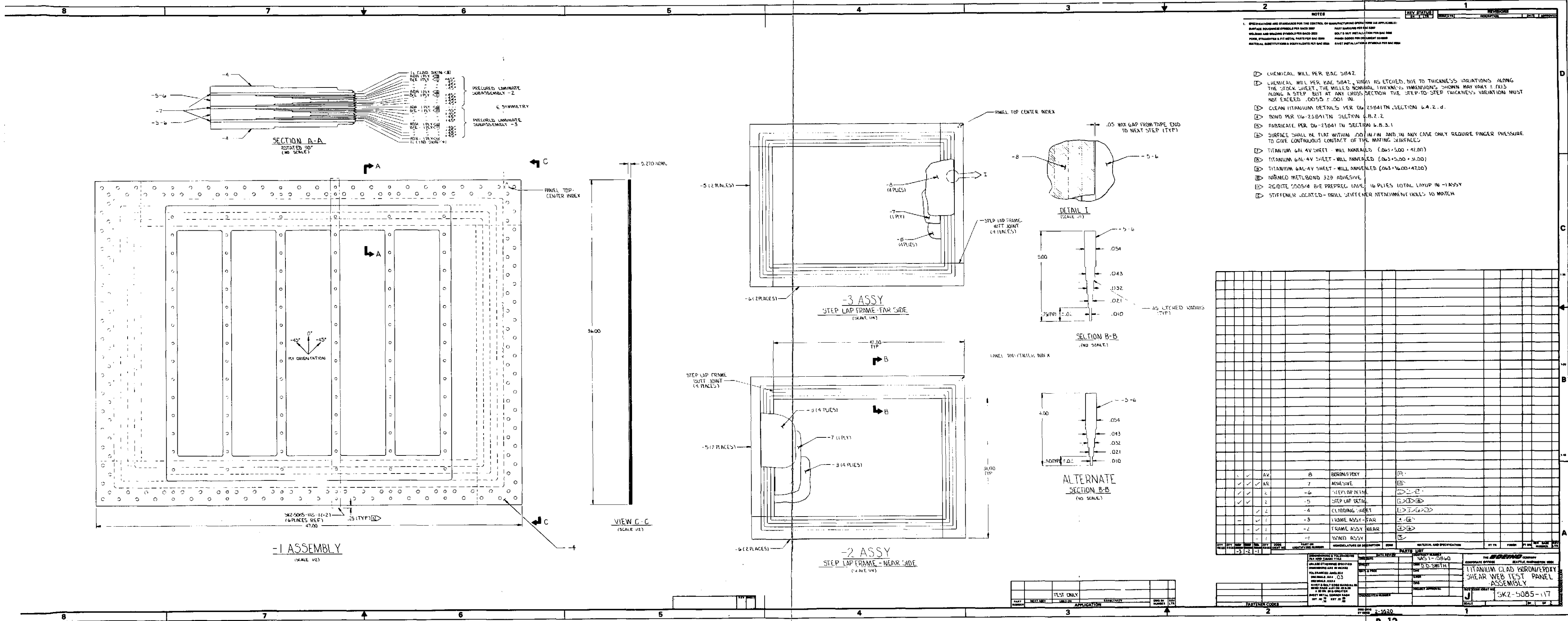
| | | | | | |
|--------------------------------------|--|-------------------------------------|--|--|---------------------|
| SEE SHEET 1 FOR PARTS LIST AND NOTES | | CONTRACT NUMBER NAS-10860 | | THE BOEING COMPANY CORPORATE OFFICES SEATTLE, WASHINGTON 98108 | |
| DATA REVIEW | | DRAWN BY LAAKSO 131-72 | | TI-CLAD B/E SHEAR WEB ELEMENT TEST PANEL | |
| STRUCT | | CHK | | | |
| MATERIALS & PRICES | | ENGR | | | |
| | | DRG | | | |
| CHANGE ITEM NUMBER | | PROJECT APPROVAL | | SIZE TEST IDENT NO. J | SK2-5085-112 |



FOLDOUT FRAME 1

FOLDOUT FRAME 2

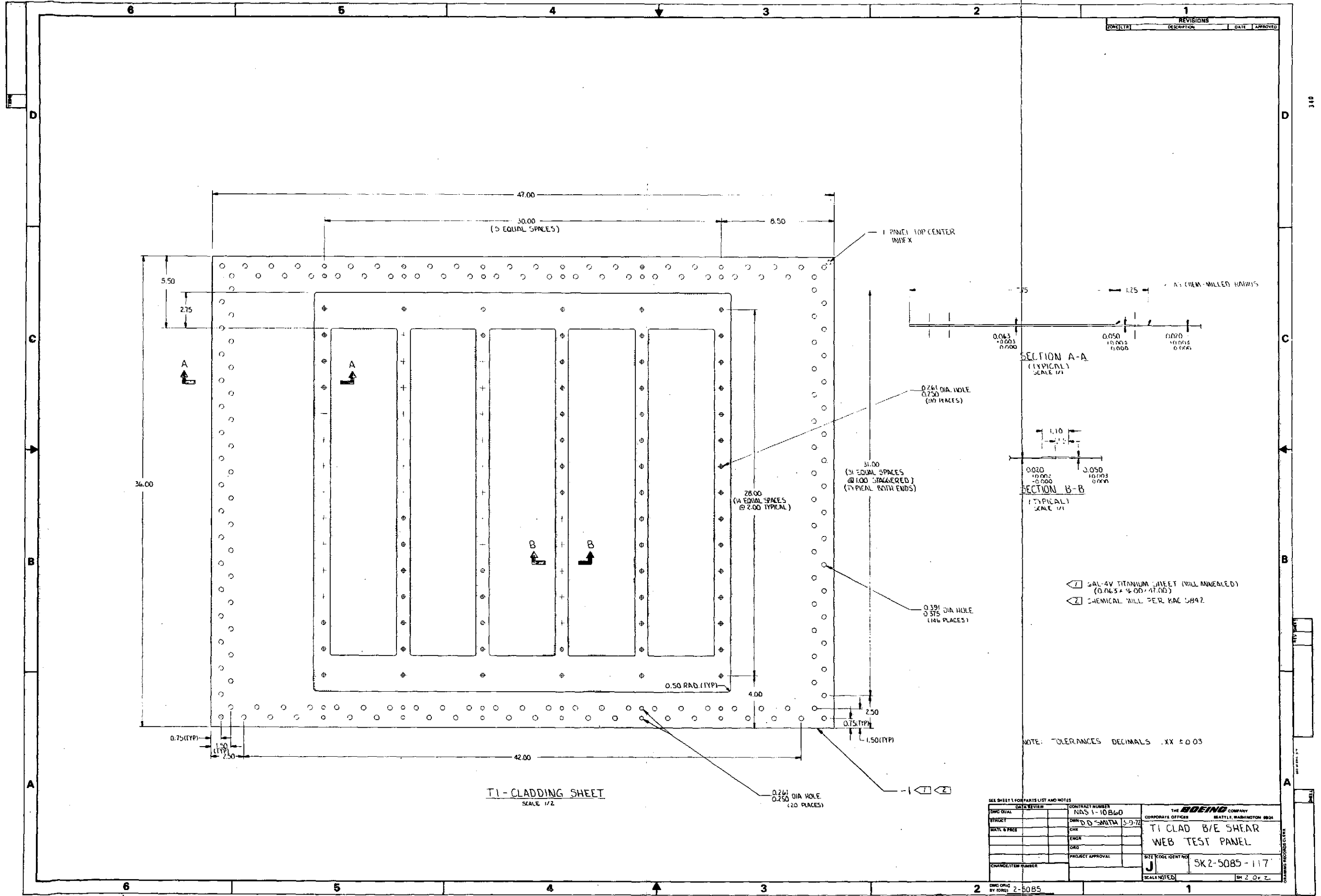
FOLDOUT FRAME 3



FOLDOUT FRAME 1

FOLDOUT FRAME 2

FOLDOUT FRAME 3



| REVISIONS | | |
|-----------|-------------|------|
| NO. | DESCRIPTION | DATE |
| 1 | | |

SECTION A-A
(TYPICAL)
SCALE 1/4

SECTION B-B
(TYPICAL)
SCALE 1/4

- 1 2AL-4V TITANIUM SHEET (MILL ANNEALED)
(0.0634 ± 0.0017)
- 2 CHEMICAL MILL PER KAC 5842

NOTE: TOLERANCES DECIMALS .XX ±0.03

| | | | | | |
|--------------------------------------|--------------|--------------------------------|-------------------|---|---------------|
| SEE SHEET 1 FOR PARTS LIST AND NOTES | | CONTRACT NUMBER NAS 1-10860 | | THE BOEING COMPANY CORPORATE OFFICE SEATTLE, WASHINGTON 9814 | |
| DWG. NO. | CA 2 REVISED | DRN | D.D. SMITH 3-9-72 | T1 CLAD B/E SHEAR WEB TEST PANEL | |
| STRUCT. | | CHK | | | |
| MAT'L & PRIC. | | ENGR | | | |
| | | DRG | | | |
| CHANGE/ITER NUMBER | | PROJECT APPROVAL | | SIZE CODE IDENT NO. | SK 2-5085-117 |
| | | | | SCALE/NOTES | SH 2 OF 2 |

FOLDOUT FRAME

FOLDOUT FRAME 2

B-14

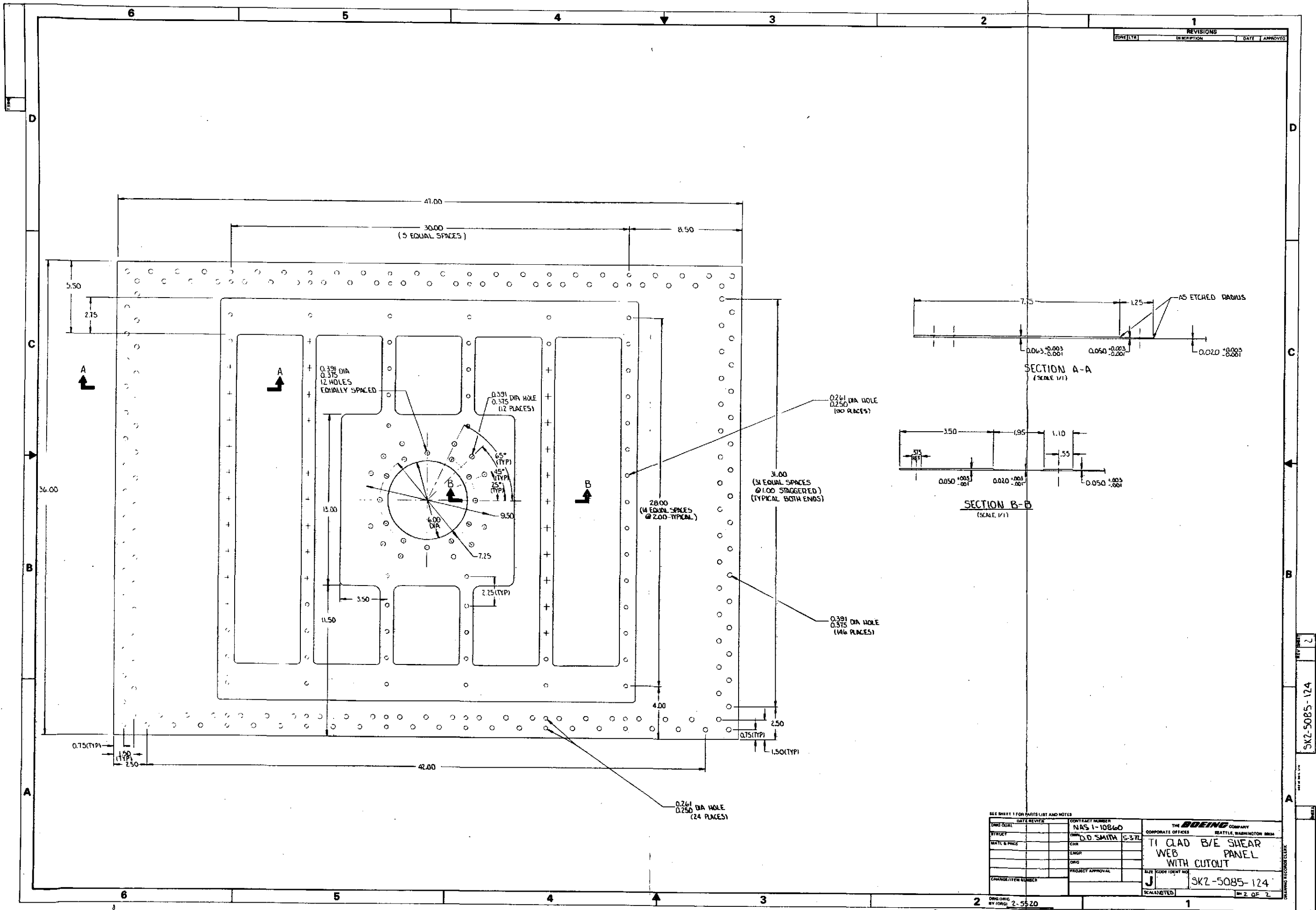
CB

FOLDOUT FRAME

FOLDOUT FRAME

2

B-17



| | | | | | |
|--------------------------------------|-------------|------------------|-------------|--------------------|---------------------------|
| SEE SHEET 1 FOR PARTS LIST AND NOTES | | CONTRACT NUMBER | | THE BOEING COMPANY | |
| DWG NO. | NAS 1-10860 | DWG NO. | NAS 1-10860 | CORPORATE OFFICES | SEATTLE, WASHINGTON 98104 |
| BY | D.D. SMITH | CHK | S-37L | TI CLAD B/E SHEAR | |
| MATL & PRG | | ENGR | | WEB PANEL | |
| | | DRG | | WITH CUTOUT | |
| CHANGE/ITER NUMBER | | PROJECT APPROVAL | | DATE | CODE IDENT NO. |
| | | | | J | SK2-5085-124 |
| | | | | SCALE/NOTES | 2 OF 2 |

SK2-5085-124

APPENDIX C

APPENDIX C - TEST PLAN FOR THE SHEAR WEB TEST COMPONENTS

C1.0 SCOPE

The test plan describes the procedures for the conduct of combined shear and bending load tests on 3-foot by 4-foot titanium shear webs reinforced with boron/epoxy composites. The tests will be conducted on three shear web designs. The testing will be performed for NASA-LRC Contract NAS 1-10860, "Evaluation of a Metal Shear Web Selectively Reinforced with Filamentary Composites for Space Shuttle Applications", and will be conducted in the 9-101 Building at The Boeing Company's Developmental Center, Seattle, Washington.

C2.0 PURPOSE

The purpose of this plan is to define the required facilities, test and instrumentation equipment, and to detail the testing procedures. The plan as described will stress the first web to limit load for 100 cycles and then load to the failure load condition. The results will be utilized to verify the structural integrity of the shear web and to correlate the analysis methodology with the experimental data. The test plan will be revised after completion of the first and second web tests.

C3.0 TEST REQUIREMENTS

The tests conducted will provide data on the structural response of the shear web versus load and shall provide sufficient data necessary for correlation with strain and buckling analyses.

C3.1 TEST SPECIMEN

Three shear webs will be fabricated and tested in the test beam frame. Test component web No. 1 will be fabricated per SK2-5085-117 and SK2-5085-118. The test beam frame construction details are shown in SK2-5085-114. (All design drawings are shown in Appendix B.) Shear web No. 2 will be similar in design to web No. 1. The test component web No. 3 design will be based on the test

results of webs 1 and 2.

C3.2 TEST EQUIPMENT

Data acquisition equipment shall be calibrated prior to use. The equipment shall be calibrated against standards which are readily traceable to national standards.

C3.2.1 Test Machine - BALDWIN - LIMA - HAMILTON 1,200,000 pound capacity universal testing machine.

C3.2.2 Data Acquisition System - HEWLETT - PACKARD Model 2012D (Option W). Range ± 100 mV and accuracy $\pm 0.4\%$.

C3.2.3 Signal Conditioner - PPM Model SG-14

C3.2.4 X-Y Plotter - ELECTRO INSTRUMENTS Model 500.

C4.0 TEST SETUP

C4.1 BEAM TEST

The shear web test panel will be mounted in the test frame shown in SK2-5085-114. Simple supports are provided to react the load applied at mid-span. Lateral support will be provided at the ends and at mid-span but will not react any of the load applied to the beam. Strain gages and EDI's will be mounted on the panel to record strains and deflections during the tests.

C4.2 CHECKOUT

Checkout of the panel test frame, load system and instrumentation equipment will be accomplished prior to the first limit load cycle to insure the correct operation of all test equipment.

C4.3 TEST SAFETY

Because of the high test loads involved, all applicable Boeing safety regulations shall be rigidly adhered to.

C5.0 INSTRUMENTATION

C5.1 Strain-gages, Electrical Deflection Indicators (EDI's), accelerometers, and Moire Fringe panels will be located on the panel per engineering instructions.

C5.1.1 Strain Gages - Micro-Measurements Type EA-05-125RD-350 with a $\pm 30,000 \mu\epsilon$ range and $\pm 1\%$ accuracy.

C5.1.2 Electrical Deflection Indicators (EDI's) - Boeing Company's short blade type with a $\pm .75$ in. deflection range and a $\pm 0.7\%$ accuracy.

C5.1.3 Moire Fringe System Equipment - The Moire test setup will consist of five 5 inch by 26 inch sections of 100 line-per-inch glass grids fixed to the test web by spring clips. Grids will be illuminated at an angle of incidence of 61° by a 1,000 watt, high-pressure Xenon light source. The fringe patterns will be recorded by a Hasselblad 500 EL camera fitted with an 80 mm lens. Photographs will be taken of the Moire fringe pattern at varying increments to the failure load.

C6.0 TEST PROCEDURES

C6.1 PHOTOGRAPHS

Photographs will be taken of:

- (1) Test panel mounted in frame before testing
- (2) Test frame setup for testing in 1,200,000 lb testing machine
- (3) Instrumented panel with Moire fringe system installed
- (4) Failed shear panel in frame
- (5) Panel close-ups of failed area

C6.2 TESTS TO LIMIT LOAD

The objective of this test is to demonstrate that the shear web can sustain the limit load condition without permanent deformation. Additionally, the cyclic limit loading will substantiate the service life capability of the web.

C6.2.1 LIMIT LOADING SCHEDULES

| <u>Cycle</u> | <u>Load</u> | <u>S/G & EDI Monitor</u> |
|--------------|-------------|----------------------------------|
| 1 | Limit | Continuous |
| 2 - 49 | Limit | - |
| 50 | Limit | Continuous |
| 50 - 99 | Limit | - |

C6.2.2 The limit load value for this test is 400 Kips.

C6.2.3 The maximum machine loading rate for the monitored load cycles is 100 k/min. For the rapid load cycle periods, the maximum loading rate is 800 k/min.

C6.2.4 A complete visual inspection of the shear web shall be performed after the limit load cycles have been made. Determine if there is any permanent set in any of the strain gages or EDI's.

C6.3 TEST TO ULTIMATE LOAD

The objectives of this test are to determine the ultimate strength of the shear web panel and the mode of failure.

C6.3.1 ULTIMATE LOADING SCHEDULE

| <u>Cycle</u> | <u>Load</u> | <u>S/G & EDI Monitor</u> |
|--------------|-------------|----------------------------------|
| 100 | Ultimate | Continuous |

C6.3.2 The ultimate load value for this test is projected to be in excess of 550 K.

C6.3.3 The maximum machine loading rate for the ultimate load cycle is 100 K/min. (Note: applies above limit load).

C6.4 POST TEST ANALYSIS

At the conclusion of the ultimate load test, the location and probable cause of

failure will be determined prior to removing the panel frame from the test machine. Any visual or acoustical phenomena observed during the test will be noted on the test log. Additional photographs to those outlined in Section 6.1 shall be taken as circumstances dictate to provide a complete photographic account of the test.